Studies in carboniferous bryozoa

A. J. Bancroft

STUDIES IN CARBONIFEROUS BRYOZOA

by A.J. Bancroft

Hatfield College

A thesis presented for the degree of Doctor of Philosophy

in the University of Durham

Volume 2 - Figures and Plates

Department of Geological Sciences,
University of Durham.

January 1984

Figure 1. Longitudinal section through the distal part of an autozooecium in a recent hornerid cyclostome showing the nature of the relationship between soft and skeletal tissues.

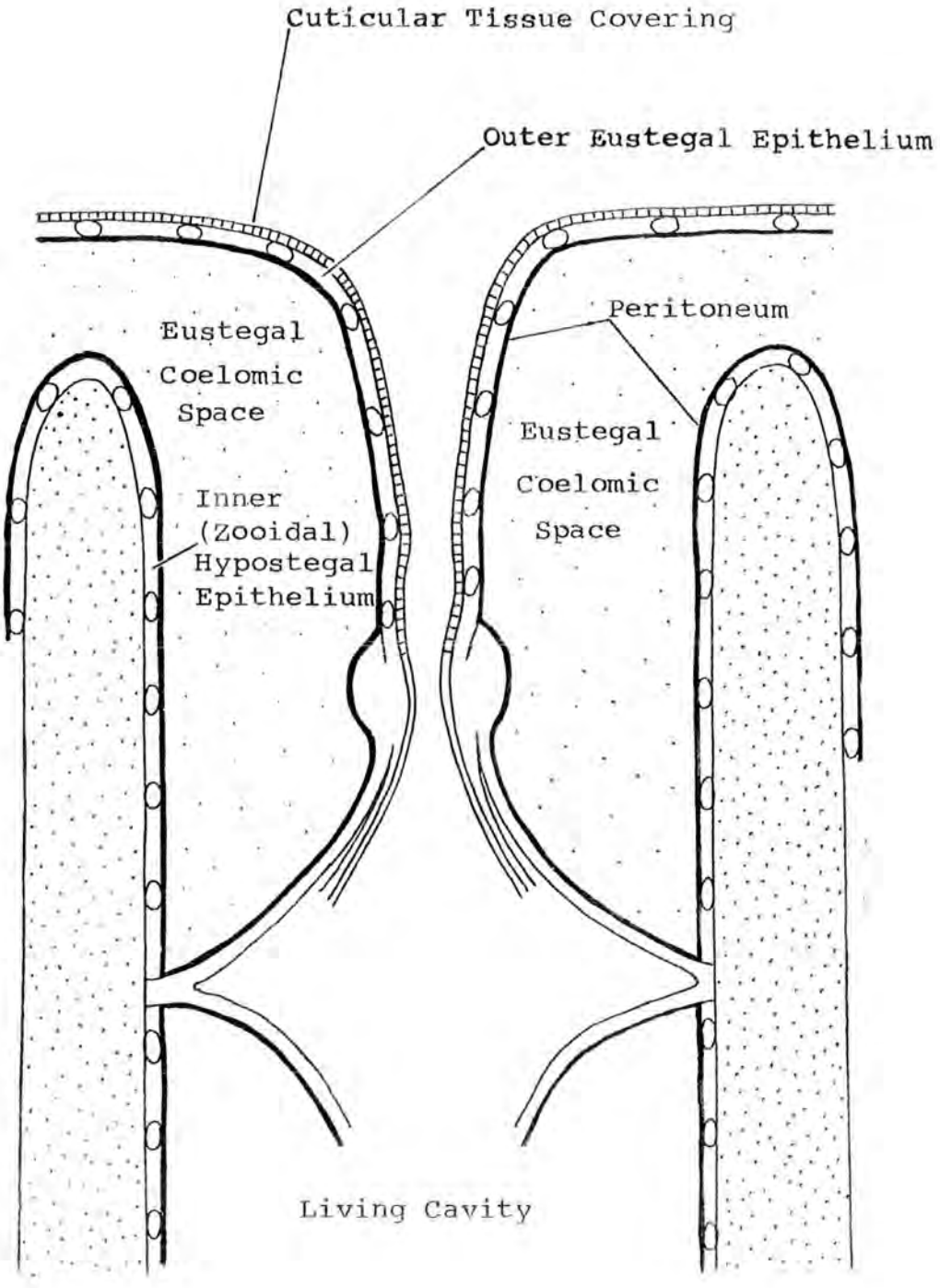
Cuticular Tissue Covering
Outer Eustegal Epithelium
Peritoneum
Eustegal
Coelomic
Space
Inner
(Zooidal)
Hypostegal
Epithelium
Eustegal
Coelomic
Space
Living Cavity

Figure 2. Longitudinal section showing the skeletal morphology of a basal diaphragm in a trepostome. Skeletal laminae of the diaphragm are orally flexed at the junction with the vertical interzooecial walls and are continuous with laminae lining interzooecial walls distal to them. The relative thicknesses of the unit comprising the basal diaphragm and interzooecial walls is shown. The thickness of the unit at a' is considerably greater than at a , because there is an increase in the number of laminae comprising the unit within interzooecial walls as new laminae are intercalated between those comprising the basal diaphragm.

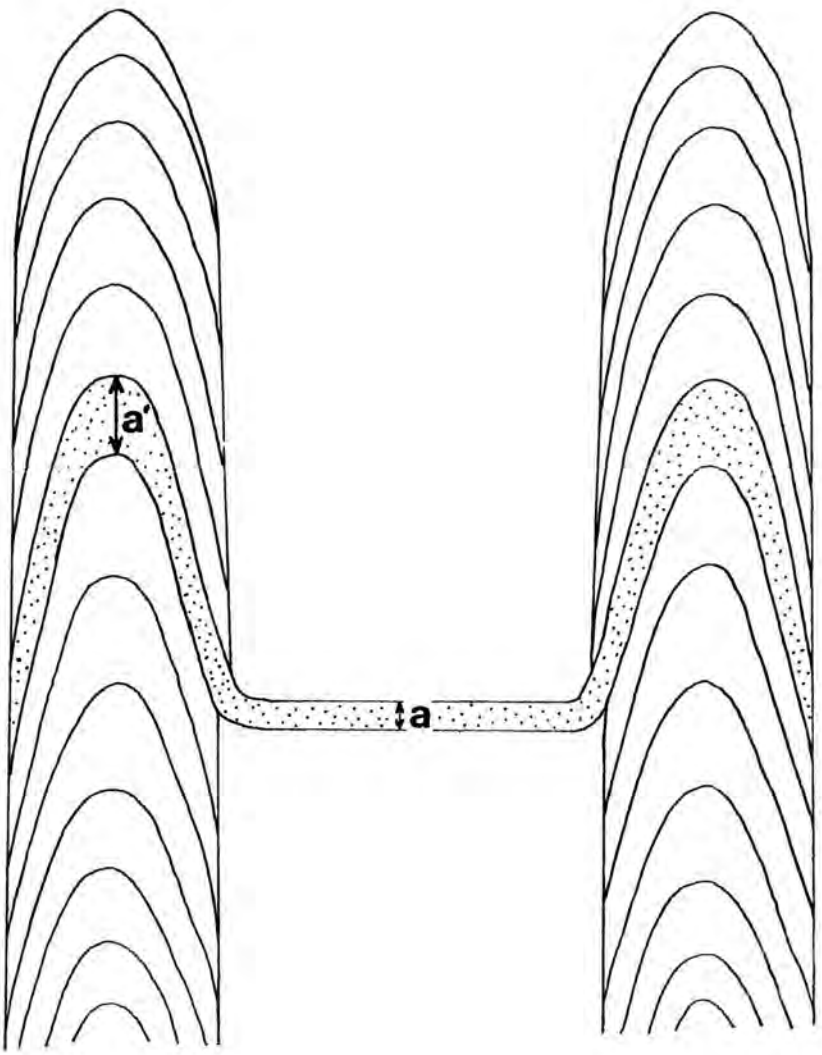
a'
a

Figure 3. Longitudinal section showing how the progressive modification of laminae deposition leads to the development of a type A stylet. (see text p.45)

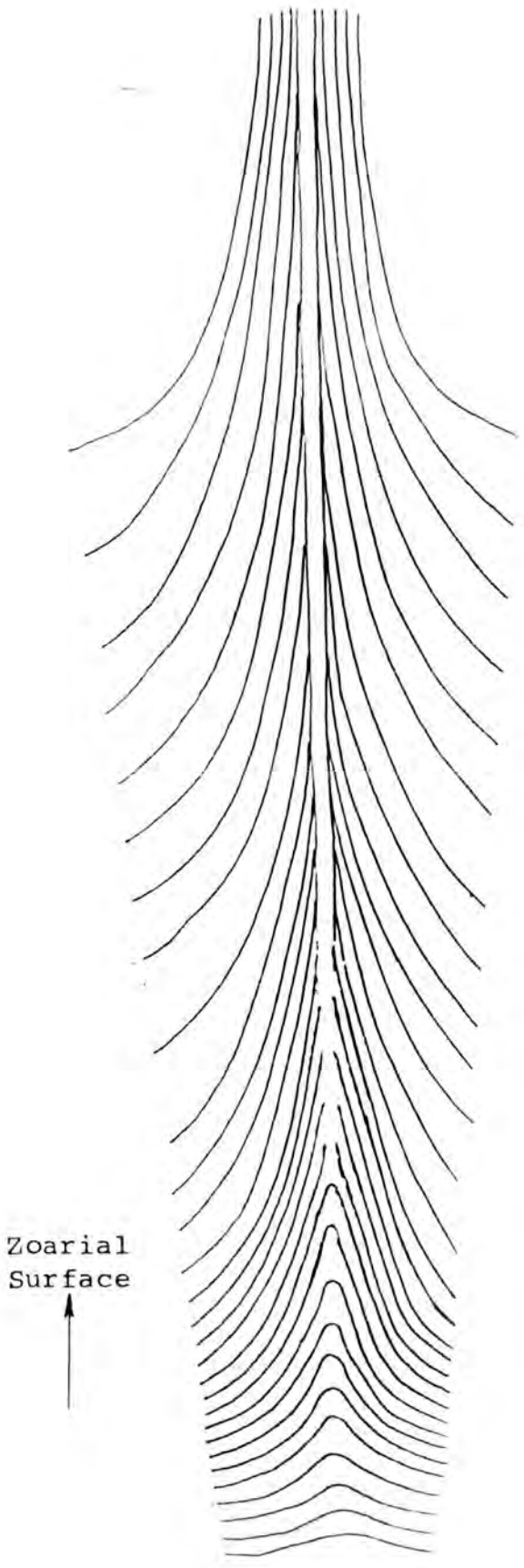
Zoarial
Surface

Figure 4. Longitudinal section showing how the progressive modification of laminae deposition leads to the development of a type B stylet. (see text p.46)

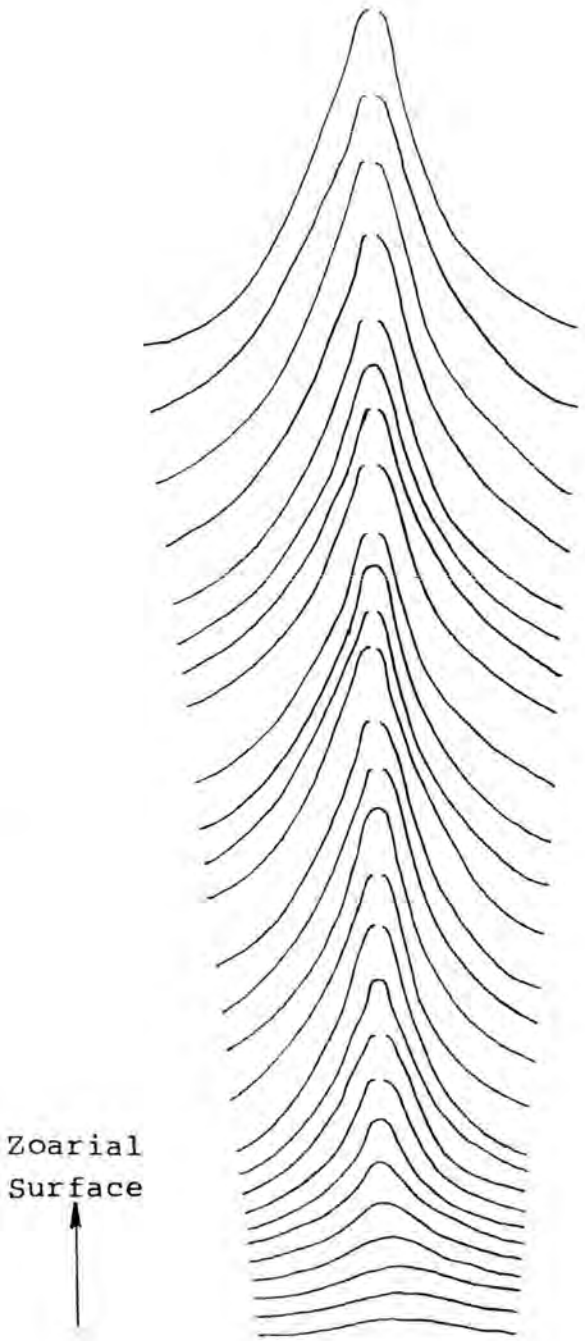
Zoarial
Surface

Figure 5. Longitudinal section showing how the progressive modification of laminae deposition leads to the development of a type C stylet. (see text p.46)

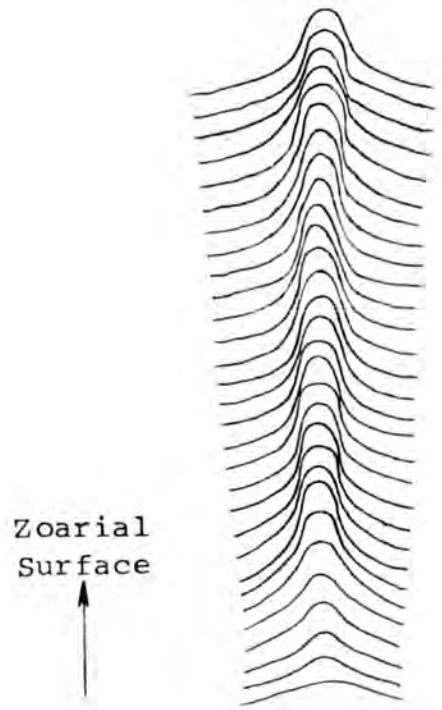
Zoarial
Surface

Figure 6. Branching types in cryptostomes

(a) Bifurcation of a primary branch: the budding axis of a branch dichotomises at the growth tip and two daughter branches are developed diverging at acute angles.

(b) Lateral branch development: a lateral branch developes on the surface of a mature stem. The exozone wall of the parent branch is completed before the lateral branch begins to develop.

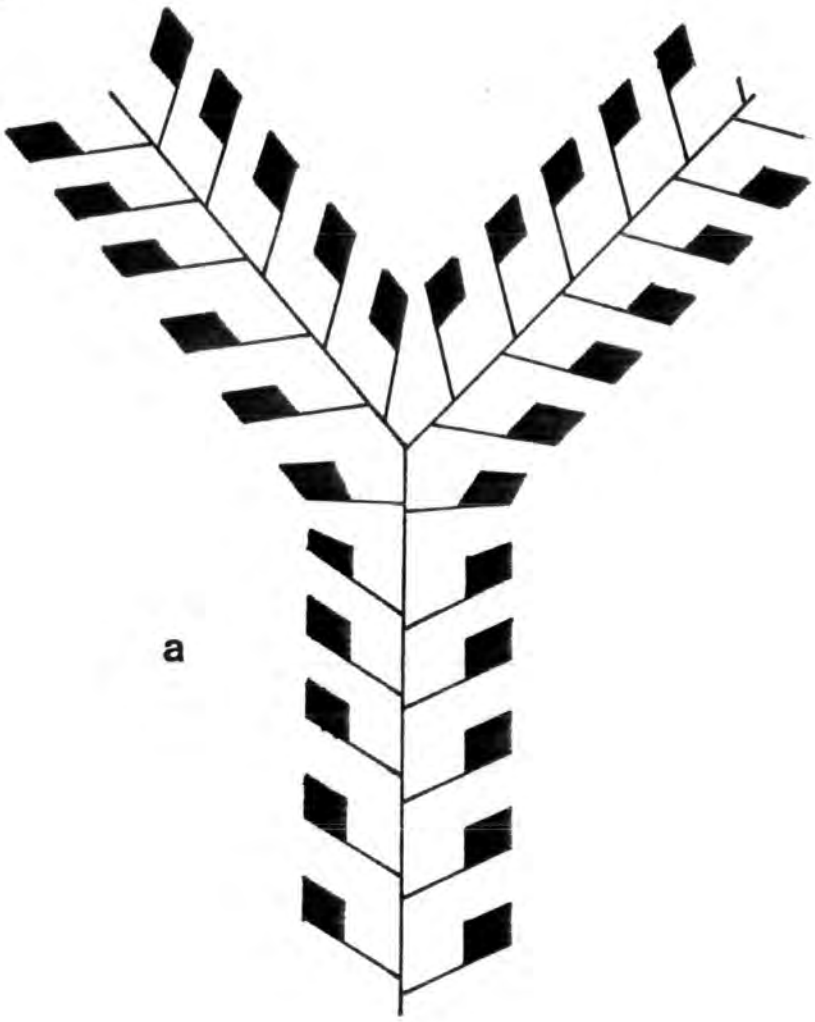

a

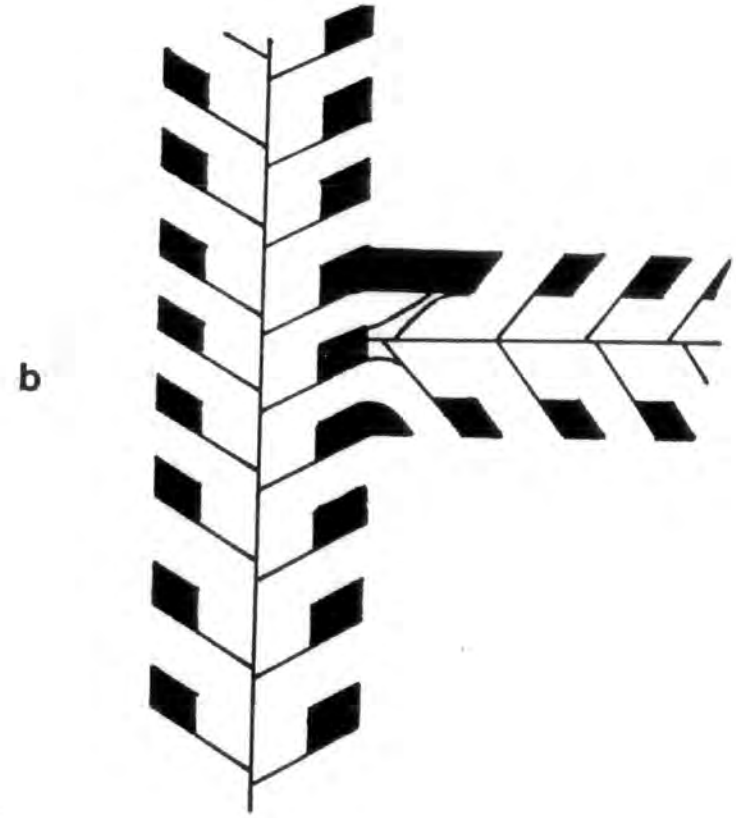

b

Figure 7. Diagram to show the morphological characters measured on cryptostomes in the present study. (For explanation of characters see text pp.64-66)

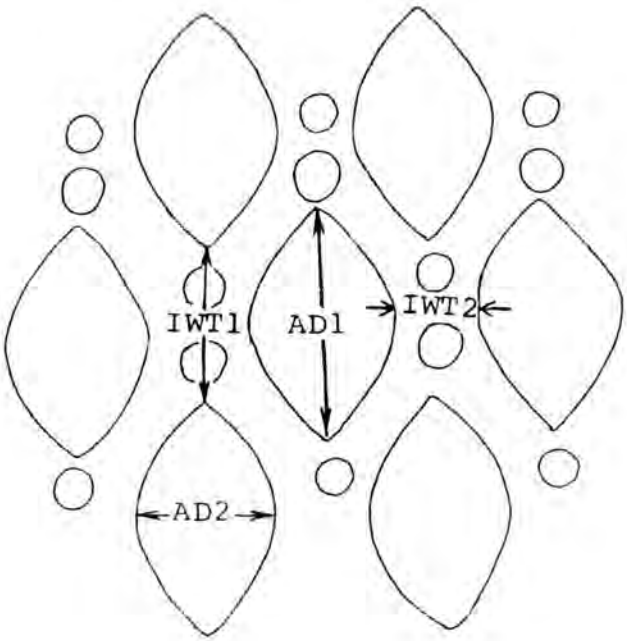
IWT1
AD1
IWT2
AD2

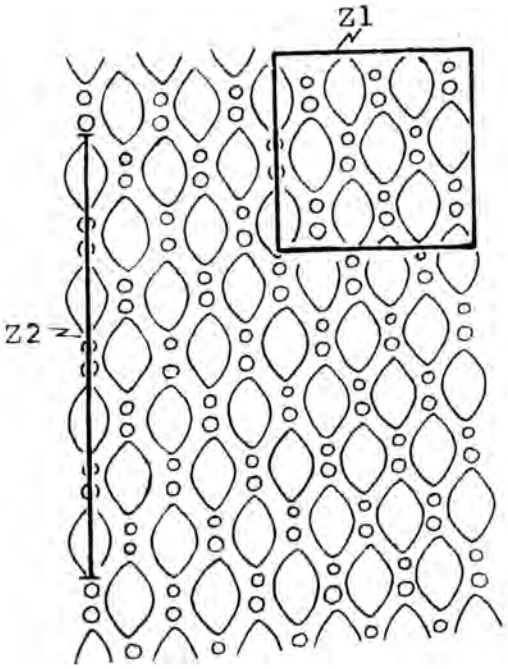
Z1
Z2

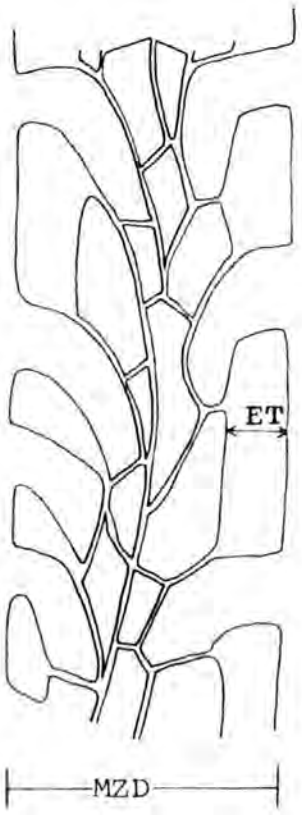
ET
MZD

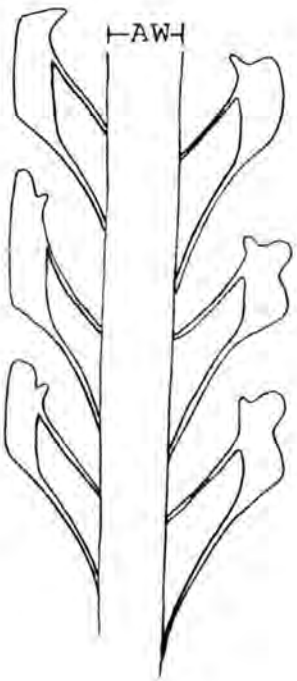
AW

Figure 8. Longitudinal section through the growth tip of a colony of Rhabdomeson showing the relationship between soft and skeletal tissues referred to in the text. (see p.69)

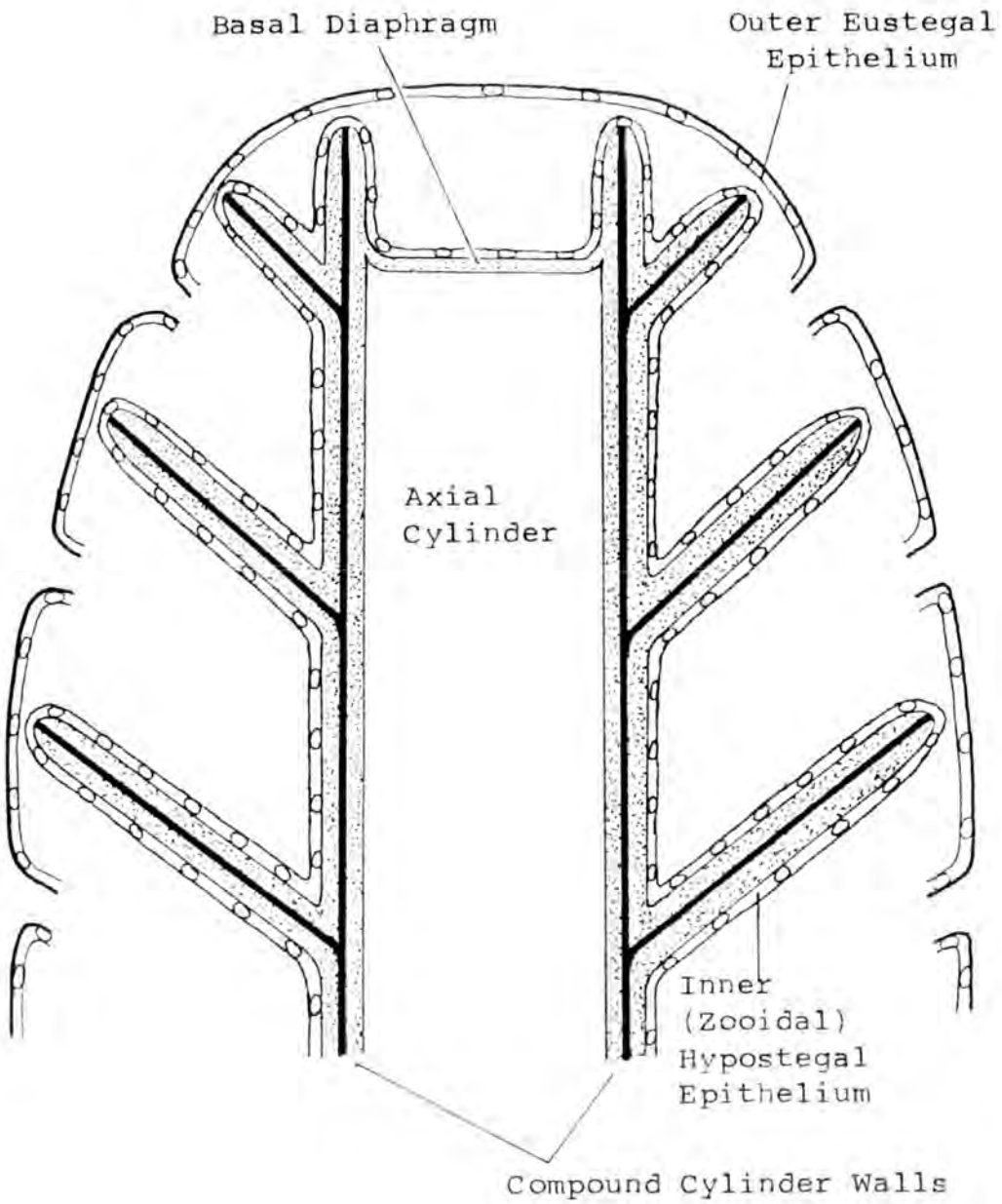
Basal Diaphragm
Outer Eustegal Epithelium
Axial Cylinder
Inner (Zooidal) Hypostegal Epithelium
Compound Cylinder Walls

Figure 9. Longitudinal section through a colony of Rhabdomeson rhombifera. The exozone wall of the parent branch was complete before the lateral branch had begun to develop. The illustration shows that a new axial cylinder was developed with the growth of a lateral branch and was unconnected to the axial cylinder of the parent branch. ABHR 234. Arnsbergian, shales above the Main Limestone, Hurst, N. Yorkshire. (Bar Scale=1mm)

Figure 10. Budding in Rhabdomeson gracilis (Phillips)

In longitudinal section beyond the axial cylinder

(a) Annular Budding: a marked bilateral symmetry is evident as autozooecia are budded in single alternate transverse planes about the axial cylinder.

(b) Spiral Budding: no bilateral symmetry is evident since autozooecia are budded in a low spire about the axial cylinder.

ABHR 212 and ABHR 214. Both Arnsbergian, shales above the Main Limestone, Hurst, N. Yorkshire.

(Bar Scale=1mm)

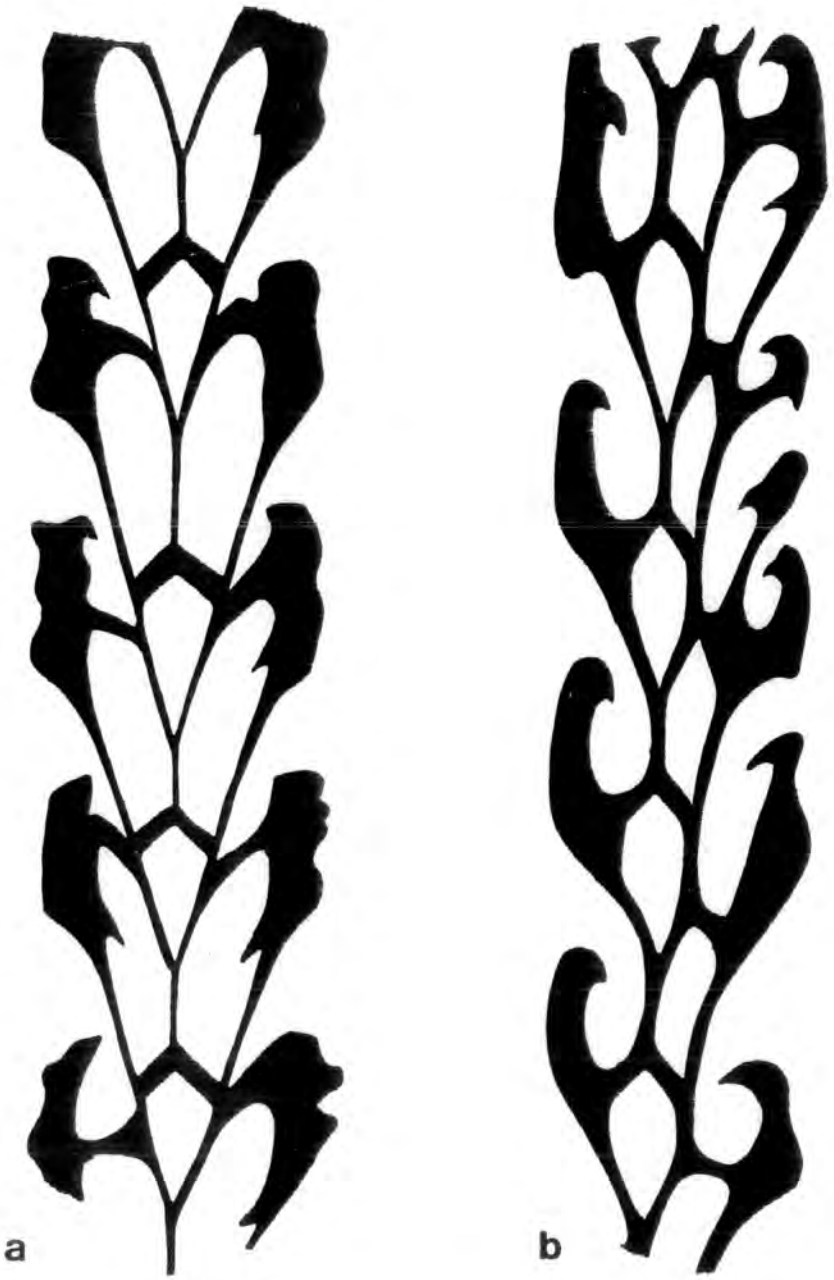
a
b

Figure 11. Budding in Rhabdomeson gracilis (Phillips)

In transverse section

(a) Annular Budding: successive tiers of alternately budded autozooecia are seen around the axial cylinder. Each tier is composed of zooecial tubes of uniform size and represent successive alternate transverse rows of budded autozooecia.

(b) Spiral Budding: no tiering is developed. The smallest tube lies adjacent to the axial cylinder, subsequent zooecia increase in size around the zoarium overlapping alternately with those adjacent to the axis spiraling outwards until the largest in a section opens onto the zoarial surface.

ABHR 209 and ABHR 207. Both Arnsbergian, shales above the Main Limestone, Hurst, N. Yorkshire. (Bar Scale=1mm)

q

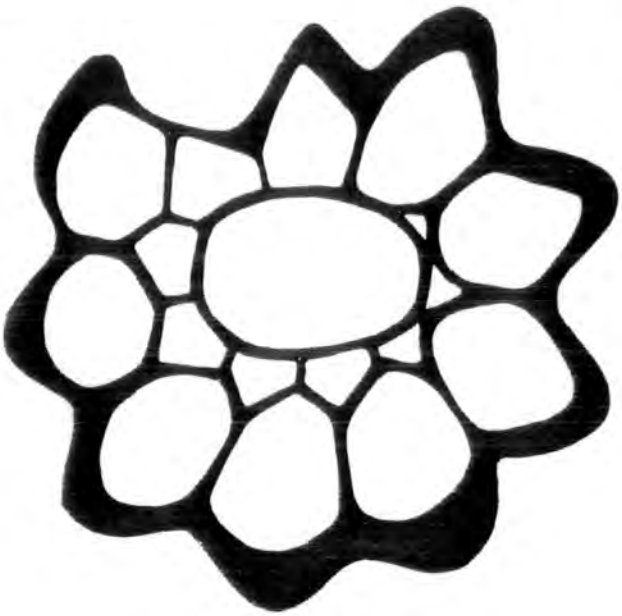

e

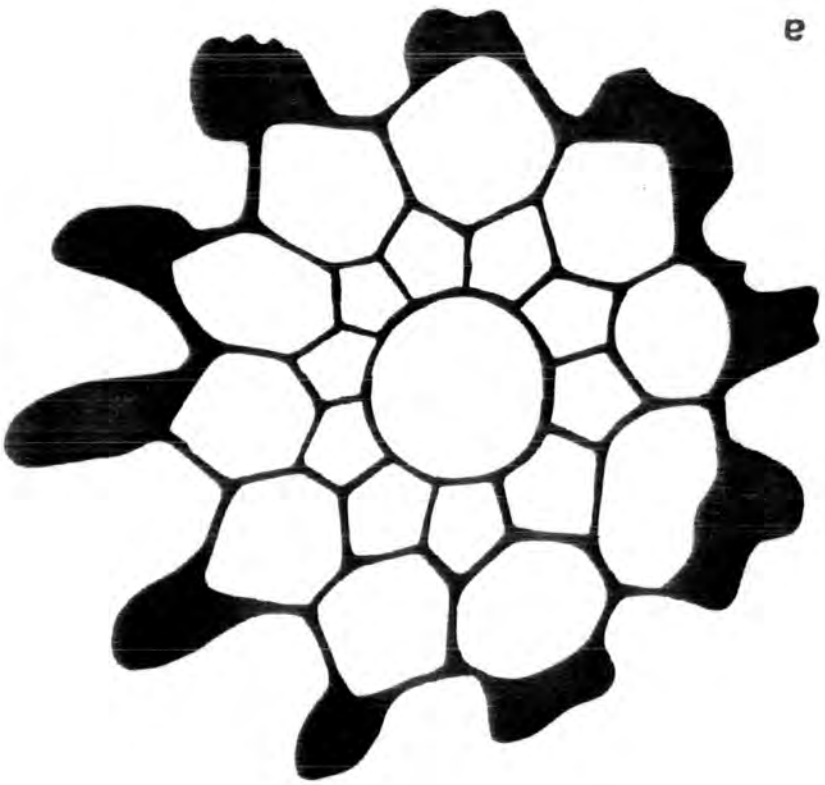

Figure 12. Rhabdomeson gracilis (Phillips)

Diagrams showing the variation in the morphology and distribution of stylets on the zoarial surface.

(a) A single large type A stylet is situated close to the distal extremity of each autozooecial aperture.

(b) Two stylets are situated along the median plane of interapertural walls. A single type A stylet is situated close to the distal extremety of each autozooecial aperture, and a single type B stylet is situated close to the proximal extremity of each aperture.

(c-e) A single large type A stylet is situated close to the distal extremity of each autozooecial aperture, and one or more type B or C stylets are situated distally to the type A stylet along the median plane of interapertural walls between apertures in the same longitudinal row.

(f) A single large type A stylet is situated close to the distal extremity of each autozooecial aperture and very small closely spaced type C stylets cover the interveining interapertural walls.

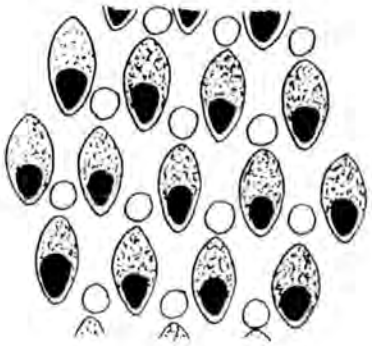

(a)

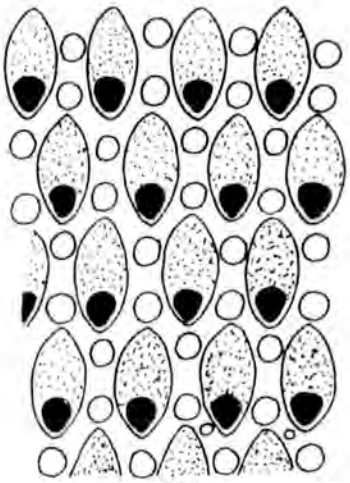

(b)

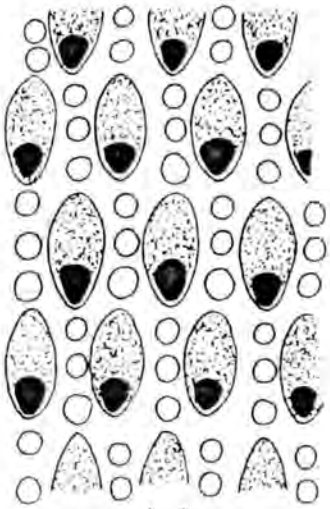

(c)

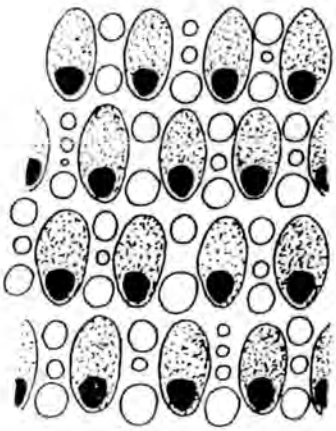

(d)

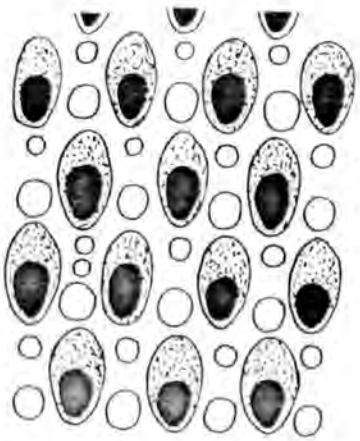

(e)

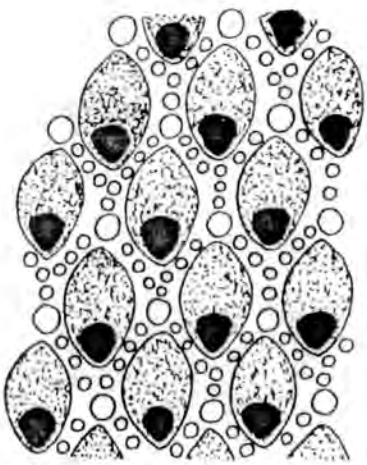

(f)

Figure 13. Rhabdomeson gracilis (Phillips)

Longitudinal section through the axial cylinder; also showing the prominent superior hemisepta, one being situated at the base of the exozone region in each autozooecial tube. HM D.103. Brigantian, Lower Limestone Group, Hosie Limestone, Hairmyres, E. Kilbride.

(Bar Scale=1mm)

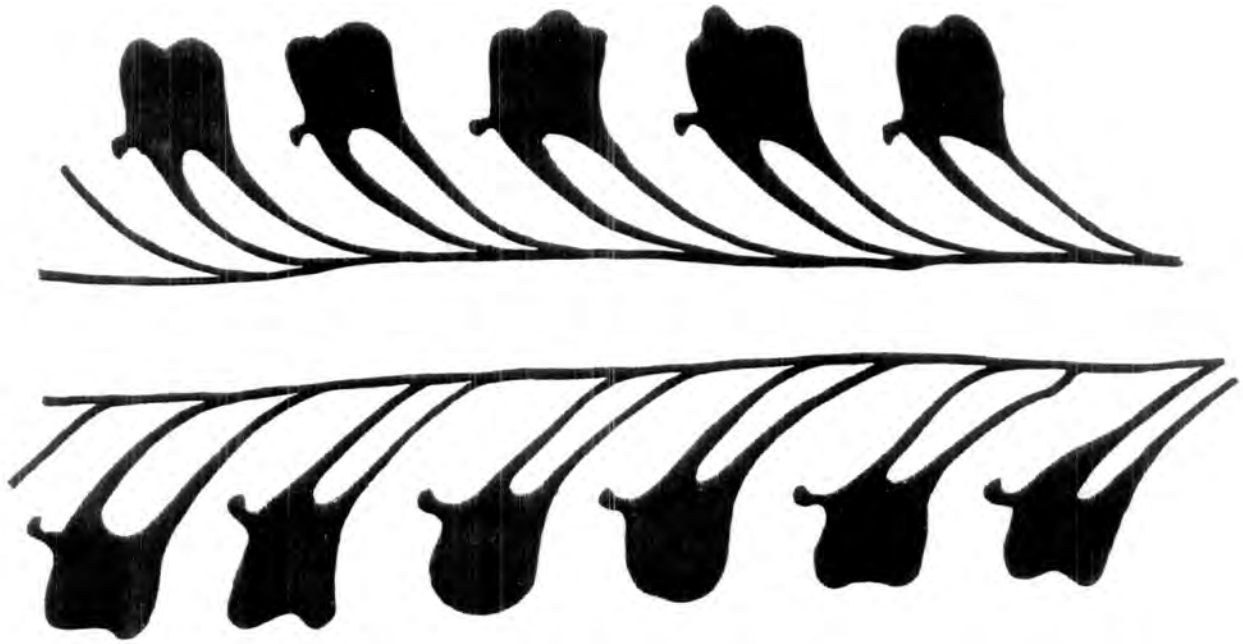

Figure 14. Rhabdomeson gracilis (Phillips)

Longitudinal section through the axial cylinder.
ABHR 205. Arnsbergian, shales above the Main Limestone, Hurst, N.Yorkshire.
(Bar Scale=1mm)

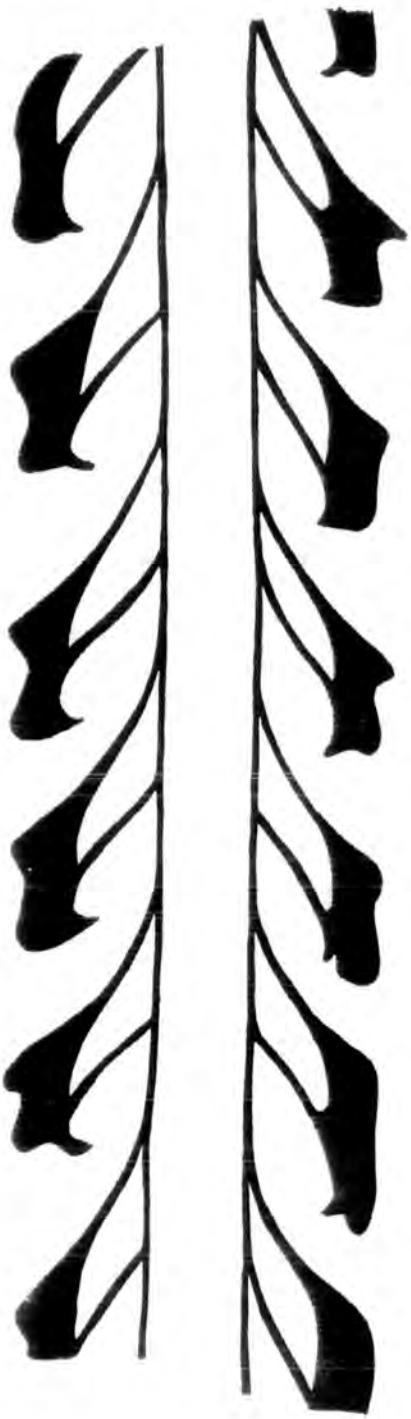

Figure 15. Rhabdomeson rhombifera (Phillips)

Zoarial surface detail showing the variation in apertural dimensions on opposite faces of a zoarium. HM D.108. Brigantian, Lower Limestone Group, Hosie Limestone, Hairmyres, E. Kilbride.

(Bar Scale=1mm)

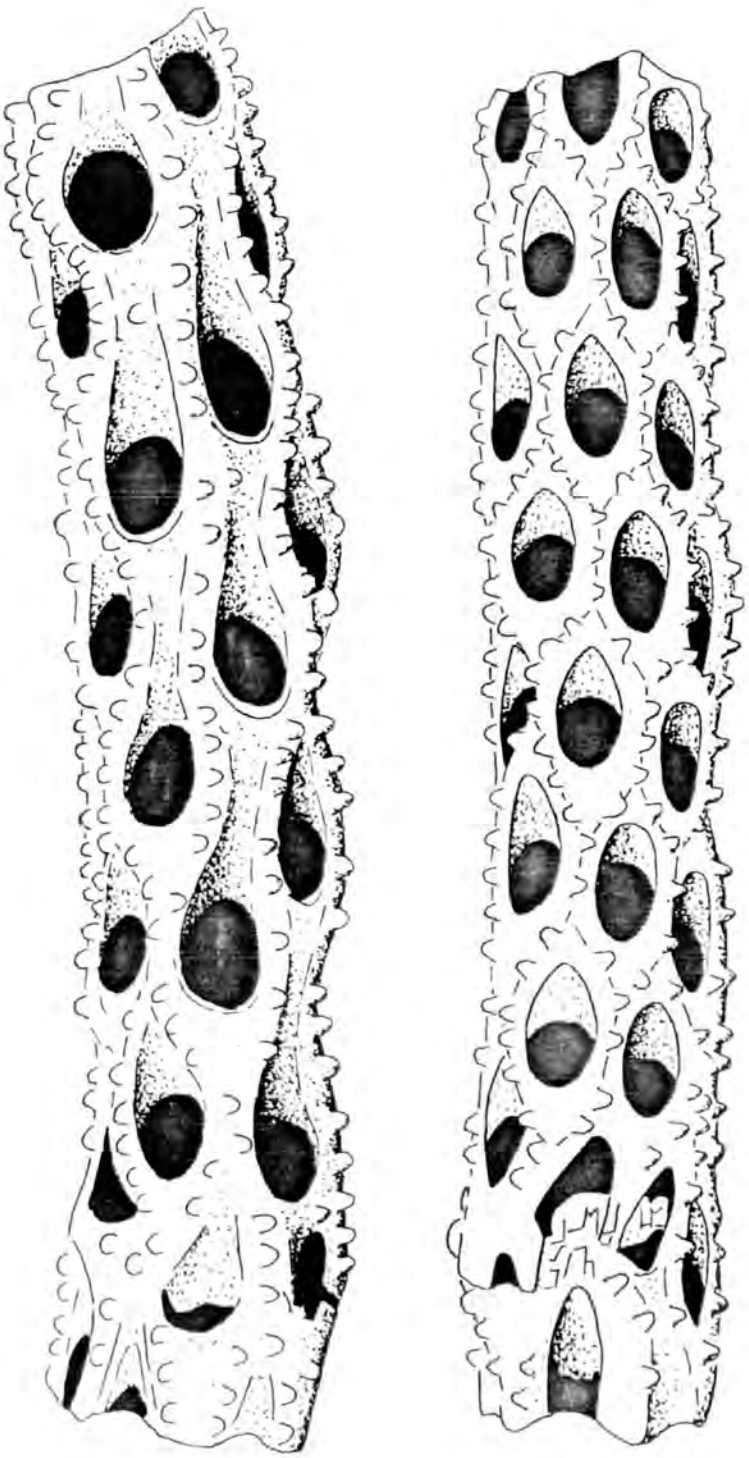

Figure 16. Rhabdomeson rhombifera (Phillips)

Graphical representation of the variation in Longitudinal Autozooecial Apertural Diameter (AD1) around a zoarium.

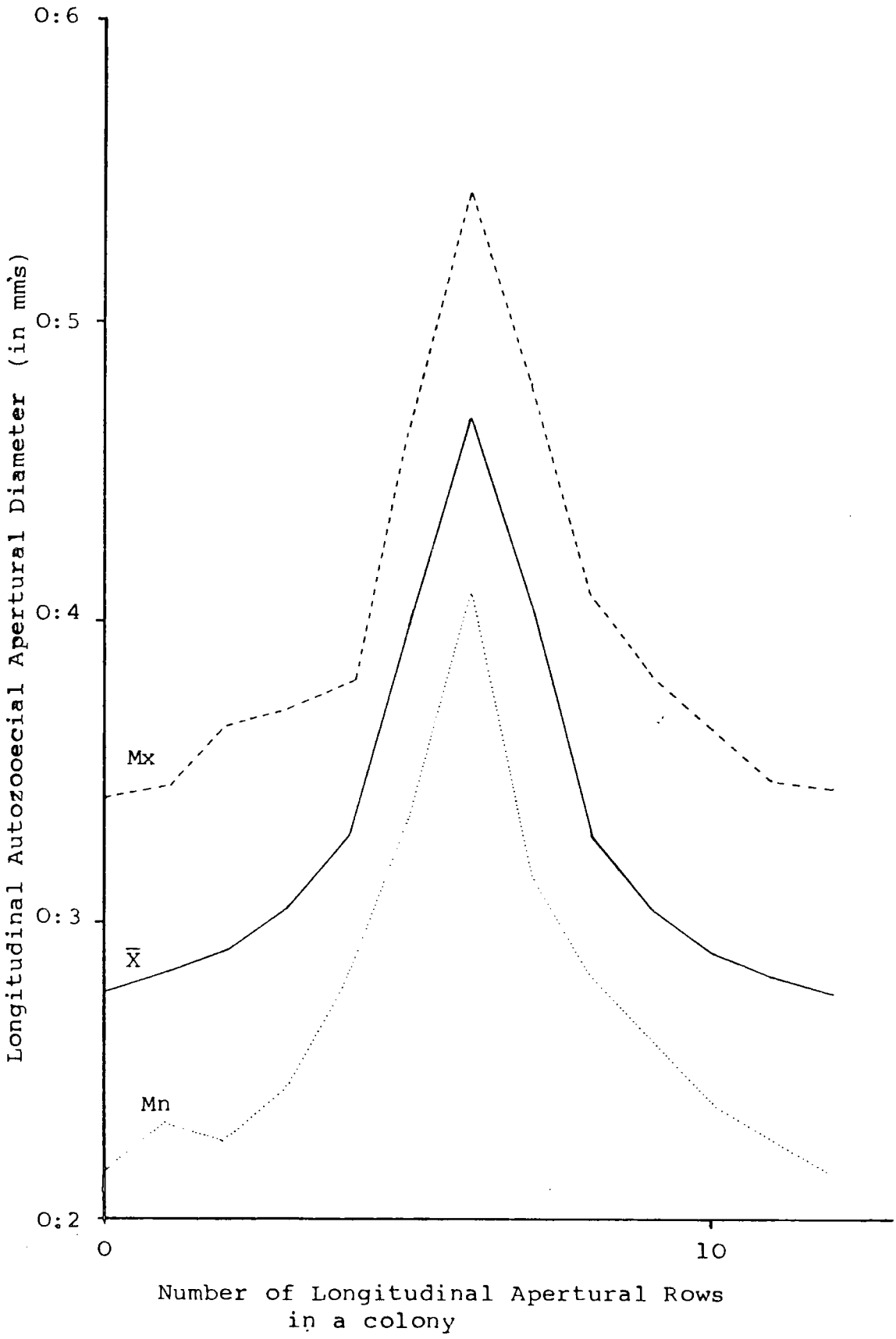
0:6
0:5
0:4
0:3
0:2
Longitudinal Autozooecial Apertural Diameter (in mms)
Mx
$\bar{X}$
Mn
0
10
Number of Longitudinal Apertural Rows
in a colony

Figure 17. Rhabdomeson rhombifera (Phillips)

Graphical representation of the variation in Transverse Autozooecial Apertural Diameter (AD2) around a zoarium.

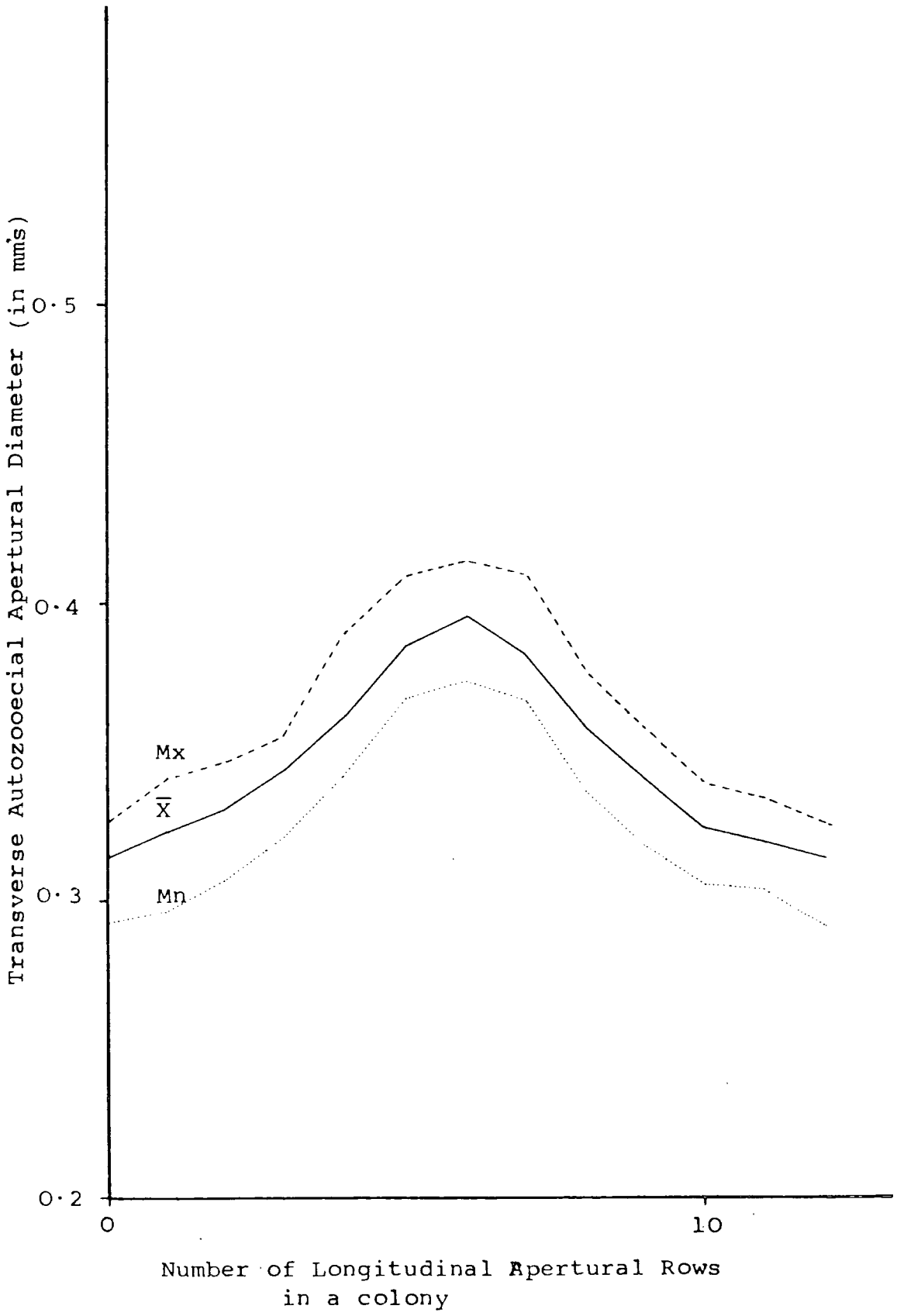
Transverse Autozooecial Apertural Diameter (in mms)
0·5
0·4
0·3
0·2
Mx
$\bar{X}$
Mn
0
10
Number of Longitudinal Apertural Rows in a colony

Figure 18. Rhabdomeson rhombifera (Phillips)

Graphical representation of the variation in Longitudinal Interapertural Wall Thickness (IWT1) around a zoarium.

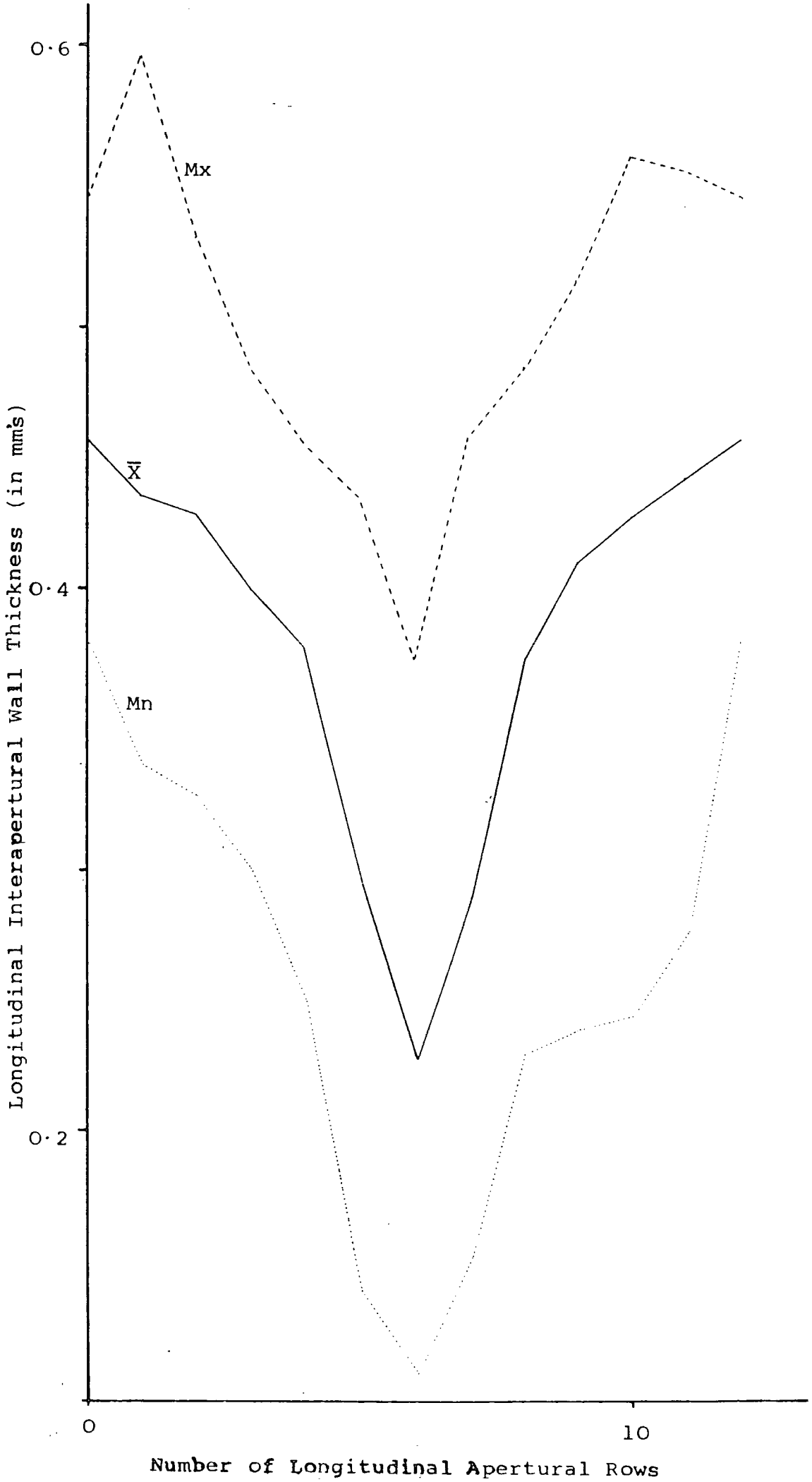
0·6
0·4
0·2
Mx
$\bar{X}$
Mn
Longitudinal Interapertural Wall Thickness (in mms)
0
10
Number of Longitudinal Apertural Rows

Figure 19. Rhabdomeson rhombifera (Phillips)

Graphical representation of the variation in Transverse Interapertural Wall Thickness (IWT2) around a zoarium.

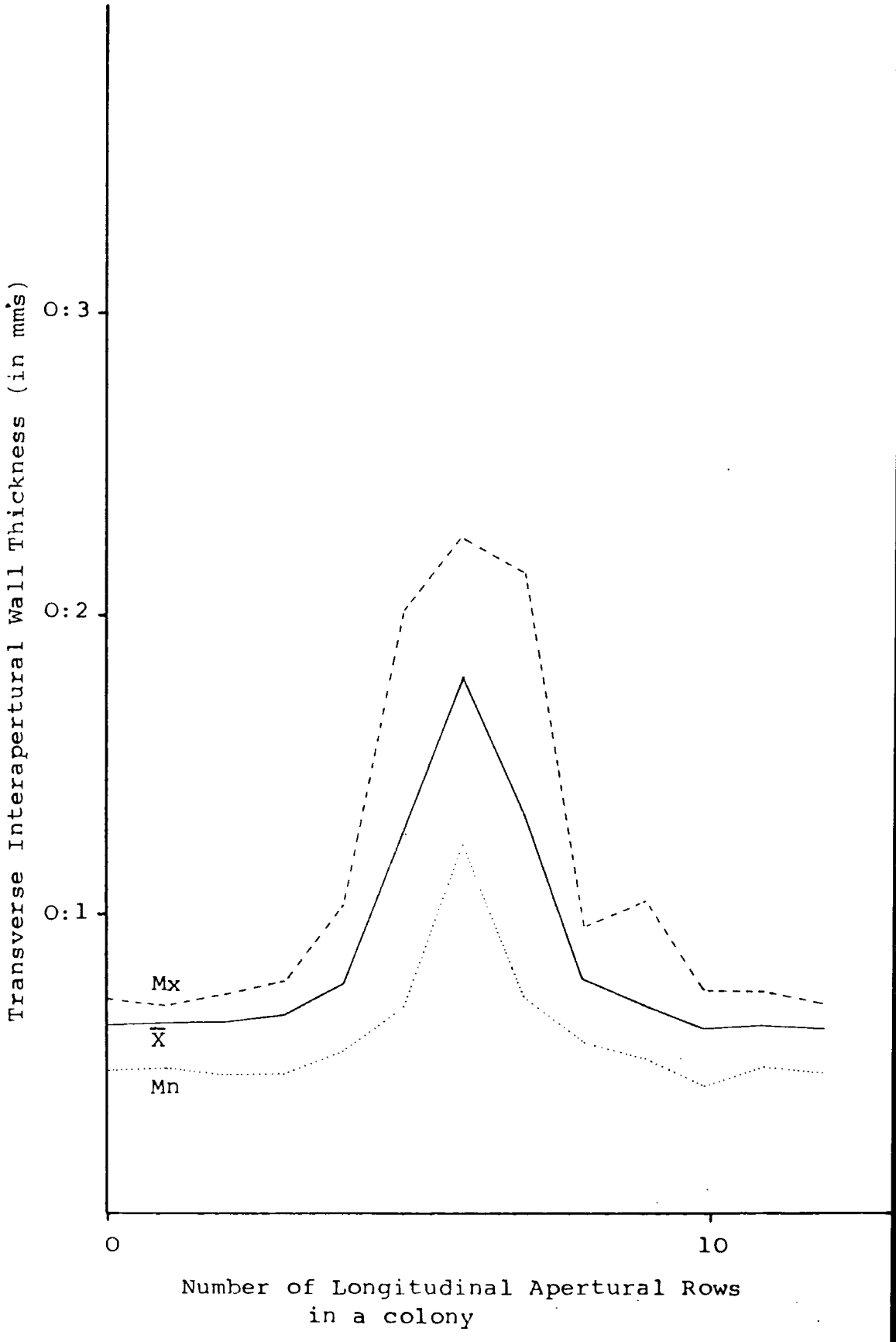
Transverse Interapertural Wall Thickness (in mms)
0:3
0:2
0:1
Mx
$\bar{X}$
Mn
0
10
Number of Longitudinal Apertural Rows
in a colony

Figure 20. Rhabdomeson rhombifera (Phillips)

Graphical representation of the variation in the number of stylets in a single row around autozooecial apertures in adjacent longitudinal rows in a colony.

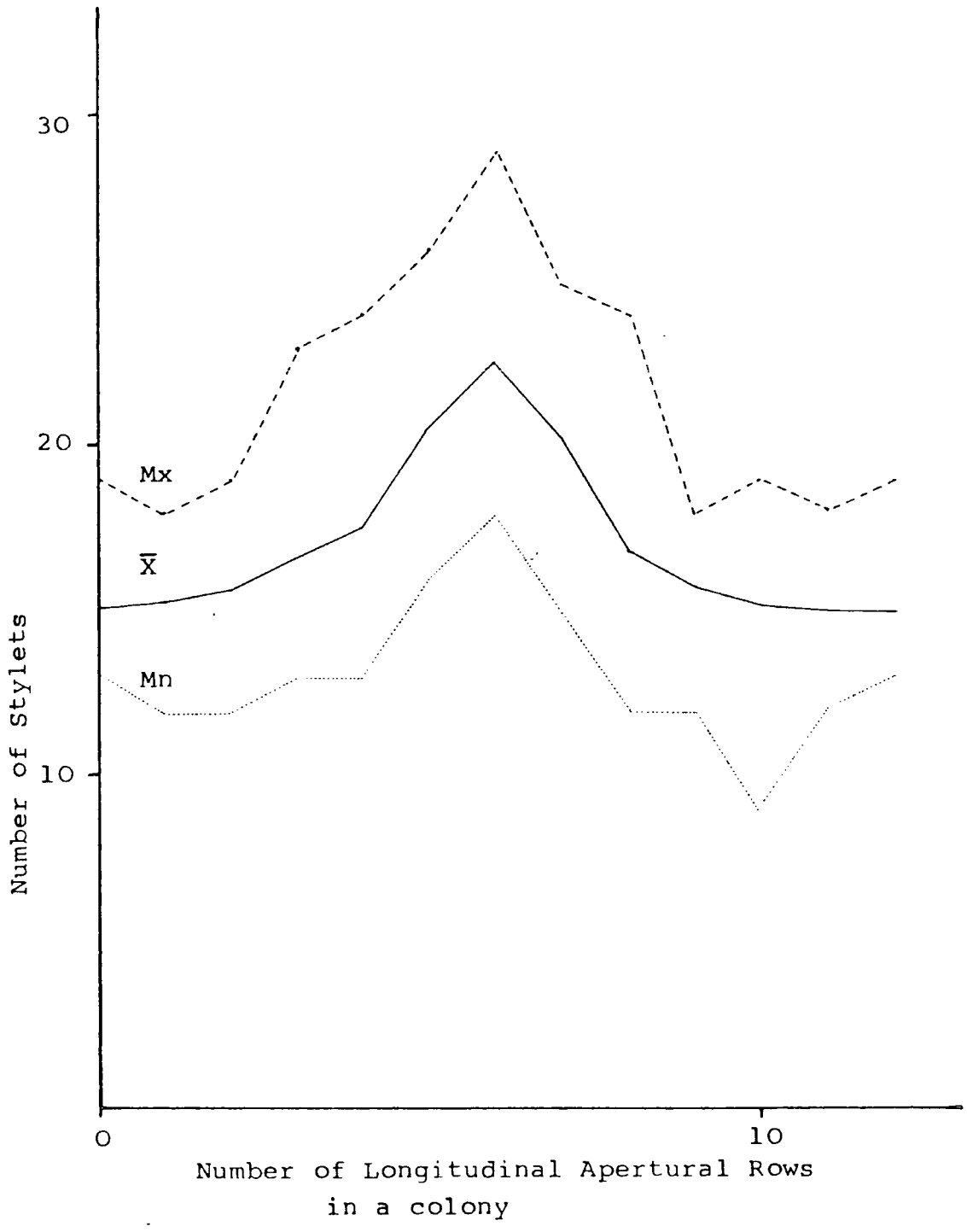
30
20
10
Mx
$\bar{X}$
Mn
Number of Stylets
0
10
Number of Longitudinal Apertural Rows
in a colony

Figure 21. Rhabdomeson rhombifera (Phillips)

Transverse section. ABHR 232. Arnsbergian, shales above the Main Limestone, Hurst, N. Yorkshire. (Bar Scale=1mm)

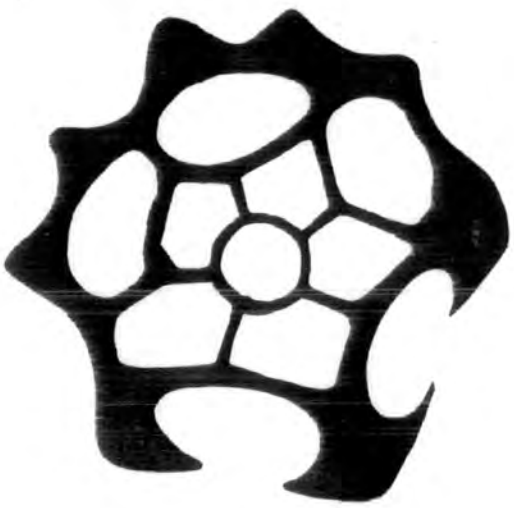

Figure 22. Rhabdomeson rhombifera (Phillips)

Longitudinal sections through the axial cylinder showing the variation in the angle of divergence of autozooecia on opposite sides of the cylinder in two colony fragments. On the left hand side of the cylinder on both specimens there is a gradual increase in the angle of divergence of the distal walls of autozooecia compared to a gradual decrease in the angle of divergence in the distal walls on the right hand side. Consequently apertural dimensions are much larger on the right hand side. ABHR 227 and 229. Both Arnsbergian, shales above the Main Limestone, Hurst, N. Yorkshire. (Bar Scale=1mm)

Figure 23. Rhombopora similis (Phillips)

Transverse section. ABHR 245 and ABHR 244. Both Arnsbergian, shales above the Main Limestone, Hurst, N. Yorkshire.

(Bar Scale=1mm)

Figure 24. Rhombopora similis (Phillips)

Longitudinal section. ABHR 238. Arnsbergian, shales above the Main Limestone, Hurst, N. Yorkshire.
(Bar Scale=1mm)

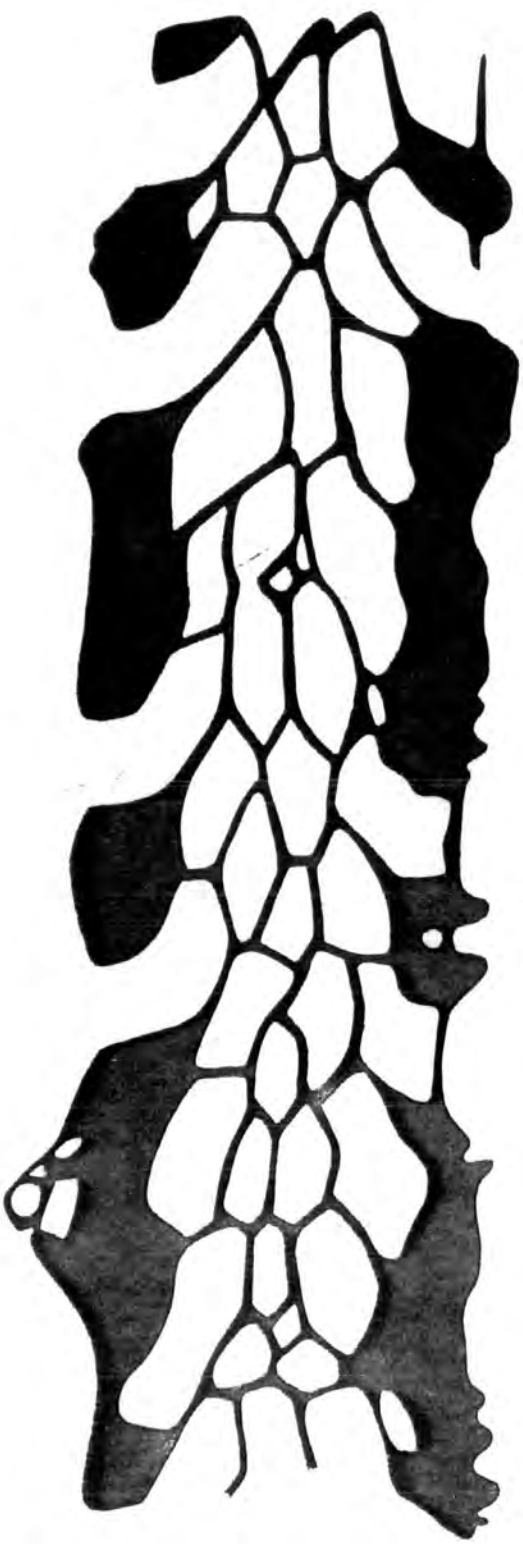

Figure 25. Rhombopora similis(Phillips)

Longitudinal section. ABHR 239. Arnsbergian, shales above the Main Limestone, Hurst, N. Yorkshire.
(Bar Scale=1mm)

Figure 26. Skeletal Structure of Fenestrate Bryozoa

Tangential section. The autozooecial chambers adjacent to the dissepiment are slightly distorted.

TANGENTIAL SECTION

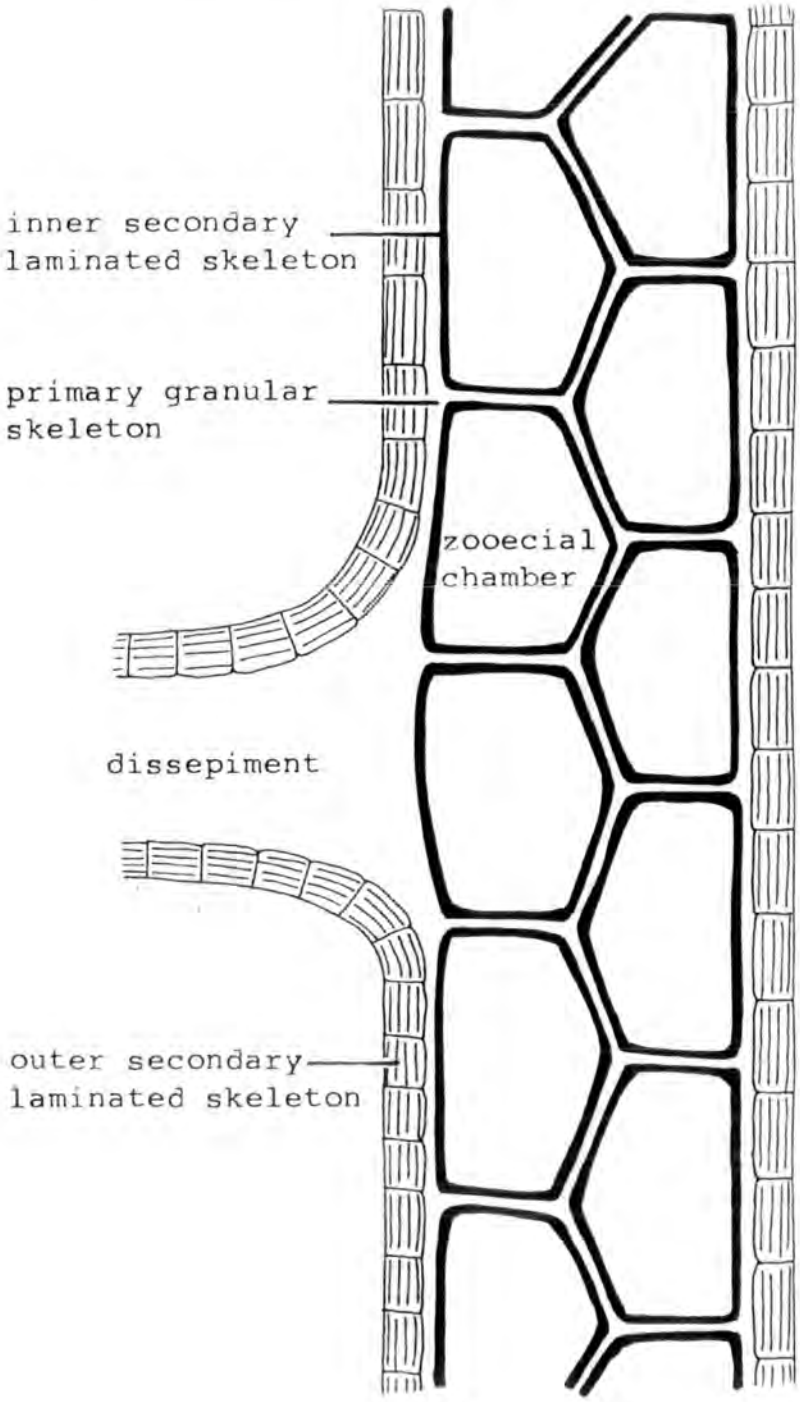

Figure 27. Skeletal Structure of Fenestrate Bryozoa

(a) Longitudinal section.

(b) Transverse section.

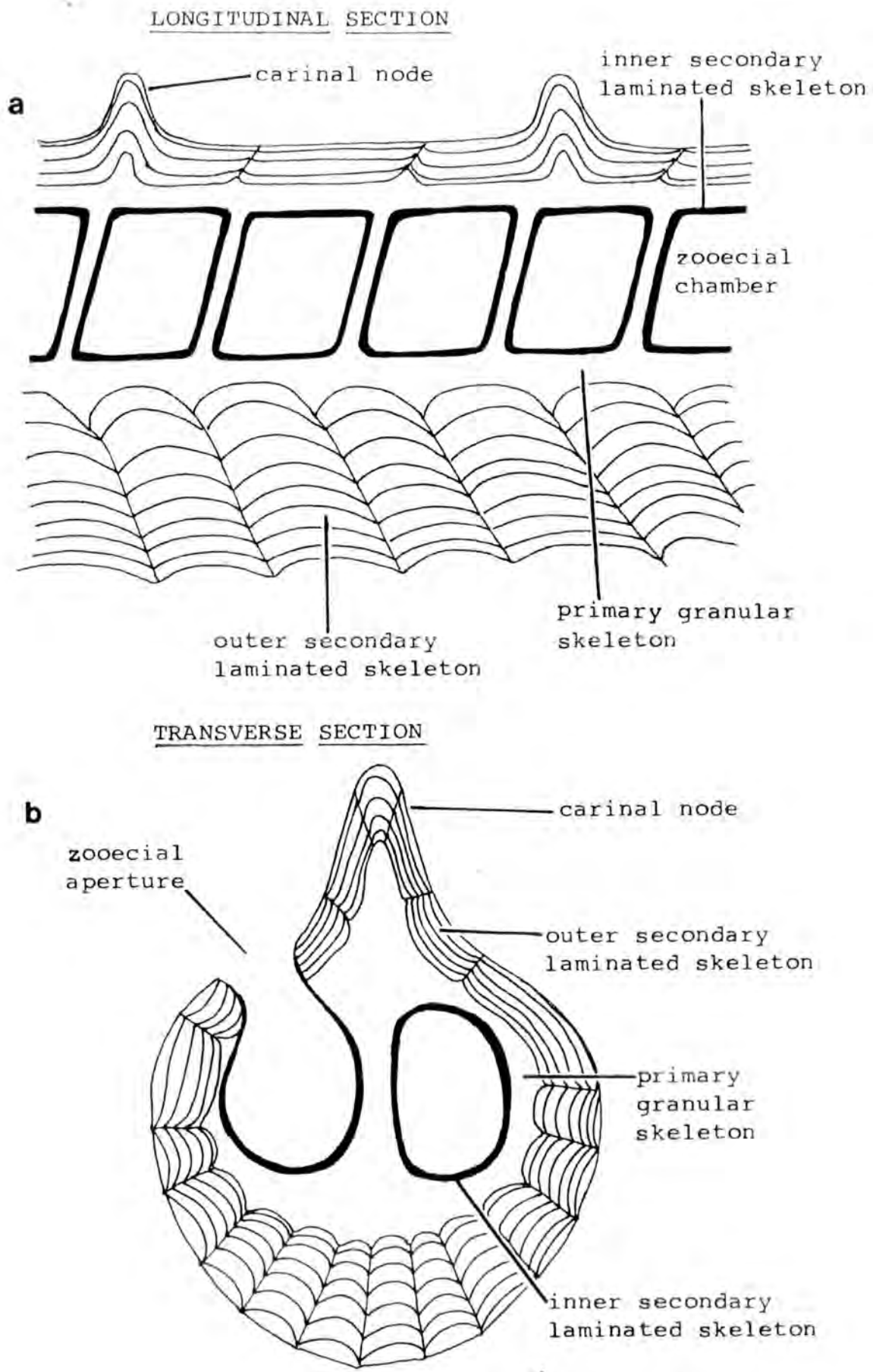
LONGITUDINAL SECTION
a
carinal node
inner secondary
laminated skeleton
zooecial
chamber
primary granular
skeleton
outer secondary
laminated skeleton
TRANSVERSE SECTION
b
carinal node
zooecial
aperture
outer secondary
laminated skeleton
primary
granular
skeleton
inner secondary
laminated skeleton

Figure 28. Skeletal Growth of Fenestrate Bryozoa

Longitudinal section showing the operation of the 'conveyor belt' principle in skeletal formation.

(see text pp.119-120.)

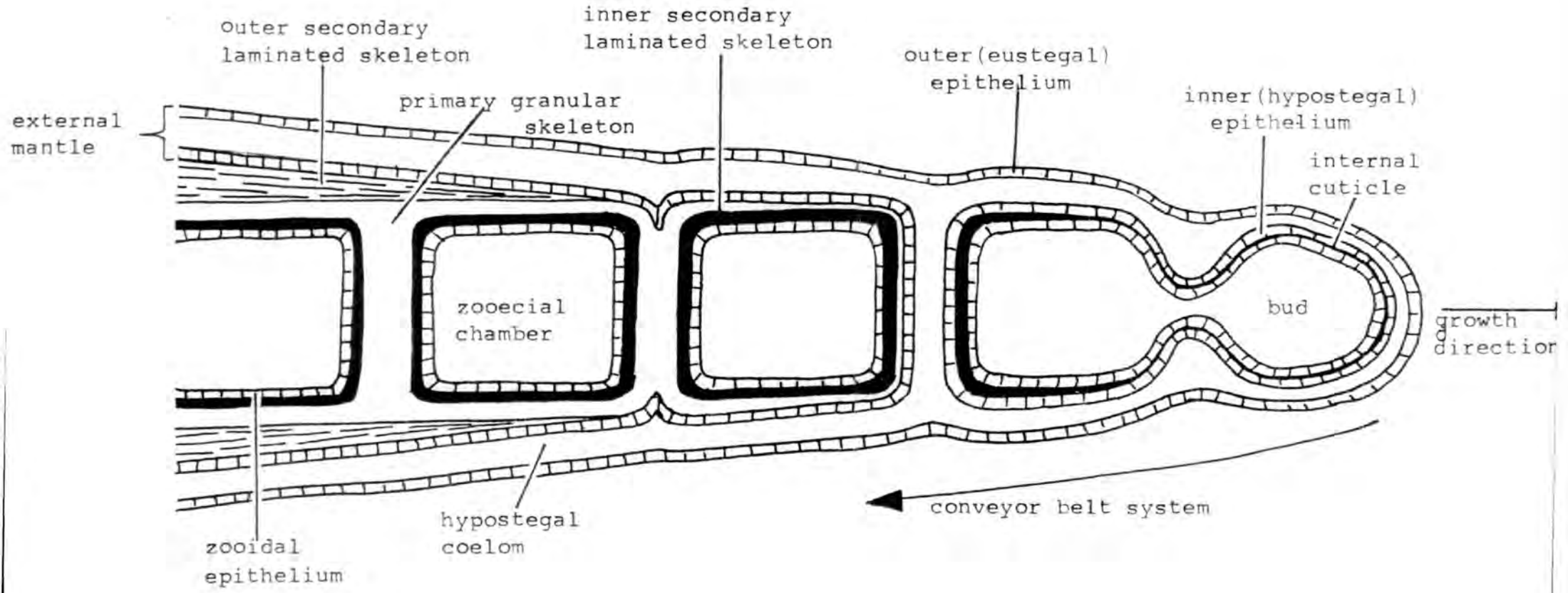
Outer secondary
laminated skeleton
inner secondary
laminated skeleton
outer(eustegal)
epithelium
inner(hypostegal)
epithelium
internal
cuticle
primary granular
skeleton
external
mantle
zooecial
chamber
bud
growth
direction
conveyor belt system
hypostegal
coelom
zooidal
epithelium

Figure 29. Diagram to show the three orientated sections utilised in the description of internal morphological details of fenestrates in the present study.

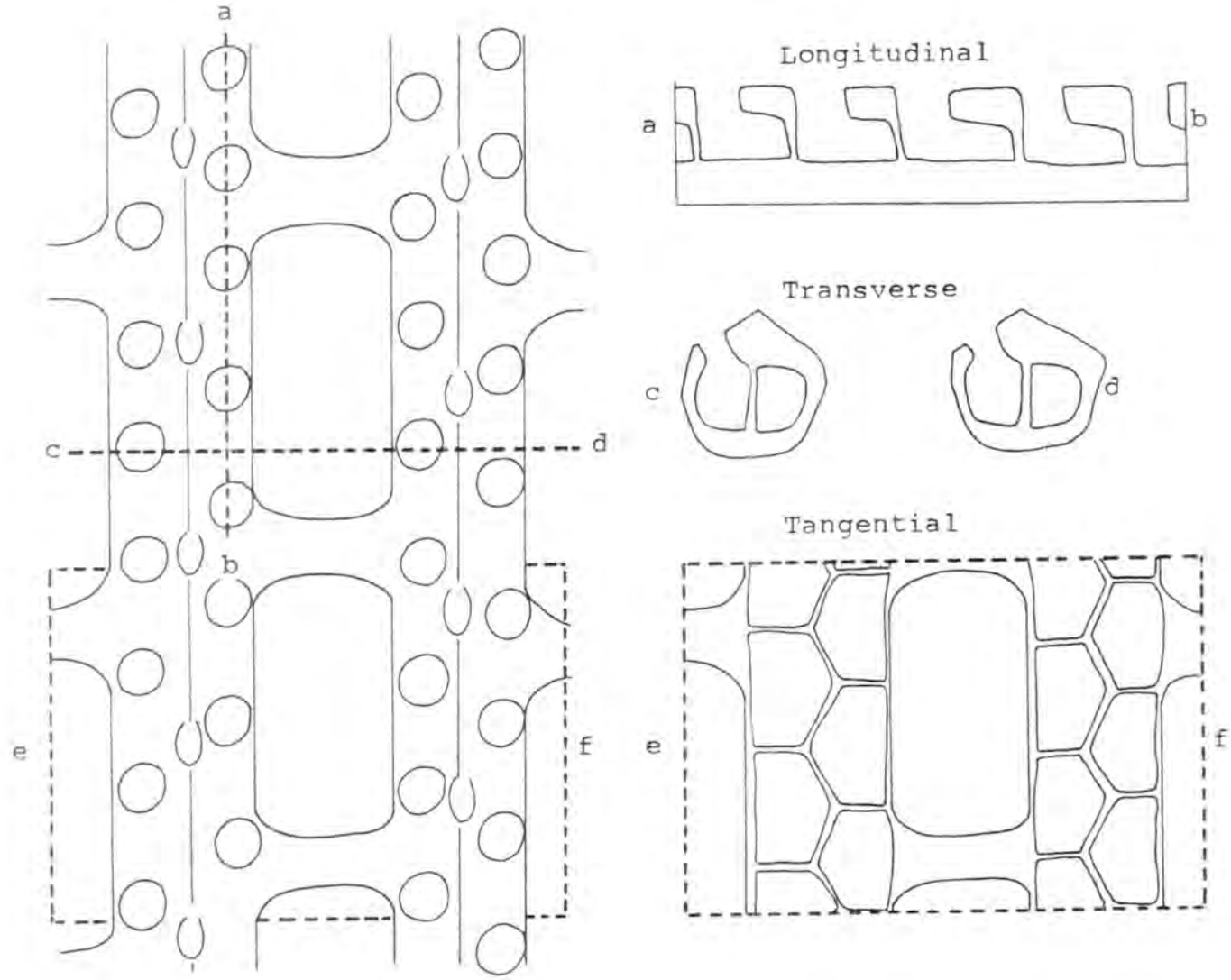
a
b
c
d
e
f
Longitudinal
a
b
Transverse
c
d
Tangential
e
f

Figure 30. Diagram to show the morphological characters measured on fenestellid and polyporid fenestrates in the present study. (For explanation of characters see text pp. 138-140)

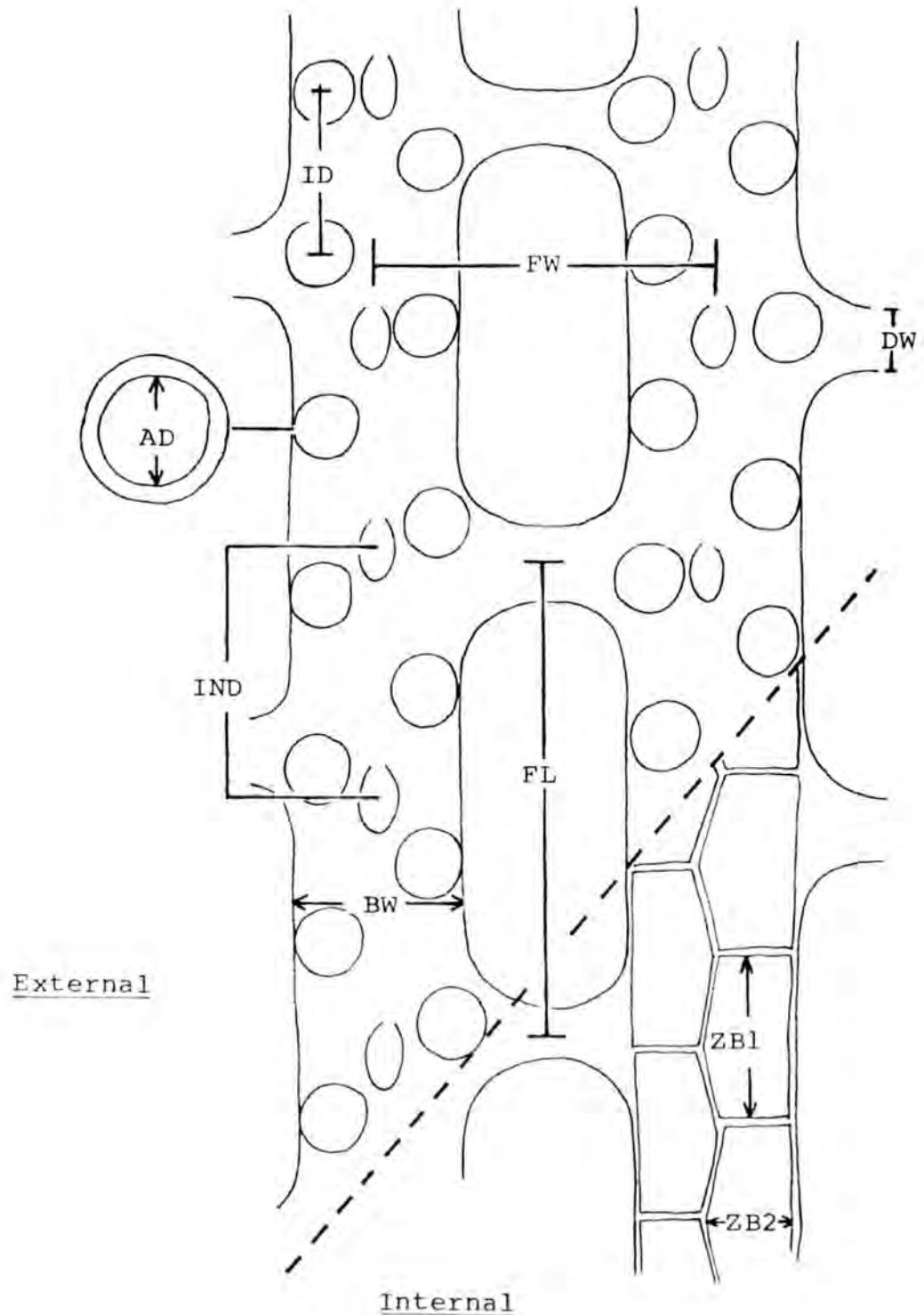
ID
FW
DW
AD
IND
FL
BW
ZB1
ZB2
External
Internal

Figure 31. Fenestella bicellulata Etheridge, Jun.

Obverse surface detail. ABP 143. Asbian, Alston Group, Fifth Limestone, Penruddock, N^{r} Penrith, Cumbria.

(Bar Scale=1mm)

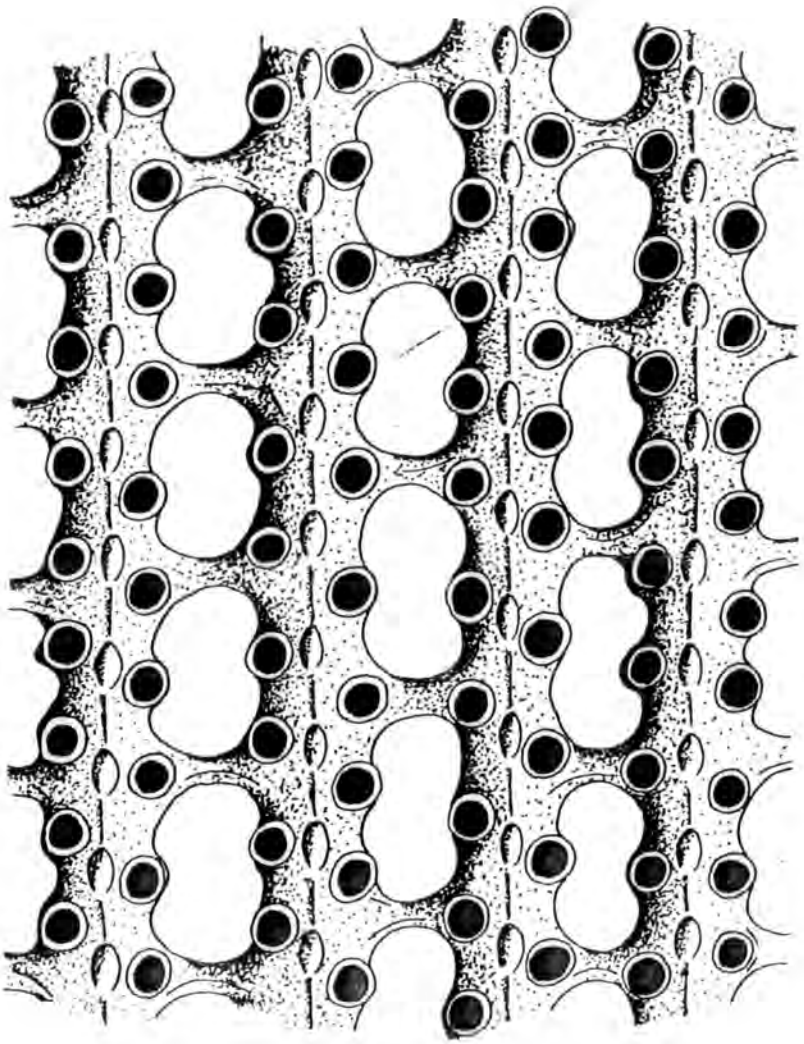

Figure 32. Fenestella bicellulata Etheridge, Jun.

Obverse surface detail. ABP 157. Asbian, Alston Group, Fifth Limestone, Penruddock, Nr Penrith, Cumbria.

(Bar Scale=1mm)

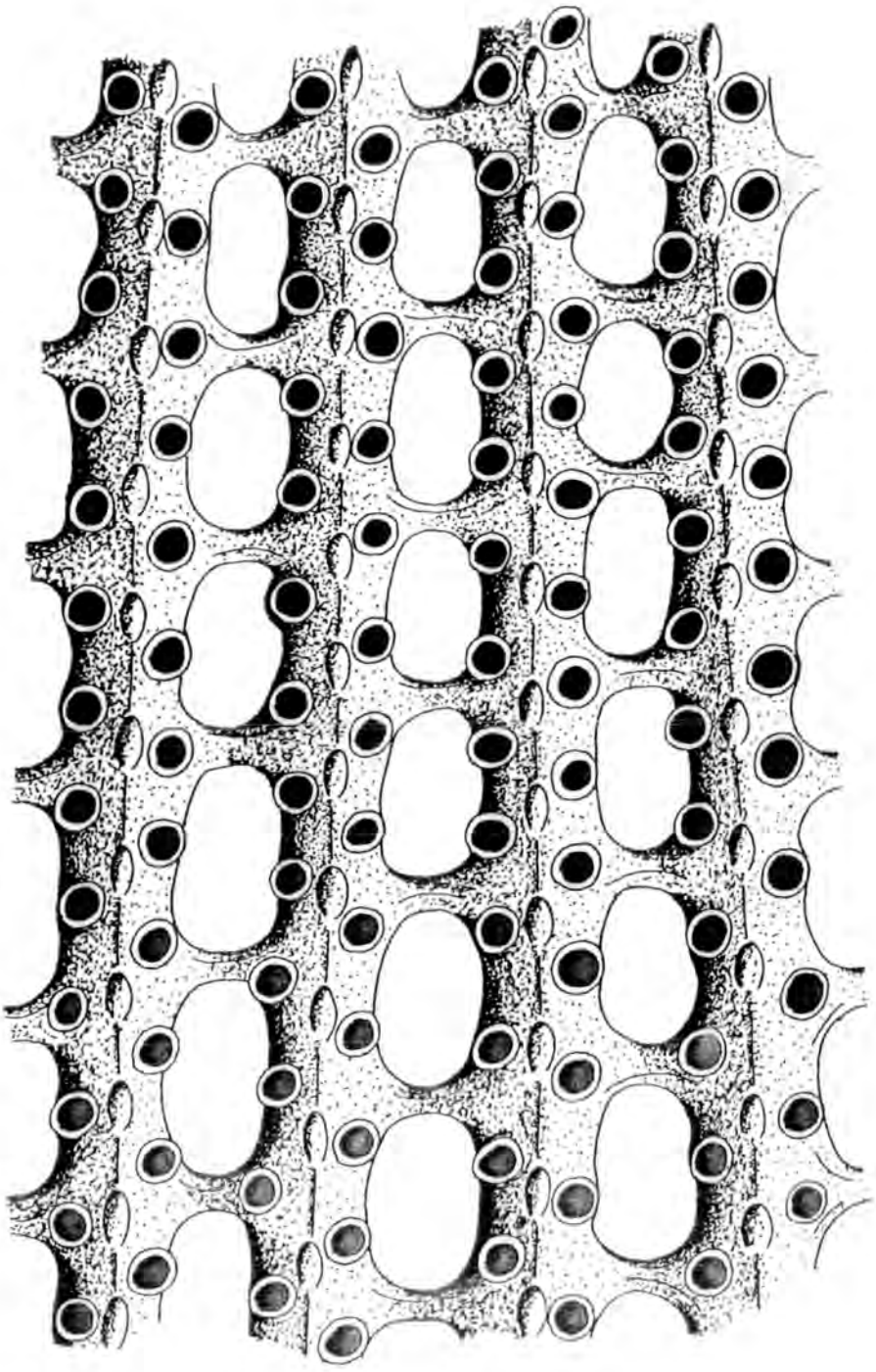

Figure 33. Fenestella bicellulata Etheridge, Jun.

Reverse surface detail. ABP 133. Asbian, Alston Group, Fifth Limestone, Penruddock, N^{r} Penrith, Cumbria.

(Bar Scale=1mm)

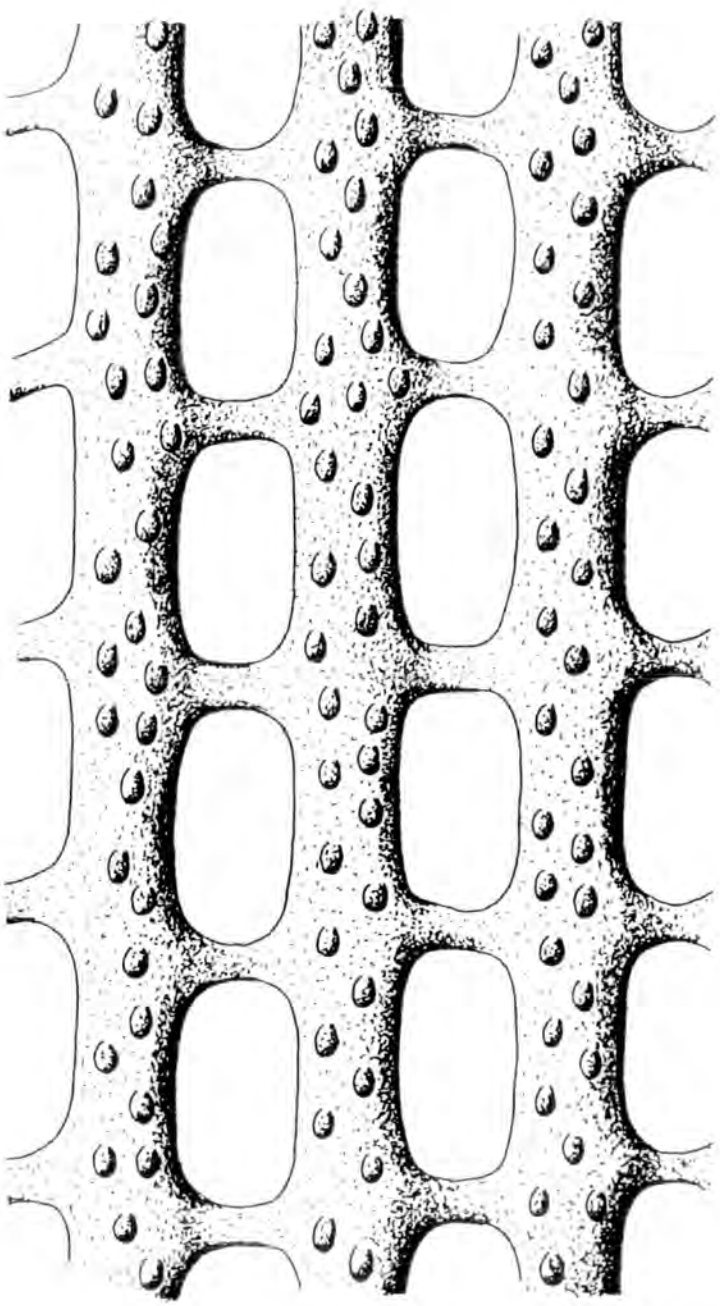

Figure 34. Fenestella ivanovi Shulga-Nesterenko

Obverse surface detail; also showing the hour-glass shape of fenestrules. ABCL 16. Asbian, Calp Shale-Upper Limestone, Carrick Lough.

(Bar Scale=1mm)

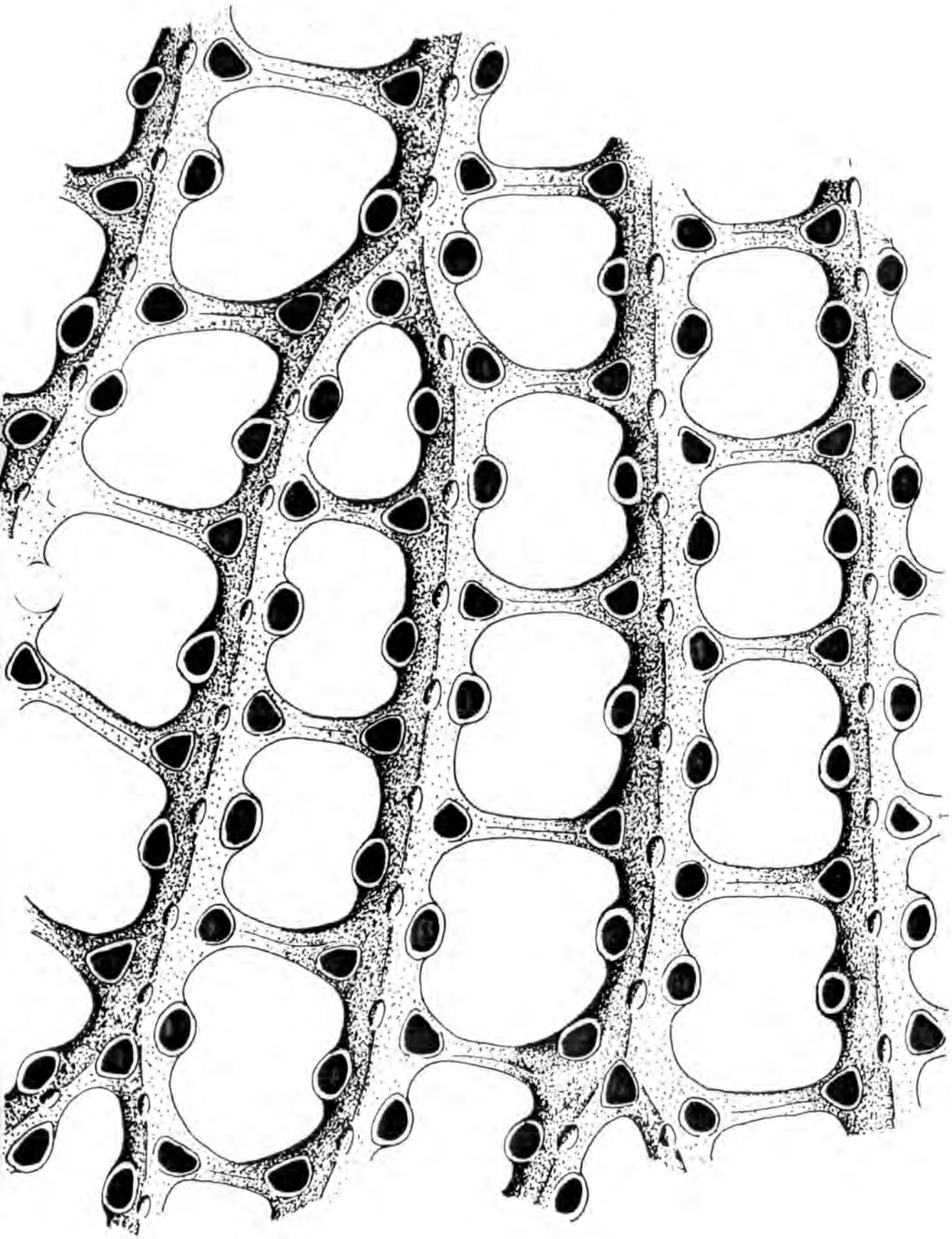

Figure 35. Fenestella ivanovi Shulga-Nesterenko

(a) Obverse surface detail- also showing some poorly preserved denticulated autozooecial apertures. ABHR 19. Arnsbergian, shales above the Main Limestone, Hurst, N. Yorkshire.
(Bar Scale=1mm)

(b) Detail of a denticulated autozooecial aperture and its pustulose peristome.
(Bar Scale=0.1mm)

a

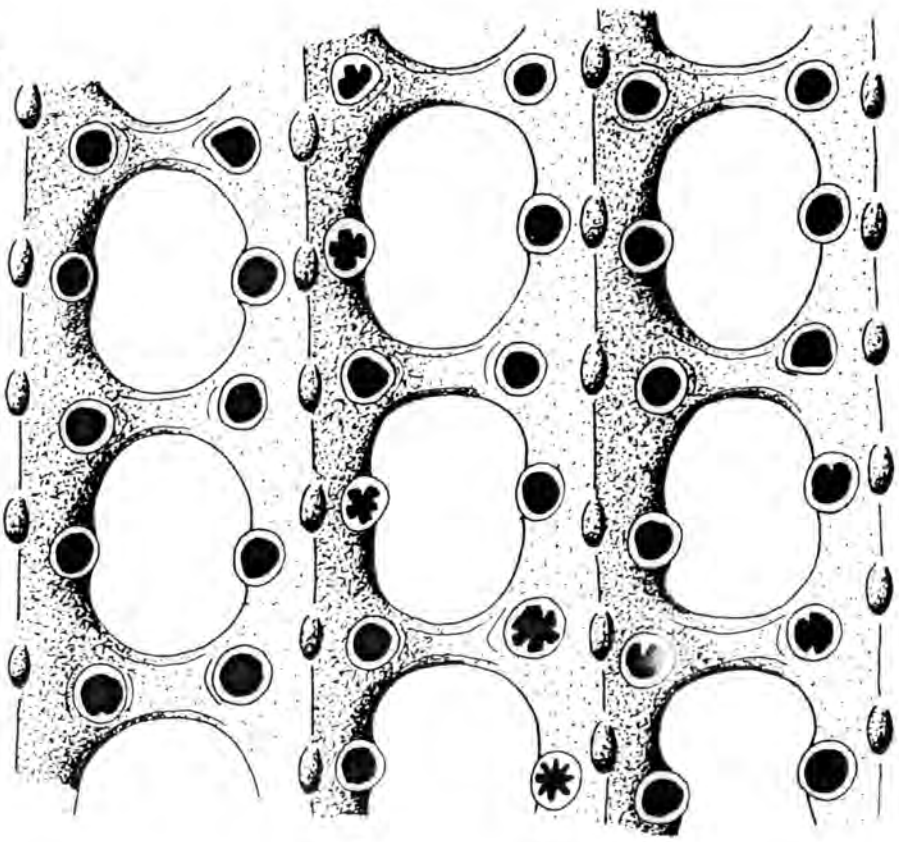

b

Figure 36. Fenestella frutex McCoy

Obverse surface detail. NH G.155.63-2. Asbian, Lower Limestone Group, Redesdale Ironstone Shale, Ridsdale, Northumberland.

(Bar Scale=1mm)

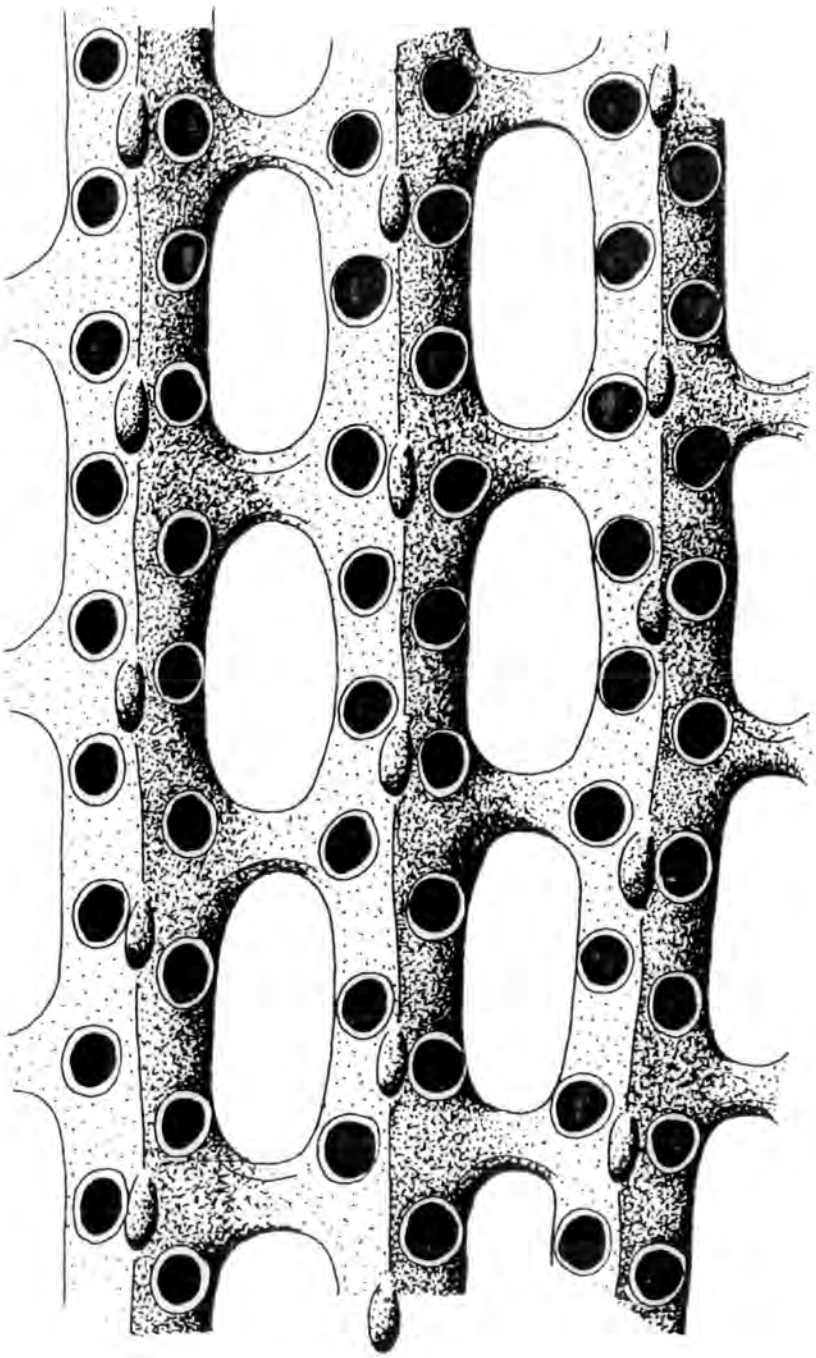

Figure 37. Fenestella frutex McCoy

Obverse surface detail. ABP 159. Asbian, Alston Group, Fifth Limestone, Penruddock, Nr Penrith,, Cumbria.

(Bar Scale=1mm)

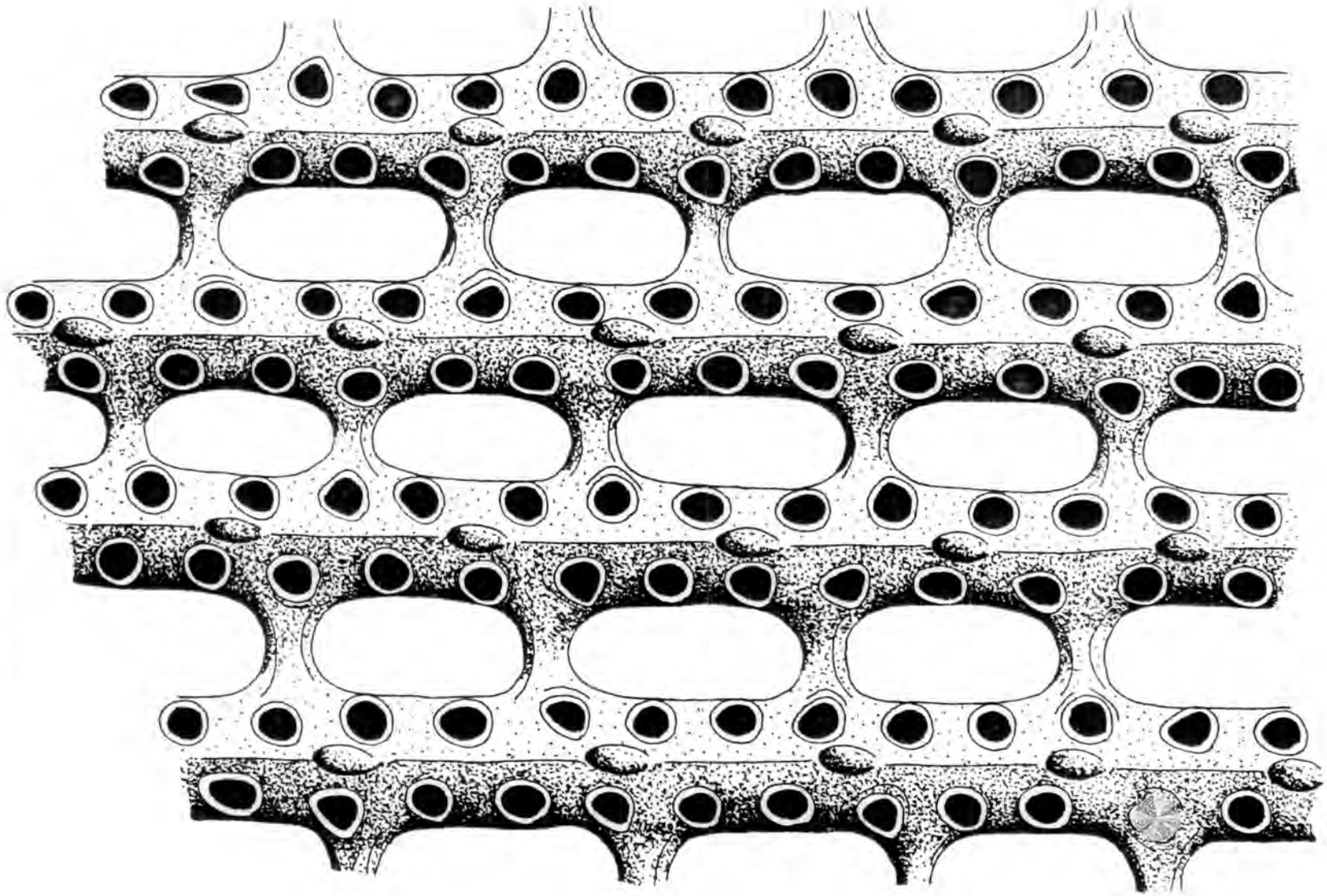

Figure 38. Fenestella frutex McCoy

Reverse surface detail. ABP 175. Asbian, Alston Group, Penruddock, Nr Penrith, Cumbria.
(Bar Scale=1mm)

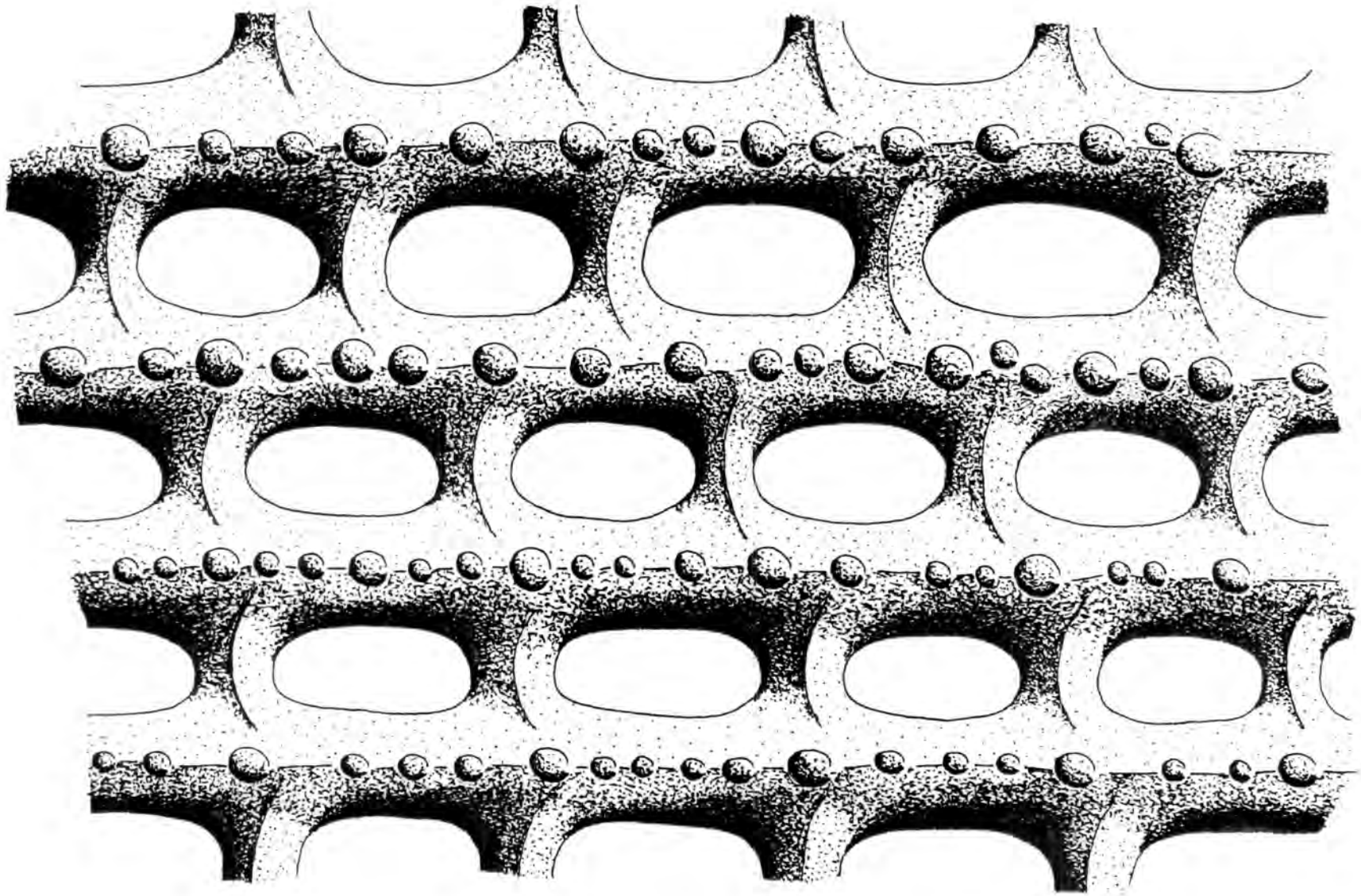

Figure 39. Fenestella frutex McCoy

Reverse surface detail. ABP 184. Asbian, Alston Group, Fifth Limestone, Penruddock, N^{r} Penrith, Cumbria.

(Bar Scale=1mm)

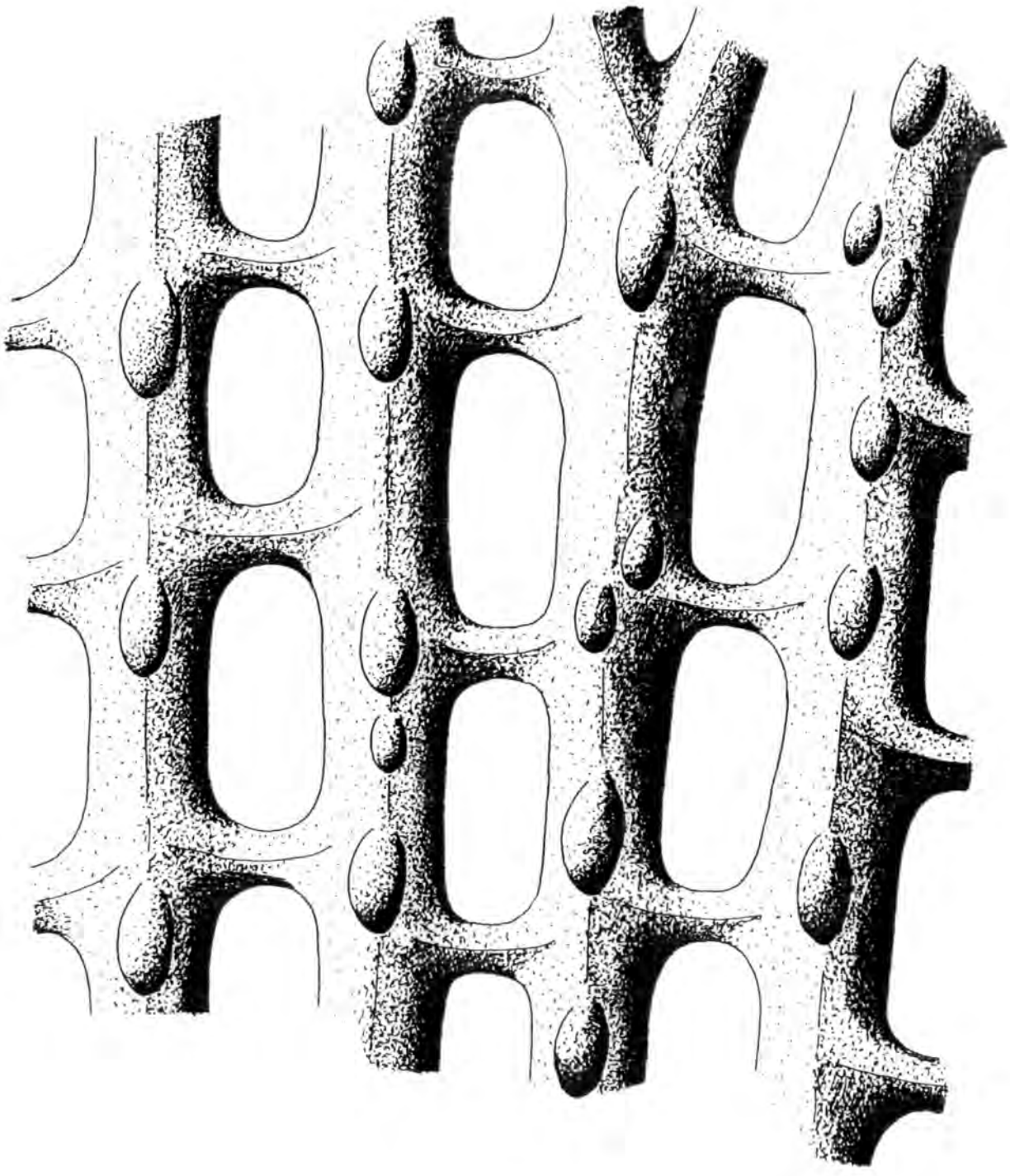

Figure 40. Fenestella multispinosa Ulrich

Obverse surface detail. ABHR 10. Arnsbergian, shales above the Main Limestone, Hurst, N. Yorkshire.
(Bar Scale=1mm)

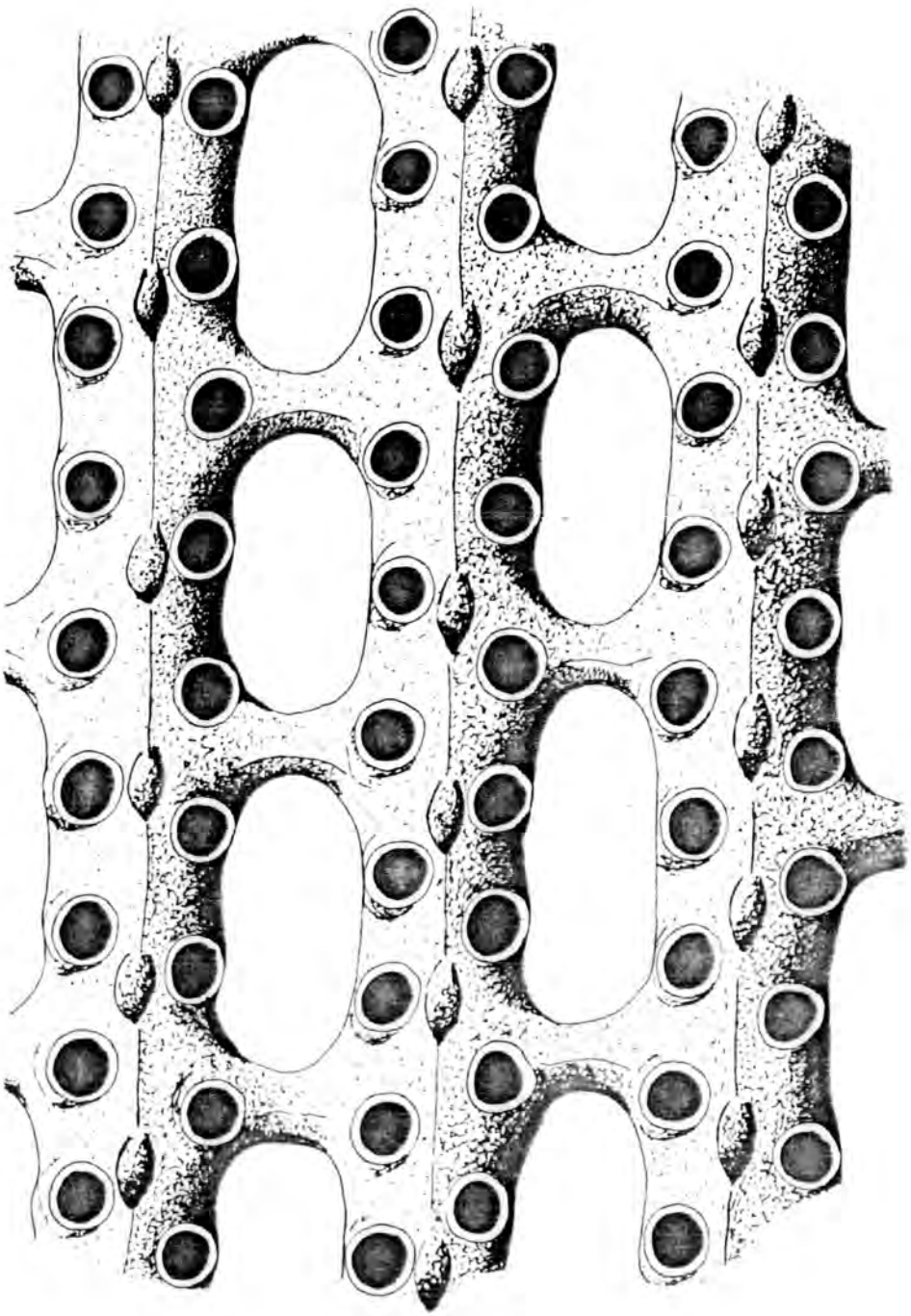

Figure 41. Fenestella tuberculo-carinata Etheridge, Jun.

Obverse surface detail. HM D44-1. Brigantian. Lower Limestone Group, Roughwood, Beith.

(Bar Scale-1mm)

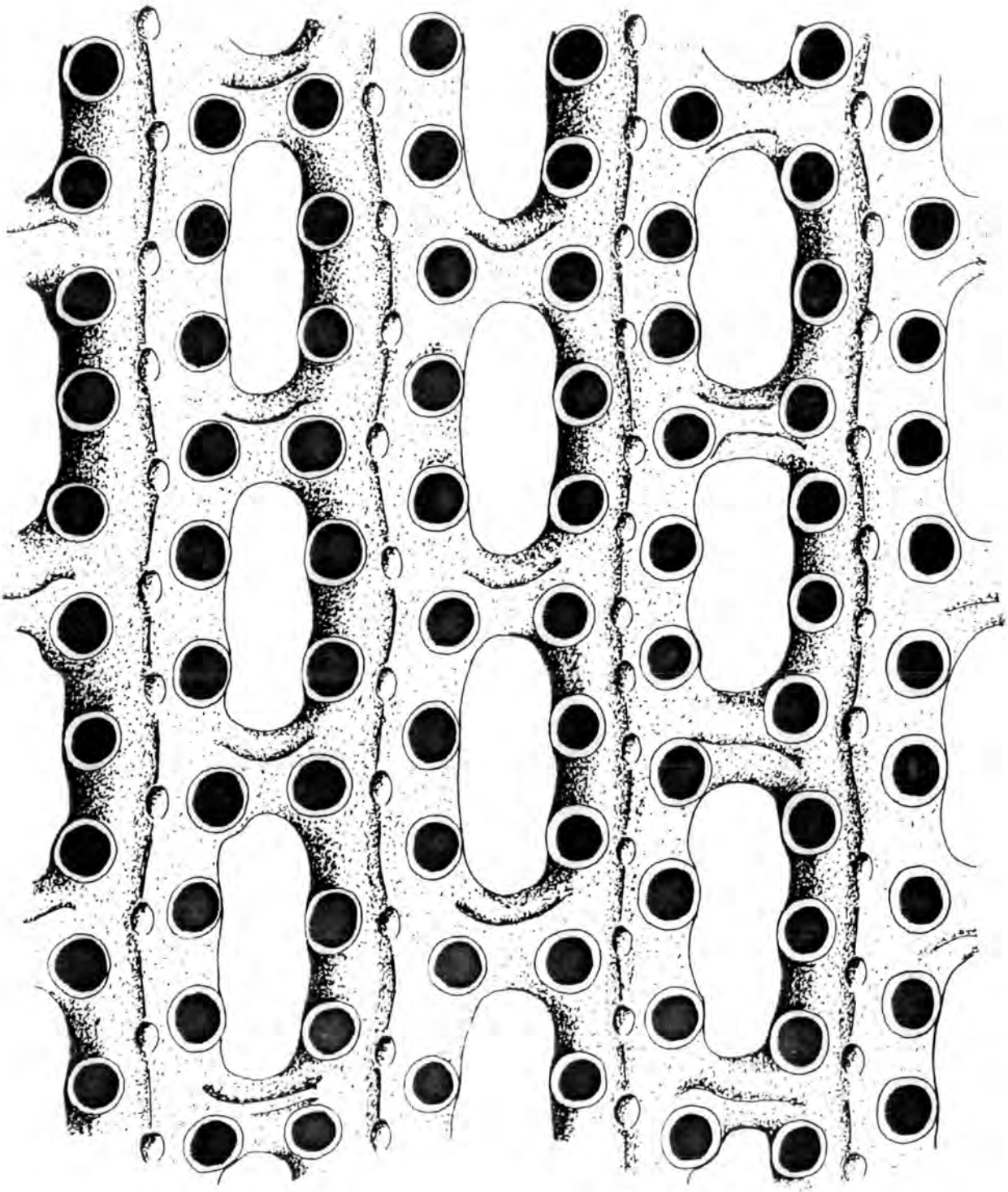

Figure 42. Fenestella tuberculo-carinata Etheridge, Jun.

Obverse surface detail. HM D.44-2. Brigantian, Lower Limestone Group, Roughwood, Beith.

(Bar Scale-1mm)

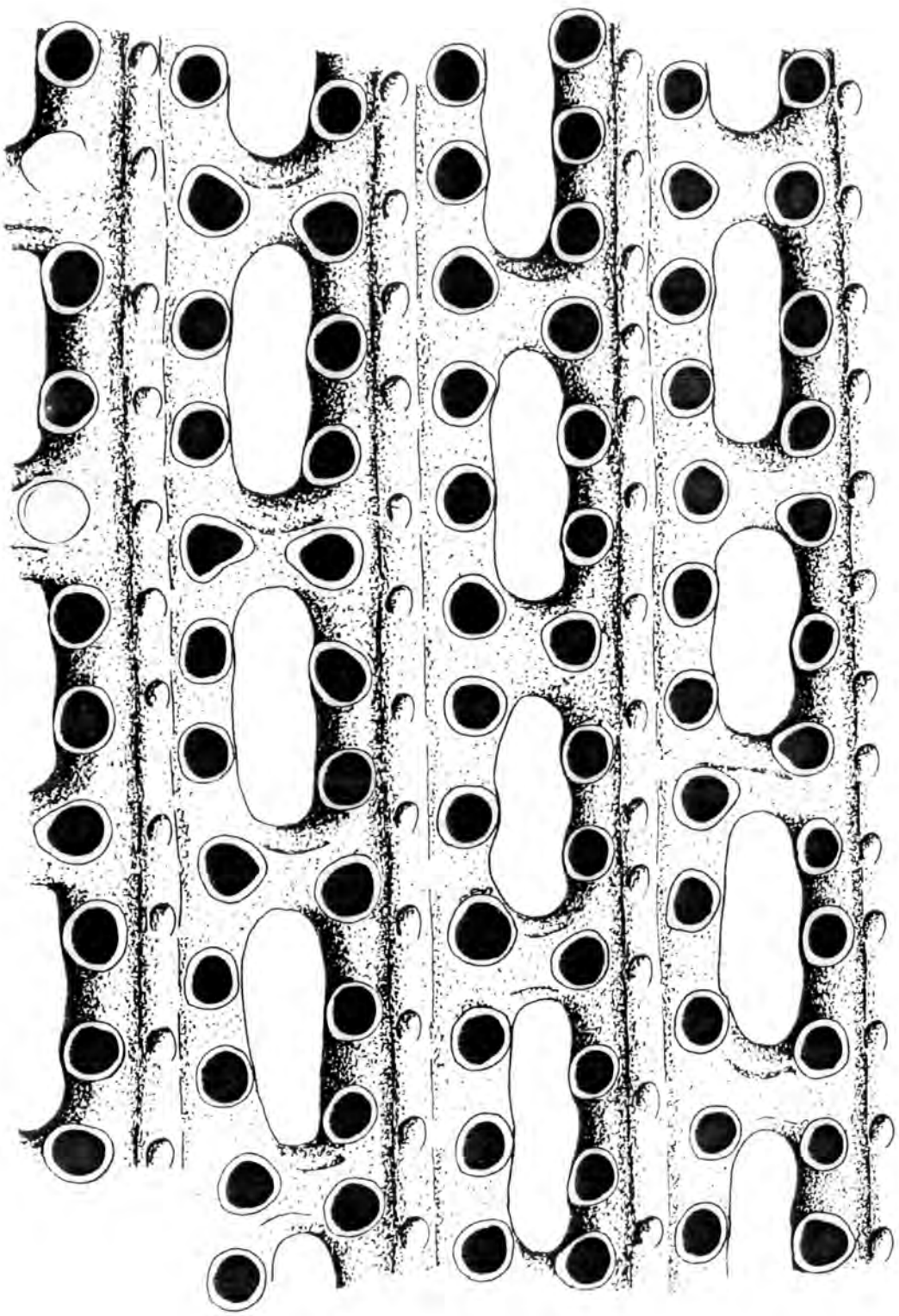

Figure 43. Fenestella plebeia McCoy

Obverse surface detail. BOM GWS+0.12. Brigantian, Carboniferous Limestone, Halkyn Mountain, Clwyd. (Bar Scale=1mm)

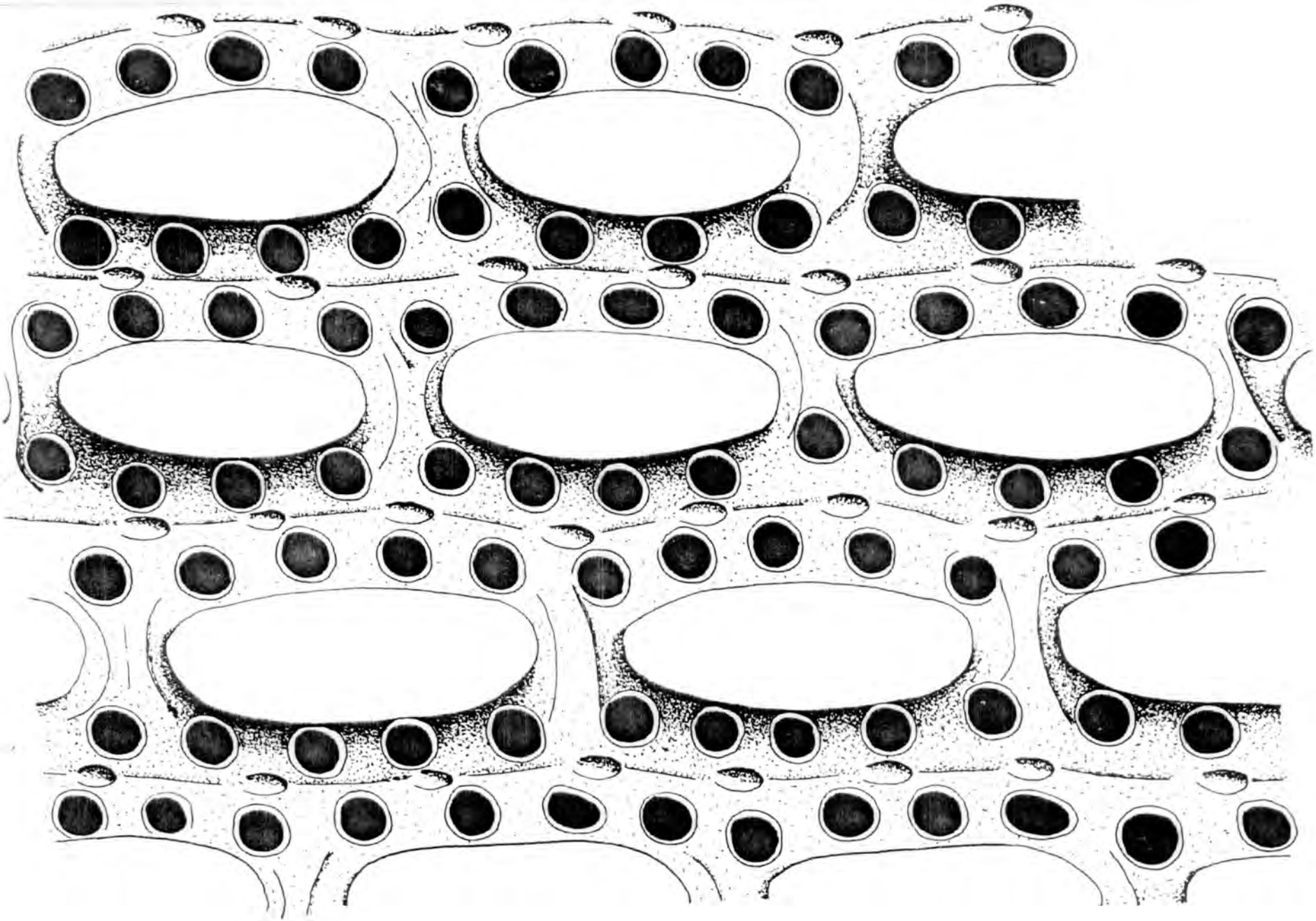

Figure 44. Fenestella plebeia McCoy

Obverse surface detail. BOM 229. Brigantian, Carboniferous Limestone, Halkyn Mountain, Clwyd. (Bar Scale=1mm)

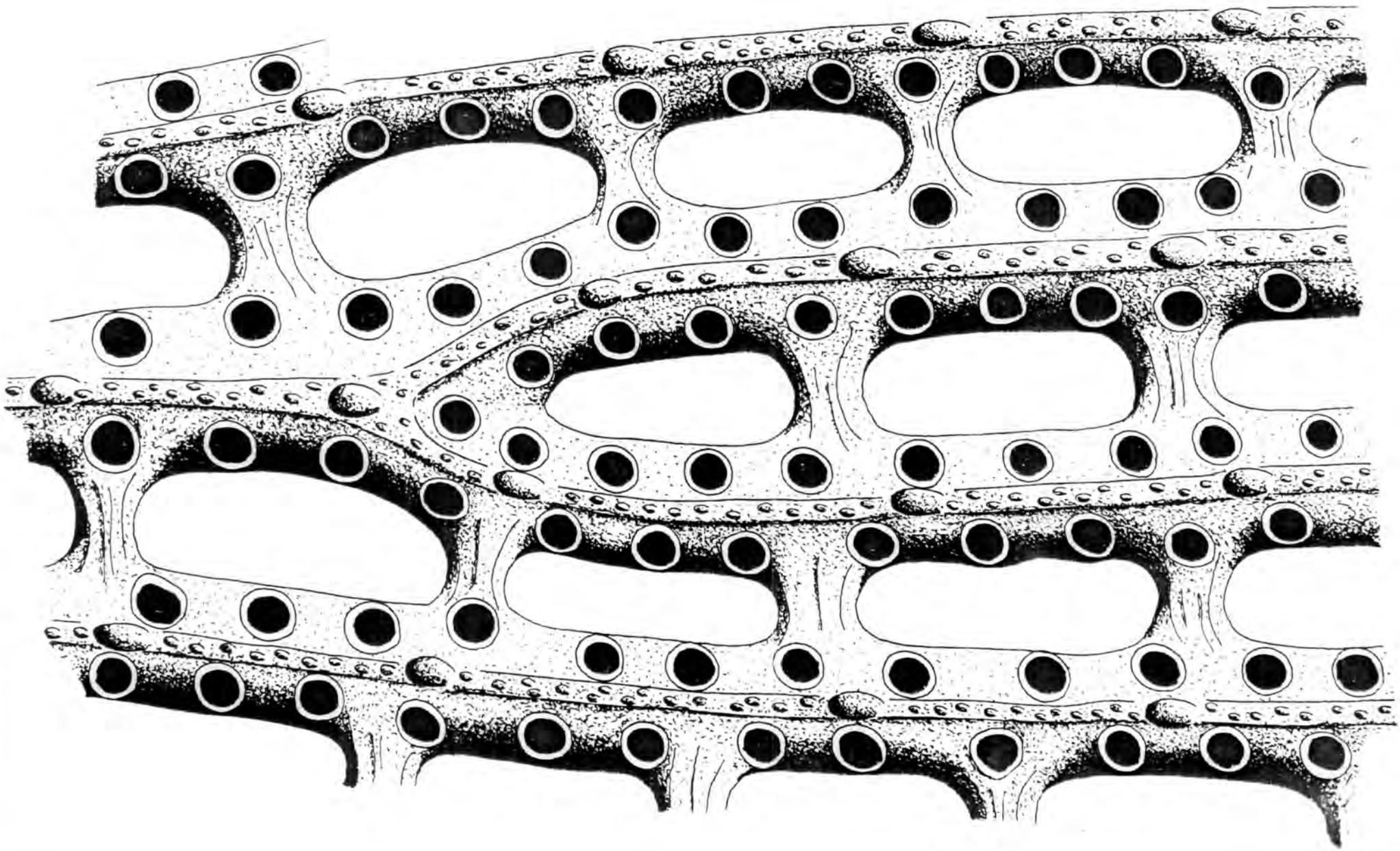

Figure 45. Fenestella plebeia McCoy

Reverse surface detail. BOM 221. Brigantian, Carboniferous Limestone, Halkyn Mountain, N^{r} Flint, Clwyd.

(Bar Scale=1mm)

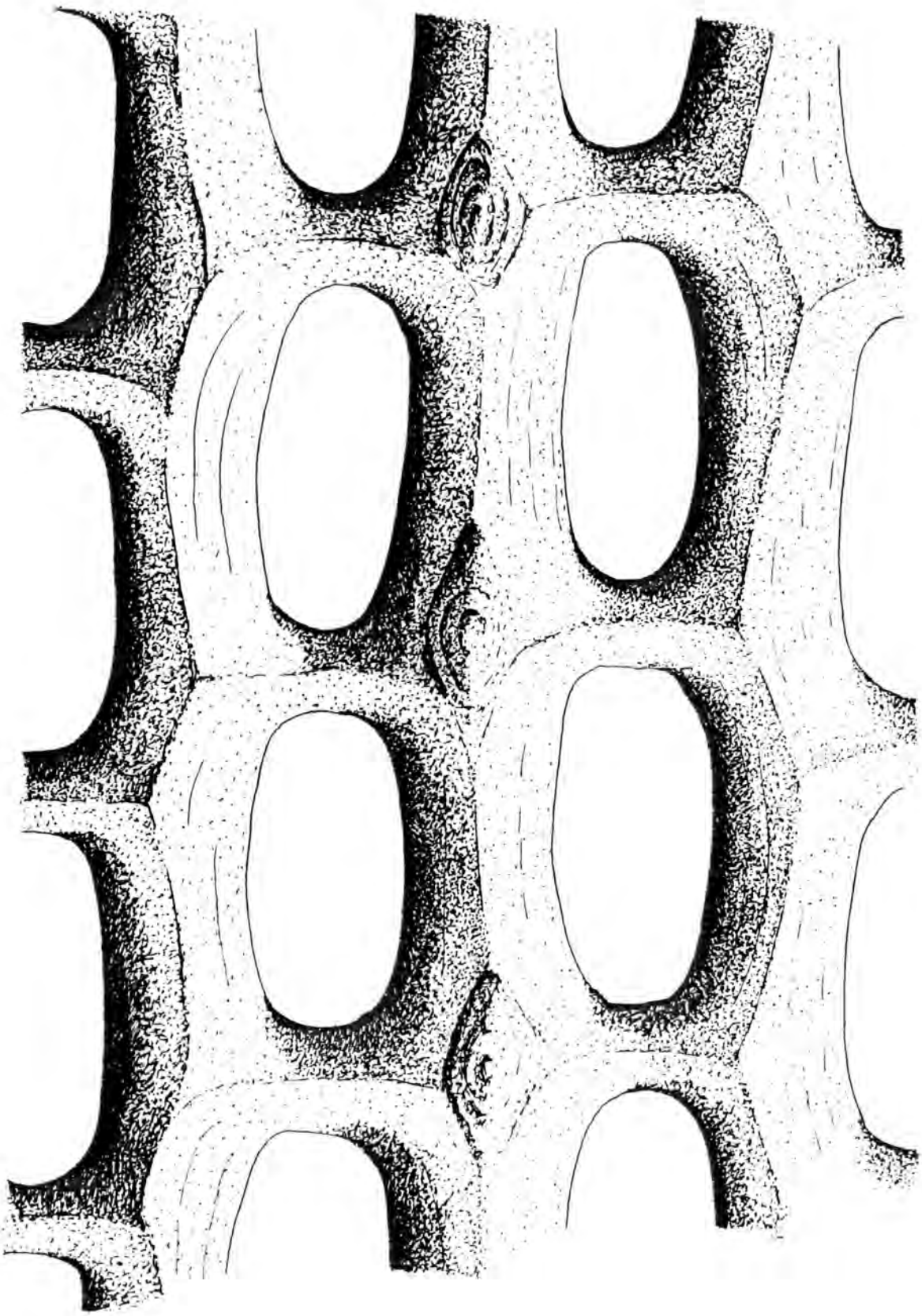

Figure 46. Fenestella polyporata (Phillips)

Obverse surface detail. ABHR 30. Arnsbergian, shales above the Main Limestone, Hurst, N. Yorkshire.
(Bar Scale=1mm)

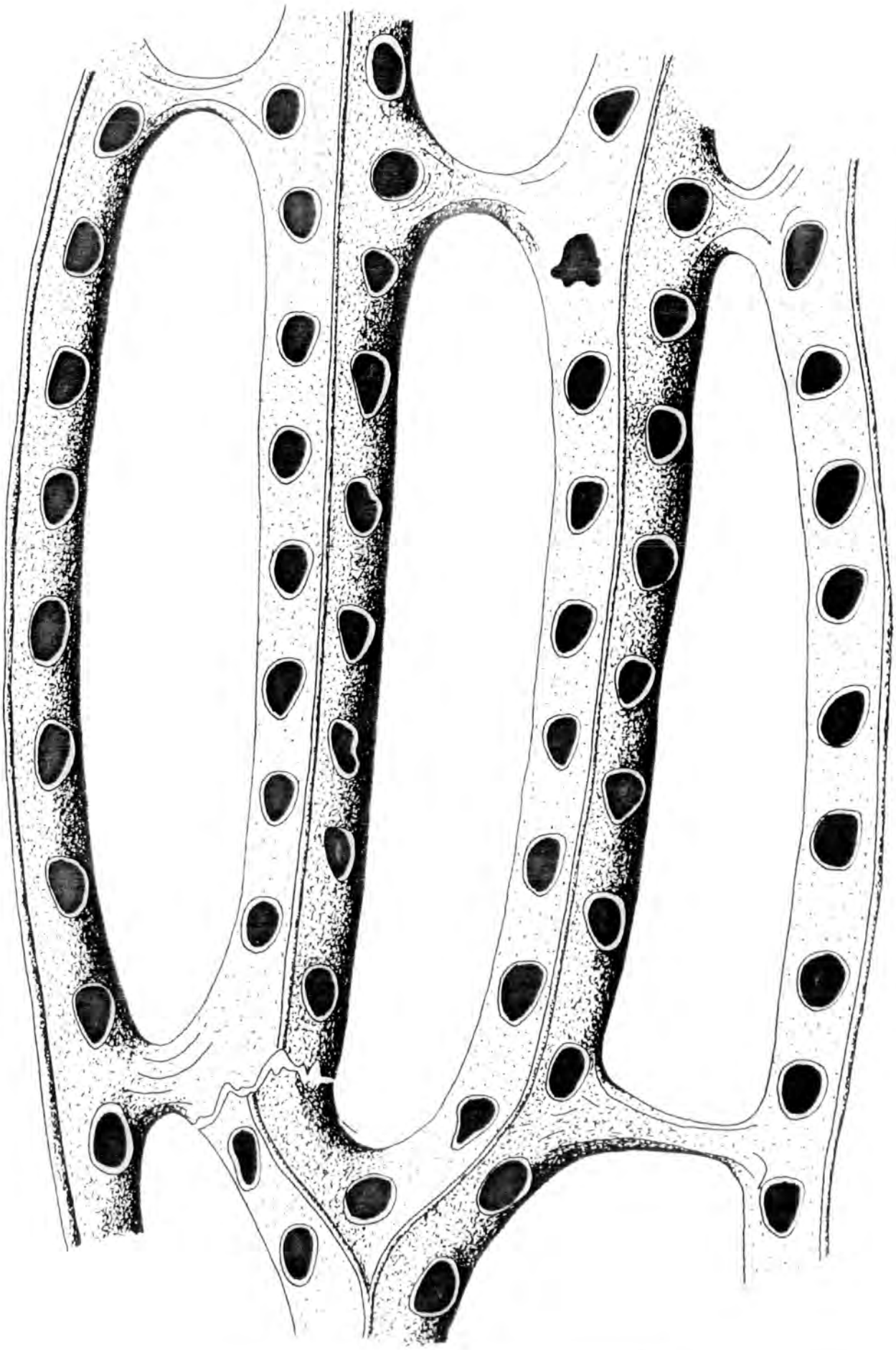

Figure 47. Fenestella polyporata (Phillips)

Obverse surface detail. ABMG 28 . Brigantian, Hardraw Shales, Mill Gill, Askrigg, N. Yorkshire.

(Bar Scale=1mm)

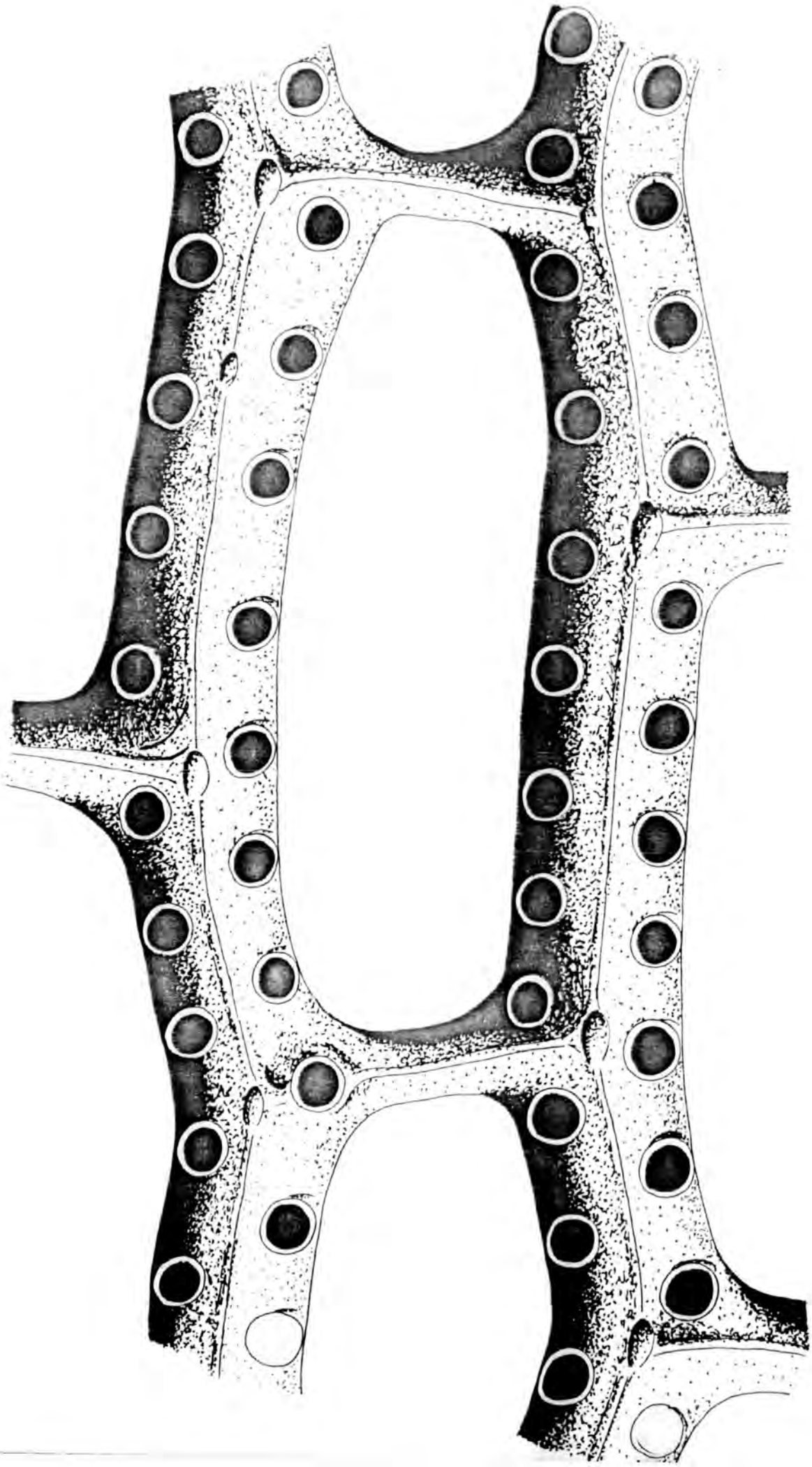

Figure 48. Fenestella polyporata (Phillips)

Autozooecial chamber bases. BOM 25-09-172. Asbian?, Carboniferous Limestone, Castleton, Derbyshire. (Bar Scale=1mm)

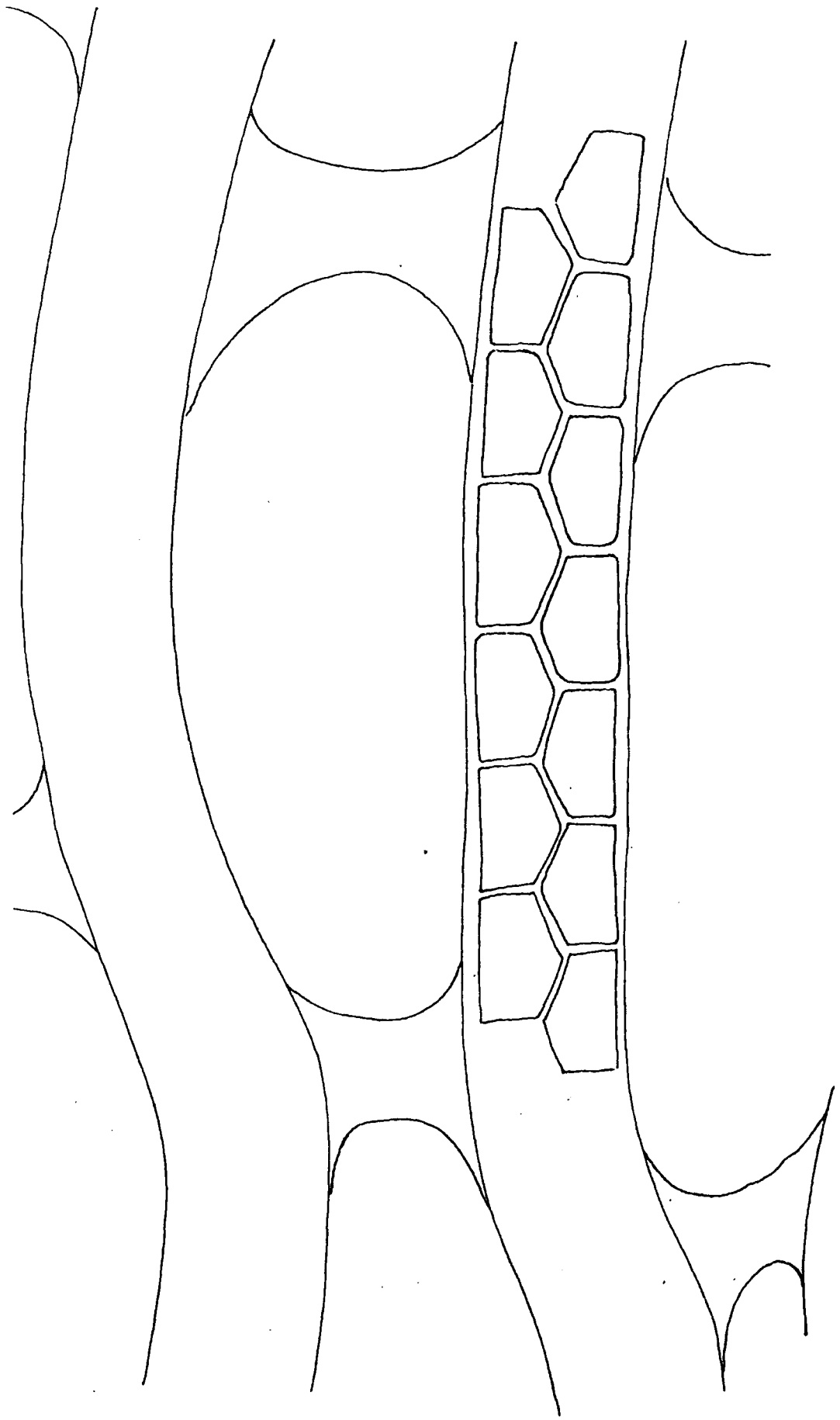

Figure 49. Minilya plummerae (Moore)

Obverse surface detail. ABP 135. Asbian, Alston Group, Penruddock, N^r Penrith, Cumbria.
(Bar Scale=1mm)

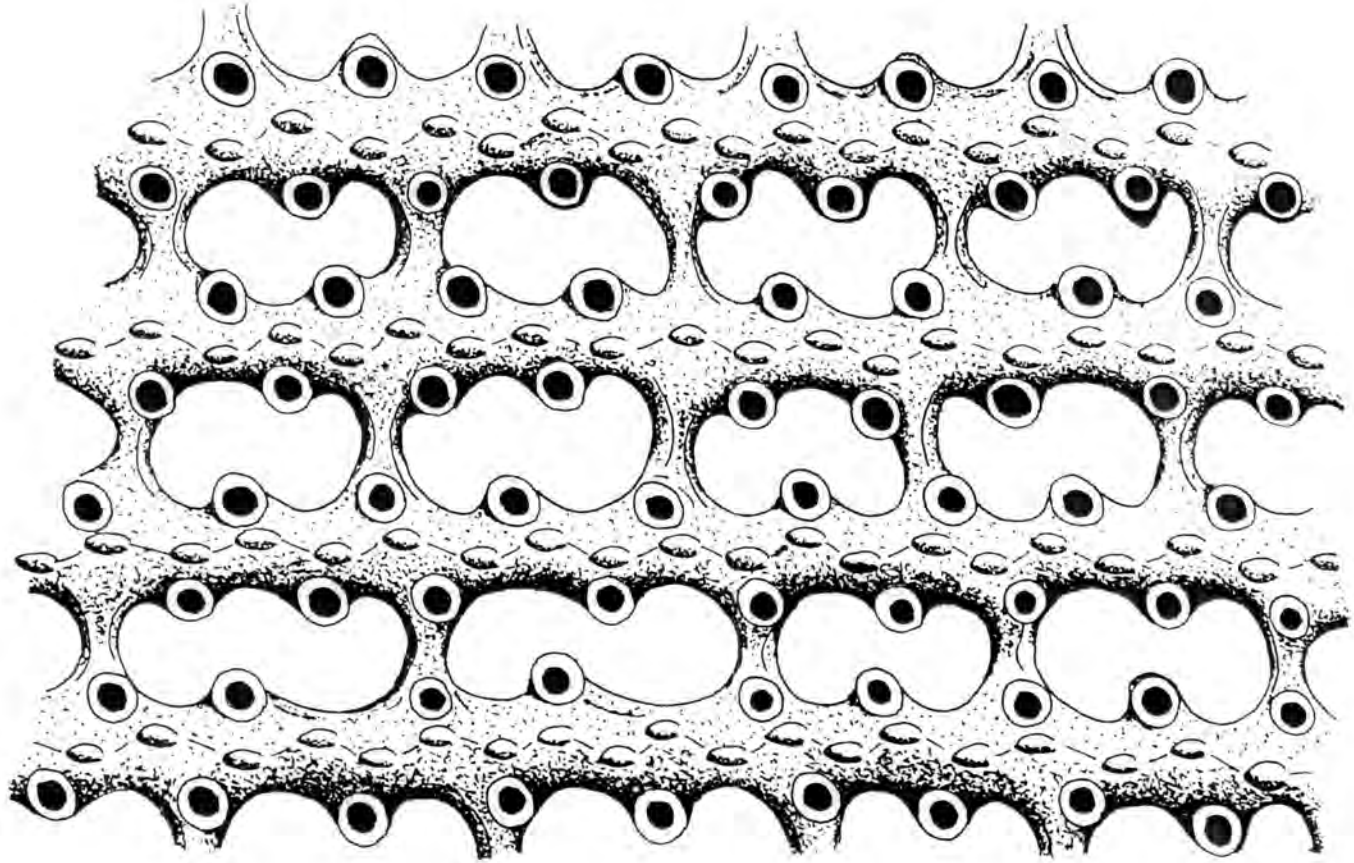

Figure 50. Minilya nodulosa (Phillips)

Obverse surface detail. ABP 153. Asbian, Alston Group, Penruddock, Nr Penrith, Cumbria.

(Bar Scale=1mm)

Figure 51. Hemitrypa hibernica McCoy

Longitudinal section showing internal skeletal details.

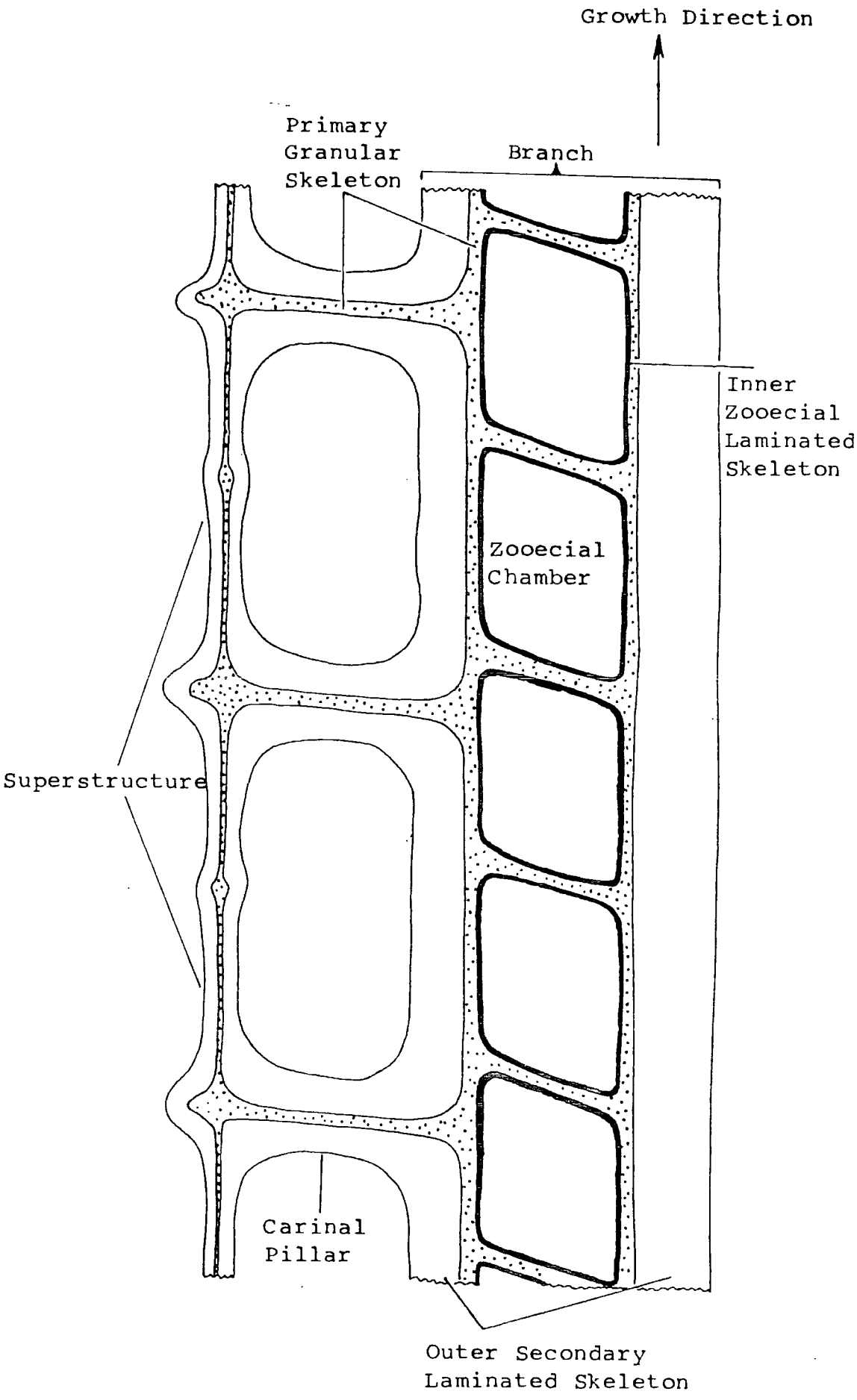
Growth Direction
Primary
Granular
Skeleton
Branch
Inner
Zooecial
Laminated
Skeleton
Zooecial
Chamber
Superstructure
Carinal
Pillar
Outer Secondary
Laminated Skeleton

Figure 52. Hemitrypa hibernica McCoy

Transverse section showing internal skeletal details.

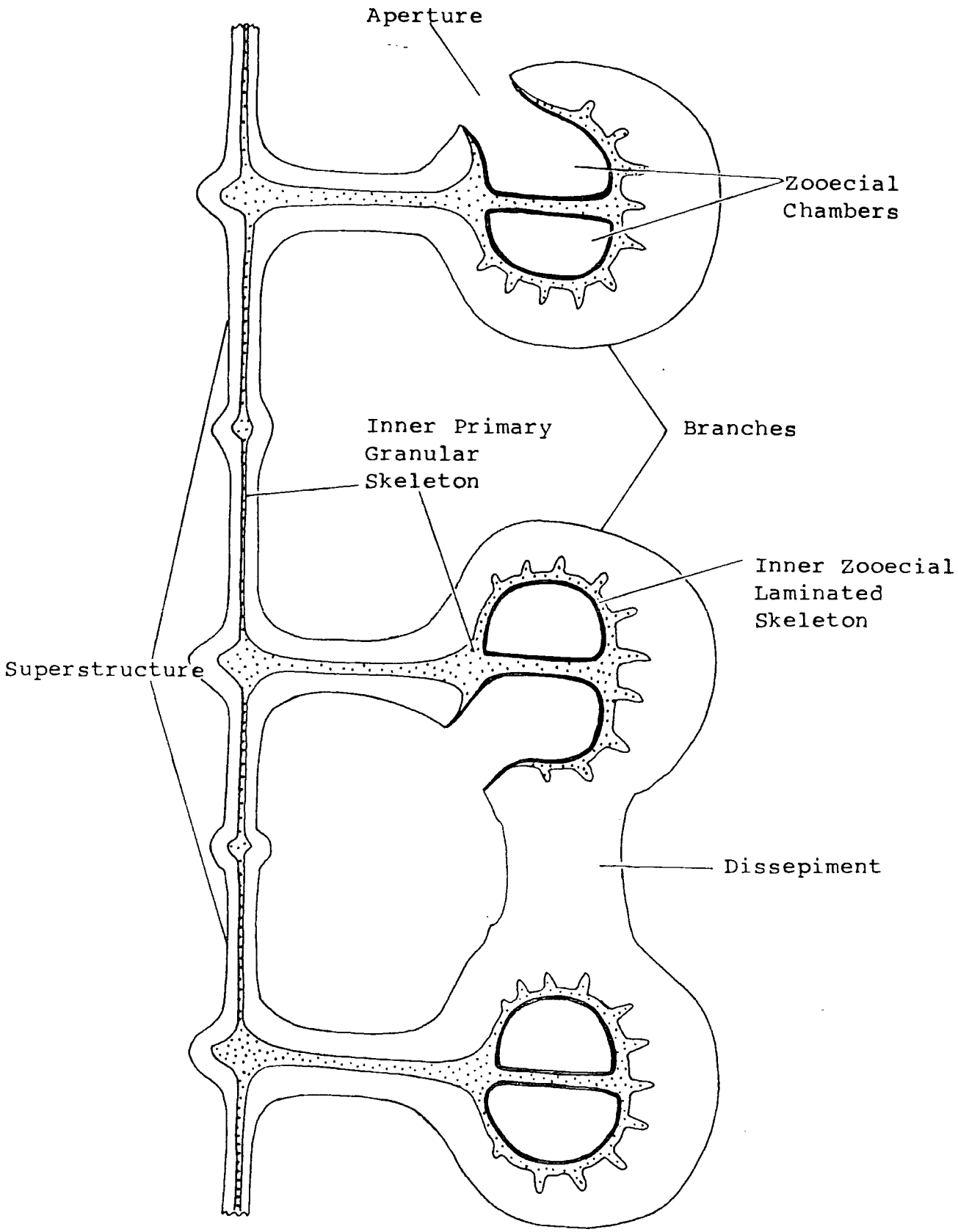
Aperture
Zooecial Chambers
Branches
Inner Primary Granular Skeleton
Inner Zooecial Laminated Skeleton
Superstructure
Dissepiment

Figure 53. Hemitrypa hibernica McCoy

Tangential section showing internal skeletal details of the superstructure.

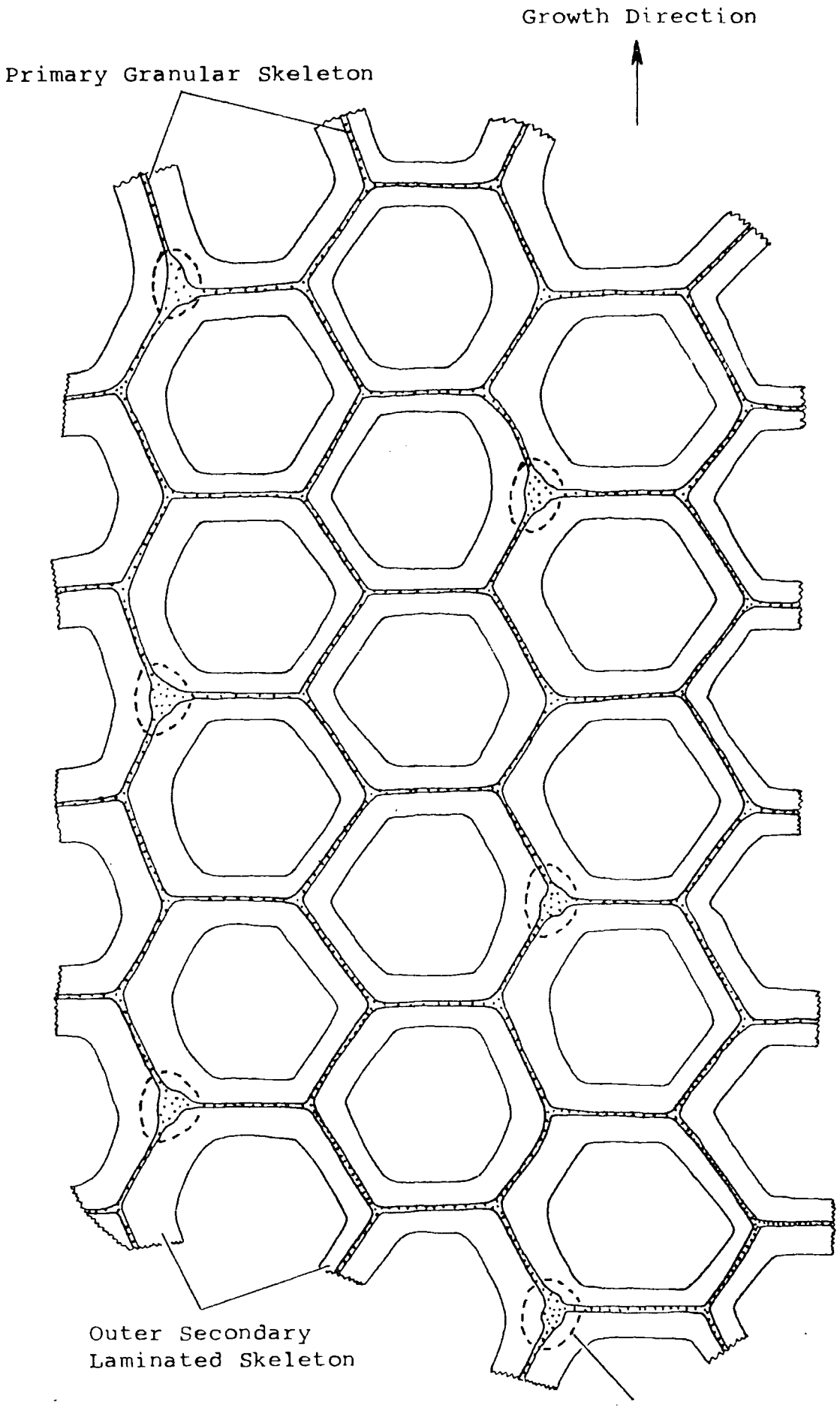
Growth Direction
Primary Granular Skeleton
Outer Secondary
Laminated Skeleton
Position of Carinal
Nodes (supporting
pillars) below the
Superstructure

Figure 54. Hemitrypa hibernica McCoy

Obverse surface detail; also showing the superstructure in place above the fenestellid meshwork. A perforation in the superstructure is situated above each autozooecial aperture. ABP 100. Asbian, Alston Group, Penruddock, N^{r} Penrith, Cumbria.
(Bar Scale=1mm)

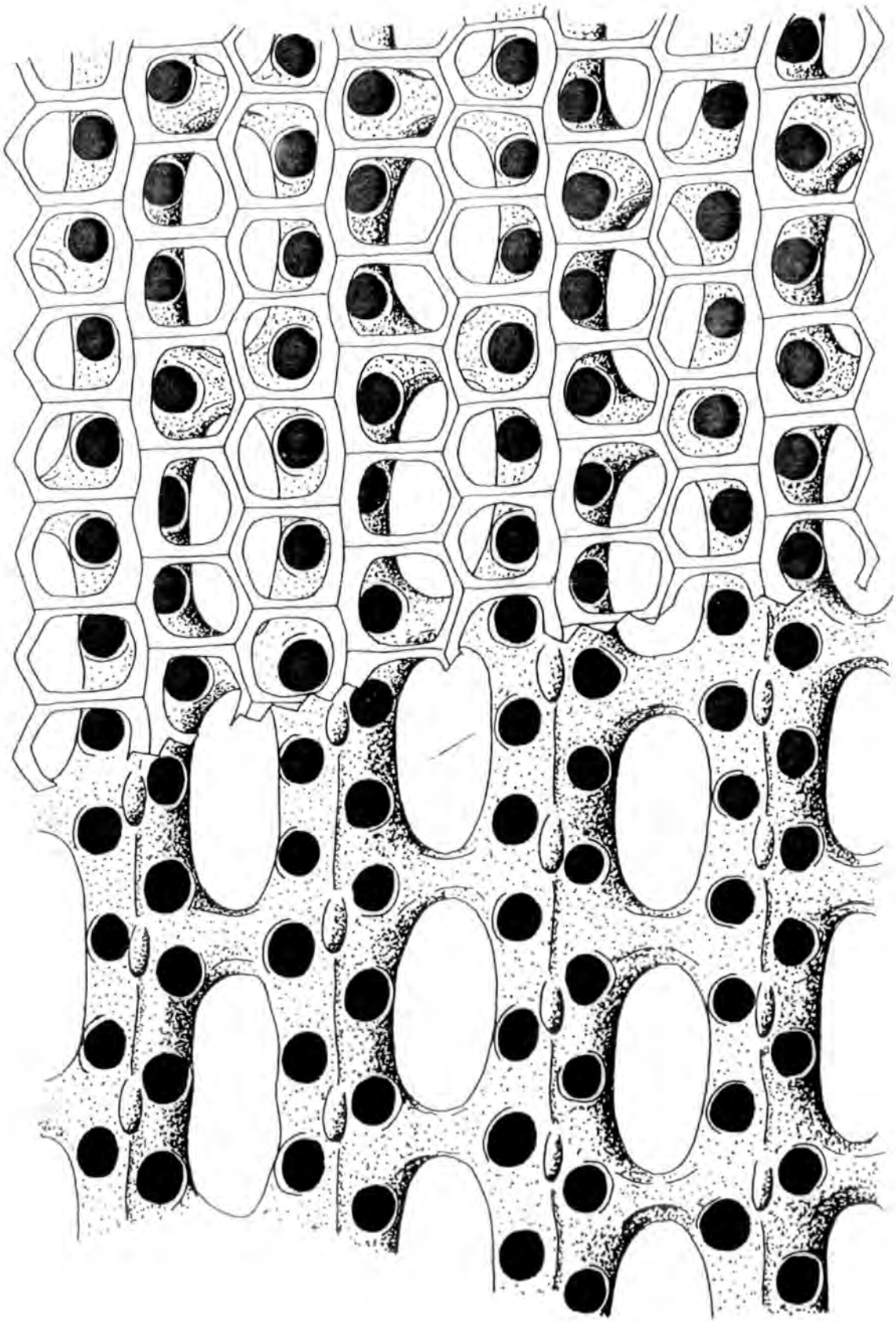

Figure 55. Diploporaria marginalis (Young and Young)

Obverse surface detail. Both specimens HM D.122. Brigantian, Lower Limestone Group, Hosie Limestone, Hairmyres, E. Kilbride.

(Bar Scale=1mm)

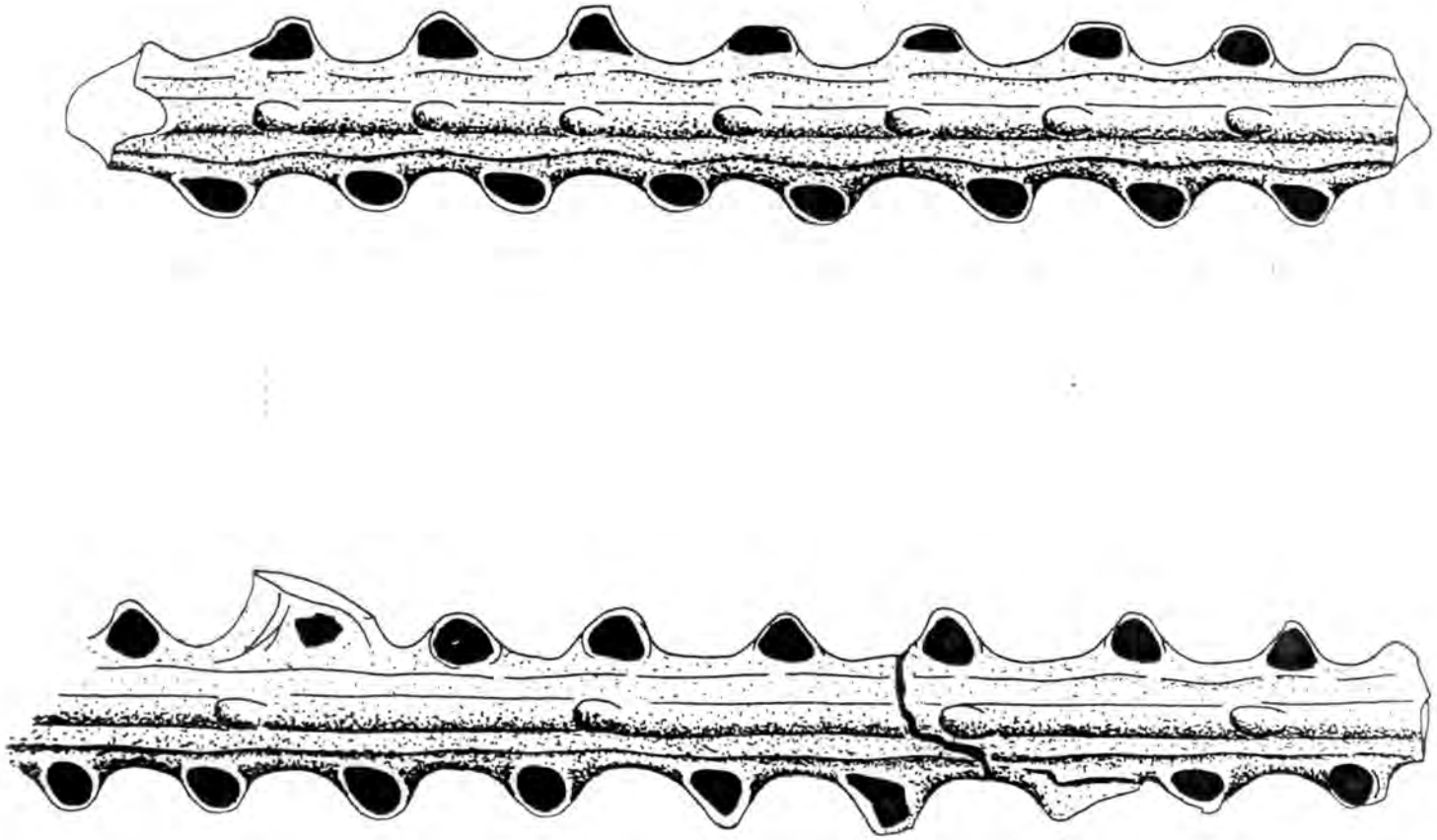

Figure 56. Diploporaria marginalis (Young and Young)

Reverse surface detail. HM D.122. Brigantian, Lower Limestone Group, Hosie Limestone, Hairmyres,. E. Kilbride.

(Bar Scale=1mm)

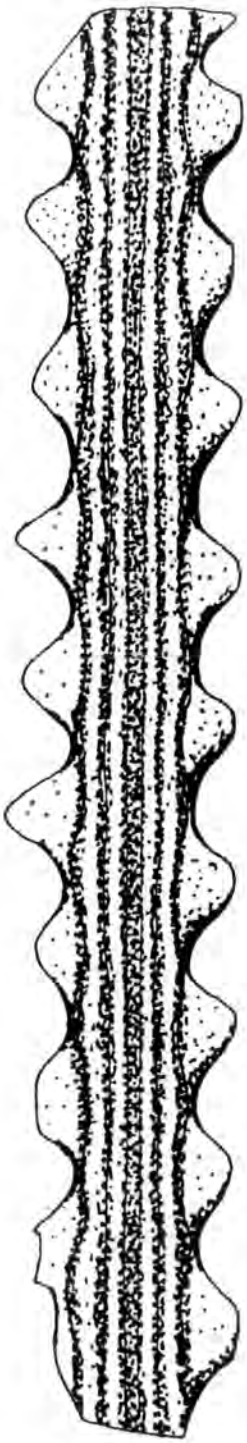

Figure 57. Colony Form in Penniretepora

(a) Pinnate zoaria: with only 1:2 minor lateral branches developed from the Mainstem (1).

(b) Bipinnate zoaria: in addition to 1:2 minor lateral branches, widely spaced 2:1 primary branches are developed along the Mainstem. These have minor branches (2:2) of their own.

(c) Tripinnate zoaria: some of the 2:2 minor lateral branches have small short lateral branches of their own.

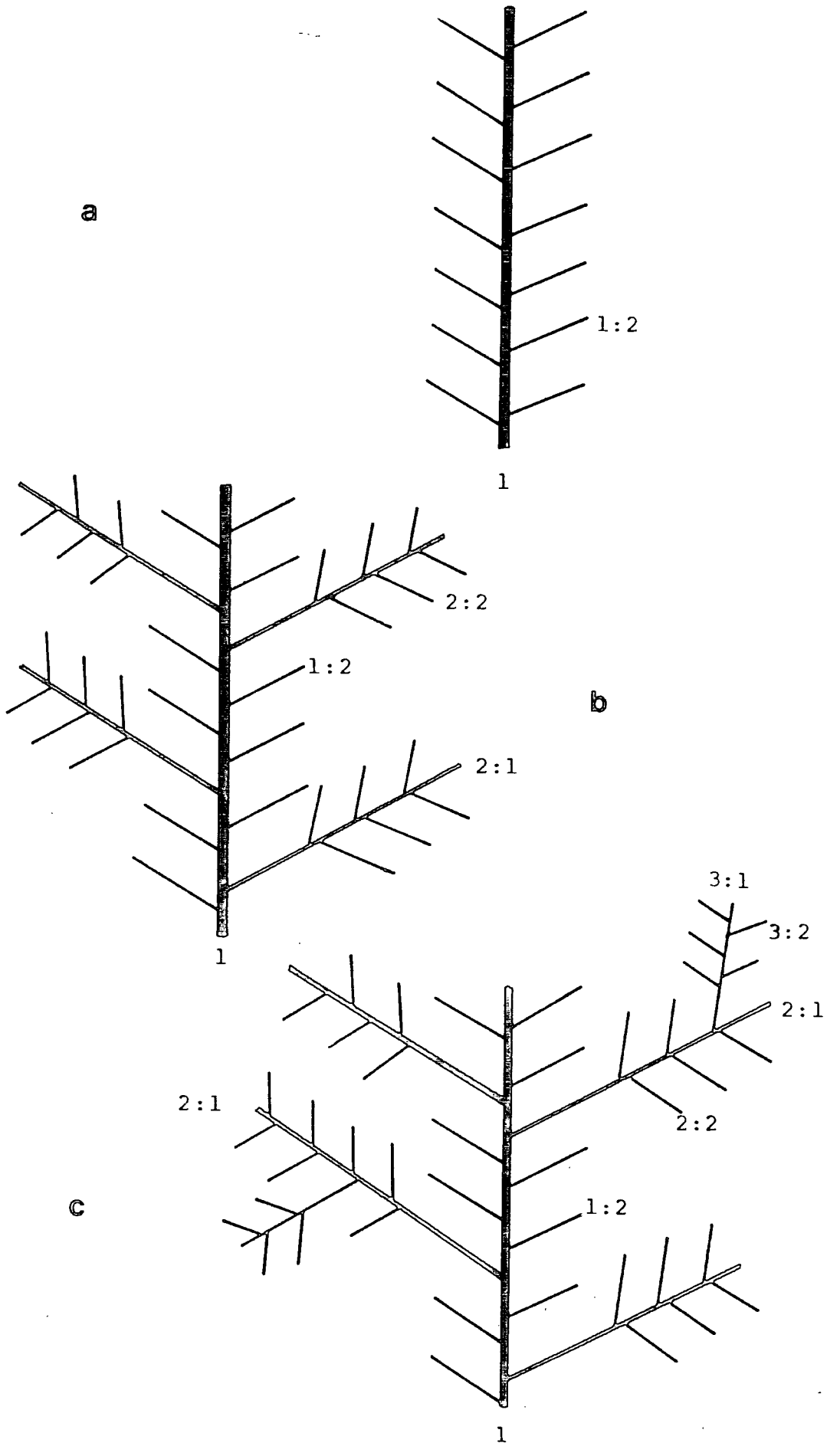
a
1:2
1
2:2
1:2
2:1
1
b
3:1
3:2
2:1
2:2
2:1
1:2
1
c

Figure 58. Diagram to show the morphological characters measured on Penniretepora in the present study. (For explanation of characters see text pp. 261-263)

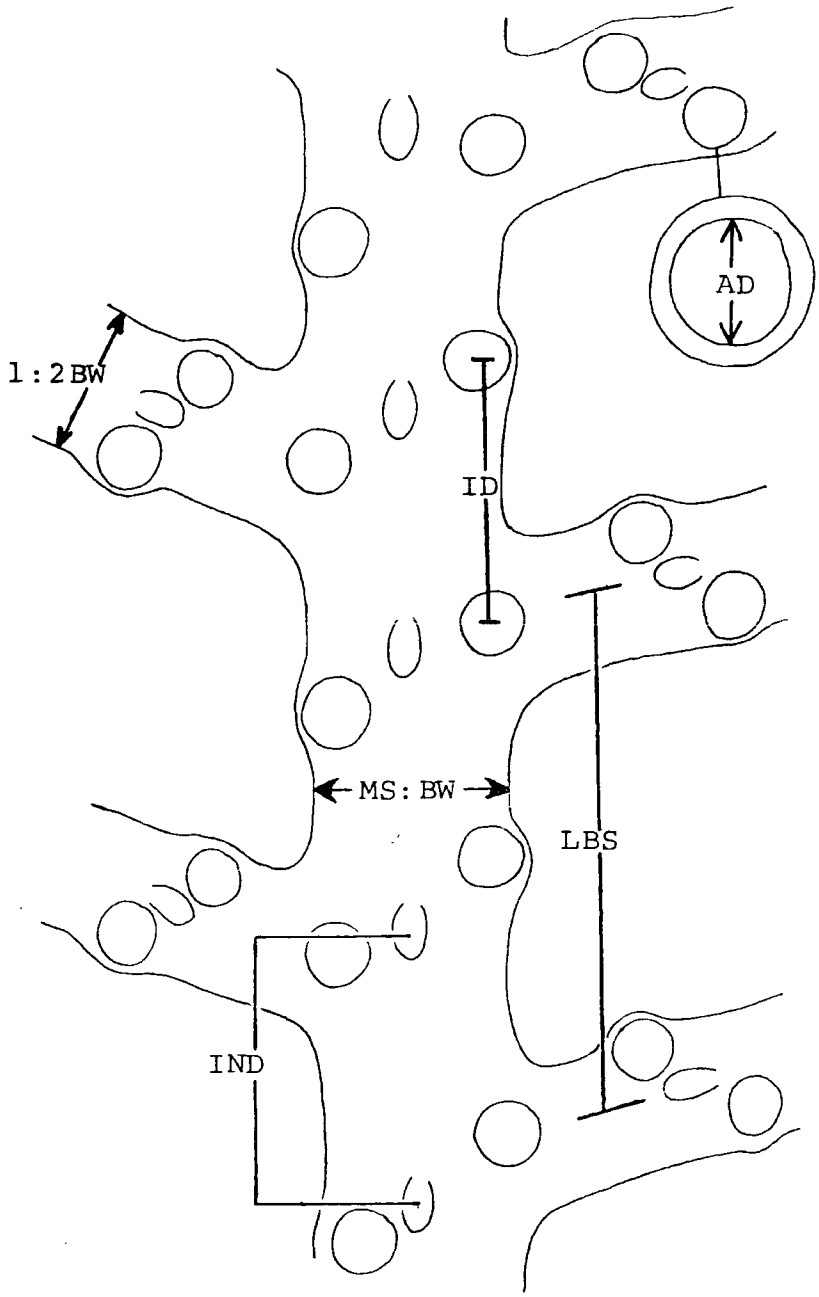
AD
1:2BW
ID
MS:BW
LBS
IND

Figure 59. Penniretepora stellipora (Young and Young)

Obverse and reverse surface detail. HM D.128-4 (The lectotype), and HM D.128-3. Both Brigantian, Lower Limestone Group, Hosie Limestone, Hairmyres, E. Kilbride.

(Bar Scale=1mm)

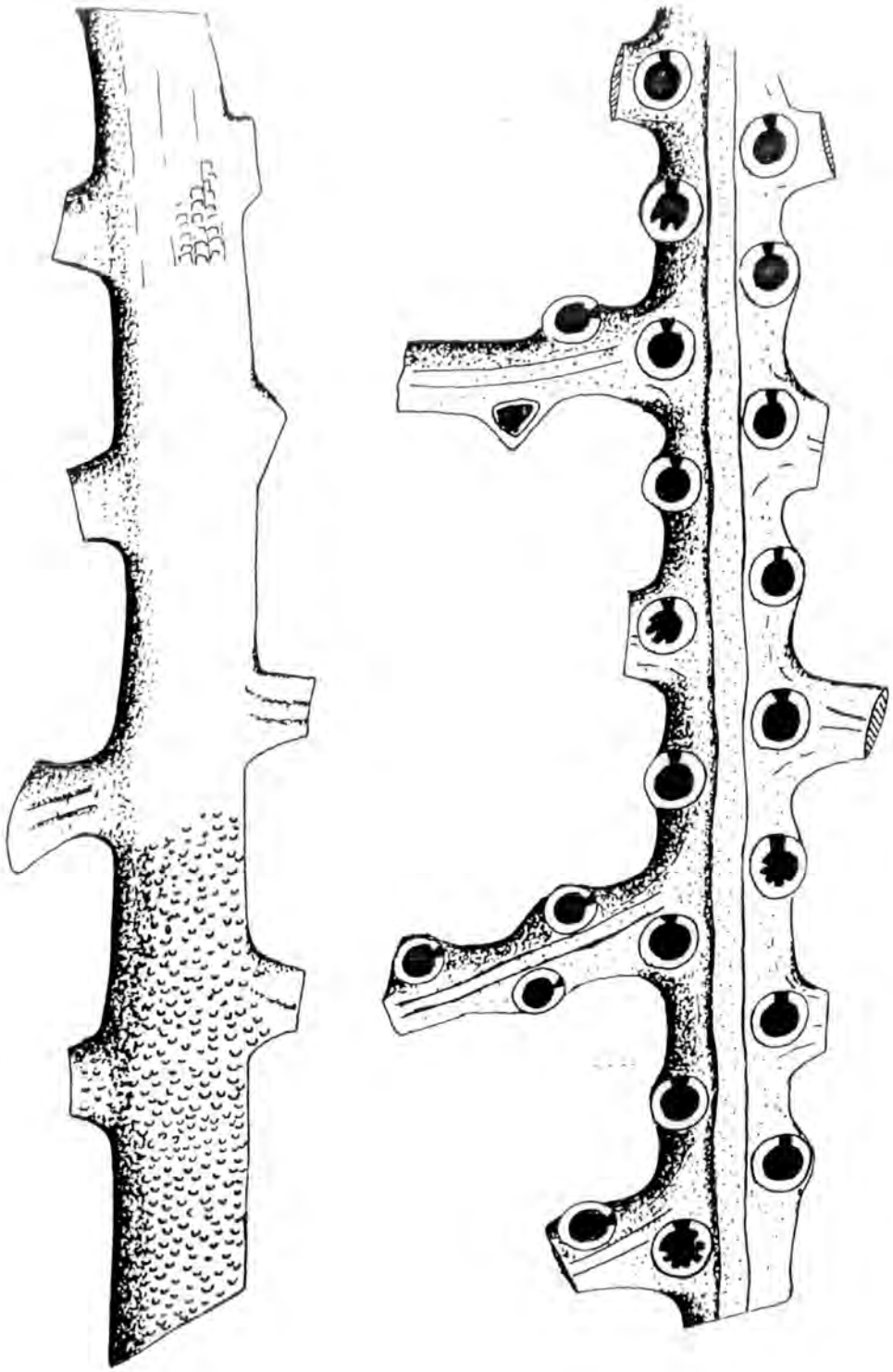

Figure 60. Penniretepora stellipora (Young and Young)

Obverse surface detail. ABHR A4-3. Arnsbergian, shales above the Main Limestone, Hurst, N. Yorkshire. (Bar Scale=1mm)

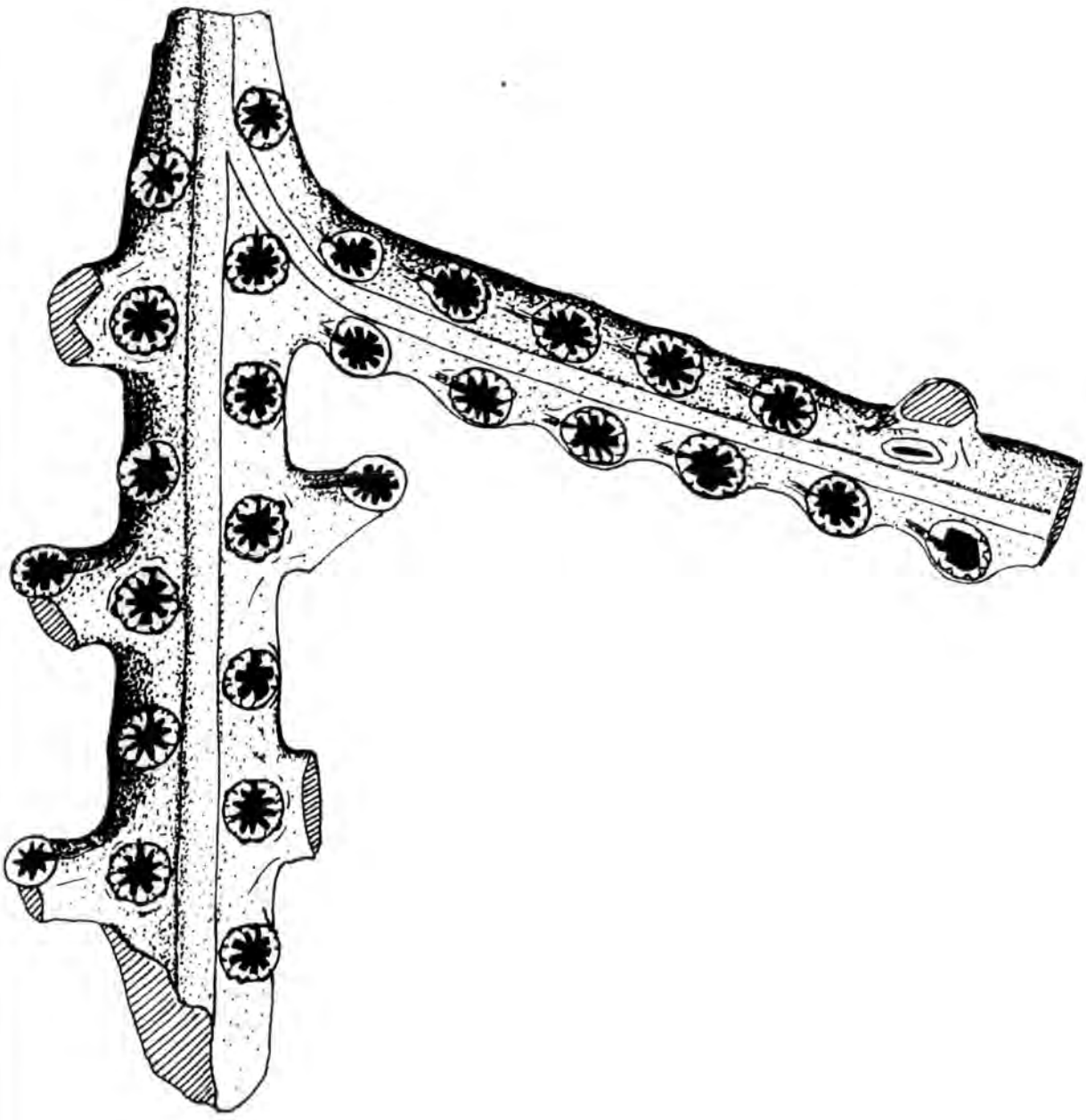

Figure 61. Penniretepora spinosa (Young and Young)

Obverse and reverse surface detail. HM D.128-14, HM D.128-3. Both Brigantian, Lower Limestone Group, Hosie Limestone, Hairmyres, E. Kilbride.
(Bar Scale=1mm)

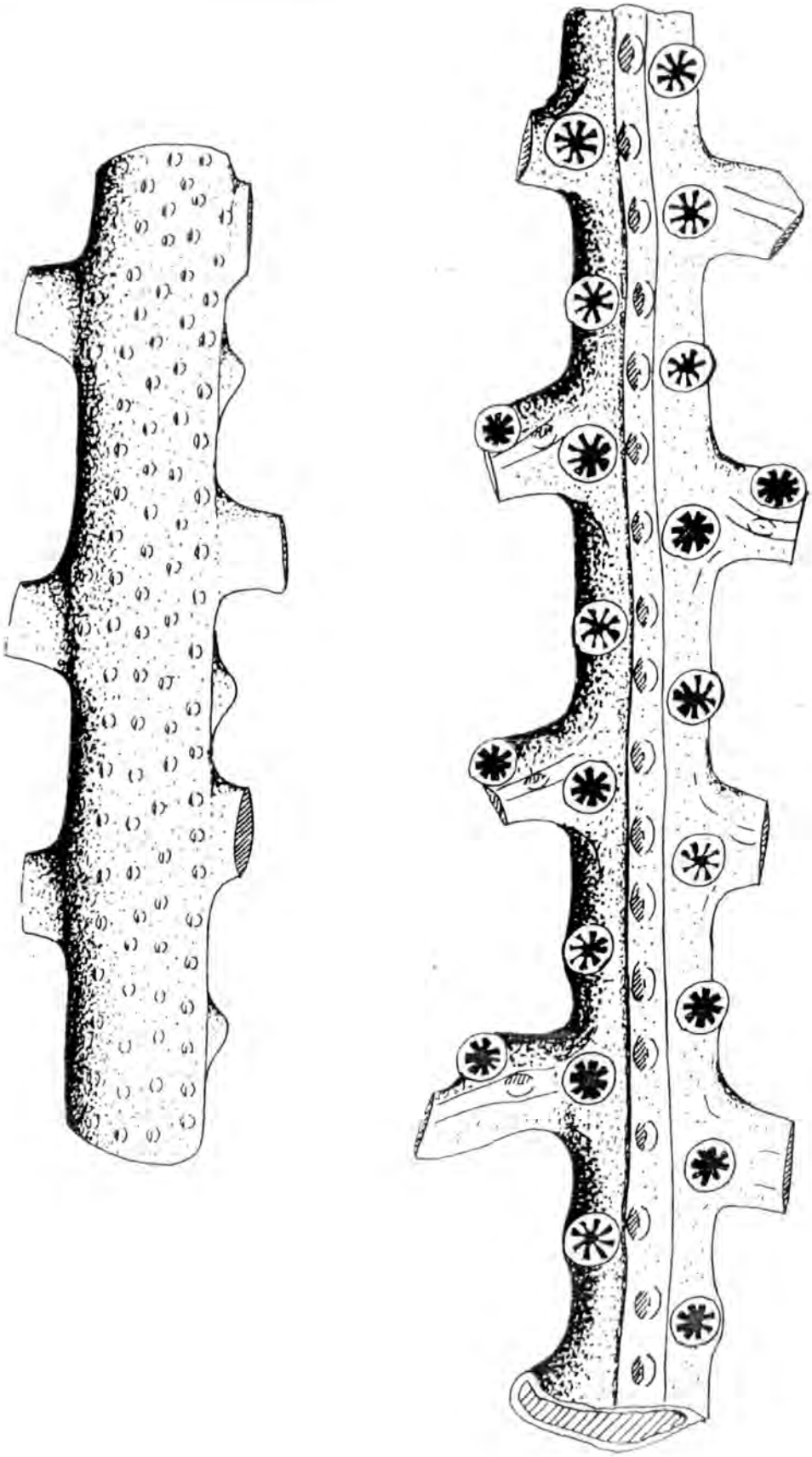

Figure 62. Penniretepora sp. nov. A

Obverse surface detail. HM D.62-2. Arnsbergian, shales above the Second Kingshaw Limestone, Carluke.

(Bar Scale=1mm)

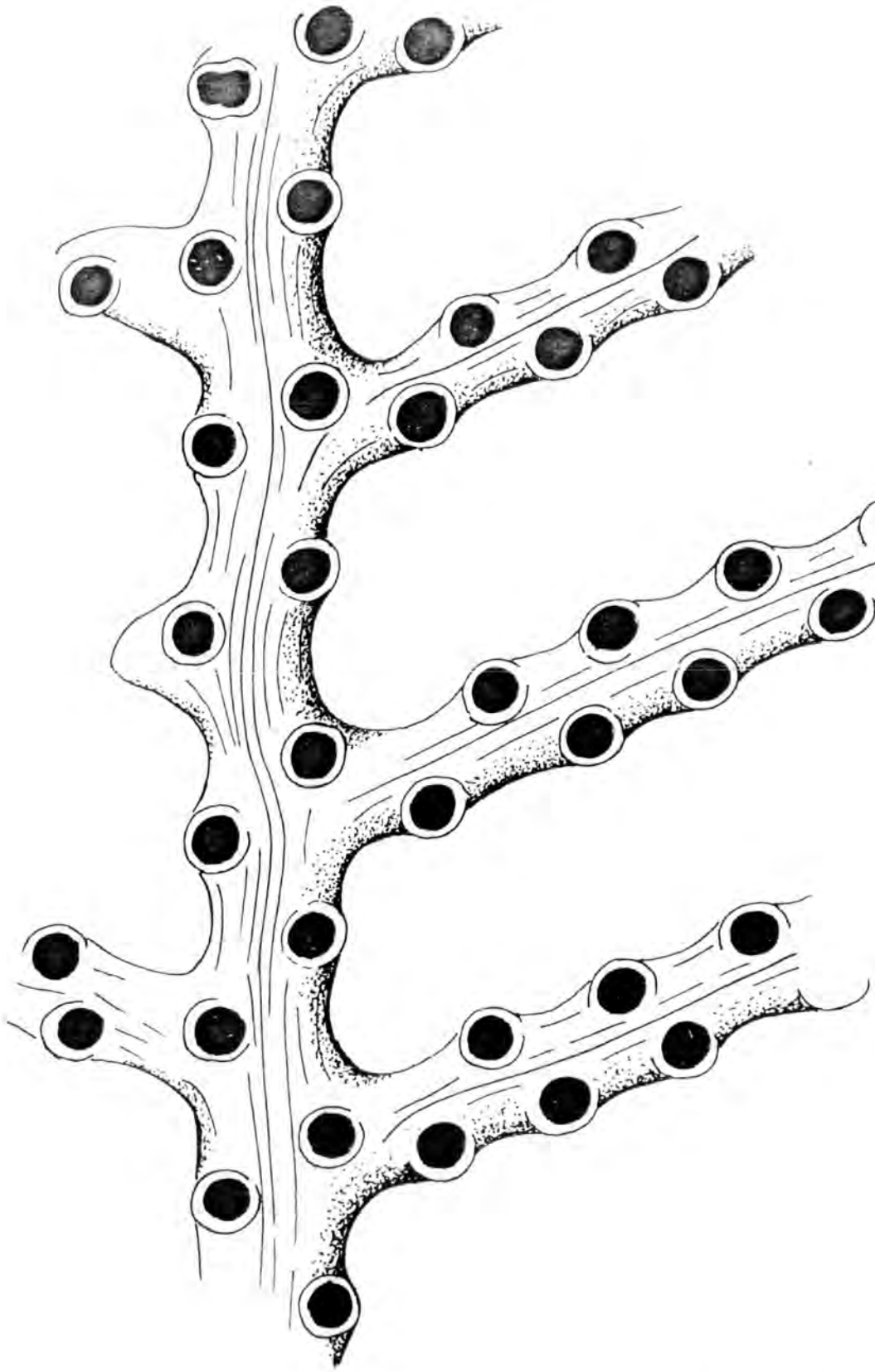

Figure 63. Penniretepora sp. nov. B

Obverse and reverse surface detail. ABHR A5-1 (Holotype), ABHR A5-3. Both Arnsbergian, shales above the Main Limestone, Hurst, N. Yorkshire. (Bar Scale=1mm)

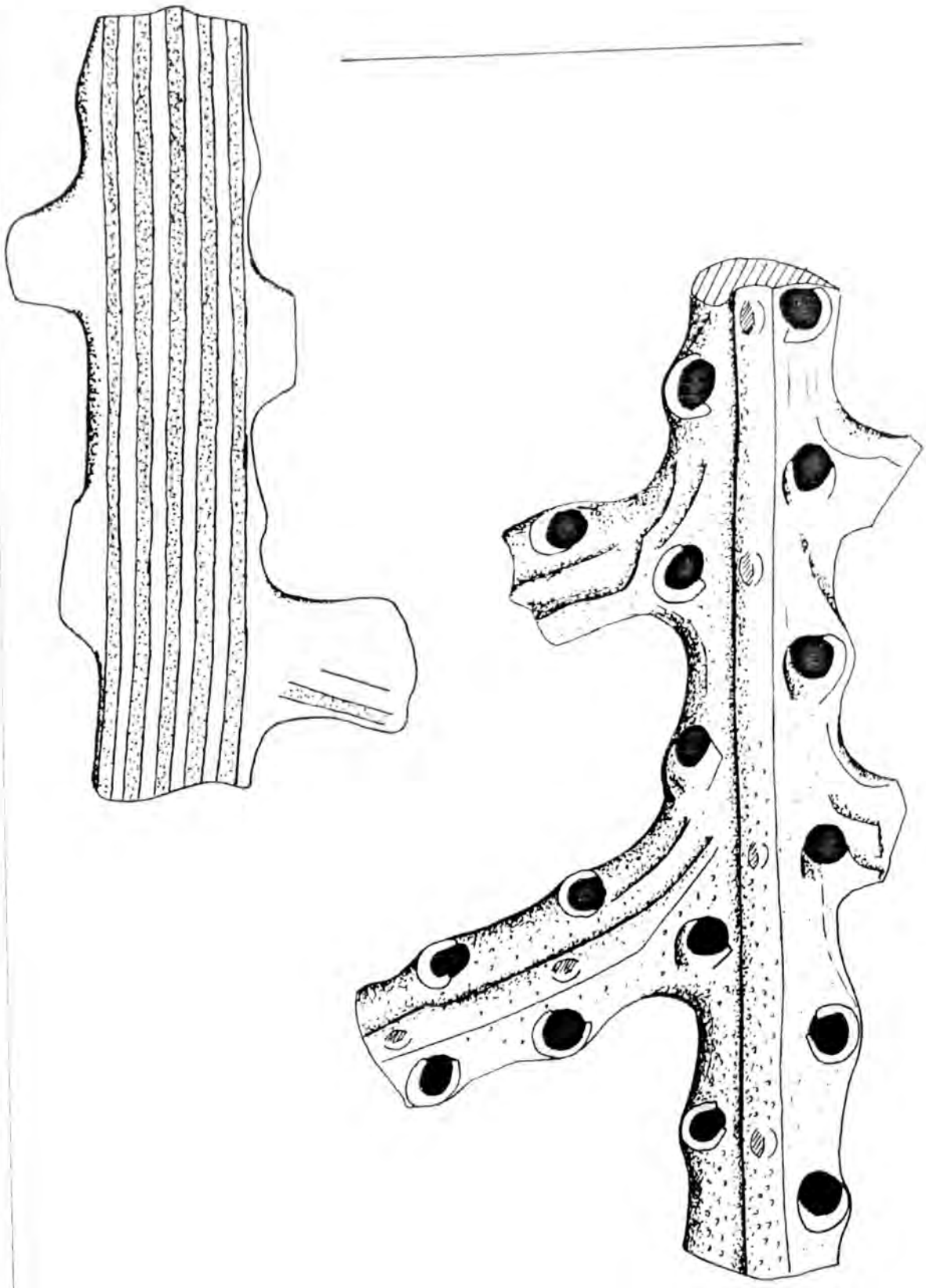

Figure 64. Penniretepora flexicarinata (Young and Young)

Obverse and reverse surface detail. HM D.120-21, HM D.121-4. Both Brigantian, Lower Limestone Group, Hosie Limestone, Hairmyres, E. Kilbride.
(Bar Scale=1mm)

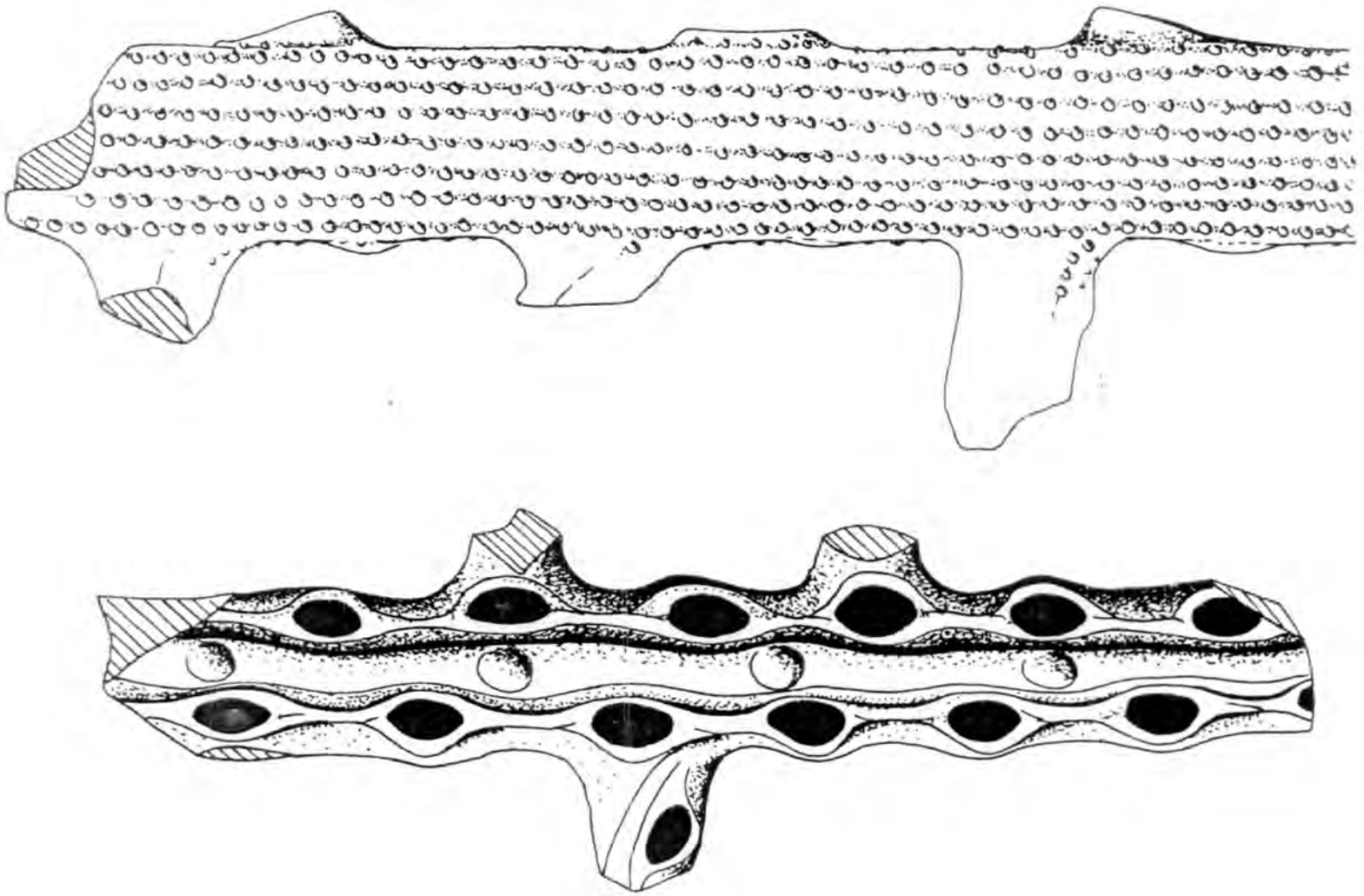

Figure 65. Penniretepora flexicarinata (Young and Young)

Obverse surface detail. HM D.121-12. Brigantian, Lower Limestone Group, Hosie Limestone, Hairmyres, E. Kilbride.

(Bar Scale=1mm)

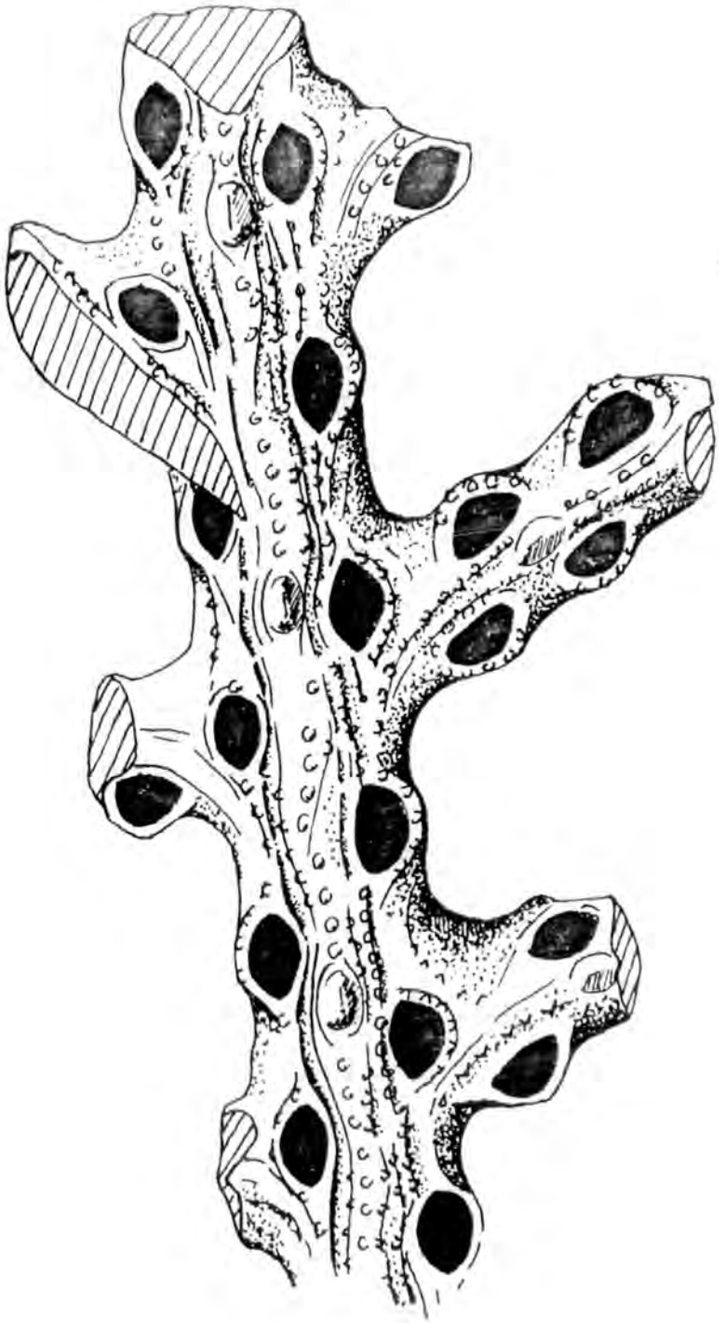

Figure 66. Penniretepora flexicarinata (Young and Young)

Obverse surface detail. HM D.121-13. Brigantian, Lower Limestone Group, Hosie Limestone, Hairmyres, E.Kilbride.

(Bar Scale=1mm)

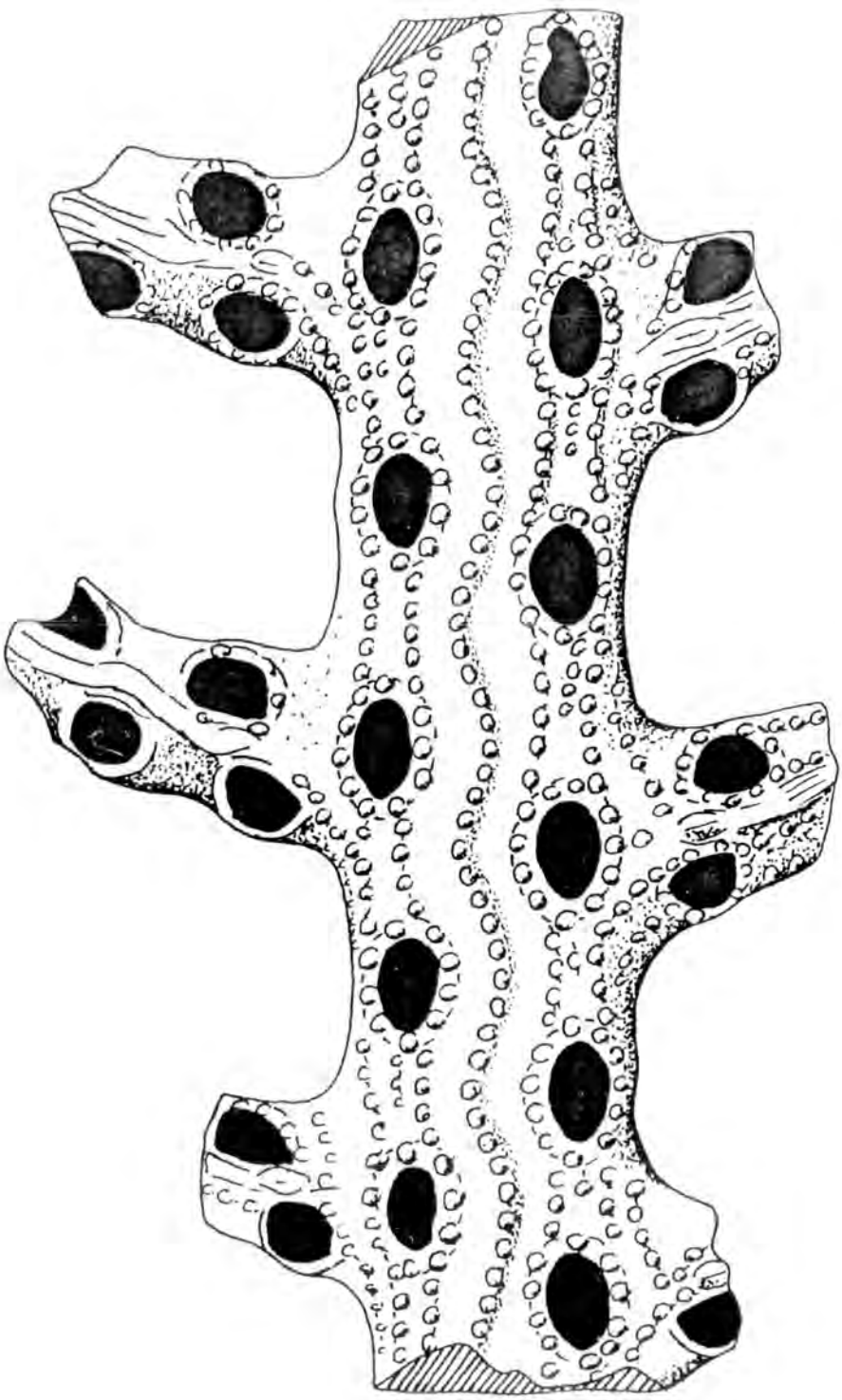

Figure 67. Penniretepora flexicarinata (Young and Young)

Obverse surface detail of the type of Penniretepora recticarinata (Young and Young); here considered to be conspecific with P. flexicarinata. HM D.455. Brigantian, Lower Limestone Group, Dykehead Pit, High Blantyre.
(Bar Scale=1mm)

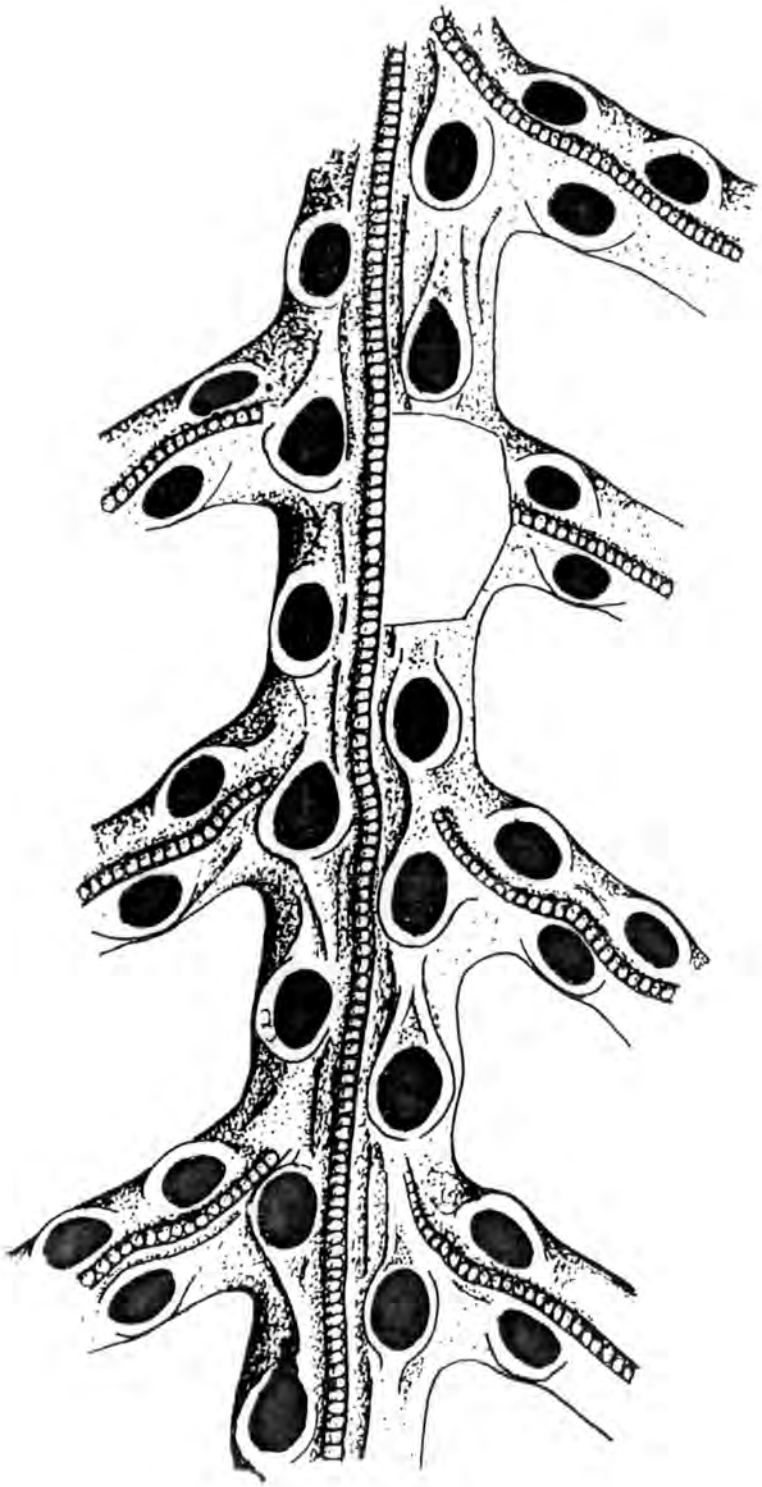

Figure 68. Penniretepora pulcherrima McCoy

Obverse surface detail. HM D.125-8. Brigantian, Lower Limestone Group, Hosie Limestone, Hairmyres, E. Kilbride. (Bar Scale=1mm)

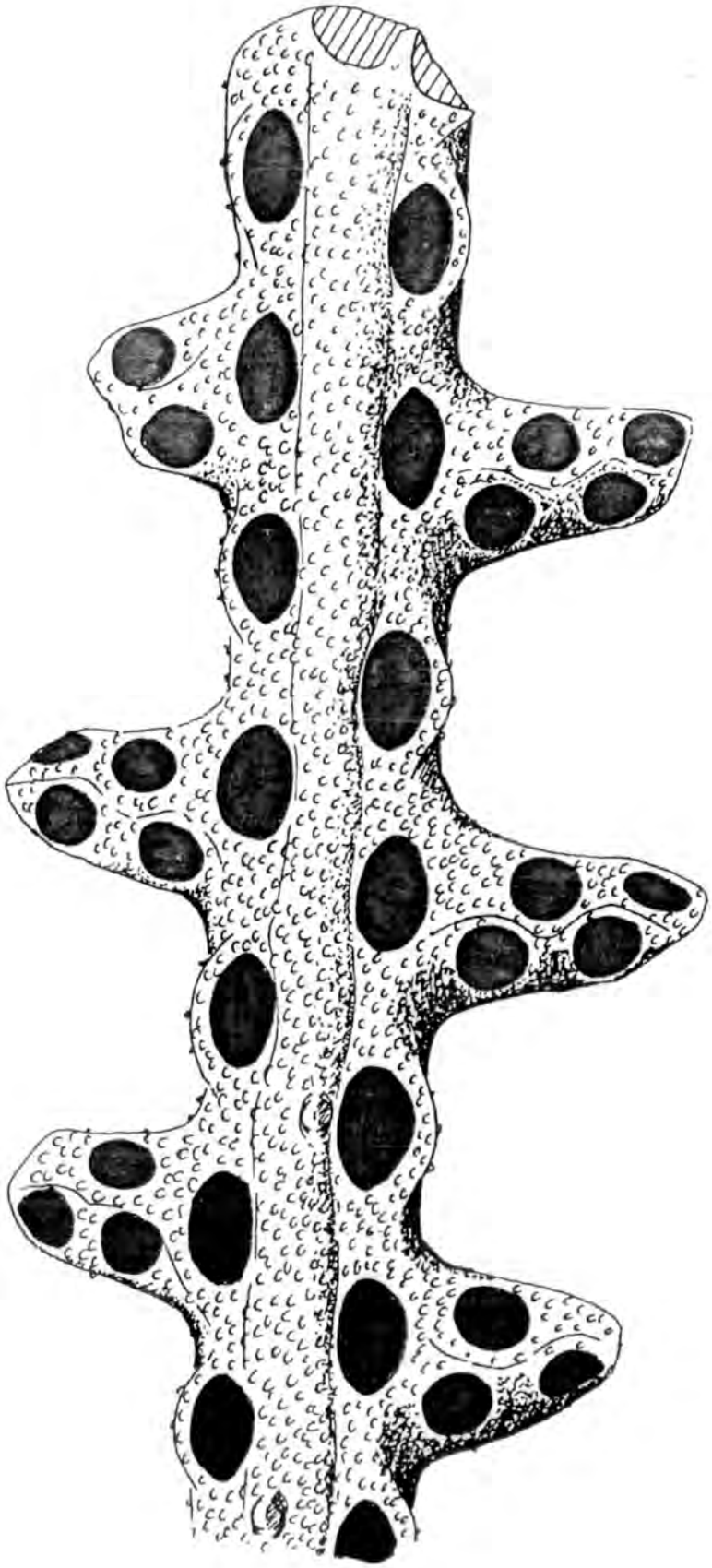

Figure 69. Penniretepora pulcherrima McCoy

Obverse surface detail. HM D.126-7. Brigantian, Lower Limestone Group, Hosie Limestone, Hairmyres, E. Kilbride.

(Bar Scale=1mm)

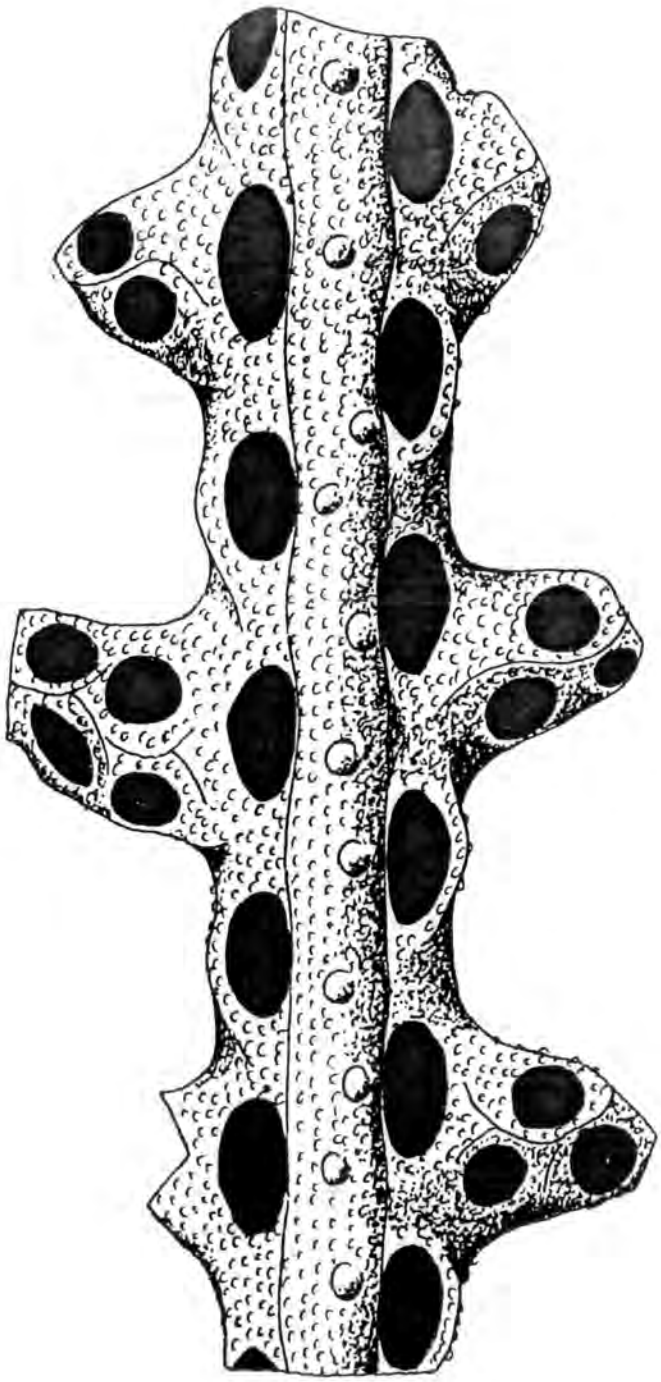

Figure 70. Pennireteporapulcherrima McCoy

Reverse surface detail. HM D.126-8. Brigantian, Lower Limestone Group, Hosie Limestone, Hairmyres, E. Kilbride.

(Bar Scale=1mm)

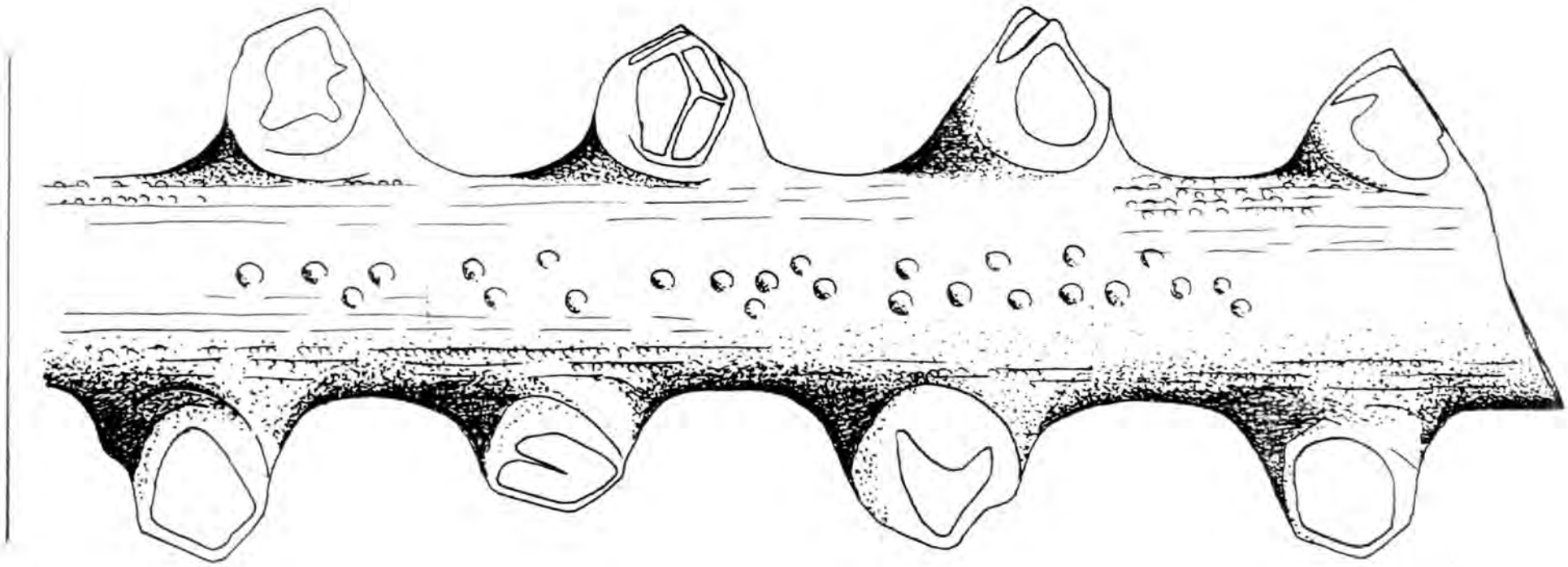

Figure 71. Pennireteporapulcherrima McCoy

Reverse surface detail. HM D.125-7, HM D.126-2.
Both Brigantian, Lower Limestone Group, Hosie Limestone,
Hairmyres, E. Kilbride.
(Bar Scale=1mm)

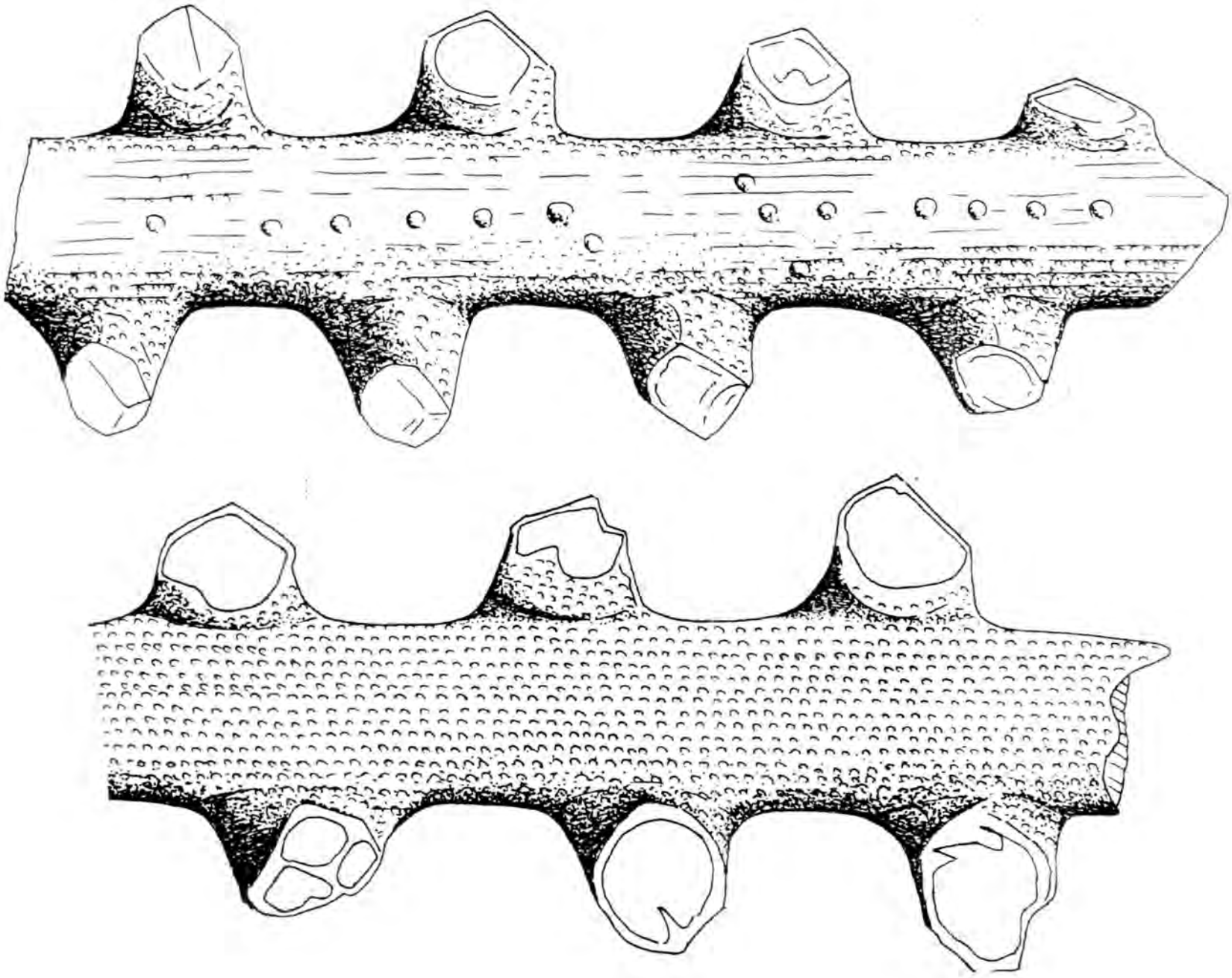

Figure 72. Penniretepora elegans (Young and Young)

Obverse surface detail. HM D.123-1. Brigantian, Lower Limestone Group, Hosie Limestone, Hairmyres, E. Kilbride.

(Bar Scale=1mm)

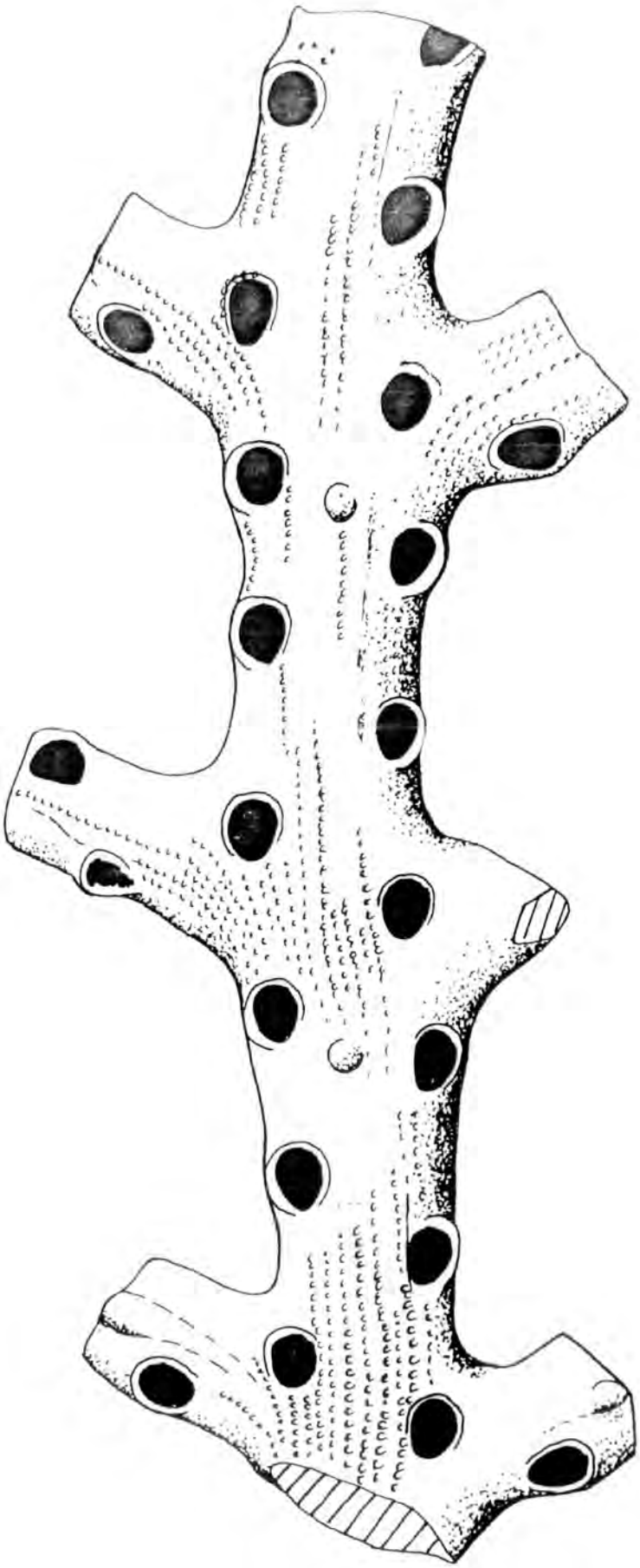

Figure 73. Penniretepora elegans (Young and Young)

Obverse surface detail. HM D.124-4. Brigantian, Lower Limestone Group, Hosie Limestone, Hairmyres. E. Kilbride.

(Bar Scale=1mm)

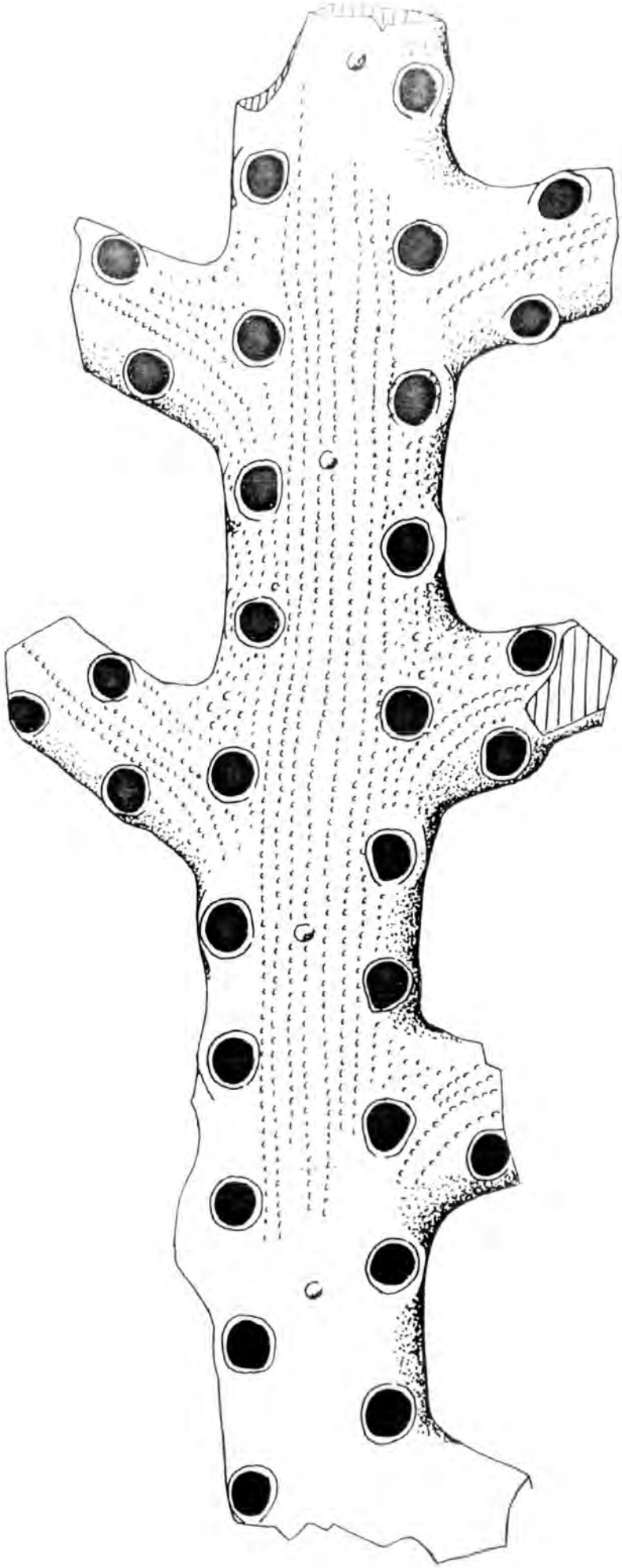

Figure 74. Penniretepora elegans (Young and Young)

Reverse surface detail. HM D.123-21. Brigantian, Lower Limestone Group, Hosie Limestone, Hairmyres, E. Kilbride.

(Bar Scale=1mm)

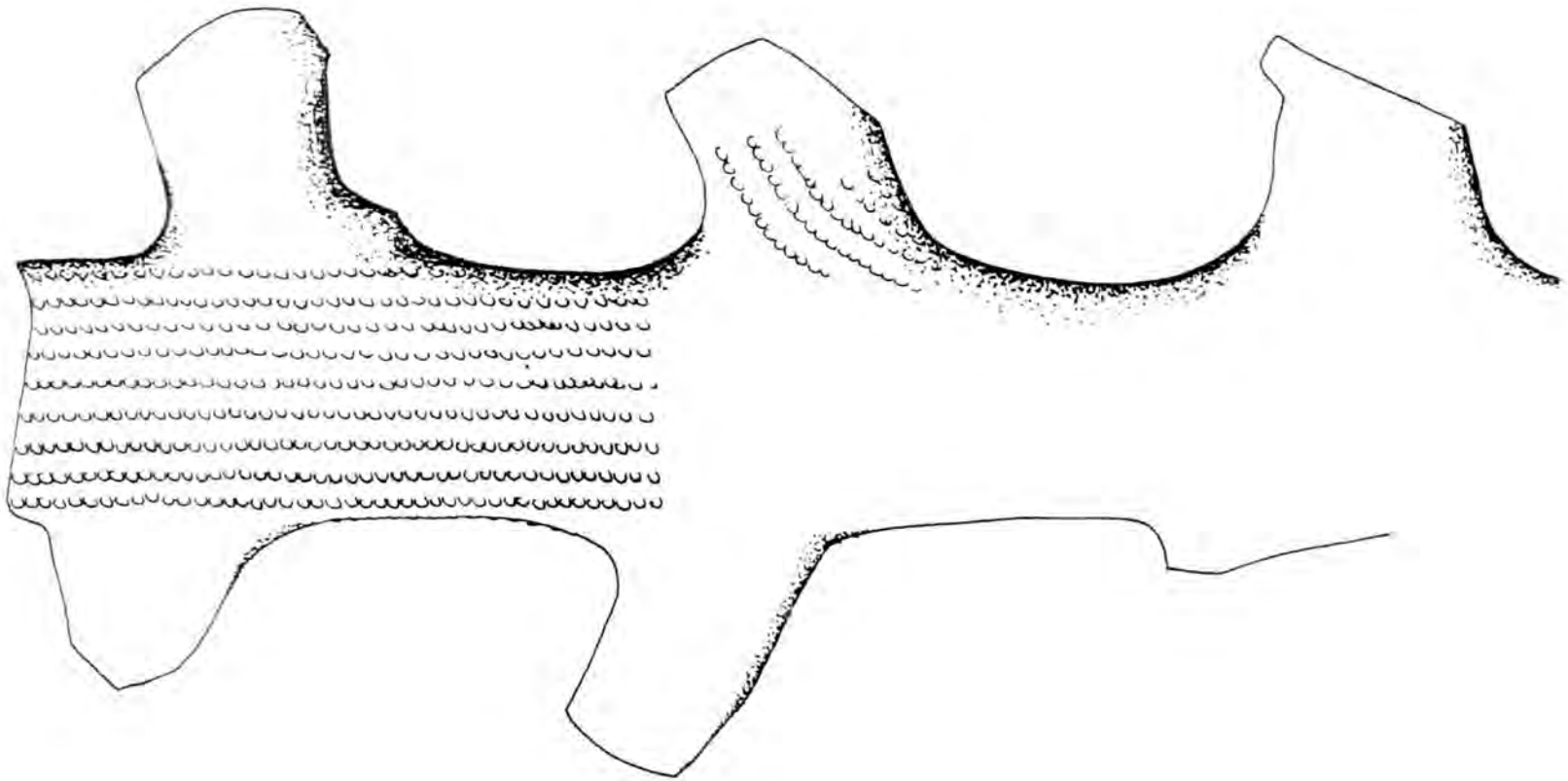

Figure 75. Penniretepora laxa (Young and Young)

Obverse surface detail. HM D.131-8. Brigantian, Lower Limestone Group, Hosie Limestone, Hairmyres, E. Kilbride.

(Bar Scale=1mm)

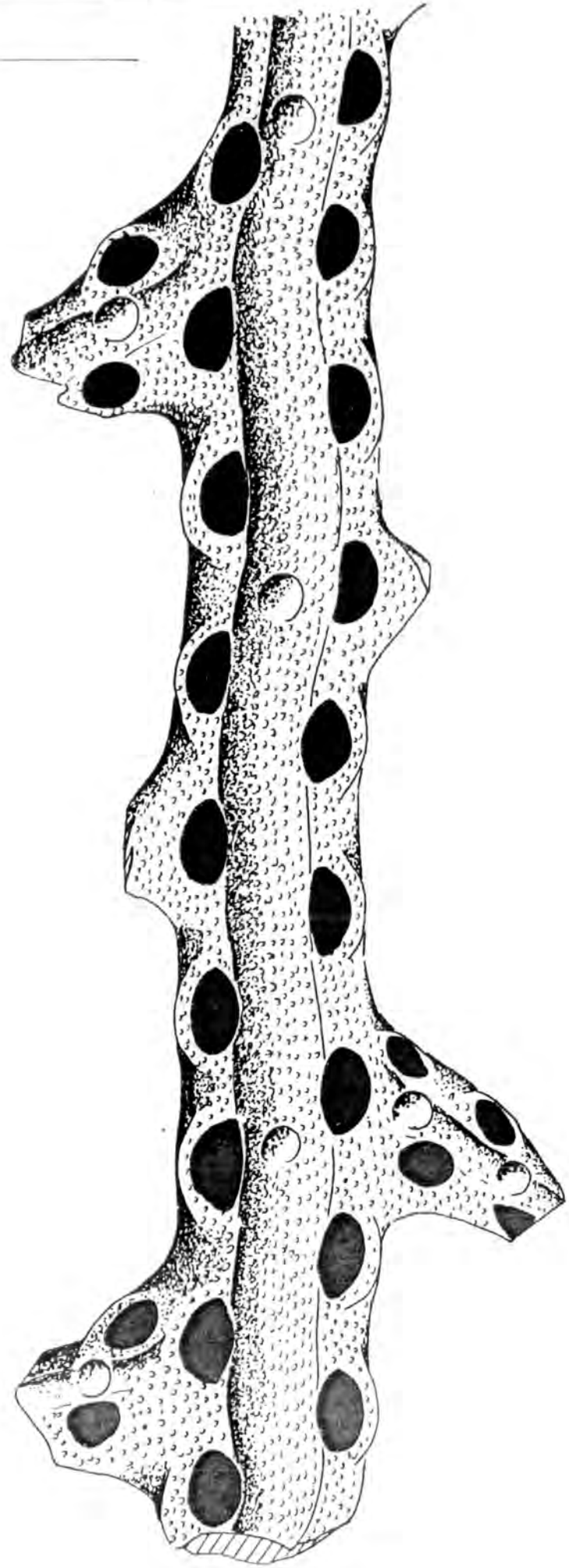

Figure 76. Penniretepora laxa (Young and Young)

Reverse surface detail. HM D.131-3. Brigantian, Lower Limestone Group, Hosie Limestone, Hairmyres. E. Kilbride.

(Bar Scale=1mm)

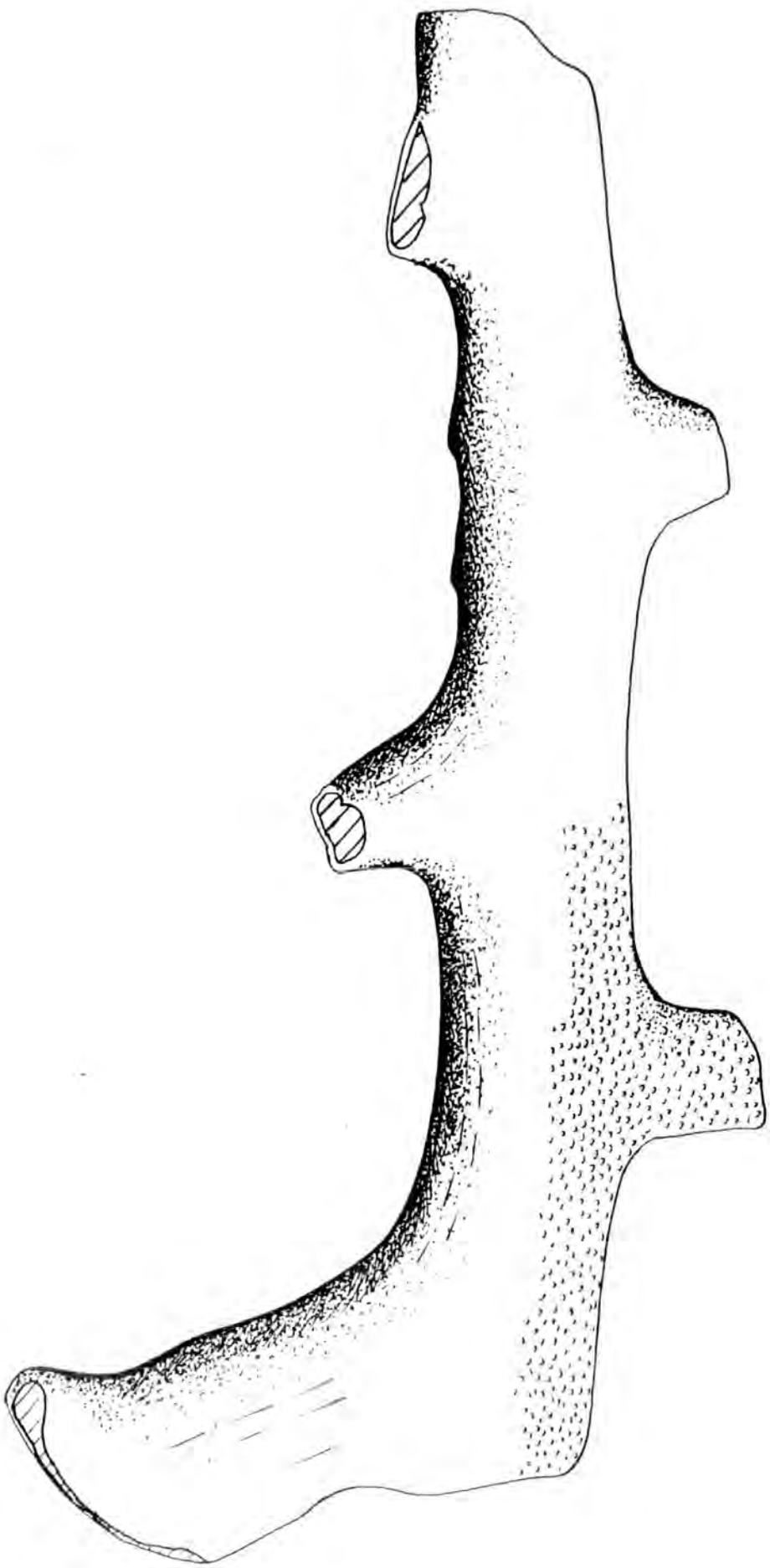

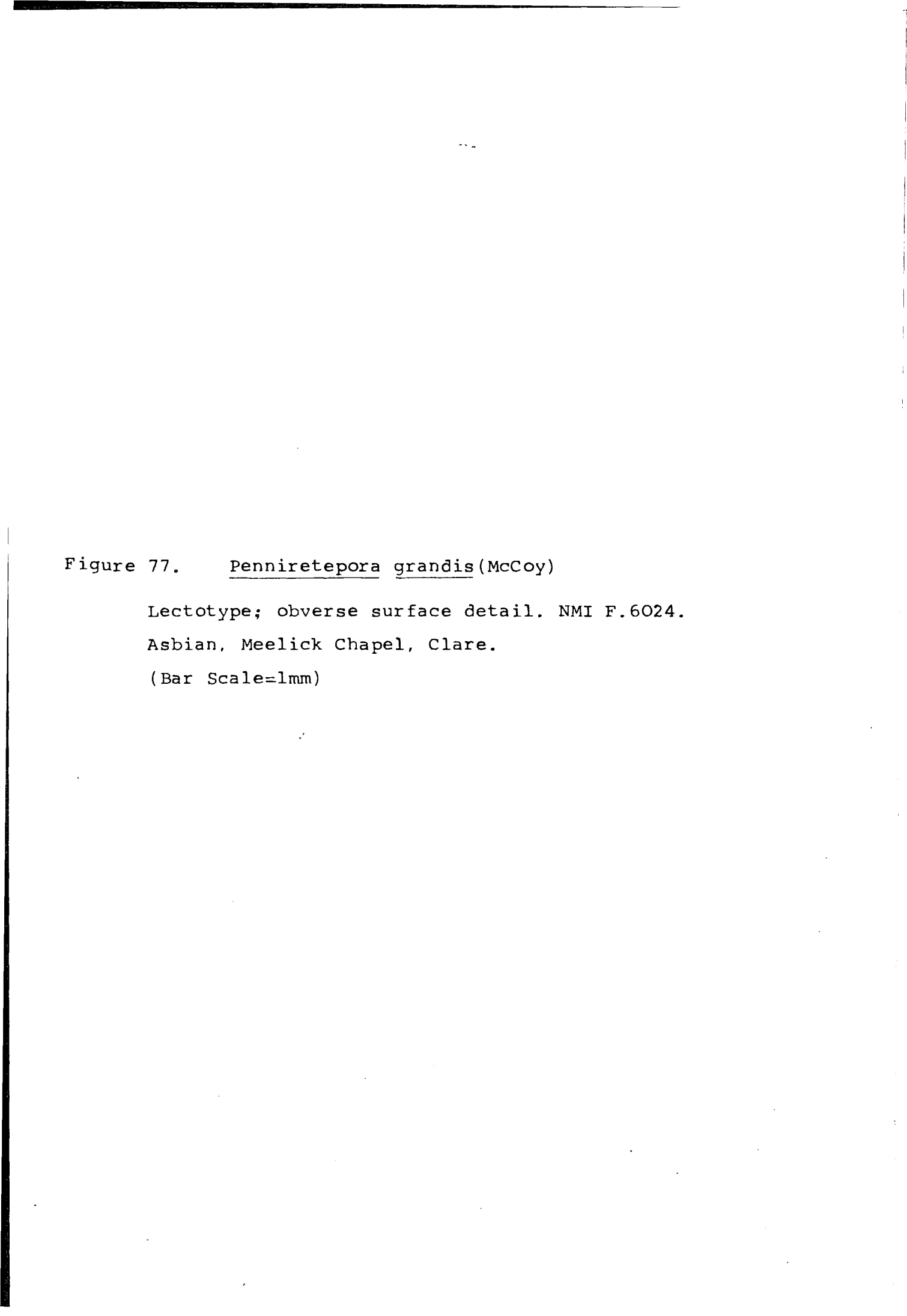

Figure 77. Penniretepora grandis (McCoy)

Lectotype; obverse surface detail. NMI F.6024.

Asbian, Meelick Chapel, Clare.

(Bar Scale=1mm)

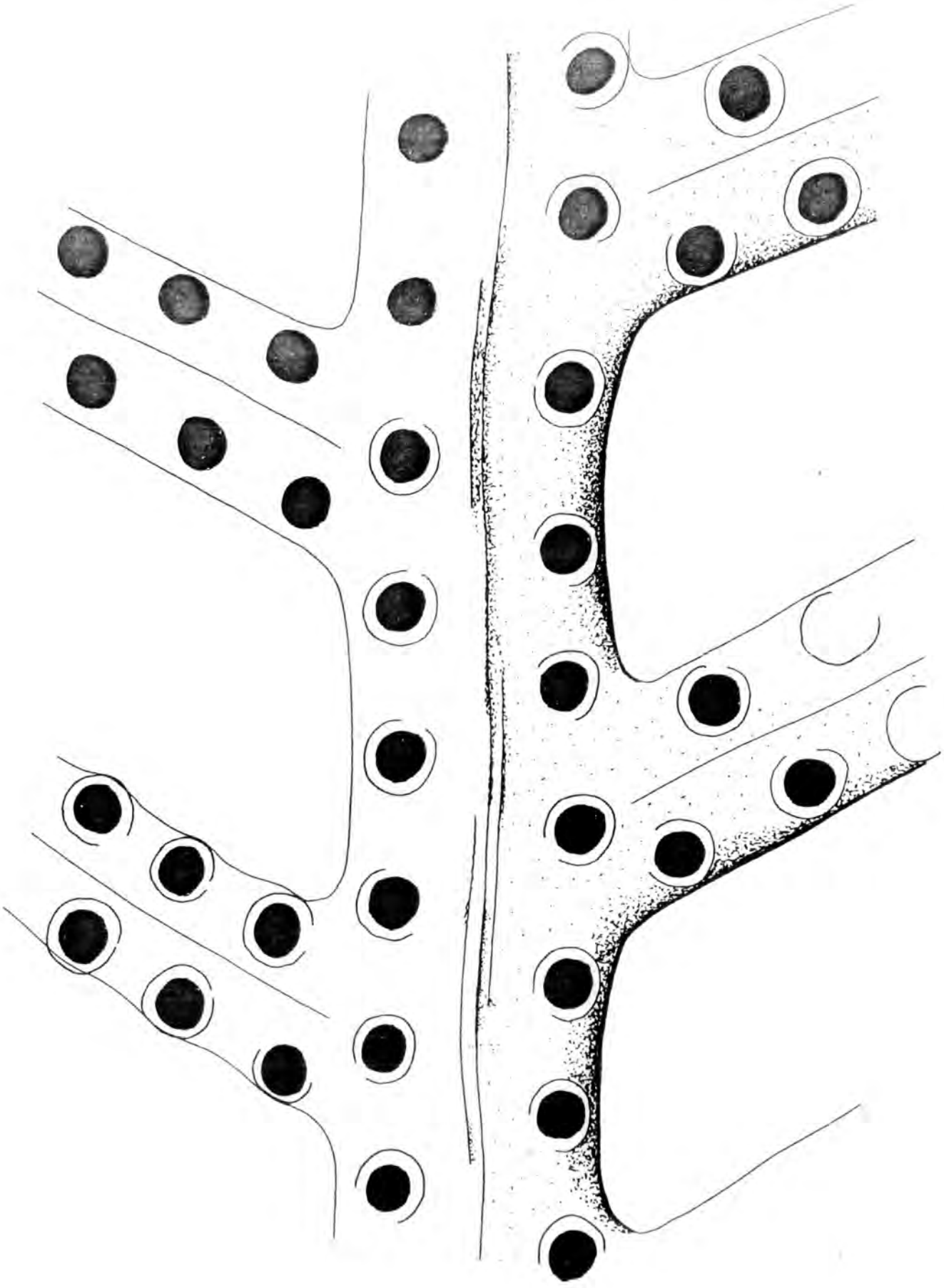

Figure 78. Diagram to show the morphological characters measured on trepostomes in the present study (For explanation of characters see text pp. 351-352)

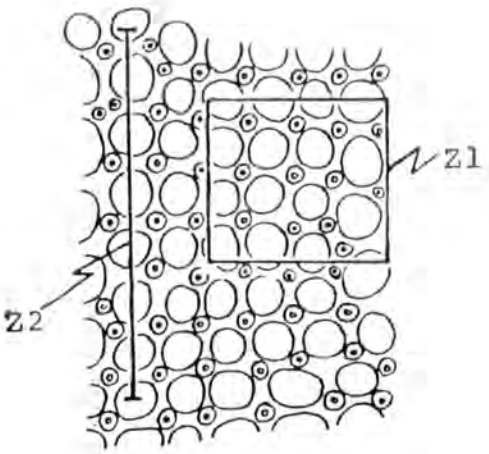
Z1
Z2

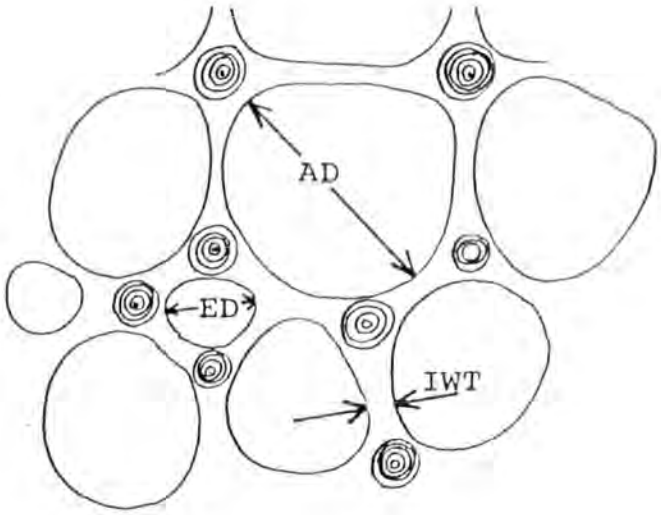
AD
ED
IWT

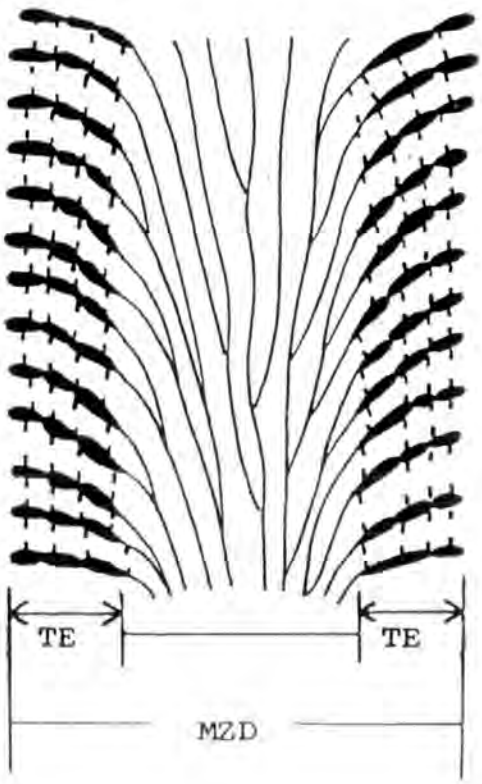
TE
TE
MZD

Figure 79. Zoarial Growth in Tabulipora

Diagram to show the incremental nature of zoarial growth in Tabulipora. A single increment (eg. a) consists of a posterior thin walled portion and an anterior thick walled portion - the monila. In all increments the central endozone portion is much longer than the corresponding exozone wall phase. The length of the wall in one increment decreases towards the exozone region continuing into the exozone where short exozone wall phases of successive increments may merge (eg. b).

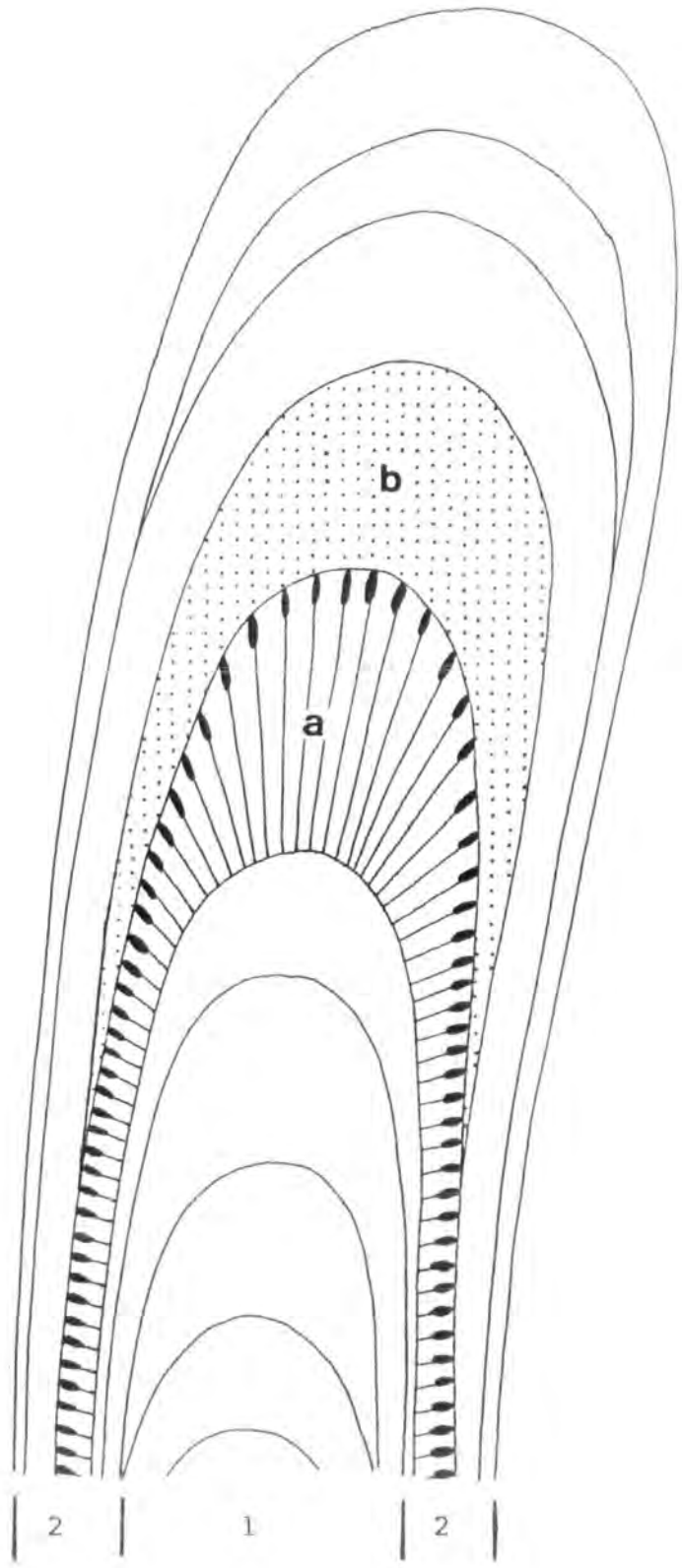

1-Endozone Region

2-Exozone Region

Figure 80. Growth of a tabuliporian ring septum indicated at selective successive stages (after Gautier 1970)

(a) A small infold of the wall laminae is developed close to the autozooecial aperture and extends part of the way around the zooecial cavity.

(b) The fold is made wider and longer by continued laminae deposition around it.

(c) The infold extends around the entire zooecial cavity. The foramen has reached its optimum size and the surrounding septal rim is thickened.

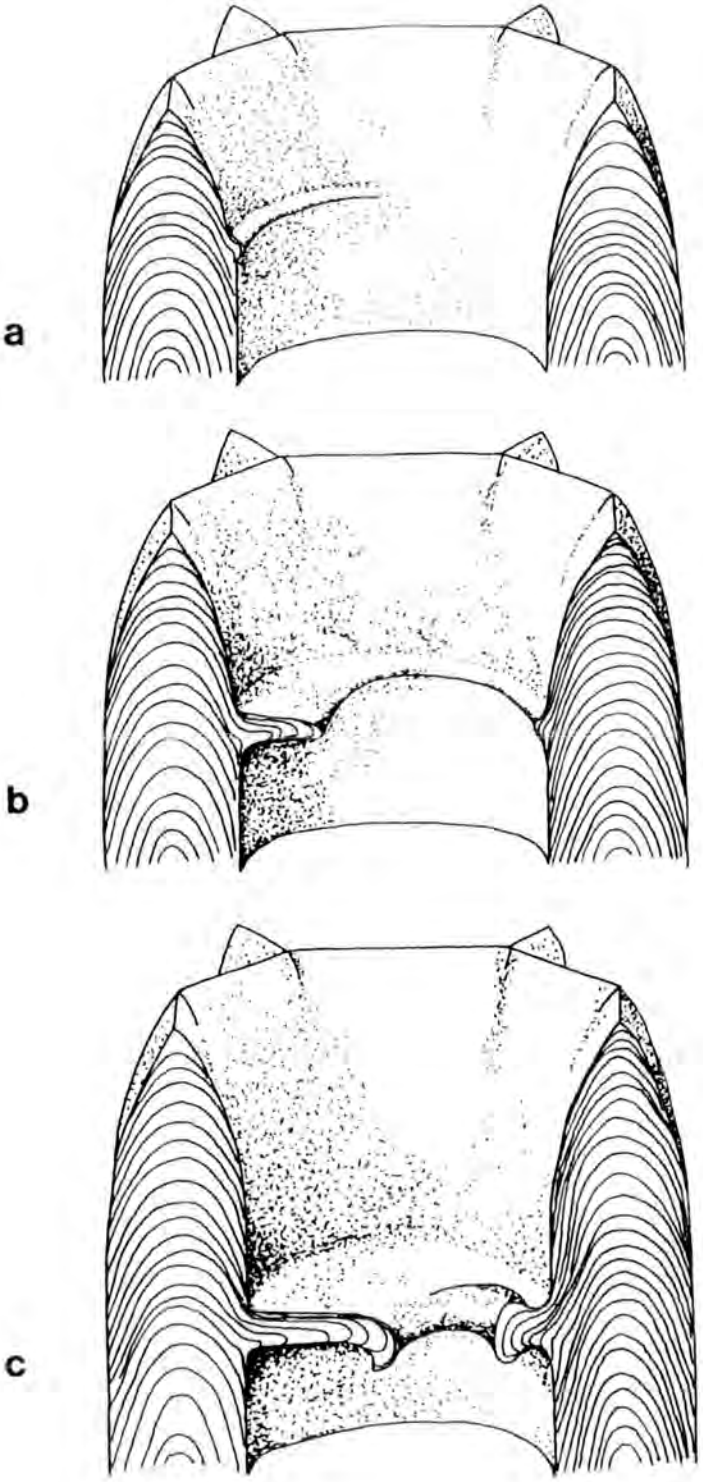
a
b
c

Figure 81. Microstructural detail of the growth of a tabuliporian ring septum

(a) A small infold of the wall laminae is developed; initially laminae of the infold are coninuous with wall laminae on anterior and posterior sides of the infold but not so distally.

(b) The infold is made longer; the dominant deposition of laminae is in a plane slightly oblique to the septums anterior surface. Proximally laminae are still partly continuous with wall laminae but not so distally.

(c) The infold still increases in length and a posterior thickening is developed with the deposition of laminae away from the anterior surface at an increased angle.

(d) The anterior portion of the septal rim is thickened by the addition of laminae onto its anterior surface.

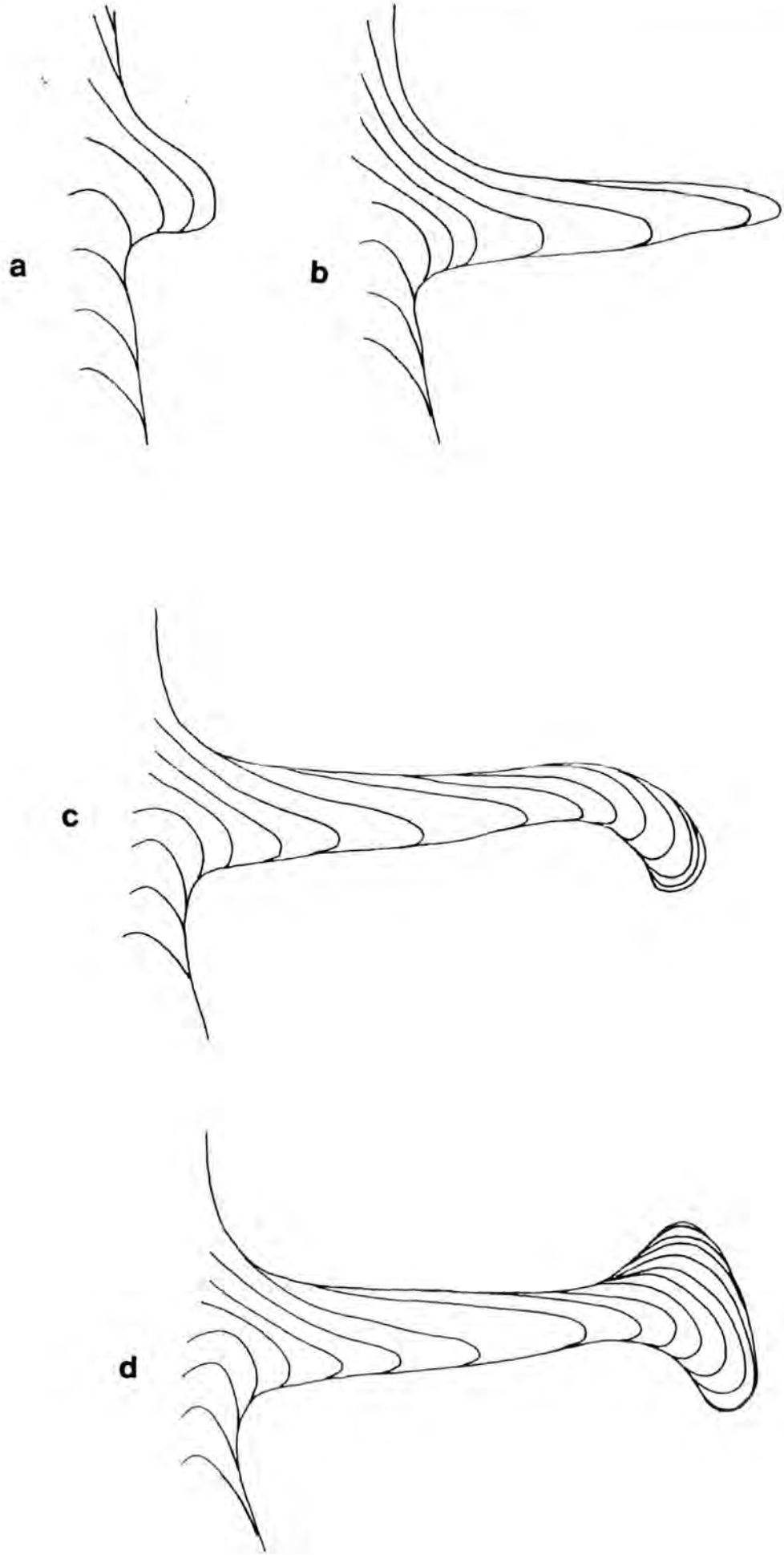
a
b
c
d

Figure 82. Diagram showing the growing edge of a colony and the successive stages of development of autozooecia in fistuliporid cystoporates.

Most new autozooecia are developed on the basal lamina and are isolate, separated by vesicular tissues. However some new autozooecia may develop above the basal lamina directly on older vesicular tissues (e.g. A). Autozooecia have a short recumbent portion and soon become erect diverging to the zoarial surface at high angles.

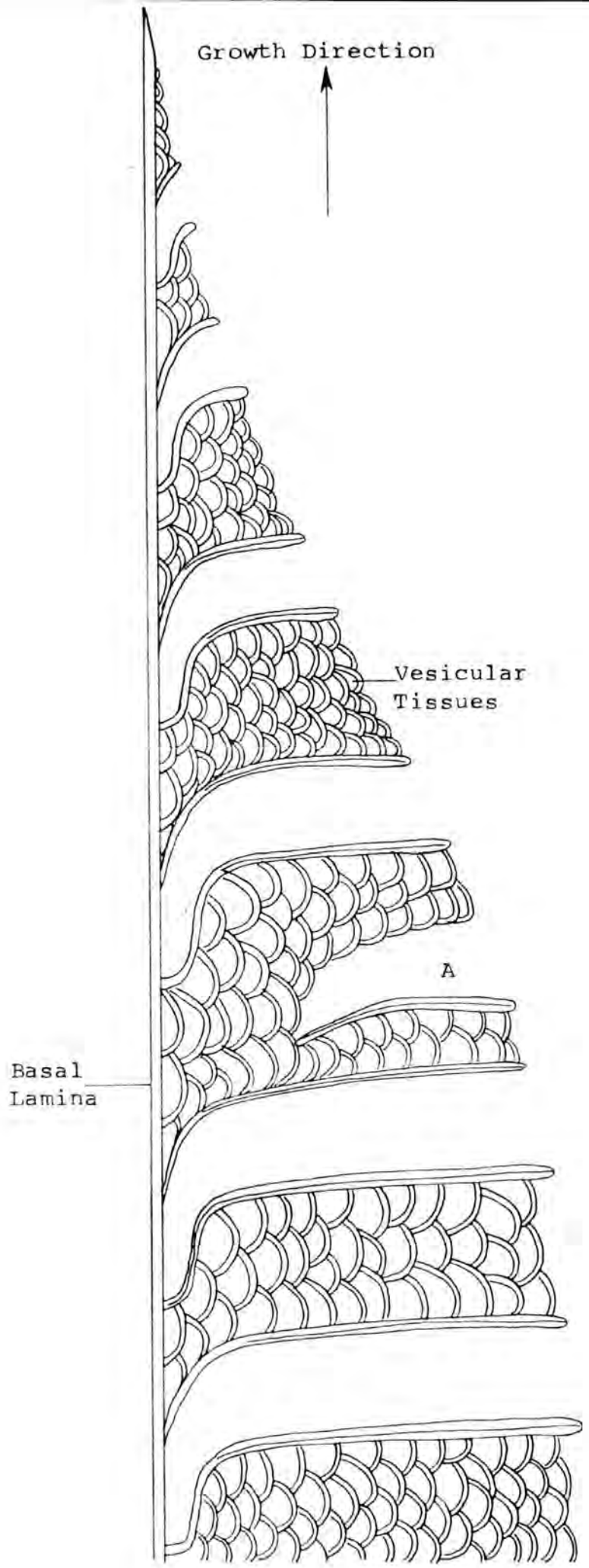
Growth Direction
Vesicular
Tissues
A
Basal
Lamina

Figure 83. Diagram showing the variation in apertural shape and wall thickness with ontogeny in fistuliporids

Section a-b. Immature portion; the autozooecium is recumbent and has a hemispherical cross-section.

Section c-d. Early mature portion; the autozooecium is now erect and has a cylindrical cross-section. The proximal lunarial wall has a slightly greater width than lateral and distal walls (with which it is structurally continuous in this case).

Section e-f. Fully mature autozooecium. The proximal lunarial wall is fully developed and is significantly thicker than lateral and distal walls.

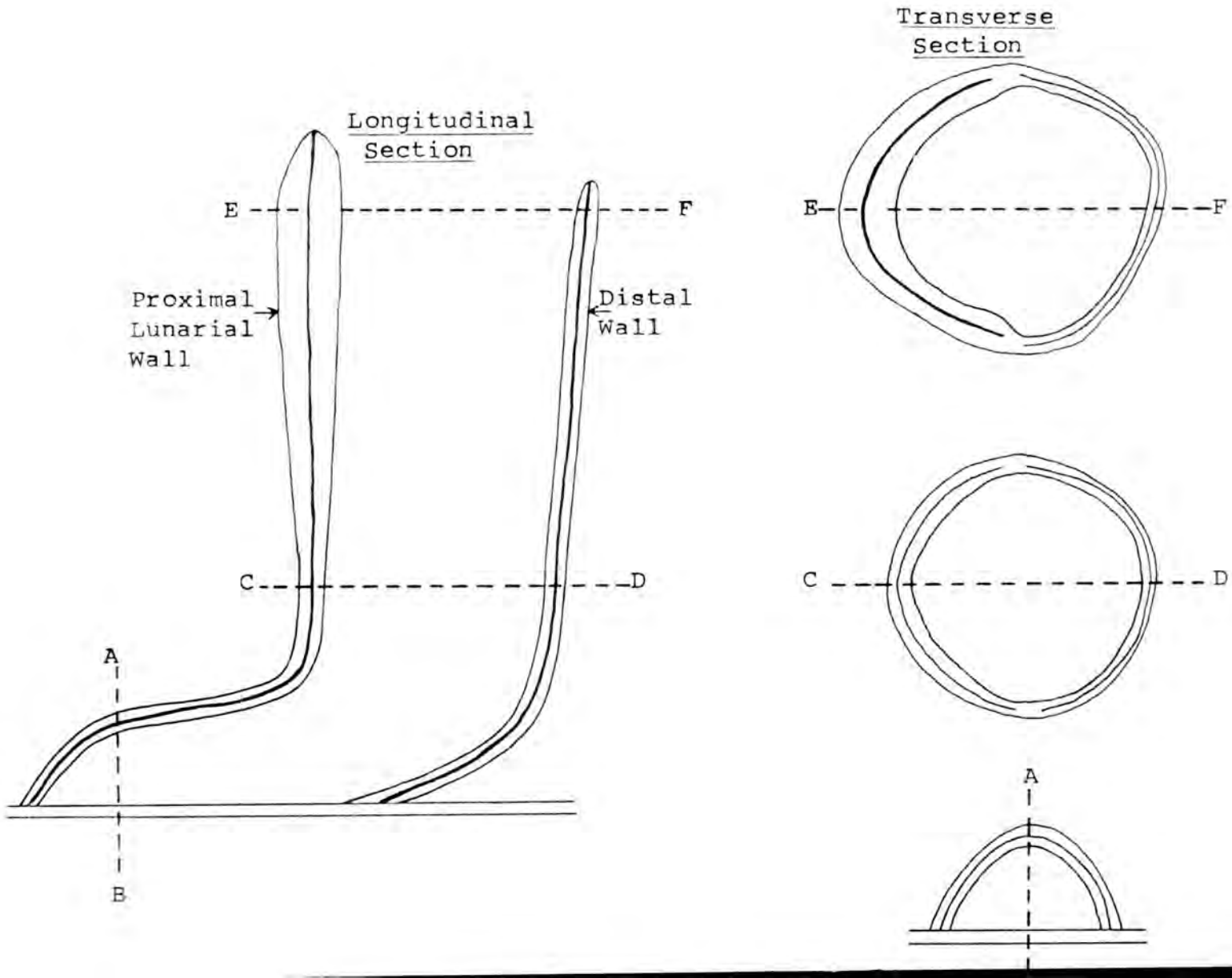
Longitudinal Section
E
F
Proximal Lunarial Wall
Distal Wall
C
D
A
B
Transverse Section
E
F
C
D
A

Figure 84. Diagram showing the variation in the shape, size and stacking of vesicles in longitudinal section in a fistuliporid

Close to the basal lamina where autozooecia are recumbent vesicles form large well rounded irregularly stacked hemispherical units. Distally where autozooecia are erect vesicles form inverted cup-like to box-like units and are more regularly arranged in vertical stacks.

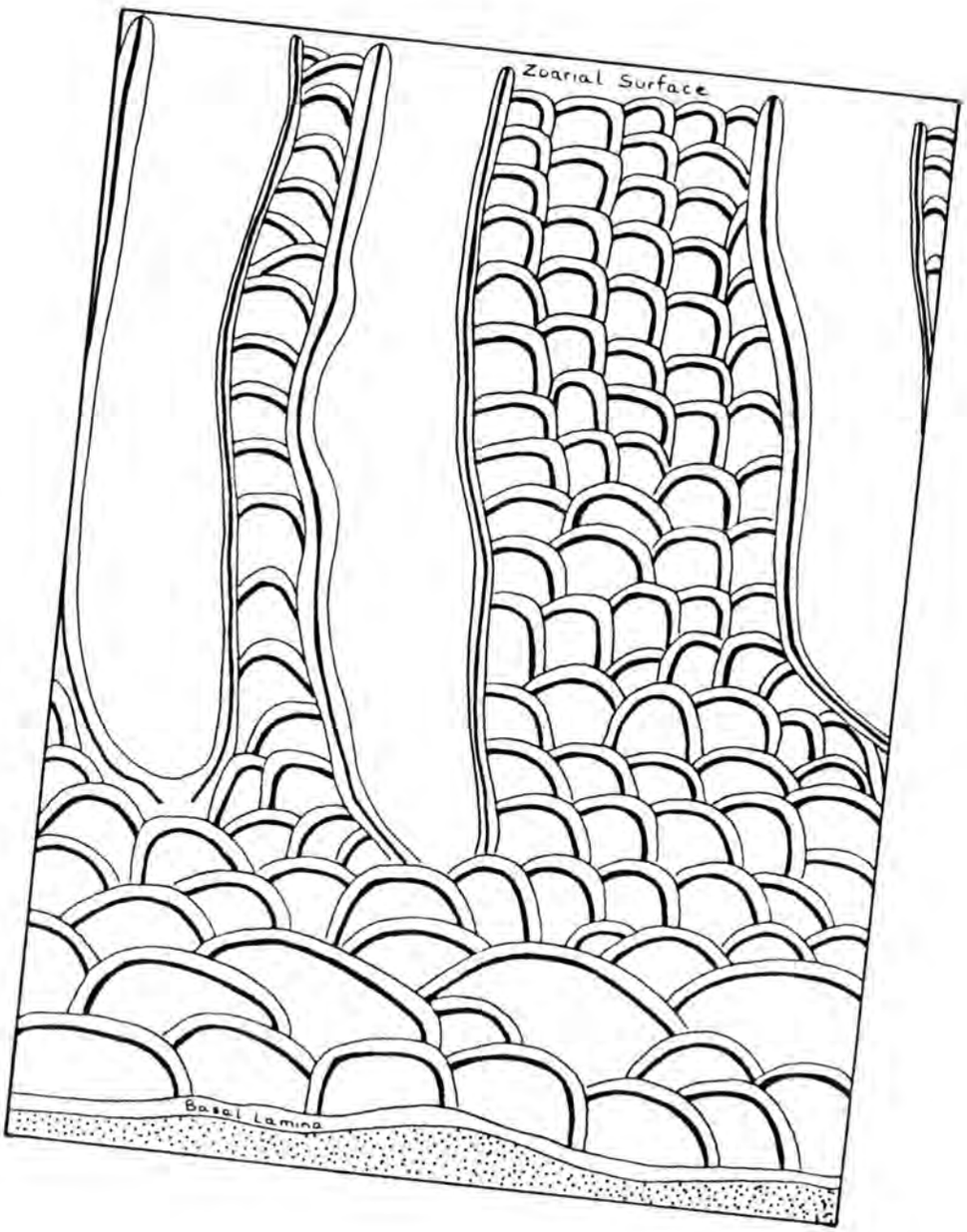
Zoarial Surface
Basal Lamina

Figure 85. Autozooecial Wall Composition in Fistuliporids

Longitudinal Section

(A) The entire wall is compound; the compound proximal lunarial wall is structurally continuous with compound lateral and distal zooecial walls. A low peristome-like rim is developed around apertures on lateral and distal walls away from the proximal lunarium.

(B) Only the proximal lunarial wall is compound, lateral and distal walls are simple and are composed of superimposed vertical stacks of vesicular tissues. As a result lateral and distal walls are quite undulatory.

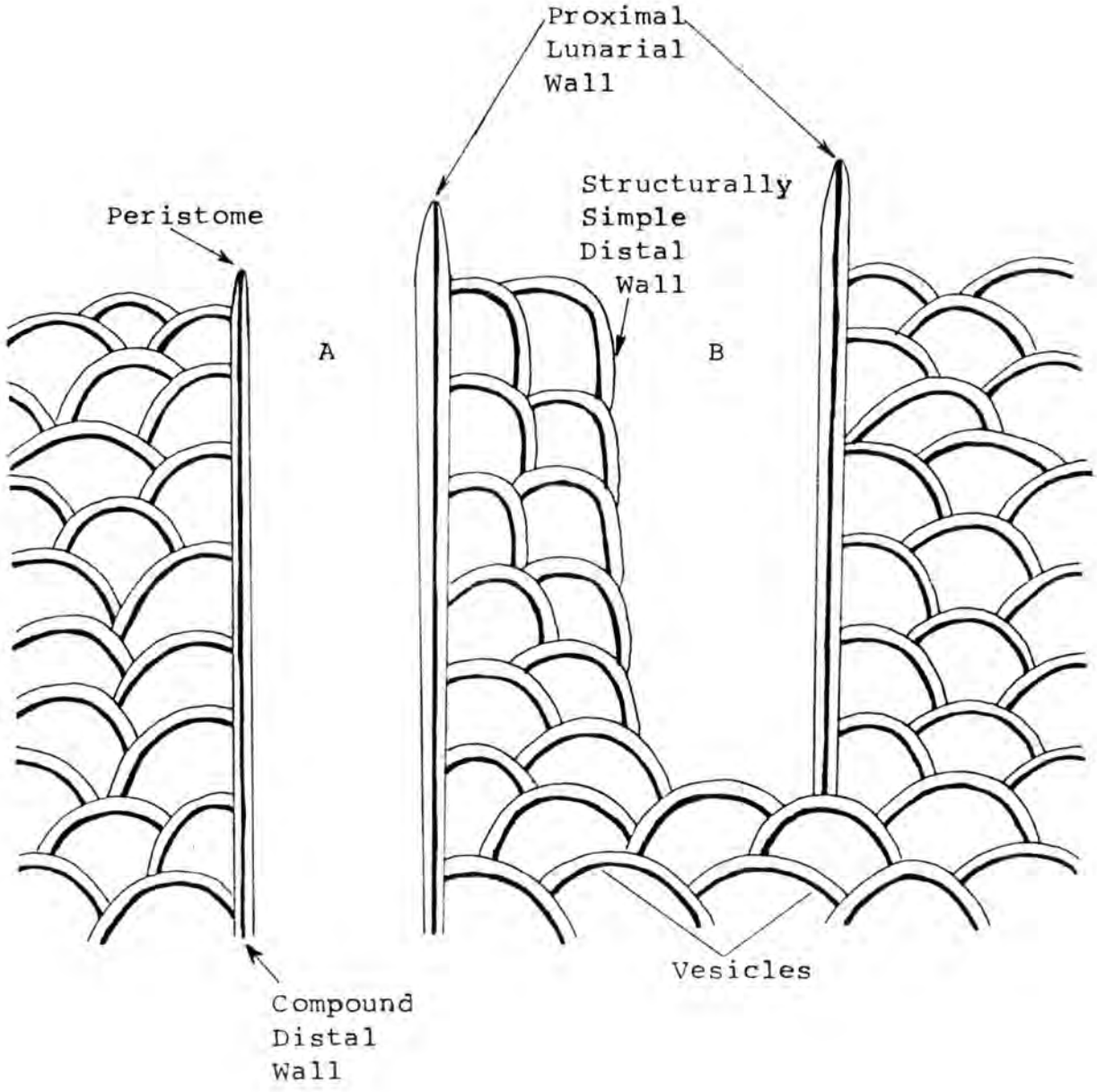
Proximal
Lunarial
Wall
Peristome
Structurally
Simple
Distal
Wall
A
B
Vesicles
Compound
Distal
Wall

Figure 86. Autozooecial Wall Composition in Fistuliporids

Tangential Section

(A) The entire wall is compound, and the compound proximal lunarial wall is microstructurally continuous with the compound lateral and distal walls.

(B) Only the proximal lunarial wall is compound. Lateral and distal walls are simple and are composed of superimposed vertical stacks of vesicles and abut abruptly against the apices of the proximal lunarial wall.

(C) As for B, but the distal apices of the compound proximal lunarial wall curve inwardly and project into the zooecial cavity.

(A) Proximal Lunarial Wall (PLW)

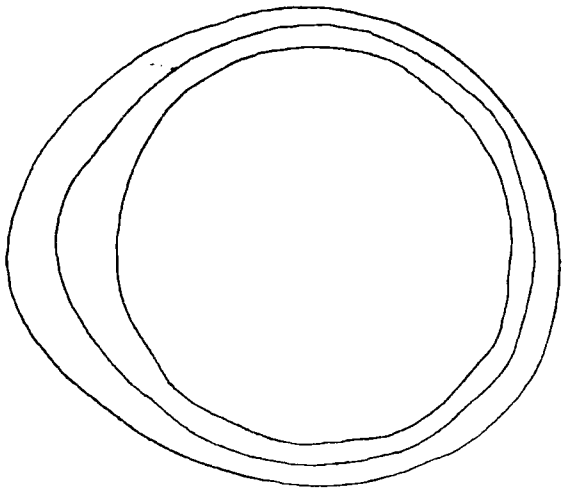

(B) PLW

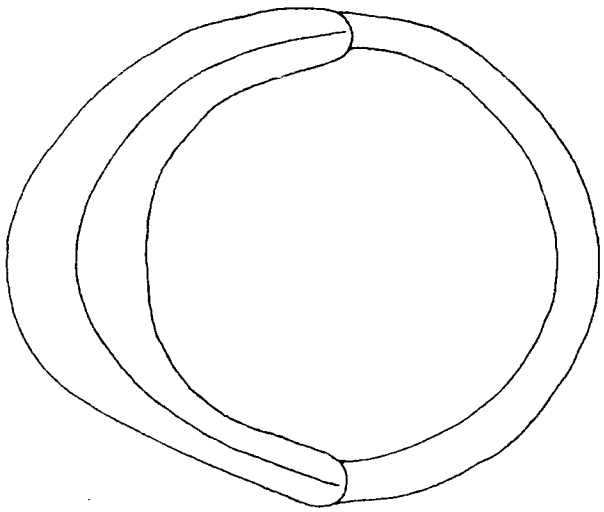

(C) PLW

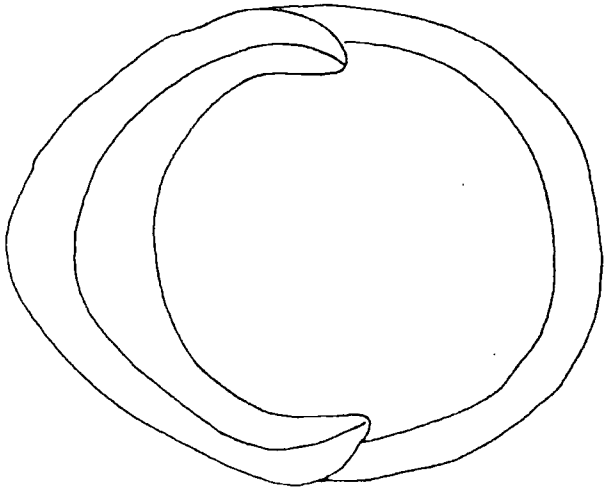

Figure 87. Diagram to show the morphological characters measured on fistuliporids in the present study. (For explanation of characters see text pp. 430 - 432)

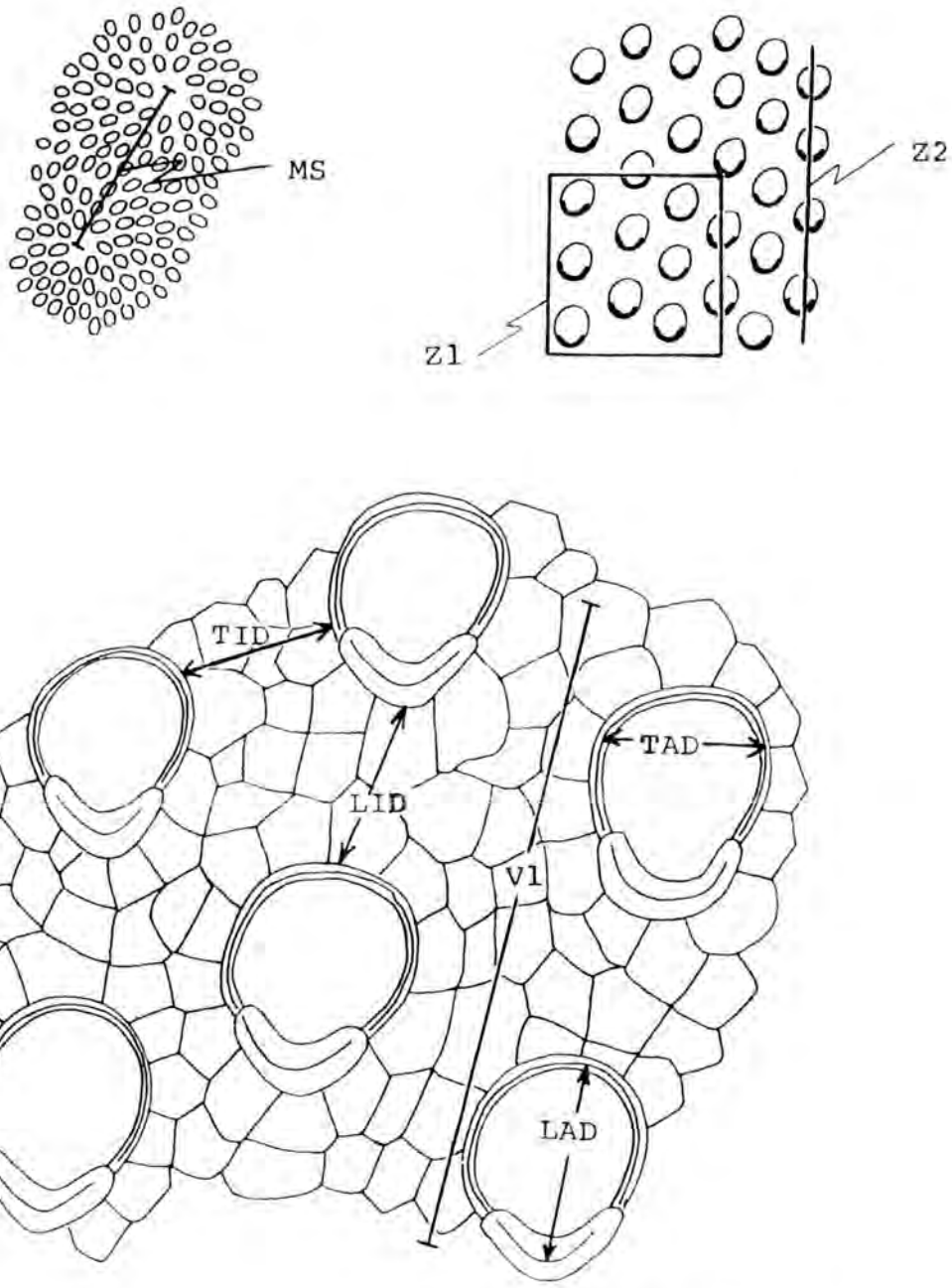
MS
Z2
Z1
TID
TAD
LID
V1
LAD
V2
LW
LD
LT

Figure 88. Fistulipora incrustans(Phillips)

Tangential section. ABHR 123. Arnsbergian, shales above the Main Limestone, Hurst, N. Yorkshire. (Bar Scale=1mm)

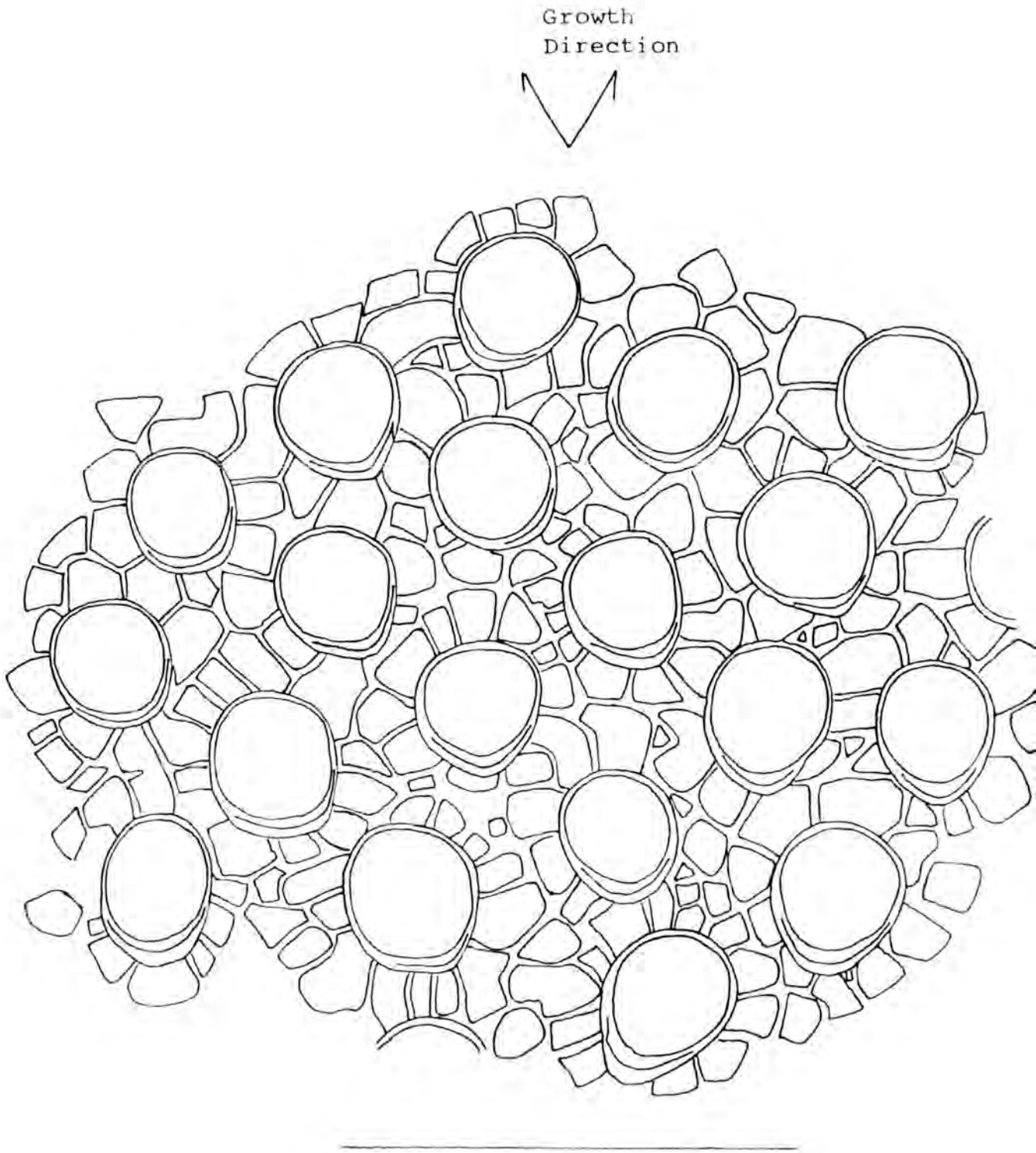
Growth
Direction

Figure 89. Fistulipora incrustans (Phillips)

Longitudinal section of a colony encrusting a branch of Dyscritella miliaria (Nicholson). ABR 212. Asbian, Lower Limestone Group, Redesdale Ironstone Shale, Ridsdale, Northumberland.

(Bar Scale=1mm)

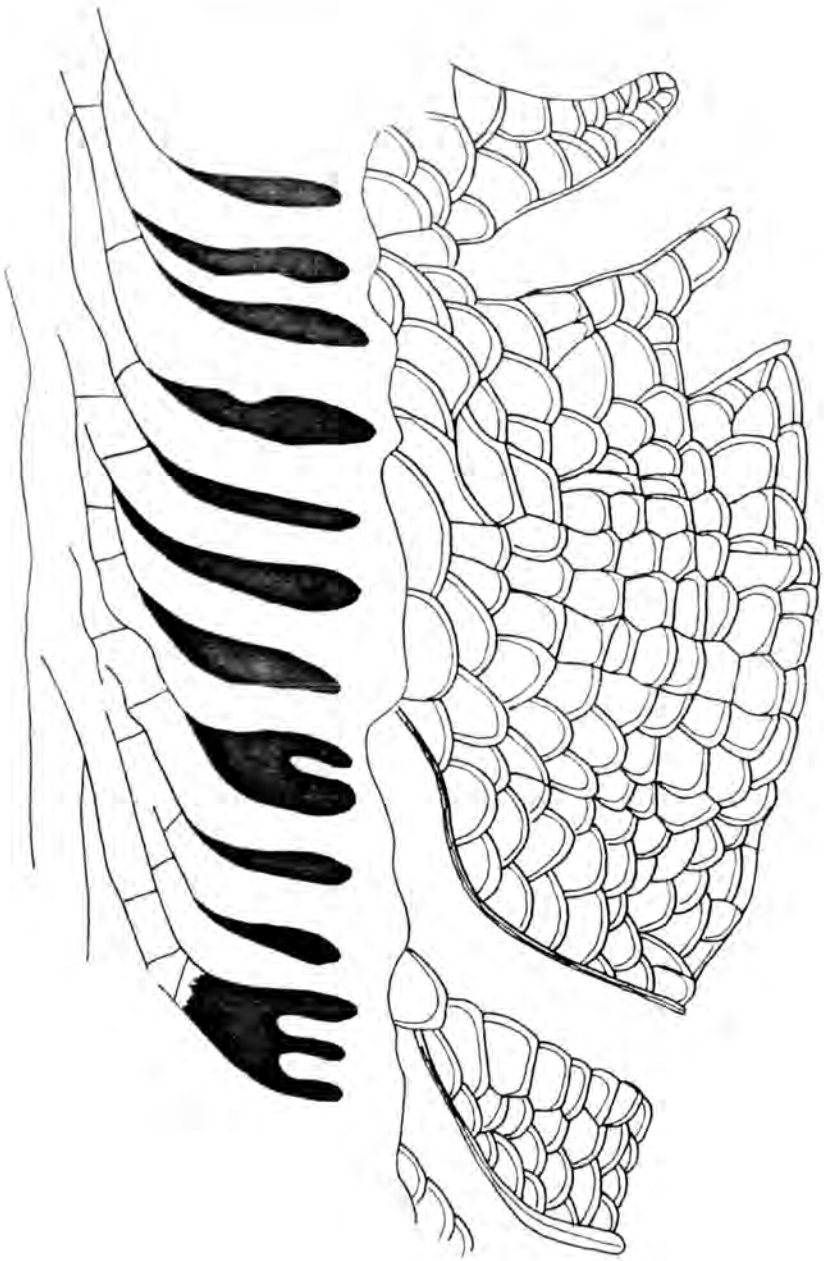

Figure 90. Eridopora beilensis Perkins and Perry

Tangential section. ABHR 101. Arnsbergian, shales above the Main Limestone, Hurst, N. Yorkshire. (Bar Scale=1mm)

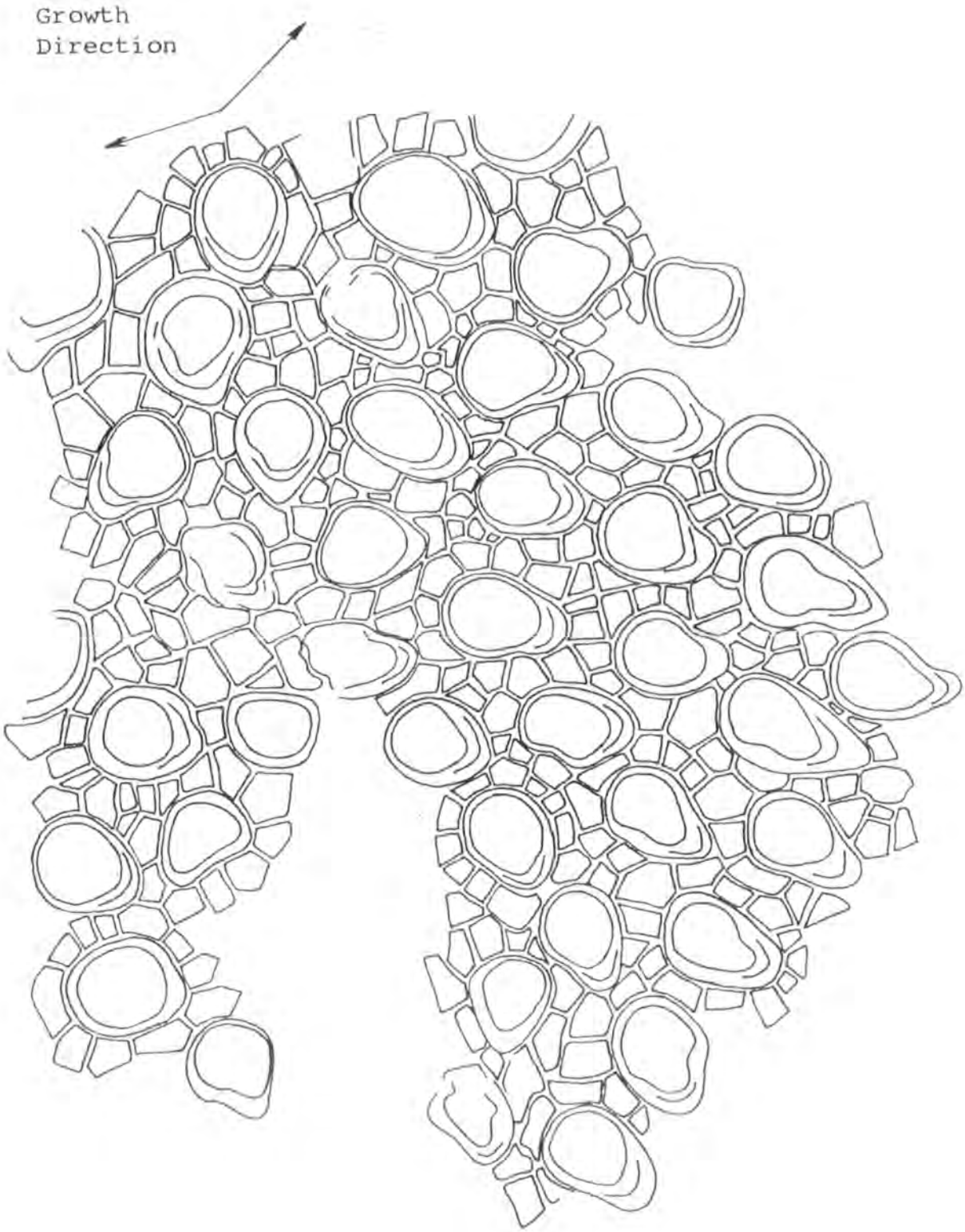
Growth
Direction

Figure 91. Eridopora macrostoma Ulrich

Tangential section showing the radial arrangement of autozooecial apertures around a monticule-like growth centre, also the poor development of vesicles. ABHR 116. Arnsbergian, shales above the Main Limestone, Hurst, N. Yorkshire.
(Bar Scale=1mm)

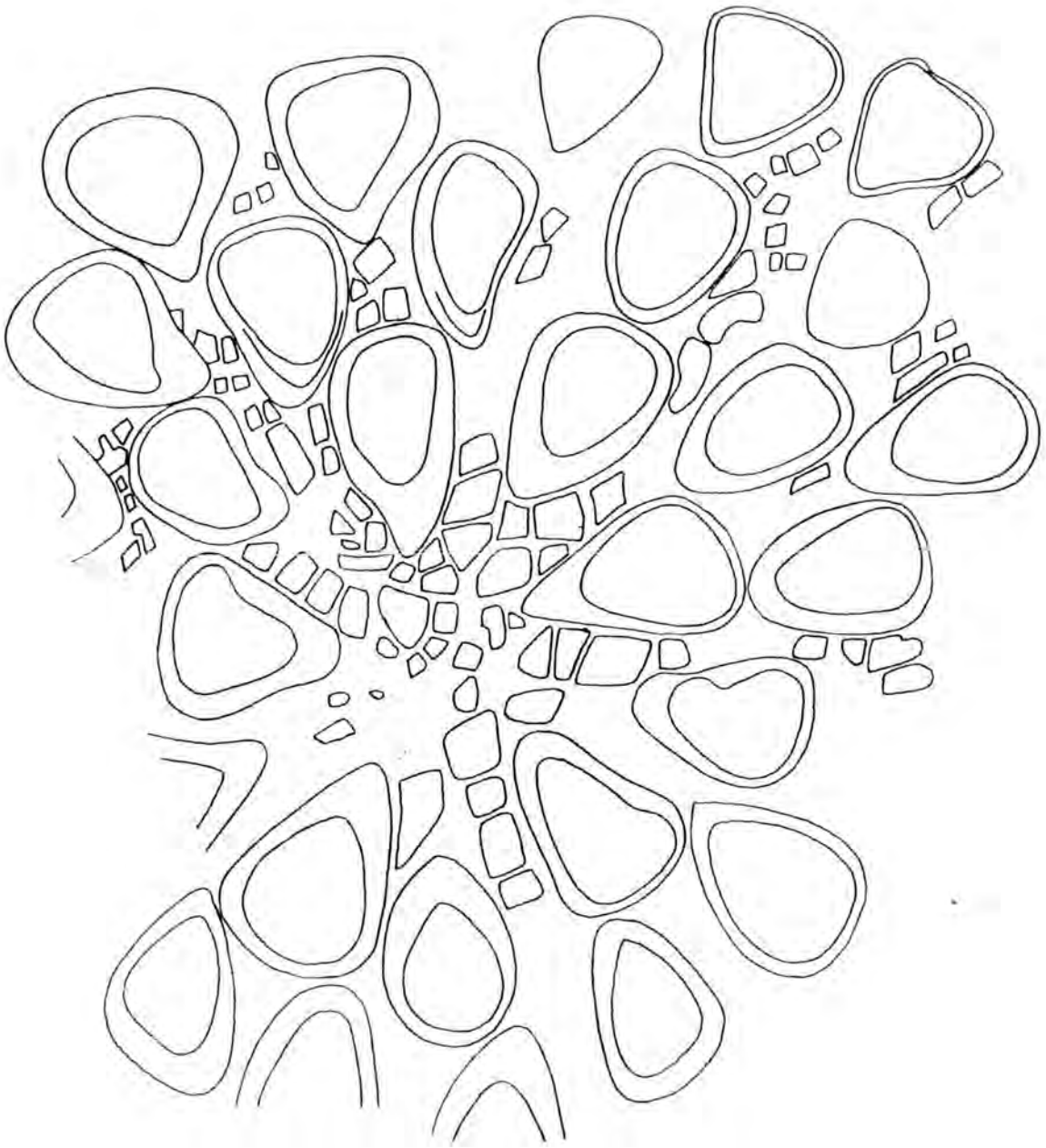

Figure 92. Eridopora macrostoma Ulrich

Longitudinal section showing the close spacing of autozooecial apertures and poor development of vesicles. ABHR 117. Arnsbergian, shales above the Main Limestone, Hurst, N. Yorkshire.
(Bar Scale=1mm)

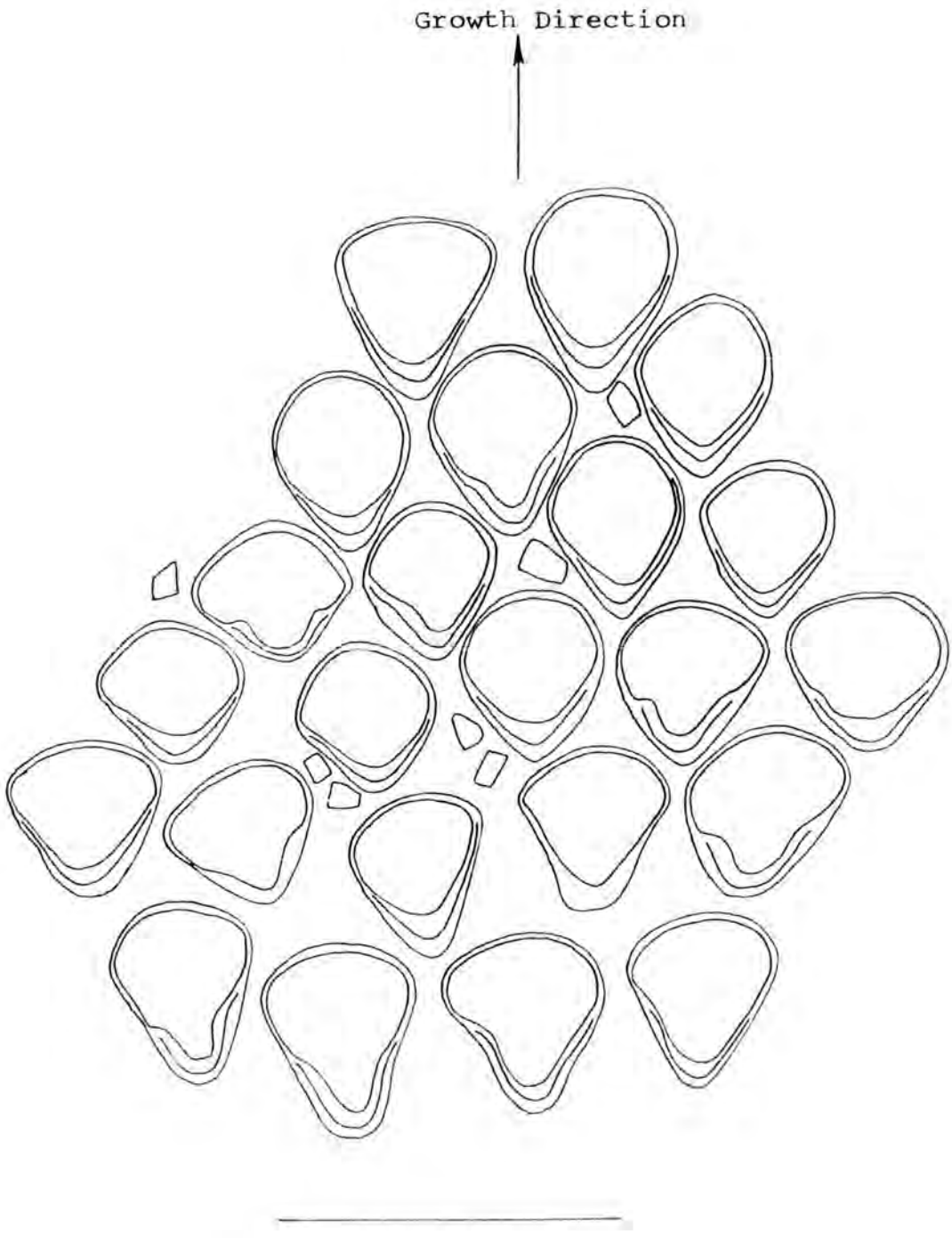
Growth Direction

Figure 93. Diagram to show the morphological characters measured on Goniocladia cellulifera in the present study. (For explanation of characters see text p.455)

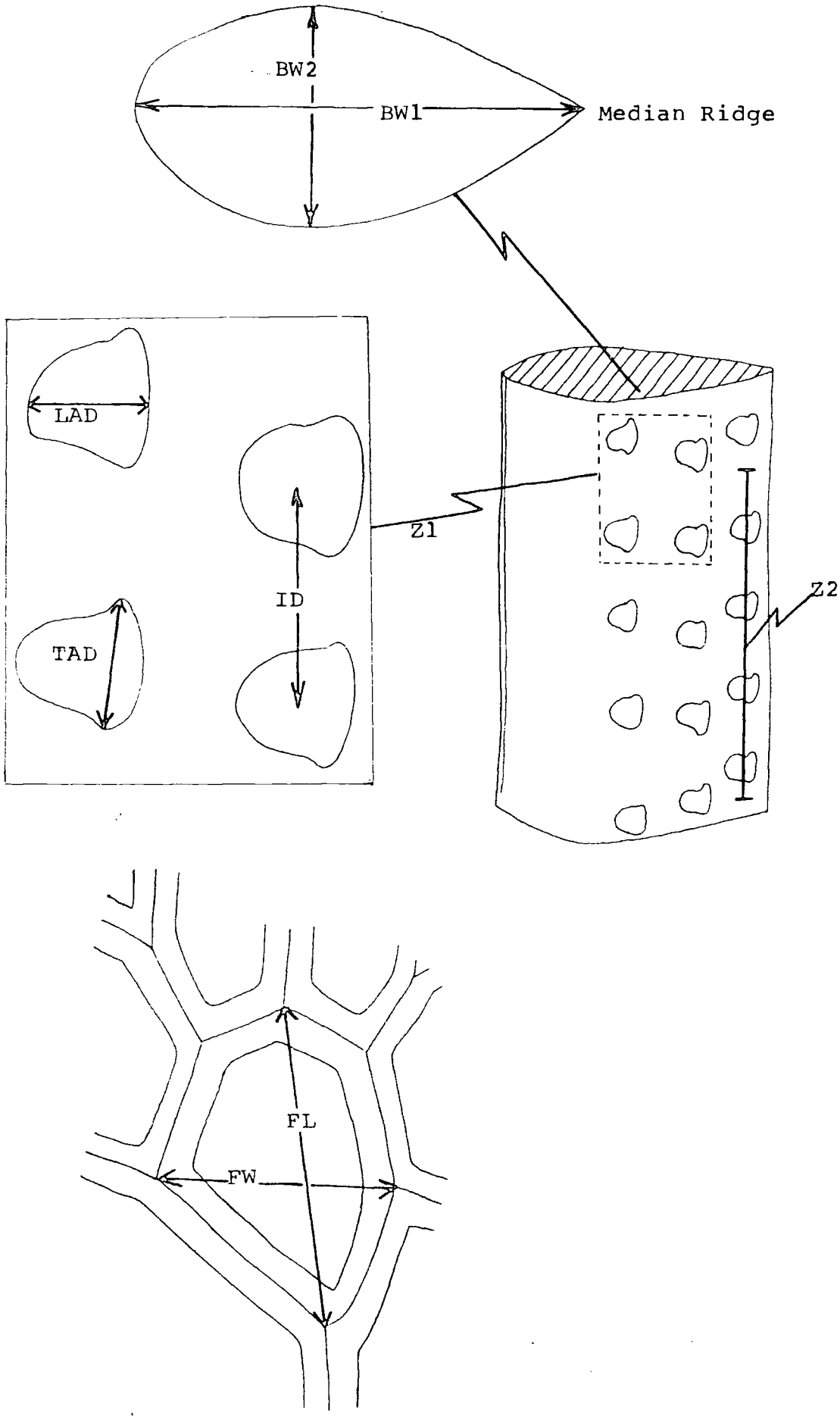
BW2
BW1
Median Ridge
LAD
ID
TAD
Z1
Z2
FL
FW

Figure 94. Goniocladia cellulifera (Etheridge Jun.)

Graphical representation of the gradation in interapertural distance (ID) in adjacent longitudinal rows towards the median ridge of branches.

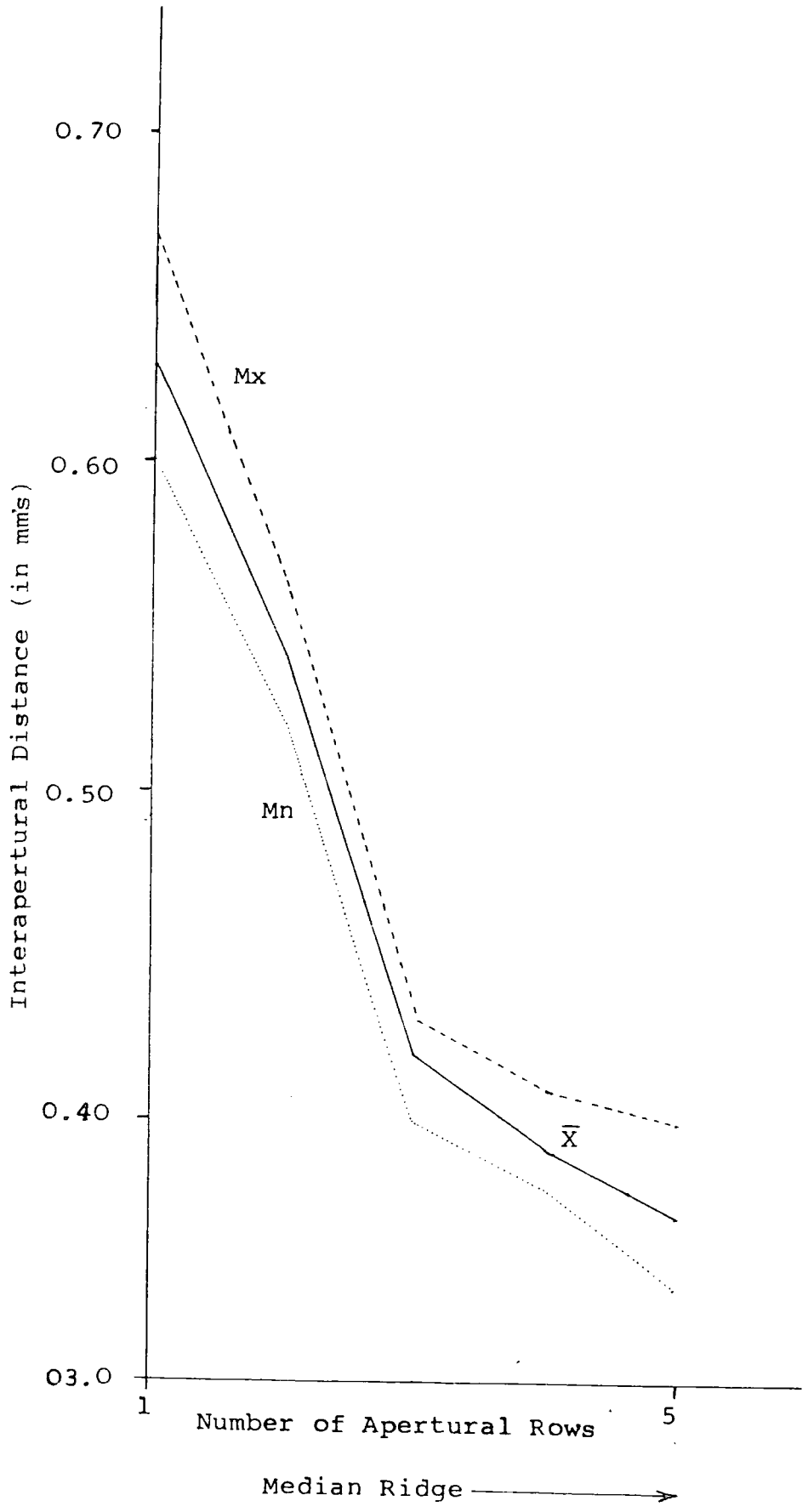
0.70
0.60
0.50
0.40
03.0
Interapertural Distance (in mm's)
Mx
Mn
$\bar{X}$
1
5
Number of Apertural Rows
Median Ridge

Plate 1. Type A stylets

fig.a. S.E.M. photomicrograph showing the solid granular cores surrounded by laminated skeletal tissues in Rhabdomeson gracilis (Phillips). ABHR 28. Arnsbergian, shales above the Main Limestone, Hurst. X830.

fig.b. Detailed morphology of a type A stylet in Rhabdomeson gracilis showing its development low down in an exozone wall and the constant diameter of the central axial core along its length. The curvature of the core corresponds to the curvature of an adjacent zooecial wall. The surrounding laminae become clustered around the core distally and become orientated parallel to the length of the core. ABHR 238. Horizon and locality as for fig.a. X238.

fig.c. Optically parallel extinction of a core along its entire length under cross polarised light in Tabulipora urii (Fleming). HM D.787c. Brigantian, Lower Limestone Group, Hosie Limestone, Hairmyres, X420.

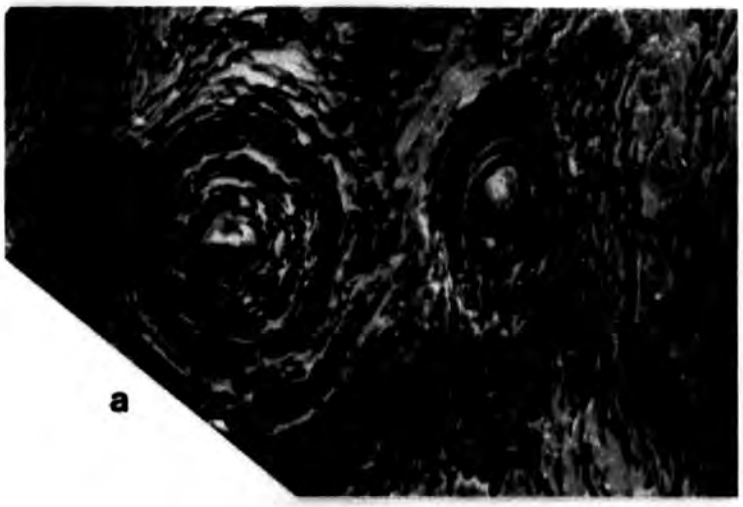
a


b

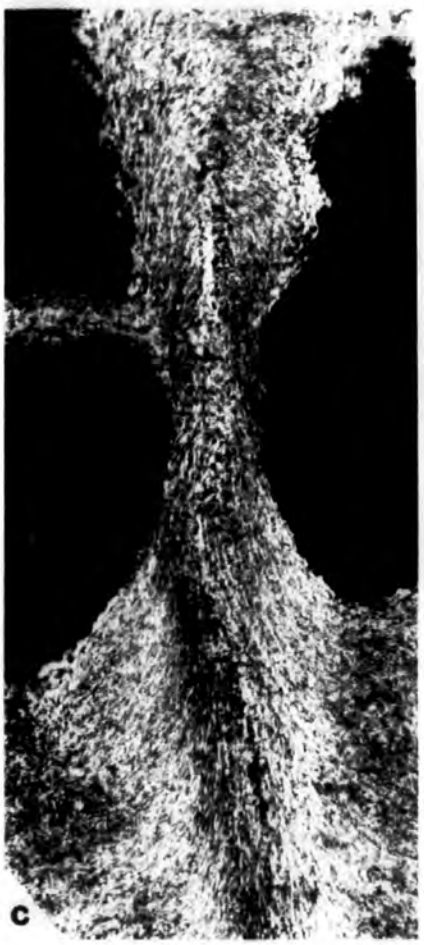
c

Plate 2. Type A stylets

fig.a. Detailed morphology of type A stylet in Rhabdomeson gracilis (Phillips), showing the clustering of skeletal laminae around the core; distally laminae become orientated parallel to the length of the core. ABHR 239. Arnsbergian, shales above the Main Limestone, Hurst. X400.

fig.b. Type A stylets developed low down in an exozone wall of Tabulipora urii (Fleming), they are straight and orientated perpendicular to the zoarial surface throughout their length. HM D.787c. Brigantian, Lower Limestone Group, Hosie Limestone, Hairmyres. X64.

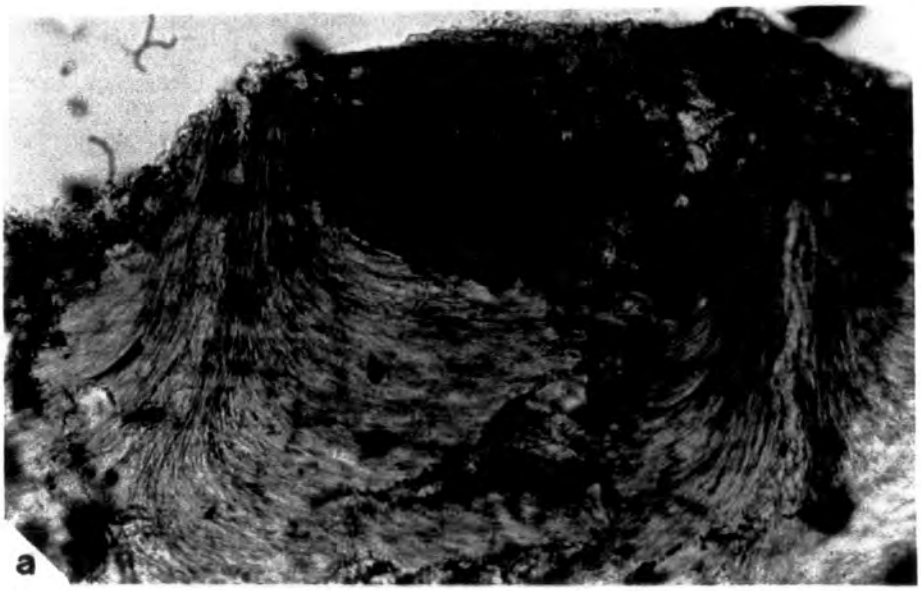
a


b

Plate 3. Type A stylets

fig.a. Tangential section of an unidentified stenoporid trepostome showing the stable positioning of large type A stylets at interzooecial angles. ABWB 210. Brigantian, Middle Limestone Group, Morpeth Scar Limestone, West Burton. X19.

fig.b. Tangential section showing the occurrence of large type A stylets at interzooecial angles in Tabulipora urii (Fleming), and how they maintain their diameter in thin walled portions of the exozone wall, between monilae, with their outer margins protruding beyond interzooecial walls and into zooecial tubes slightly. HM D.787b. Brigantian, Lower Limestone Group, Hosie Limestone, Hairmyres. X104.


a

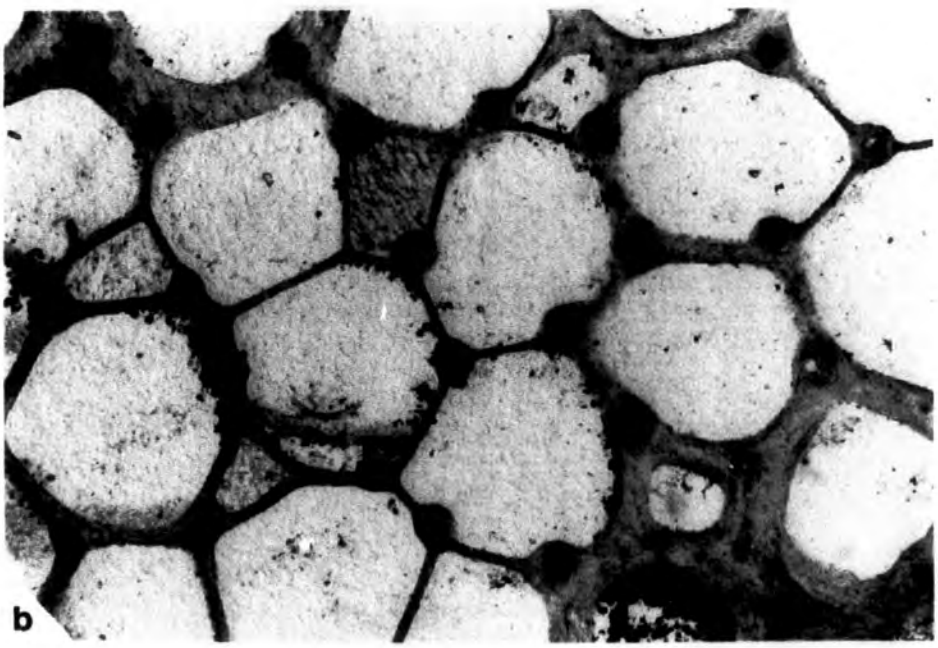
b

Plate 4. Type B stylets

fig.a. Longitudinal section showing the detailed morphology of a type B stylet (right hand side) in Rhabdomeson gracilis (Phillips). The central granular is crossed infrequently by the surrounding orally flexed sheath laminae. Sheath laminae are deflected orally for only short distances around the core, and most appear to terminate against it. The morphology of the type B stylet contrasts with the type A stylet to the left of it. HM D.106. Brigantian, Lower Limestone Group. Hosie Limestone, Hairmyres. X210.

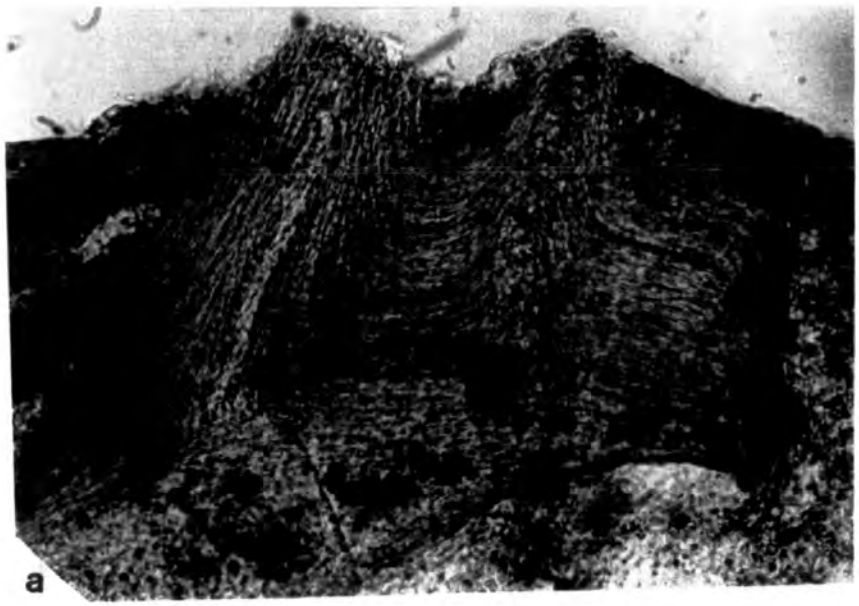
a

Plate 5. Type C stylets

Fig.a. Longitudinal section showing the development of type C stylets in the upper exozone wall of Rhabdomeson rhombifera (Phillips). No granular cores are defined and laminae are tightly orally flexed for only a very short distance. ABHR 231. Arnsbergian, shales above the Main Limestone, Hurst. X204.

fig.b. Stenoporid trepostome showing the regular distribution of type C stylets in closely spaced uniserial rows along interzooecial walls between the larger type A stylets situated at interzooecial angles. ABWB 210. Middle Limestone Group, Morpeth Scar Limestone, West Burton. X64.


a

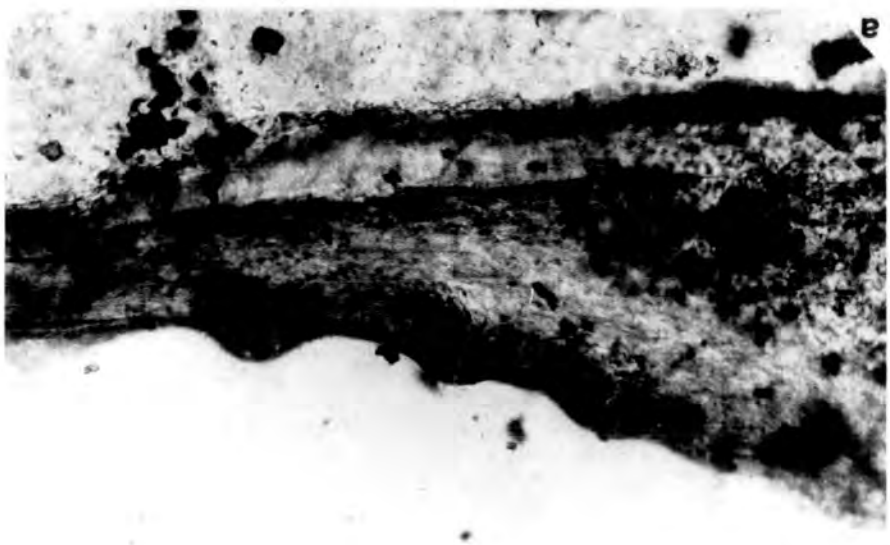
e

Plate 6. Budding in rhabdomesid cryptostomes

fig.a. Longitudinal section through Rhombopora sp. showing autozooecia budded around a linear axial zone. ABHH 200. Courceyan, Hookhead Formation, Hookhead. X45.

fig.b. Transverse section through Rhombopora sp. showing autozooecia budded around a linear axial zone. ABHH 200. Horizon and locality as for fig.a. X45.

fig.c. Longitudinal section through Rhabdomeson gracilis (Phillips) showing autozooecia budded around a central axial cylinder. ABHR 206. Arnsbergian, shales above the Main Limestone , Hurst. X45.

fig.d. Transverse section through Rhabdomeson gracilis showing autozooecia budded around a central axial cylinder. AB 224. Horizon and locality as for fig .c. X45.

fig.e. Longitudinal section through Ascopora florata Shulga-Nesterenko showing autozooecia budded around a central axial bundle. Visean. X15.

fig.f. Transverse section through Ascopora florata showing autozooecia budded around a central axial bundle. Visean. X15.

(figs e and f are reproduced from Shulga-Nesterenko 1955, Pl.26,figs.1,2.)


a


c

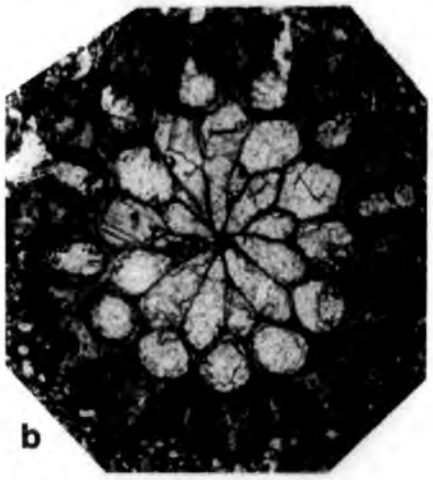
b

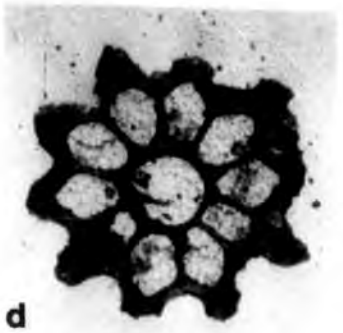
d

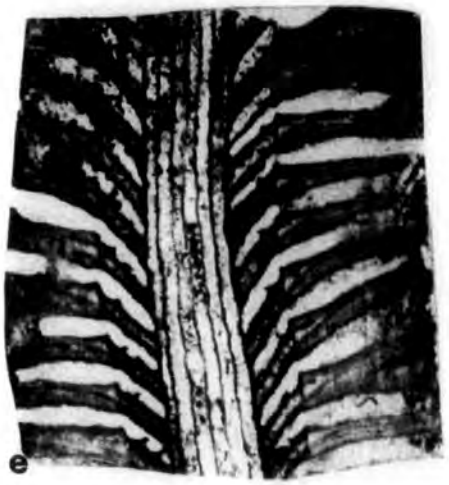
e

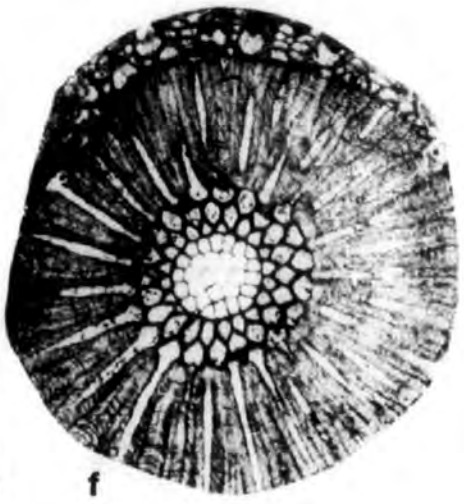
f

Plate 7. Rhabdomeson gracilis (Phillips)

fig.a. Large colony fragment with branches dichotomising at widely spaced intervals. HM D.288. Brigantian, Lower Limestone Group, Hairmyres. X1.1.

figs b to f show zoarial surface detail; autozooecial apertures are arranged in quincunx, a single large type A stylet always occurs on interapertural walls between apertures in the same longitudinal row, occasionally with a smaller type B stylet situated distally to it.

fig.b. ABHR 35. Arnsbergian, shales above the Main Limestone, Hurst. X20.

fig.c. S.E.M. photomicrograph. ABHR 25. Horizon and locality as for fig.b. X26.

fig.d. HM D.105. Horizon and locality as for fig.a. X20.

fig.e. ABHR.IR.3. Horizon and locality as for fig.b. X20.

fig.f. ABHR.IR.4. Horizon and locality as for fig.b. X20.

fig.h. Broken colony fragment revealing the central axial cylinder around which autozooecia are regularly budded. HM D.105. Horizon and locality as for fig.a. X20.

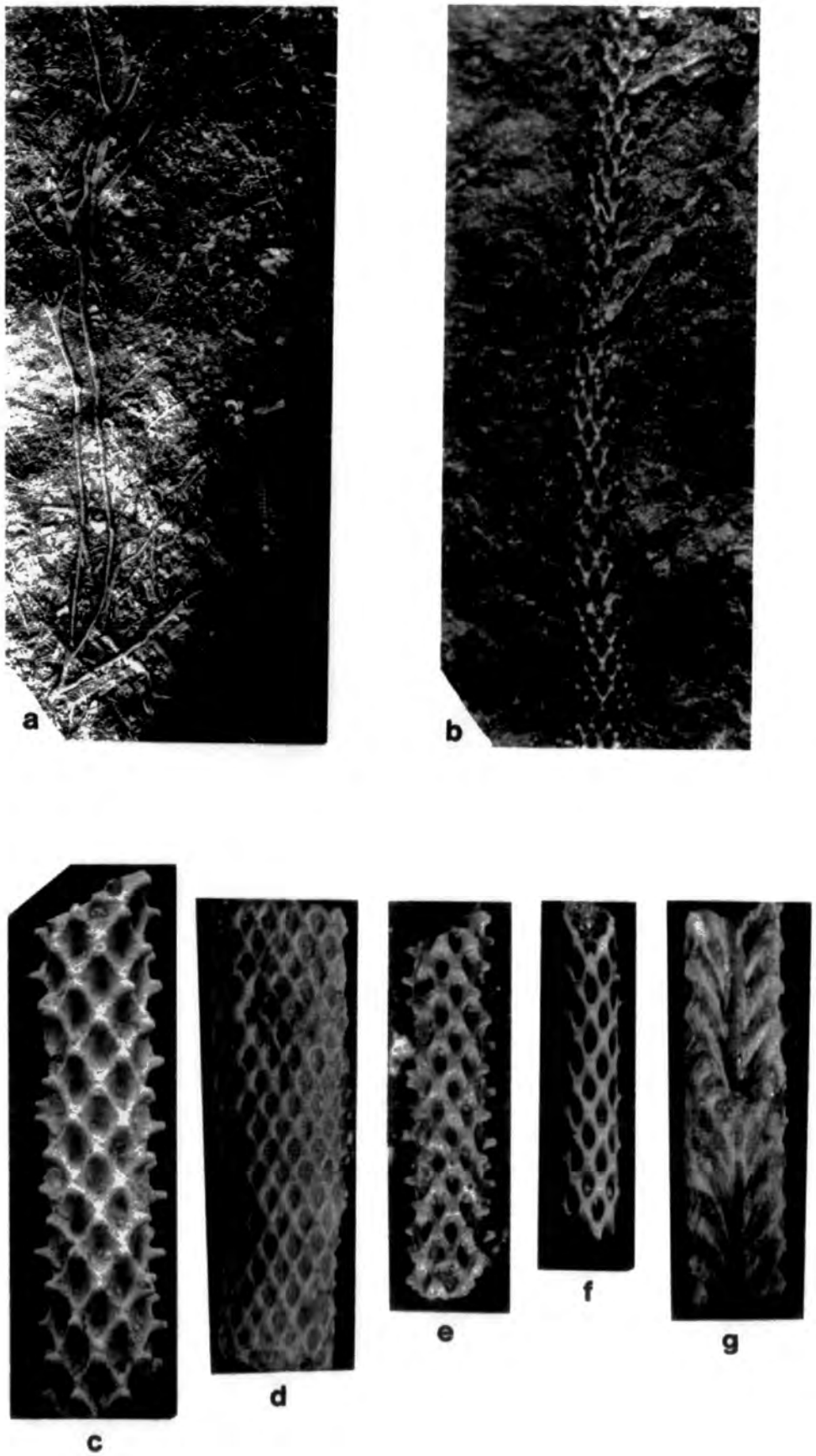
a
b
c
d
e
f
g

Plate 8. Rhabdomeson gracilis (Phillips)

fig.a. S.E.M. photomicrograph showing rhomb-shaped autozooecial apertures with very thin subangular interveining interapertural walls and, the occurrence of a single large type A stylet situated immediately distal to each aperture. ABHR 25. Arnsbergian, shales above the Main Limestone, Hurst. X80.

fig.b. S.E.M. photomicrograph showing oval-shaped autozooecial apertures with narrow well rounded interveining interapertural walls, and the occurrence of a single large type A stylet situated immediately distal to each aperture with a smaller type B stylet situated distally to each type A stylet. ABH 11. Brigantian, Lower Limestone Group, Hosie Limestone, Hairmyres. X50.

fig.c. S.E.M. photomicrograph showing the growth tip of a colony with the axial cylinder opening at the zoarial surface. ABH 40. Horizon and locality as for fig.b. X80.

fig.d. S.E.M. photomicrograph showing detail of the growth tip with immature autozooecia budded around the axial cylinder. ABH 40. Horizon and locality as for fig.b. X150.

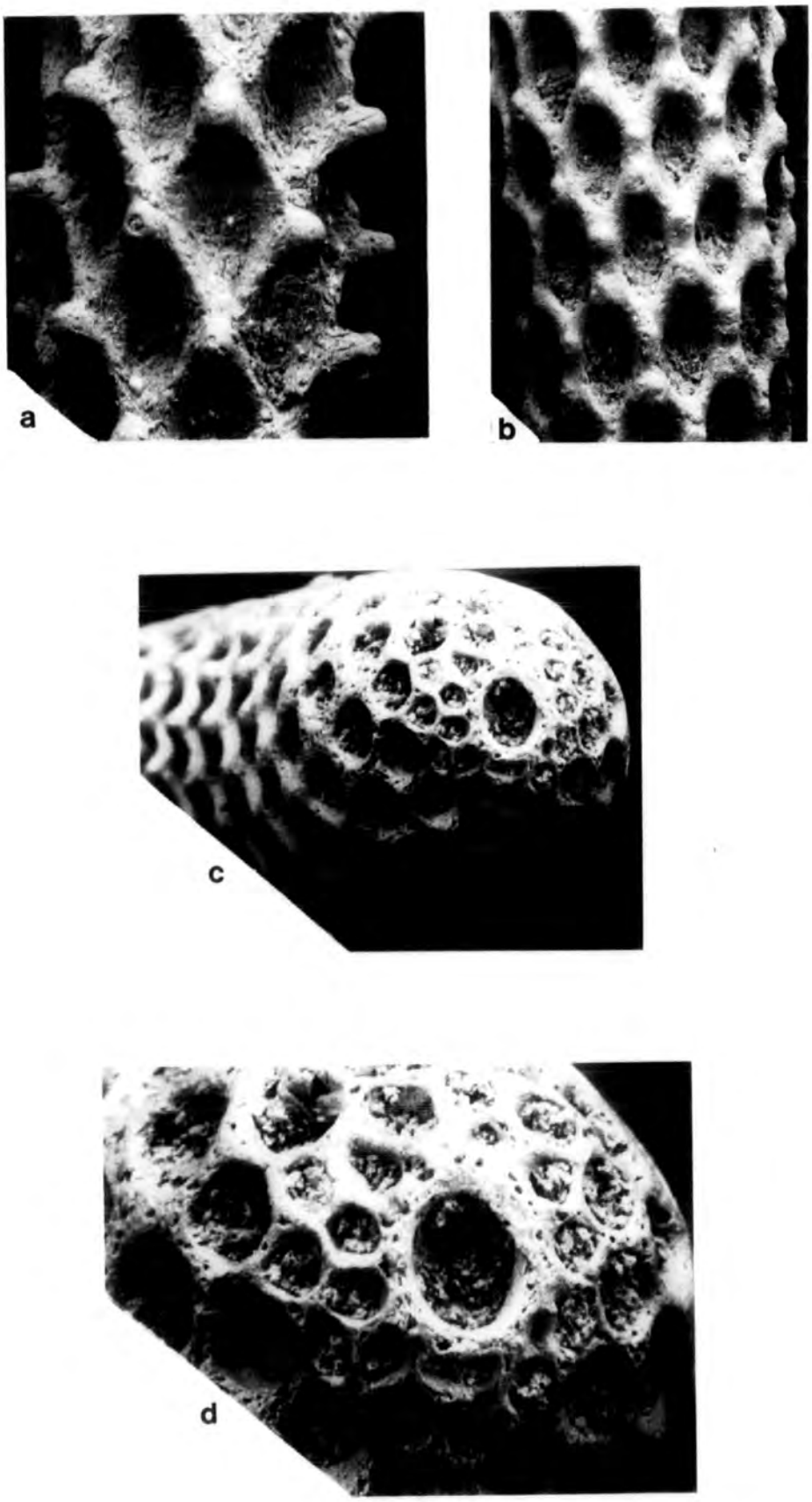
a
b
c
d

Plate 9. Rhabdomeson gracilis (Phillips)

figs a to e illustrate the two forms of budding as seen in transverse section.

fig.a. Annular budding seen in transverse section of a broken silicified colony fragment. ABCL 24. Asbian, Calp Shale - Upper Limestone, Carrick Lough. X20.

fig.b. Annular budding. ABHR 209. Arnsbergian, shales above the Main Limestone, Hurst. X90.

fig.c. Annular budding. ABHR 210. Horizon and locality as for fig.b. X90.

fig.d. Annular budding. ABHR 210. Horizon and locality as for fig.b. X240.

fig.e. Spiral budding. ABHR 217. Horizon and locality as for fig.b. X150.


a

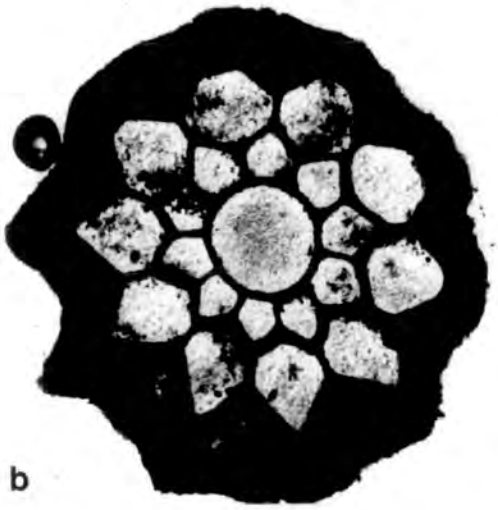
b

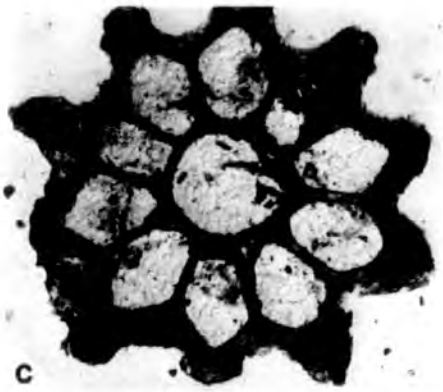
c

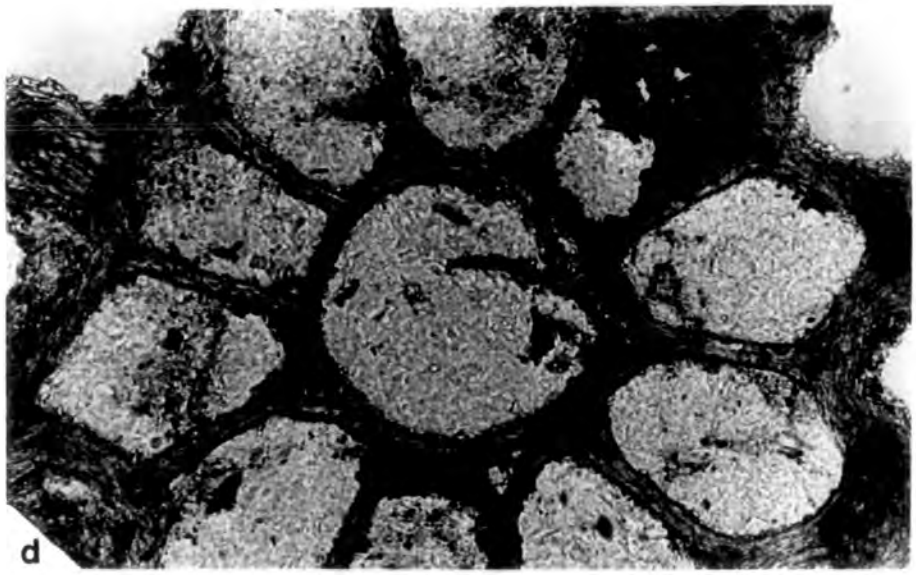
d

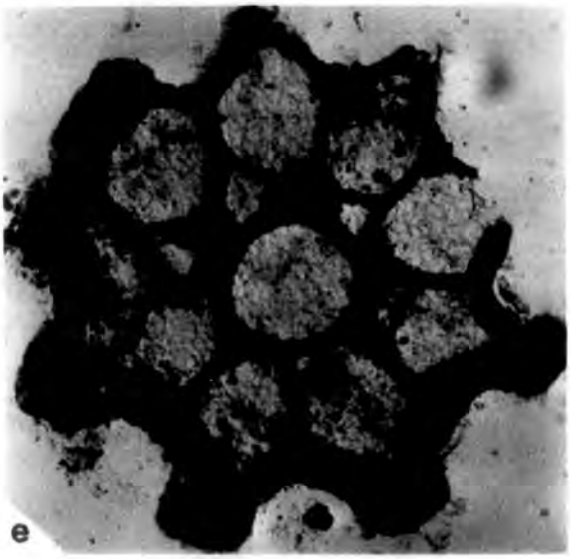
e

Plate 10. Rhabdomeson gracilis (Phillips)

fig.a. Longitudinal section through the central axial cylinder showing the regularity of budding and the constancy of the angle of divergence of successive autozooecia away from the axial cylinder. Consequently autozooecial tubes are all the same length. A single superior hemiseptum is situated at the base of the vestibular region in each autozooecium. HM D.103. Brigantian, Lower Limestone Group, Hosie Limestone, Hairmyres. X40.

fig.b. Longitudinal section showing the constancy in the angle of divergence of successive autozooecia from the axial cylinder, and the occurrence of a single superior hemiseptum situated at the base of the vestibular region in each autozooecium. HM D.103. Horizon and locality as for fig.a. X100.

fig.c. Detail of hemisepta. HM D.103. Horizon and locality as for fig.a. X240.


a


b


c

Plate 11. Rhabdomeson gracilis (Phillips)

fig.a. Longitudinal section through the central axial cylinder showing the regularity of budding and the constancy in the angle of divergence of successive autozooecia away from the axial cylinder. Large type A stylets are situated at the proximal extremities of exozone walls between adjacent autozooecia. HM D.106. Brigantian, Lower Limestone Group, Hosie Limestone, Hairmyres. X100.

fig.b. Longitudinal section through the central axial cylinder. ABHR 205. Arnsbergian shales above the Main Limestone, Hurst. X40.

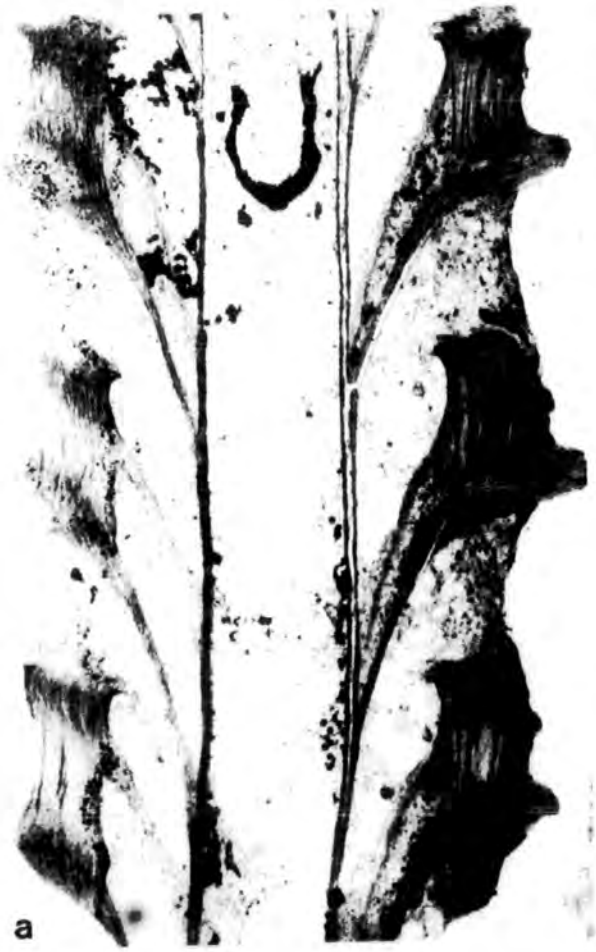
a


b

Plate 12. Rhabdomeson gracilis (Phillips)

fig.a. Longitudinal section showing a transverse imperforate diaphragm across the axial cylinder. ABHR 200. Arnsbergian, shales above the Main Limestone, Hurst. X100.

fig.b. As for fig.a., but showing detail of the imperforate diaphragm across the axial cylinder. X270.


a


b

Plate 13. Rhabdomeson gracilis (Phillips)

fig.a. Longitudinal section beyond the axial cylinder showing the annular budding of autozooecia. The zoarium shows a marked bilateral symmetry. ABHR 212. Arnsbergian, shales above the Main Limestone, Hurst. X55.

fig.b. As for fig.a. ABHR 213. Horizon and locality as for fig.a. X55.

fig.c. Longitudinal section beyond the axial cylinder showing the spiral budding of autozooecia. The zoarium shows no bilateral symmetry. ABHR 214. Horizon and locality as for fig.a. X55.


a


b


c

Plate 14. Rhabdomeson rhombifera (Phillips)

fig.a. S.E.M. photomicrograph showing zoarial surface detail; the variation in apertural dimensions between adjacent longitudinal rows and the occurrence of type C stylets that are closely spaced in uniserial rows between apertures. ABHR.2R.12. Arnsbergian, shales above the Main Limestone, Hurst. X16.

fig.b. S.E.M. photomicrograph, details as for fig.a. ABH 13. Brigantian, Lower Limestone Group, Hosie Limestone, Hairmyres. X16.

fig.c. S.E.M. photomicrograph showing the pyriform shape of the larger autozooecial apertures and the closely spaced type C stylets in uniserial rows on interapertural walls. ABH 13. Horizon and locality as for fig.b. X40.

fig.d. S.E.M. photomicrograph showing the slightly outward curving proximal margins of autozooecial apertures. ABHR.2R.12. Horizon and locality as for fig.a. X90.

fig.e. S.E.M. photomicrograph showing the morphology of type C stylets. ABH 12. Horizon and locality as for fig.a. X89.

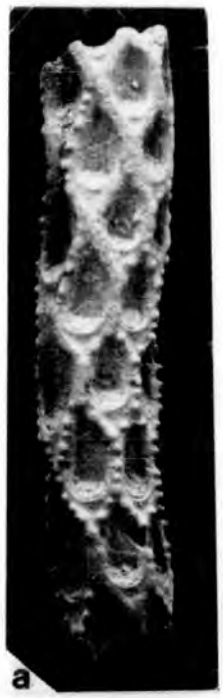
a


b

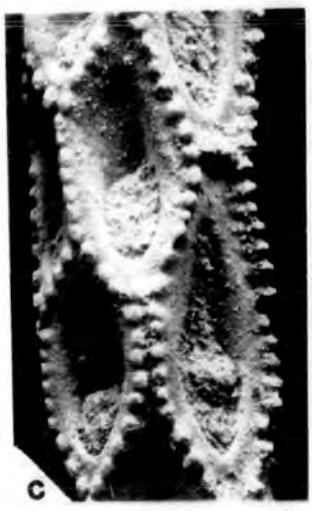
c


d

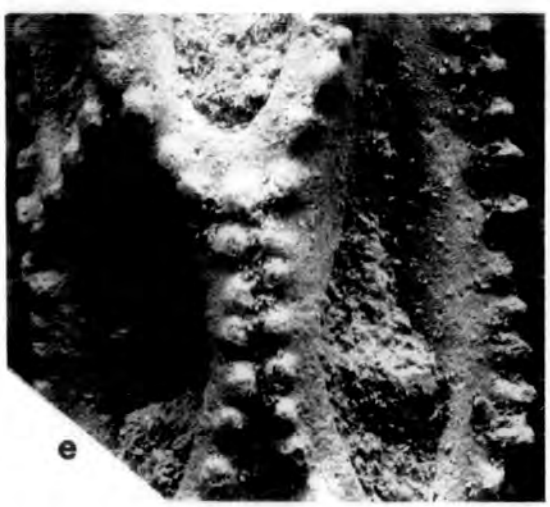
e

Plate 15. Rhabdomeson rhombifera (Phillips)

fig.a. Transverse section. ABHR 232. Arnsbergian, shales above the Main Limestone. X65.

fig.b. Longitudinal section through the axial cylinder. ABHR 228. Horizon and locality as for fig.a. X37.

fig.c. Longitudinal section through the central axial cylinder showing the variation in the angle of divergence of autozooecia on opposite sides of the cylinder. On the left hand side there is a gradual increase in the angle of divergence of the distal wall of an autozooecium away from the cylinder compared to a gradual decrease in the angle of divergence of the distal wall on the right hand side. Consequently apertural dimensions are much larger on the right hand side of the axial cylinder. ABHR 226. Horizon and locality as for fig.a. X37.

fig.d. As for fig.c. X54.


a
b
c
d

Plate 16. Rhabdomeson rhombifera (Phillips)

fig.a. Longitudinal section through the axial cylinder showing the variation in the angle of divergence of autozooecia on opposite sides of the cylinder resulting in the variation in apertural size. Closely spaced type C stylets stand out above the general level of the zoarial surface in the top left hand side of the section. ABHR 229. Arnsbergian, shales above the Main Limestone, Hurst. X37.

fig.b. Longitudinal section through the central axial cylinder. ABHR 227. Horizon and locality as for fig.a. X27.

fig.c. As for fig.b. X53.

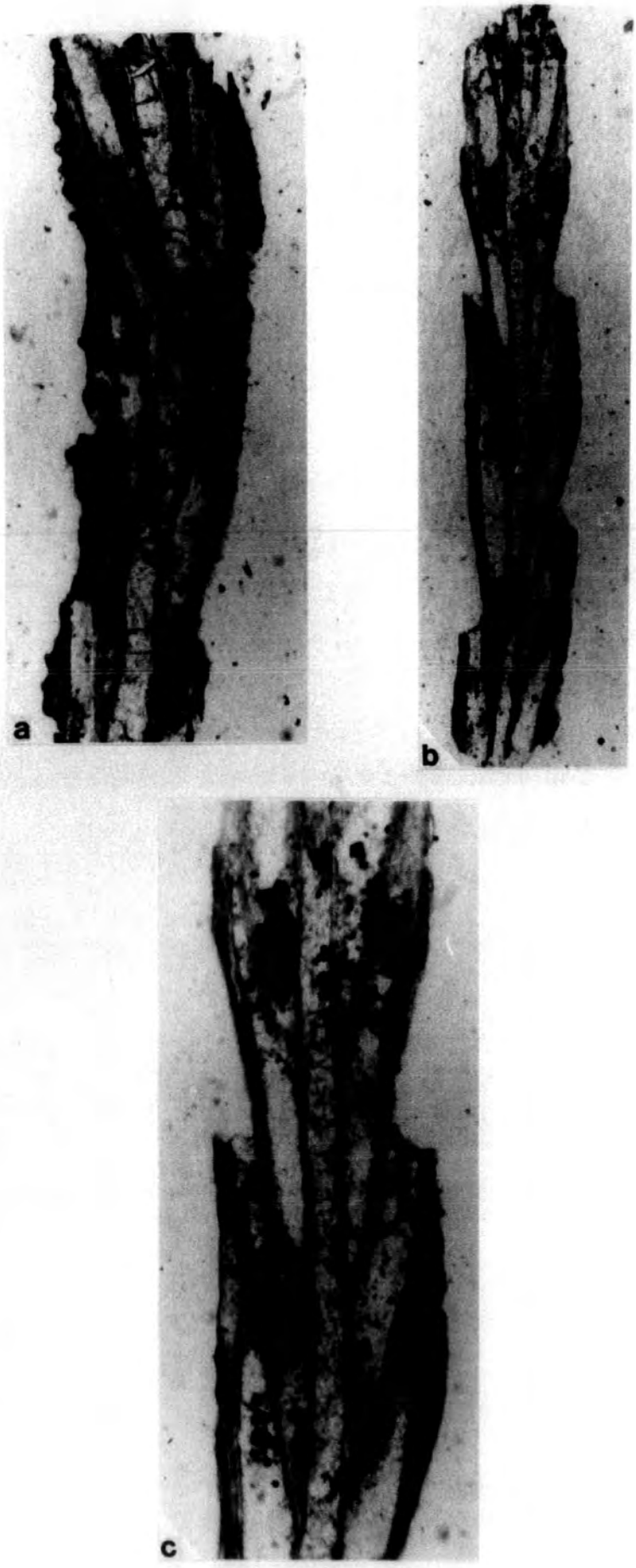
a
b
c

Plate 17. Rhabdomeson rhombifera (Phillips)

fig.a. Longitudinal section showing the development of a lateral branch from the parent branch. The lateral branch was developed after completion of the exozone region of the parent branch. A new axial cylinder is developed with the development of a lateral branch by the modification of an autozooecium. ABHR 234. Arnsbergian, shales above the Main Limestone, Hurst. X35.

fig.b. Longitudinal section showing detail of the axial cylinder wall with its compound structure. ABHR 227. Horizon and locality as for fig.a. X171.

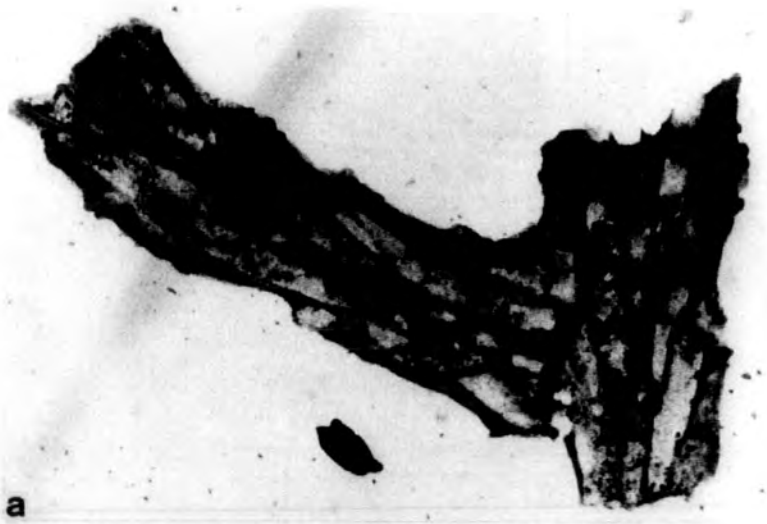

a

b

Plate 18. Rhabdomeson rhombifera (Phillips)

fig.a. Longitudinal section showing detail of type C stylets developed in the upper portion of the exozone wall. ABHR 226. Arnsbergian, shales above the Main Limestone, Hurst. X173.

fig.b. As for fig.a. but also showing the outward curvature of the proximal margin of an autozooecial aperture. ABHR 228. Horizon and locality as for fig.a. X173.


q

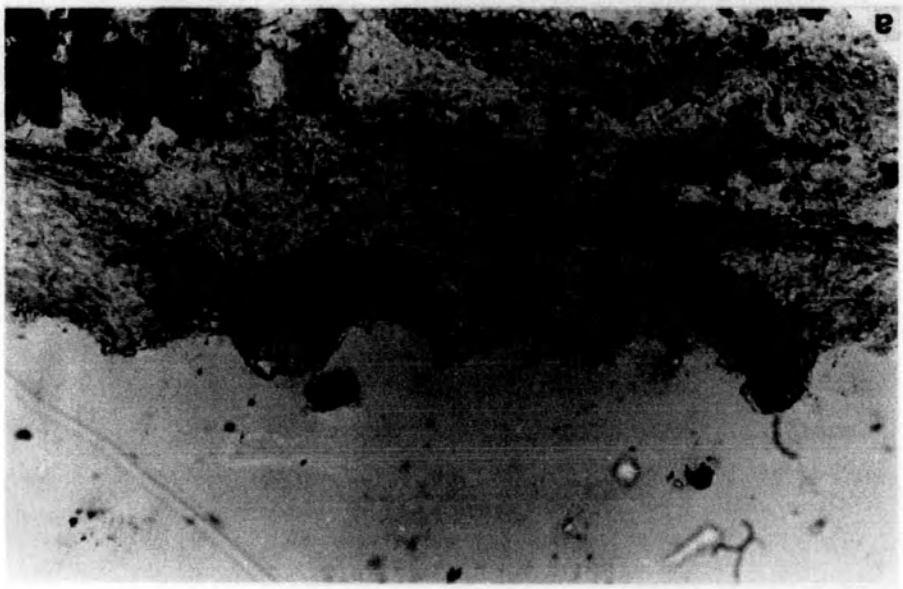
e

Plate 19. Rhombopora similis (Phillips)

figs a to e show zoarial surface detail; budding patterns are generally obscured by the occurrence of exilazooecia.

fig.a. HM D.110. Brigantian, Lower Limestone Group, Hosie Limestone, Hairmyres. X17.

fig.b. As for fig.a. X17.

fig.c. ABHR.3R.5. Arnsbergian, shales above the Main Limestone, Hurst. X18.

fig.d. S.E.M. photomicrograph showing the abundance of stylets on the interapertural walls. ABHR.3R.20. Horizon and locality as for fig.c. X17.

fig.e. S.E.M. photomicrograph showing zoarial surface detail, with the large oval autozooecial apertures surrounded by abundant large type A stylets and very abundant smaller type C stylets. ABHR.3R.20. Horizon and locality as for fig.c. X66.

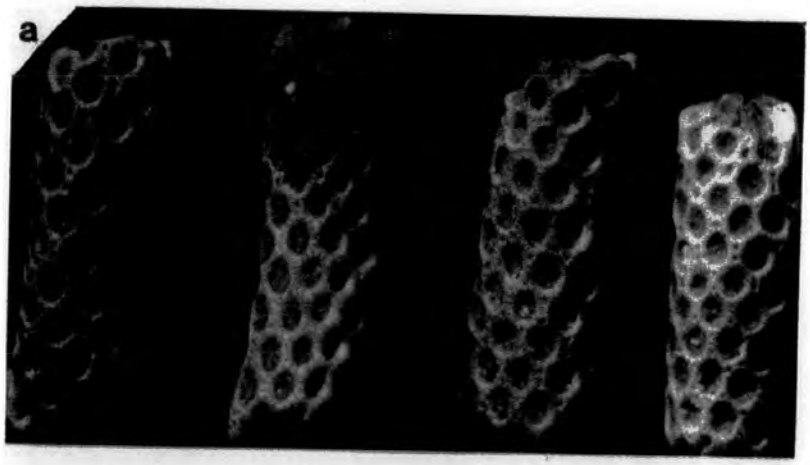
a

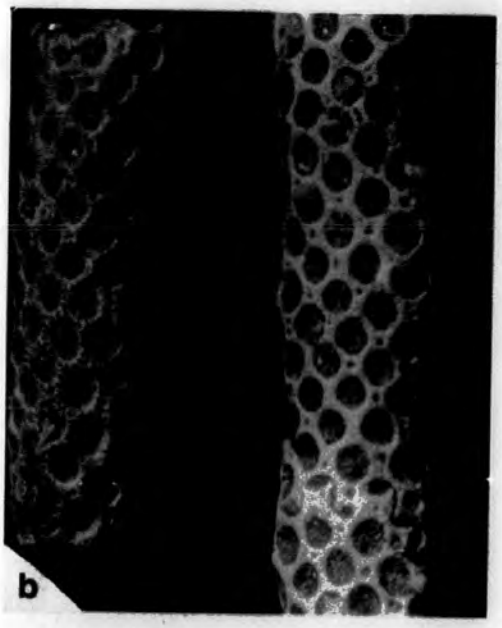
b


c

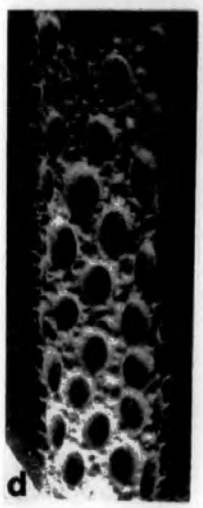
d

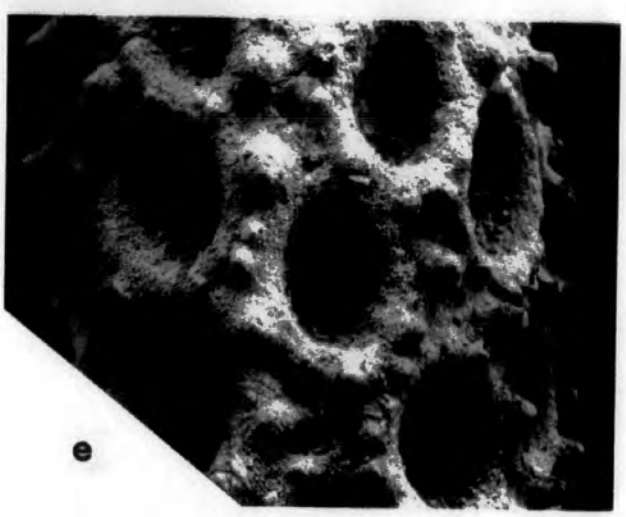
e

Plate 20. Rhombopora similis (Phillips)

fig.a. S.E.M. photomicrograph showing zoarial surface detail of stylets. ABHR.3R.20. Arnsbergian, shales above the Main Limestone, Hurst. X170.

fig.b. Transverse section. ABHR 244. Horizon and locality as for fig.a. X43.

fig.c. Transverse section. ABHR 245. Horizon and locality as for fig.a. X43.

a

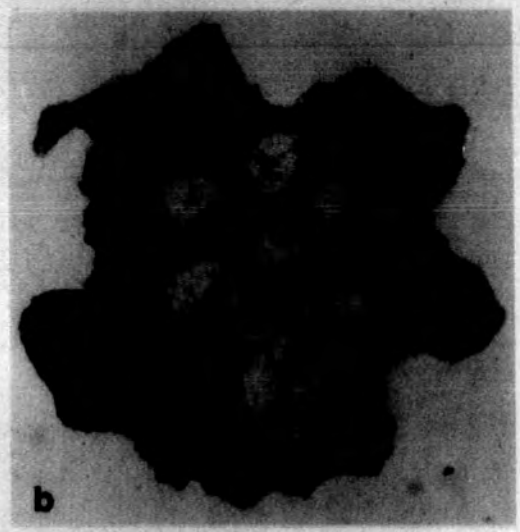

b

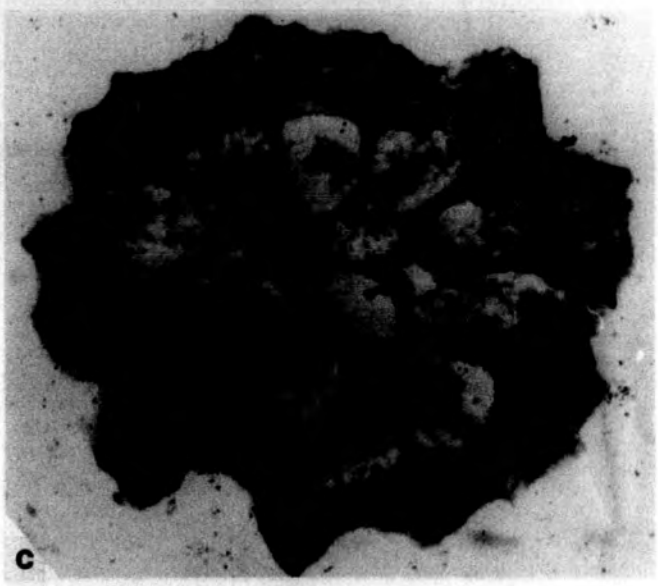

c

Plate 21. Rhombopora similis (Phillips)

fig.a. Longitudinal section. ABHR 238. Arnsbergian, shales above the Main Limestone, Hurst. X43.

fig.b. Longitudinal section showing autozooecial apertures sealed by terminal diaphragms. ABHR 248. Horizon and locality as for fig.a. X43.

fig.c. Longitudinal section showing detail of the terminal diaphragms sealing autozooecial apertures. ABHR 248. Horizon and locality as for fig.a. X85.


a
b
c

Plate 22. Rhombopora similis (Phillips)

fig.a. Longitudinal section showing detail of exozone interzooecial walls. HM D.145. Brigantian, Lower Limestone Group, Hosie Limestone, Hairmyres. X144.

fig.b. Longitudinal section showing detail of exozone wall with type C stylets orientated at right angles to the zoarial surface and intrastylets extending at oblique angles through the exozone wall. HM D.145. Horizon and locality as for fig.a. X230.


a

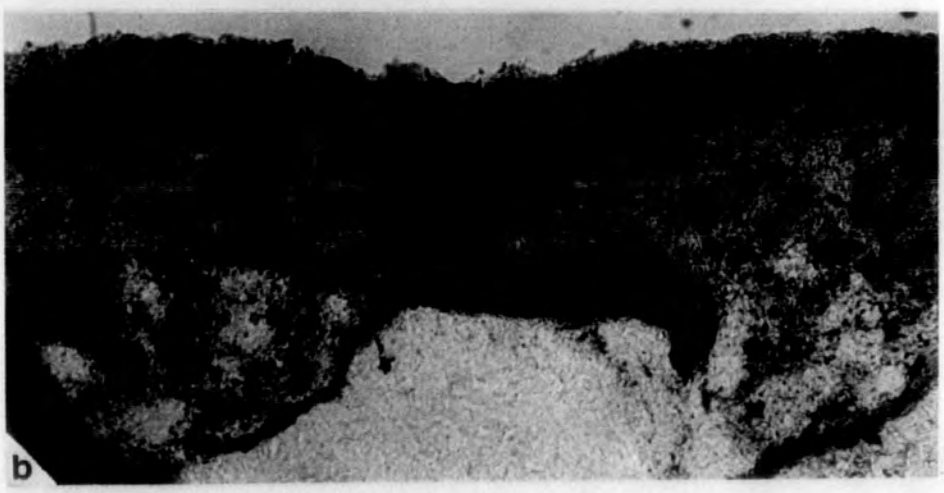
b

Plate 23. Rhombopora similis (Phillips)

fig.a. Longitudinal section showing morphology of stylets in the exozone wall; type A stylets are developed low down in the exozone wall. ABHR 238. Arnsbergian, shales above the Main Limestone, Hurst. X220.

fig.b. Longitudinal section showing detail of stylets in the exozone wall with two large type A stylets developed low down in the exozone wall and two small type C stylets developed close to the zoarial surface. ABHR 239. Horizon and locality as for fig.a. X220.

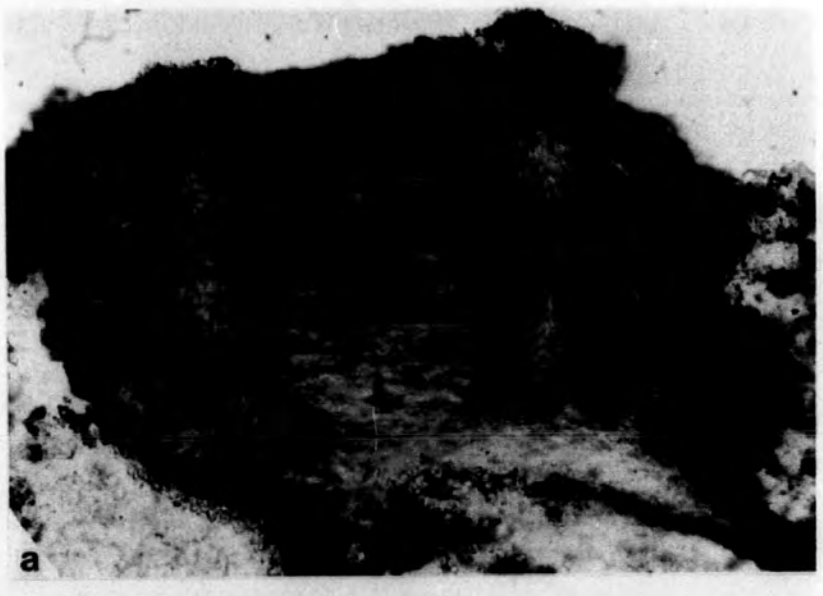
a

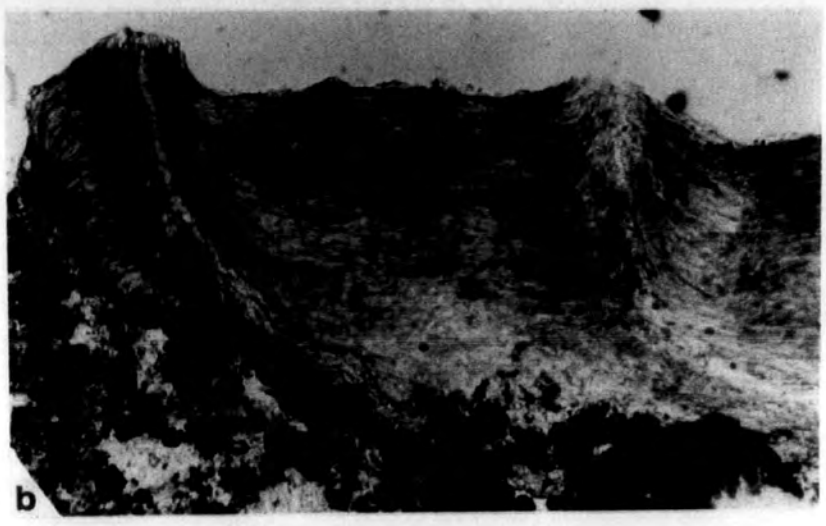
b

Plate 24. Secondary Nanozooids

figs a to e are S.E.M. photomicrographs of secondary nanozooids in Penniretepora elegans (Young and Young) ABH 20. Brigantian, Lower Limestone Group, Hosie Limestone, Hairmyres.

fig.a. Each autozooecial aperture is sealed by a secondary nanozooid. X47.

fig.b. Detail of apertures sealed by secondary nanozooids. X135.

fig.c. Detail of the central elevated perforation of the secondary nanozooid. X670.

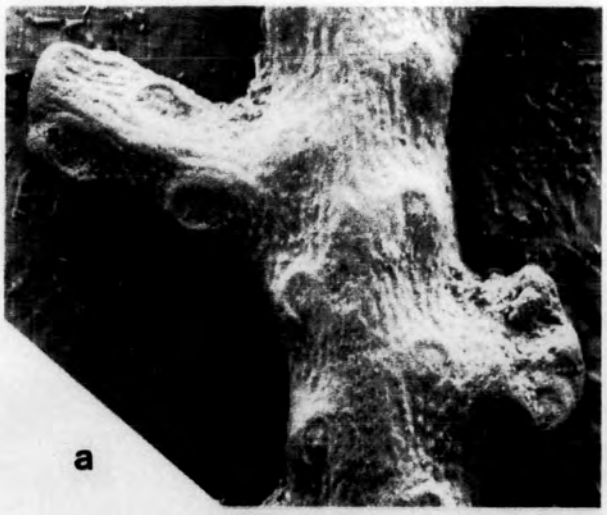

a

b

c

Plate 25. Ovicells

fig.a. Small colony fragment of Fenestella fanata Whidborne var carrickensis showing an unusual abundance of ovicells. Individual ovicells are well depressed into branches and the swellings are quite small and do not affect the disposition of adjacent autozooecial apertures. ABCL 100. Asbian, Calp Shale-Upper Limestone, Carrick Lough. X17.

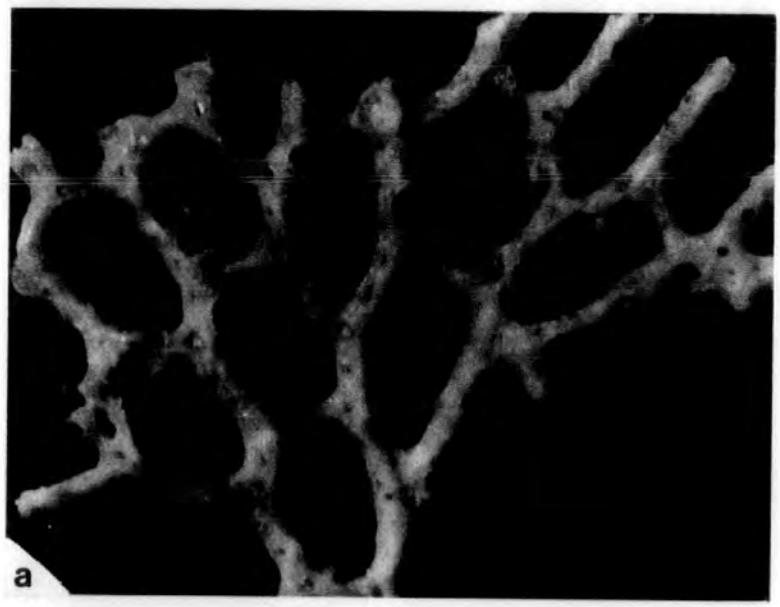
a

Plate 26. Fenestella bicellulata Etheridge,Jun.

fig.a. Neotype, obverse surface detail. GSE 1944. Brigantian,shales between First and Second Calderwood Limestone, Boghead. X25. (the photograph is reproduced from Miller 1961, Pl.27, fig.1.)

fig.b. Colony form. ABP 115. Asbian, Alston Group, Fifth Limestone, Penruddock. X2.2.

fig.c. Obverse surface detail. ABP 157. Horizon and locality as for fig.b. X15.

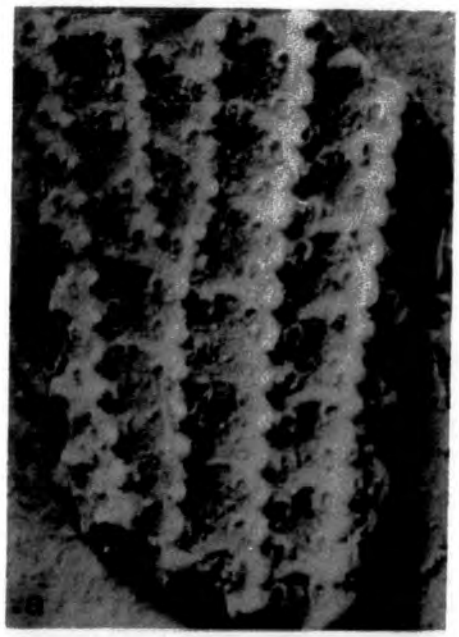


b

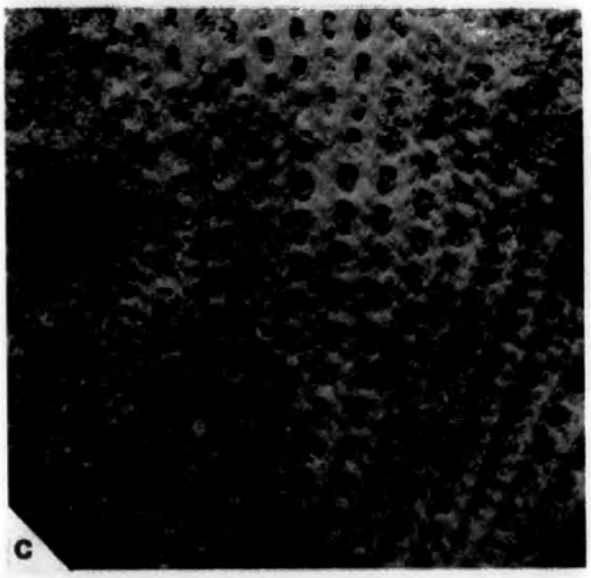
c

Plate 27. Fenestella bicellulata Etheridge,Jun

fig.a. Obverse surface detail. ABP 141. Asbian, Alston Group, Fifth Limestone, Penruddock. X15.

fig.b. Obverse surface detail showing the prominent very closely spaced carinal nodes. ABP 158. Horizon and locality as for fig.a. X15.

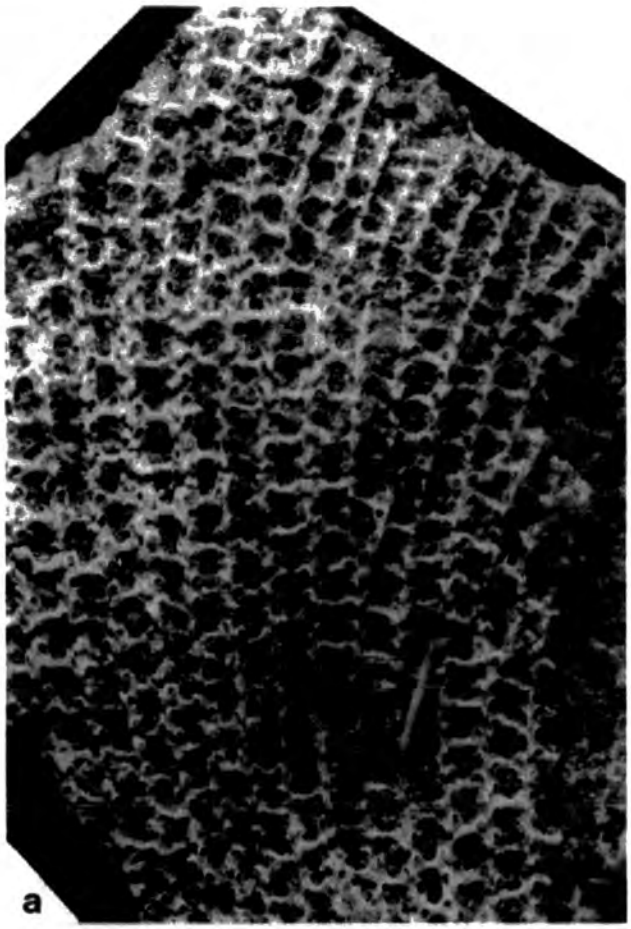
a

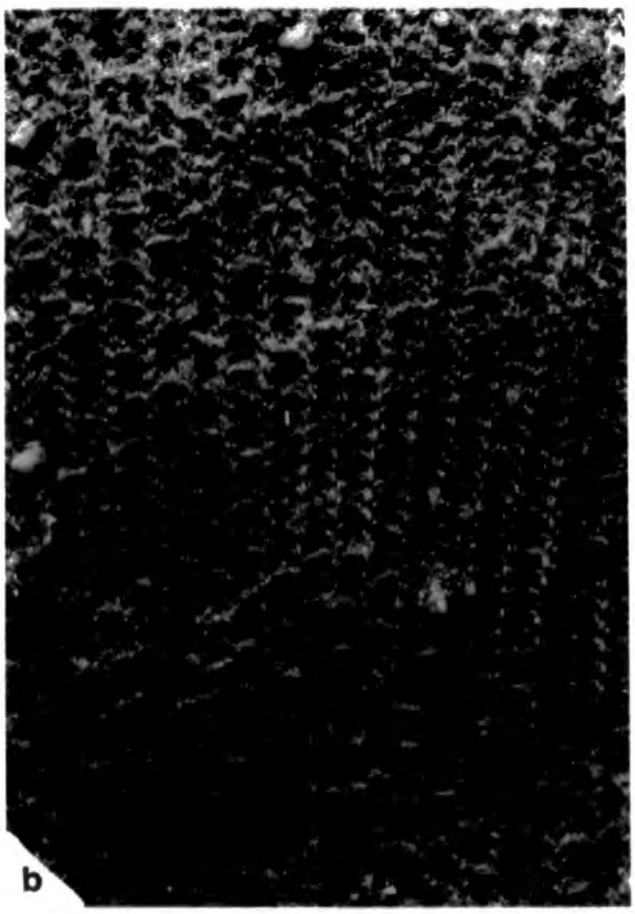
b

Plate 28. Fenestella bicellulata Etheridge, Jun

fig.a. Obverse surface detail. ABP 166. Asbian, Alston Group, Fifth Limestone, Penruddock. X15.

fig.b. S.E.M. photomicrograph showing obverse surface detail. GAGM 01-53aaL. Brigantian, Lower Limestone Group, Hairmyres. X19.

fig.c. S.E.M. photomicrograph of obverse surface detail, showing the closely spaced carinal nodes and denticulated autozooecial apertures. GAGM 01-53aaL. Horizon and locality as for fig.b. X60.

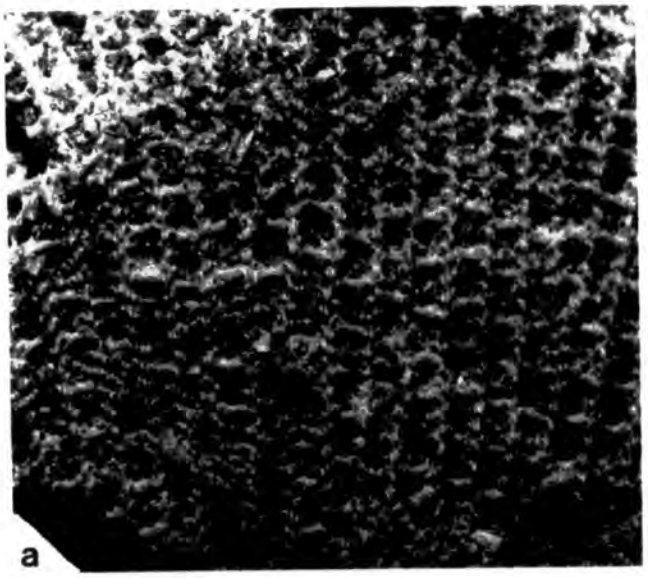
a

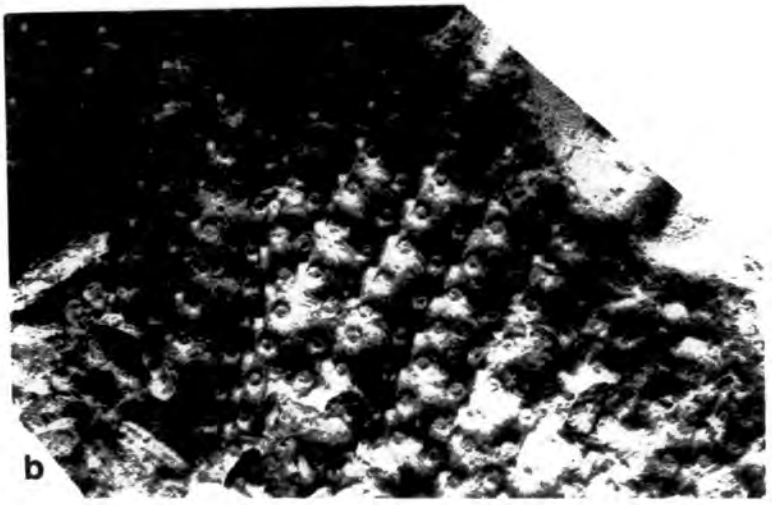
b

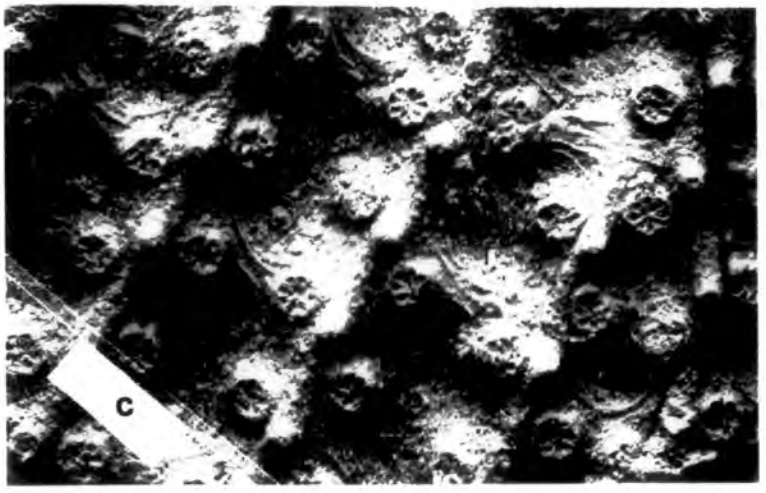
c

Plate 29. Fenestella bicellulata (Etheridge, Jun.)

fig.a. S.E.M. photomicrograph showing detail of denticulated autozooecial apertures. GAGM 01-53aaL. Brigantian, Lower Limestone Group, Hairmyres. X120.

fig.b. Reverse surface detail. ABP 178. Asbian, Alston Group, Fifth Limestone, Penruddock. X15.

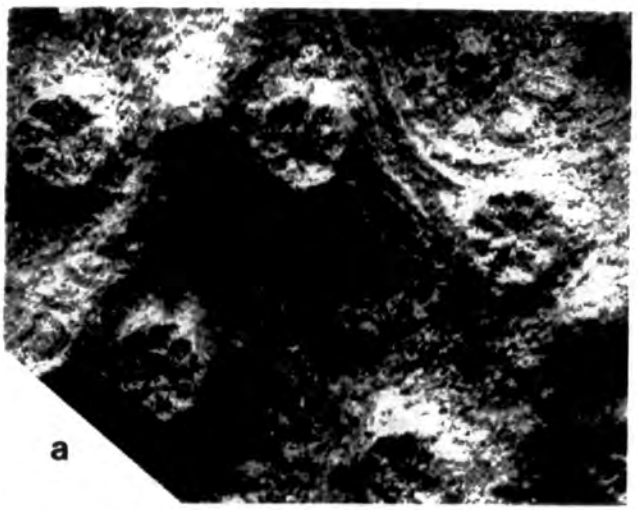
a


b

Plate 30. Fenestella bicellulata (Etheridge, Jun.)

fig.a. Reverse surface detail. ABP 168. Asbian, Alston Group, Fifth Limestone, Penruddock. X15.

fig.b. Reverse surface detail. A small immature colony of Fistulipora incrustans (Phillips) is encrusting part of the zoarium. ABP 133. Horizon and locality as for fig.a. X15.

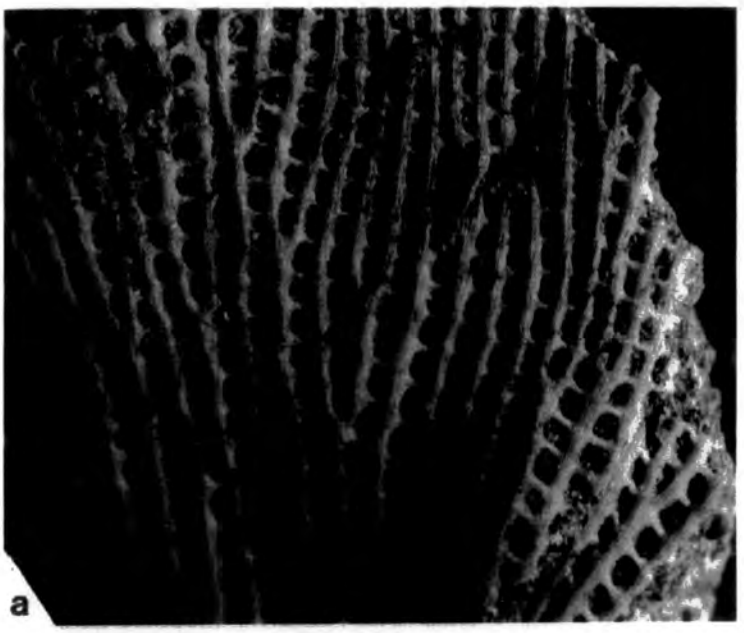
a


b

Plate 31. Fenestella bicellulata (Etheridge, Jun.)

fig.a. Reverse surface detail. ABP 192. Asbian, Alston Group, Fifth Limestone, Penruddock. X15.

fig.b. Oblique tangential section showing the variation in autozooecial chamber shape with depth. GAGM 01-53aap. Brigantian, Lower Limestone Group, Hosie Limestone. Hairmyres. X36.

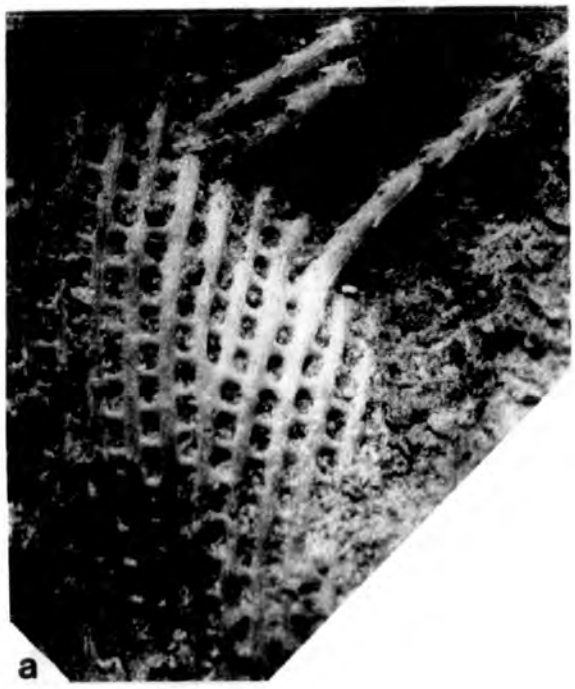

a

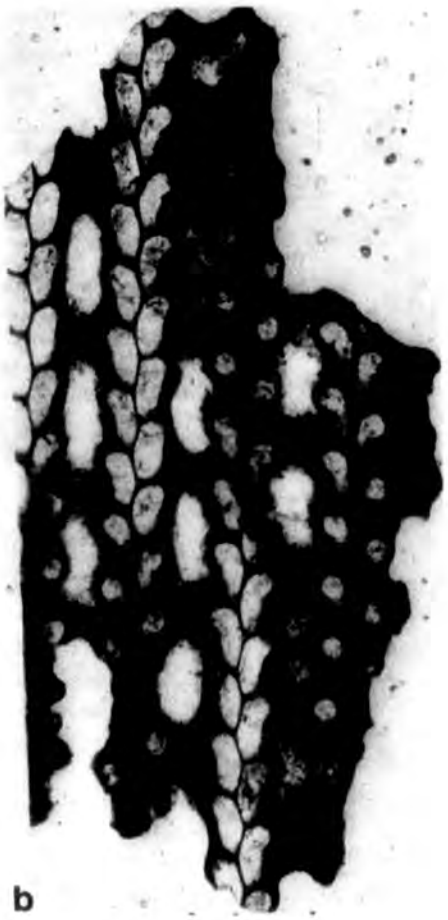

b

Plate 32. Fenestella bicellulata (Etheridge, Jun.)

fig.a. Oblique tangential section showing the variation in autozooecial chamber shape with depth. GAGM 01-53aap(2). Brigantian, Lower Limestone Group, Hairmyres. X39.

fig.b. Tangential section through denticulated autozooecial apertures. GAGM 01-53aap(2). Horizon and locality as for fig.a. X140.

fig.c. As for fig.b. but at a higher magnification. X220.


a


b

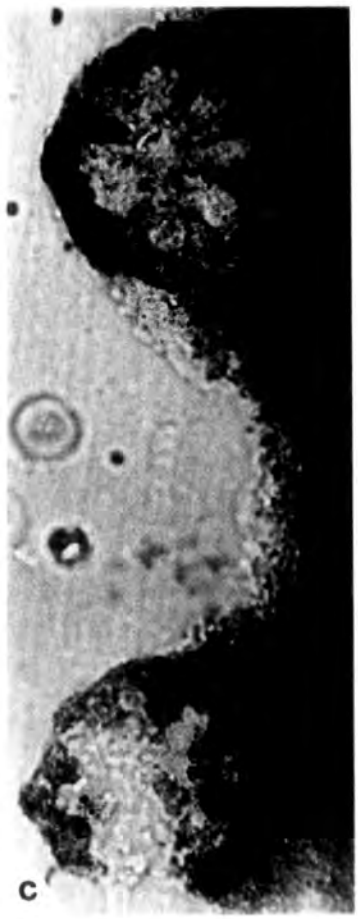
c

Plate 33. Fenestella ivanovi Shulga-Nesterenko

figs a to c show obverse surface detail; the positions of autozooecial apertures is stabilised with one situated above the dissepiment-branch junction and one midway along fenestrule margins projecting out from branch sides and giving fenestrules their characteristic hour-glass shape.

fig.a. ABCL 16. Asbian, Calp Shale-Upper Limestone, Carrick Lough. X12.

fig.b. Part of the obverse surface is encrusted by a serpulid on which a colony of Fistulipora incrustans (Phillips) has developed. ABCL 16. Horizon and locality as for fig.a. X12.

fig.c. S.E.M. photomicrograph showing the former positions of carinal nodes. ABCL 16. Horizon and locality as for fig.a. X25.

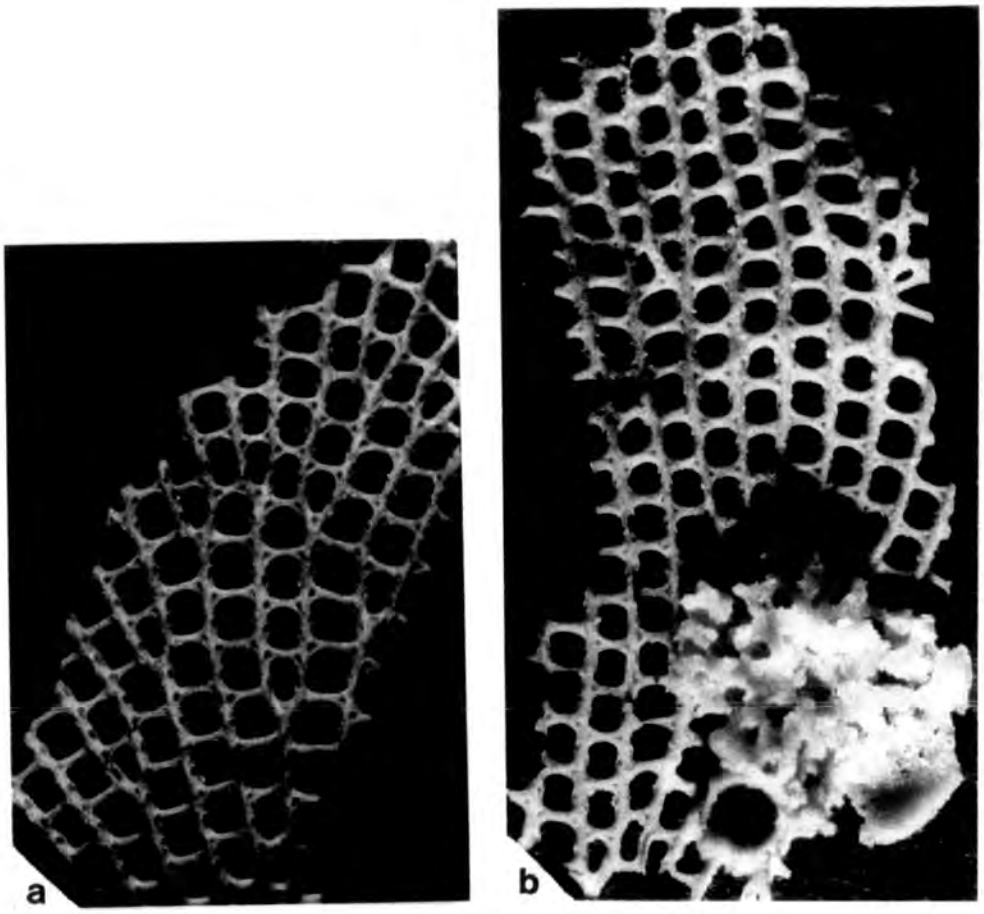
a
b

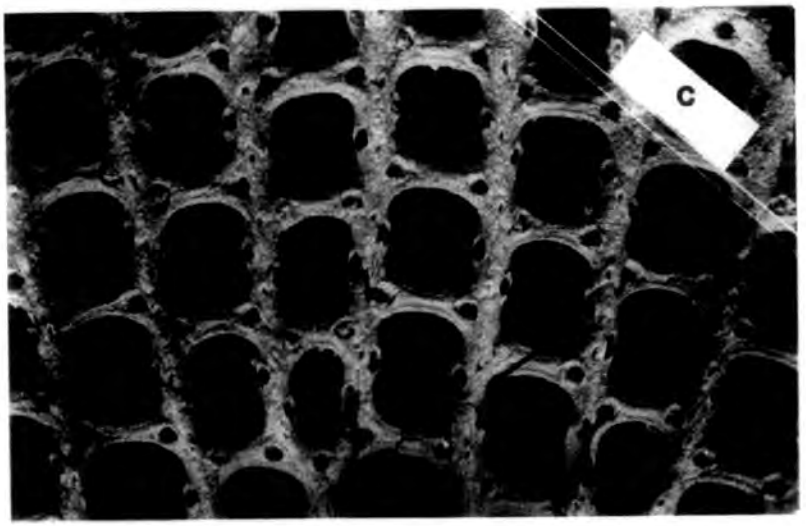
c

Plate 34. Fenestella ivanovi Shulga-Nesterenko

fig.a. Reverse surface detail. ABCL 16. Asbian, Calp Shale- Upper Limestone, Carrick Lough. X18.

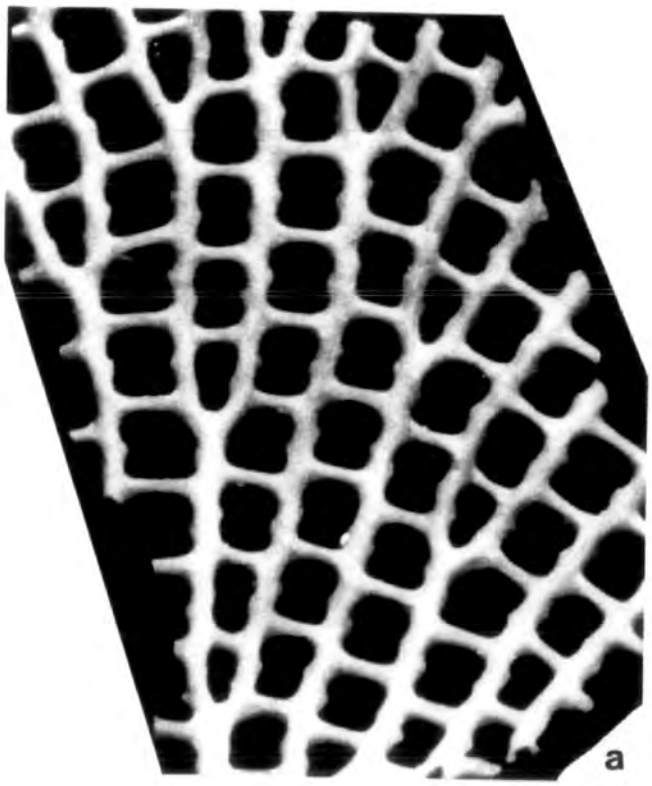
a

Plate 35. *Fenestella frutex* McCoy

fig.a. Lectotype; reverse surface detail. NMI F.6038. Asbian, Killymeal, Dungannon. X19.

fig.b. Detail of Millers (1961, p.232) syntype of *F. frutex* here referable to *Fenestella ivanovi* Shulga-Nesterenko. NMI F.6041. Asbian, Killymeal, Dungannon. X19.

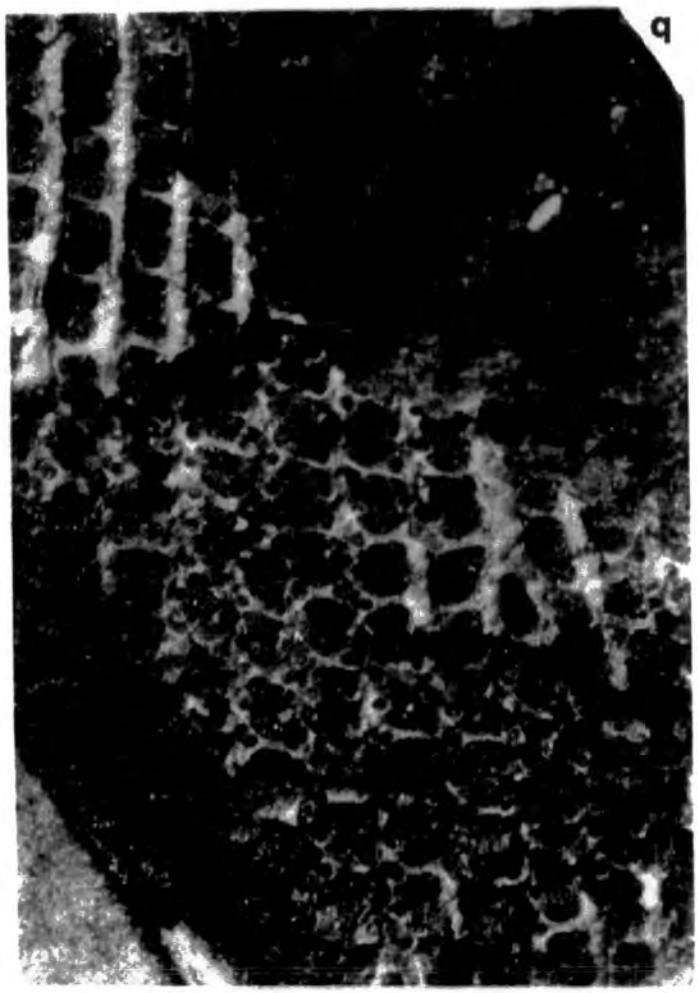
q

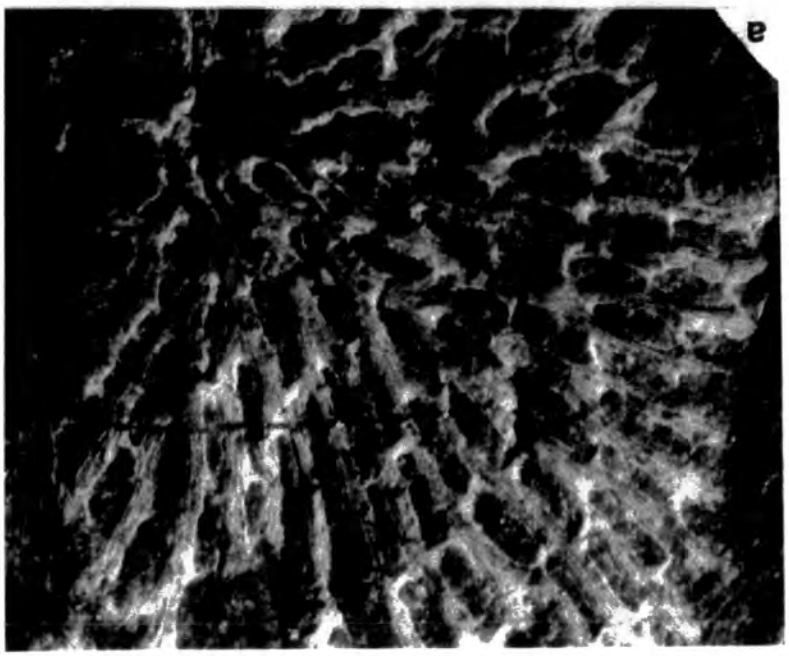
e

Plate 36. Fenestella frutex McCoy

fig.a. Obverse surface detail. ABP 159. Asbian, Alston Group, Fifth Limestone, Penruddock. X15.

fig.b. Obverse surface detail. ABP 159. Horizon and locality as for fig.a. X15.

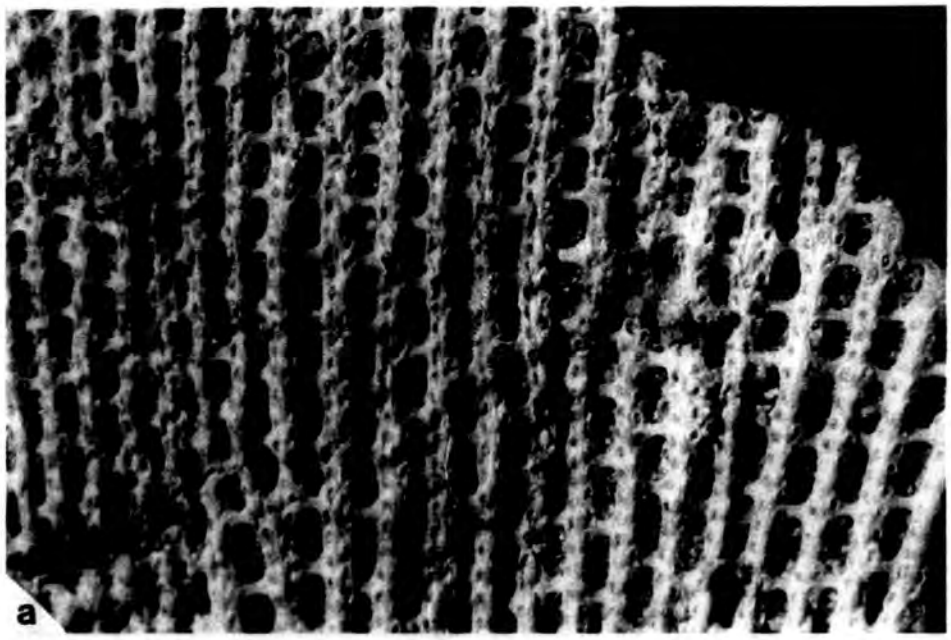
a

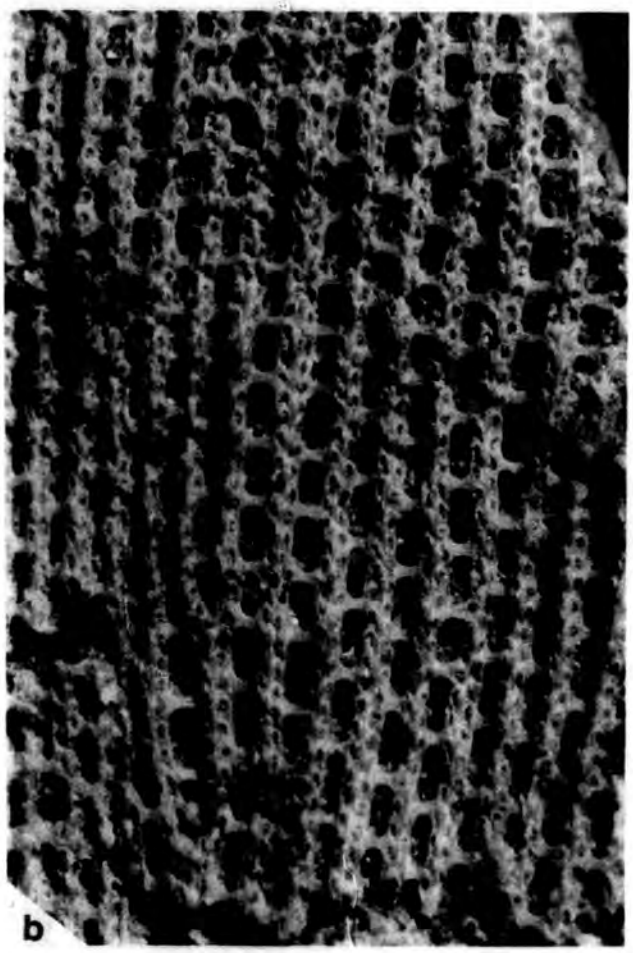
b

Plate 37. Fenestella frutex McCoy

fig.a. Colony origin. NH G155.67.11. Asbian, Lower Limestone Group, Redesdale Ironstone Shale, Ridsdale. X19.

fig.b. Reverse surface detail; the planar spiral encrustation is a serpulid. ABP 175. Asbian, Alston Group, Fifth Limestone, Penruddock. X16.

a

b

Plate 38. Fenestella frutex McCoy

fig.a. Reverse surface detail. ABP 195. Asbian, Alston Group, Fifth Limestone, Penruddock. X15.

fig.b. Oblique tangential section. ABP 306. Horizon and locality as for fig.a. X15.

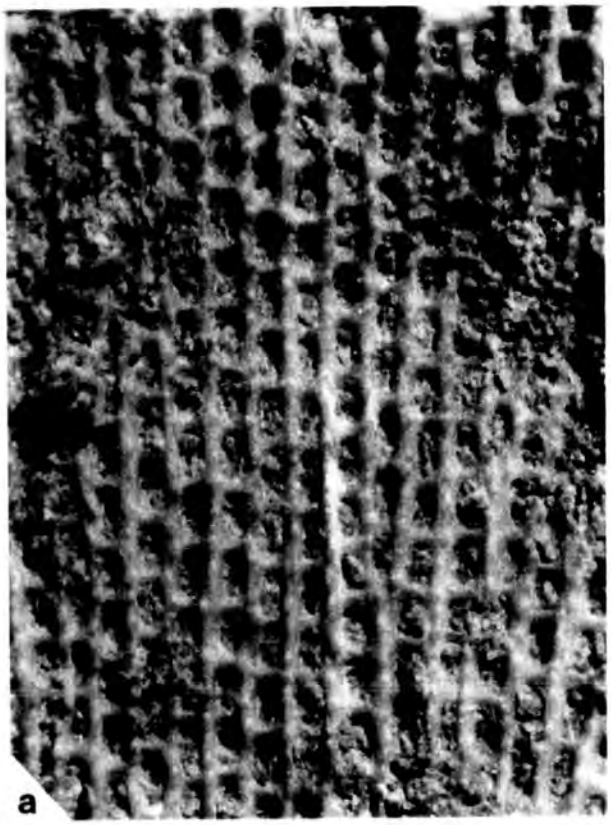

a

b

Plate 39. Fenestella frutex McCoy

fig.a. Oblique tangential section. ABP 305. Asbian, Alston Group, Fifth Limestone, Penruddock. X17.

fig.b. Tangential section through autozooecial chamber bases showing detail of skeletal tissues. ABP 305. Horizon and locality as for fig.a. X220.


a


b

Plate 40. Fenestella multispinosa Ulrich

fig.a. Obverse surface detail. ABCL 17. Asbian, Calp Shale- Upper Limestone, Carrick Lough. X17.

fig.b. Reverse surface detail; part of the specimen has been ground down to reveal obverse surface detail. BOM 25-09-206. Brigantian, Black Limestone, Halkyn Mountain, Clwyd. X11.


a

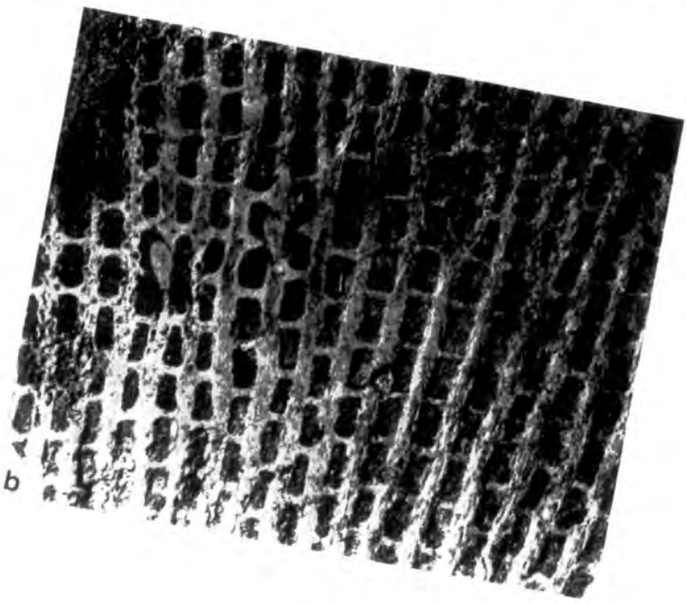
b

Plate 41. Fenestella multispinosa Ulrich

fig.a. Colony form. BOM 25-09-206. Brigantian, Black Limestone, Halkyn Mountain, Clwyd. X5.

fig.b. Reverse surface detail. HM D.454. Brigantian, Carboniferous Limestone Shale, High Blantyre. X16.

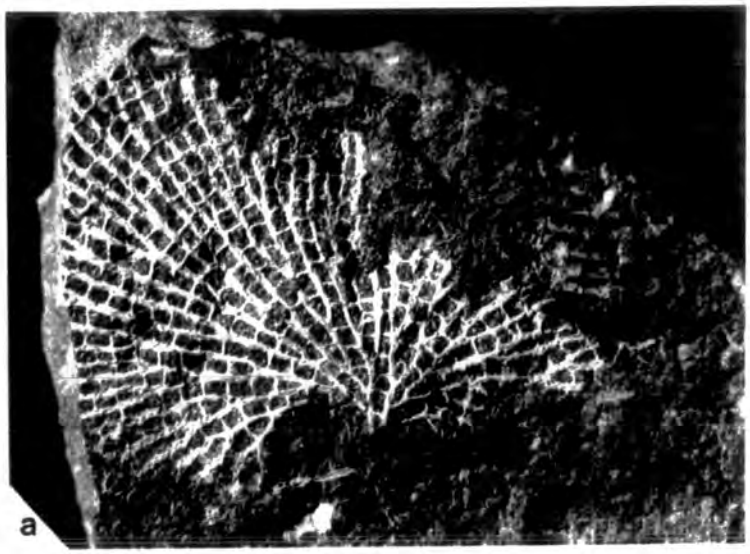
a

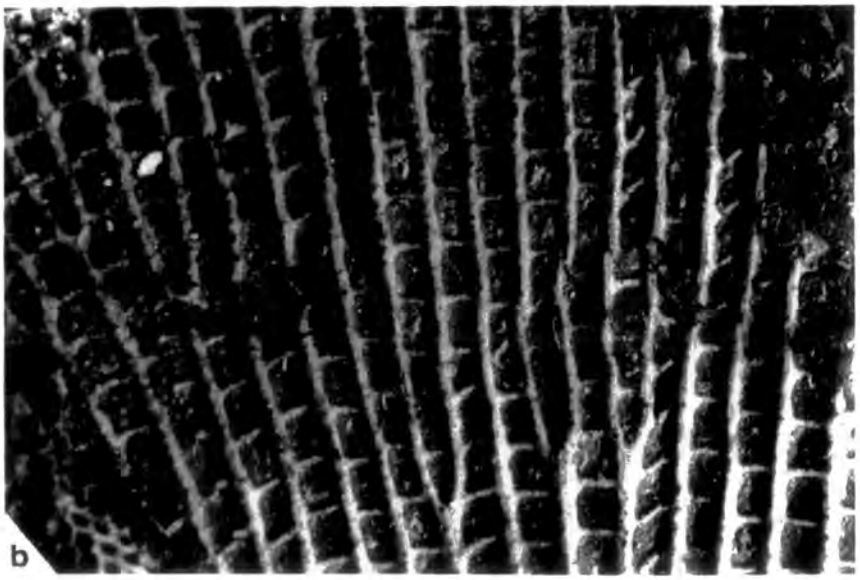
b

Plate 42. Fenestella multispinosa Ulrich

fig.a. Reverse surface detail. HM D.454. Brigantian, Carboniferous Limestone Shale, High Blantyre. X16.


a

Plate 43. Fenestella tuberculo-carinata Etheridge, Jun.

fig.a. Neotype; obverse surface detail.
GSE 89041-03. Brigantian, shale below the Hosie Limestone, Mouse Water, Wilsontown.
X26.
(this photograph is reproduced from Miller 1961, Pl.27, fig.2.)

fig.b. Obverse surface detail; the positions of some of the carinal nodes are indicated.
HM D.41. Brigantian, Lower Limestone Group, Roughwood, Beith. X16.

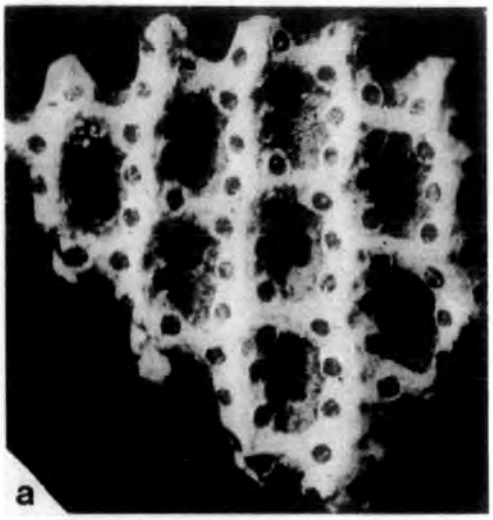
a

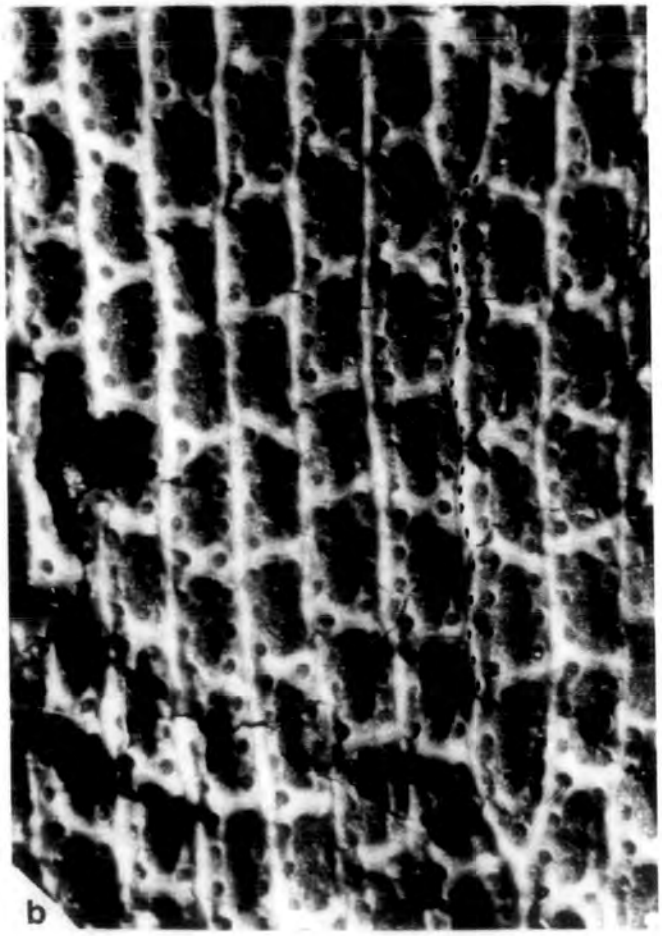
b

Plate 44. Fenestella tuberculo-carinata Etheridge, Jun.

fig.a. Obverse surface detail. HM D.41. Brigantian, Lower Limestone Group, Roughwood, Beith. X16.

fig.b. As for fig.a. X16.

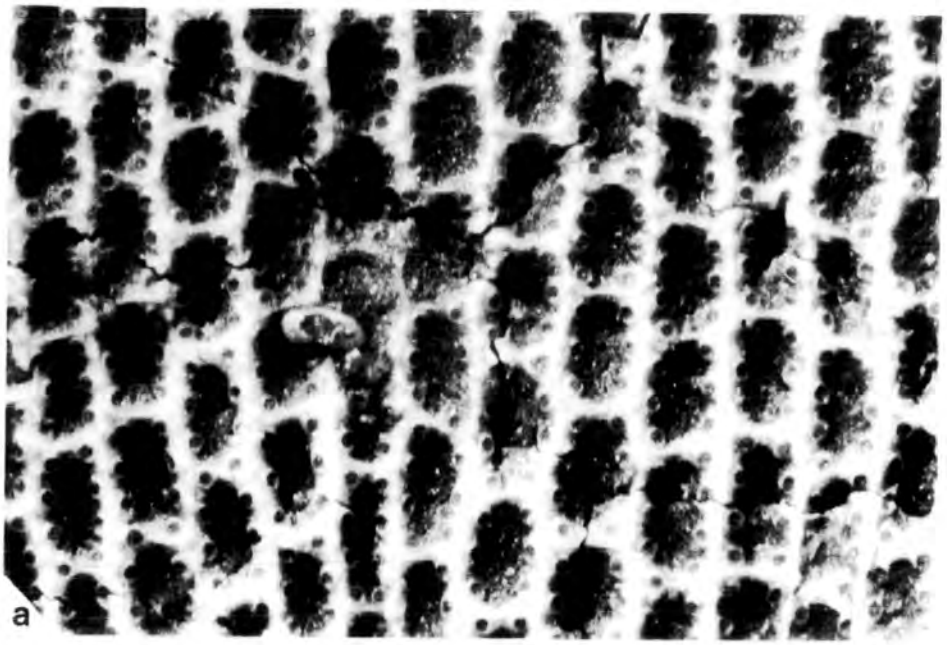
a

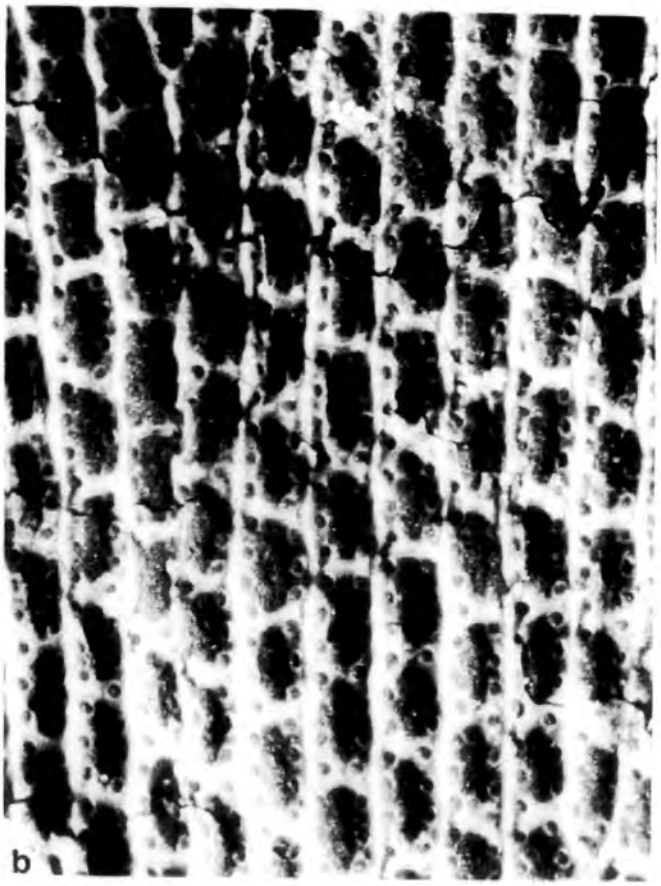
b

Plate 45. Fenestella tuberculo-carinata Etheridge, Jun.

fig.a. Reverse surface detail. HM D.44. Brigantian, Lower Limestone Group, Roughwood, Beith. X11.


a

Plate 46. Fenestella tuberculo-carinata Etheridge,Jun.

fig.a. Oblique tangential section showing the variation in autozooecial chamber shape with depth. HM D.45. Brigantian, Lower Limestone Series, Laigh, Baidland, Dalry. X36.

fig.b. As for fig.a. HM D.46. Horizon and locality as for fig.a. X36.

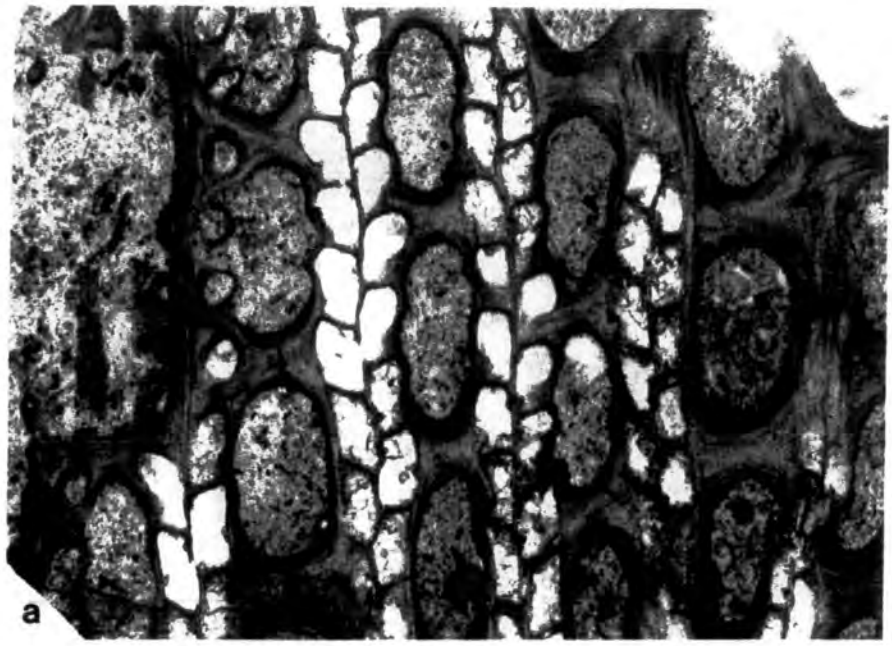

a

b

Plate 47. Fenestella tuberculo-carinata Etheridge, Jun.

fig.a. Shallow tangential section through the reverse side of branches. HM D.46. Brigantian, Lower Limestone Series, Laigh, Baidland, Dalry. X16.

fig.b. Shallow tangential section through the reverse side of branches showing the occurrence of small cores of the primary granular skeleton. HM D.45. Horizon and locality as for fig.a. X36.

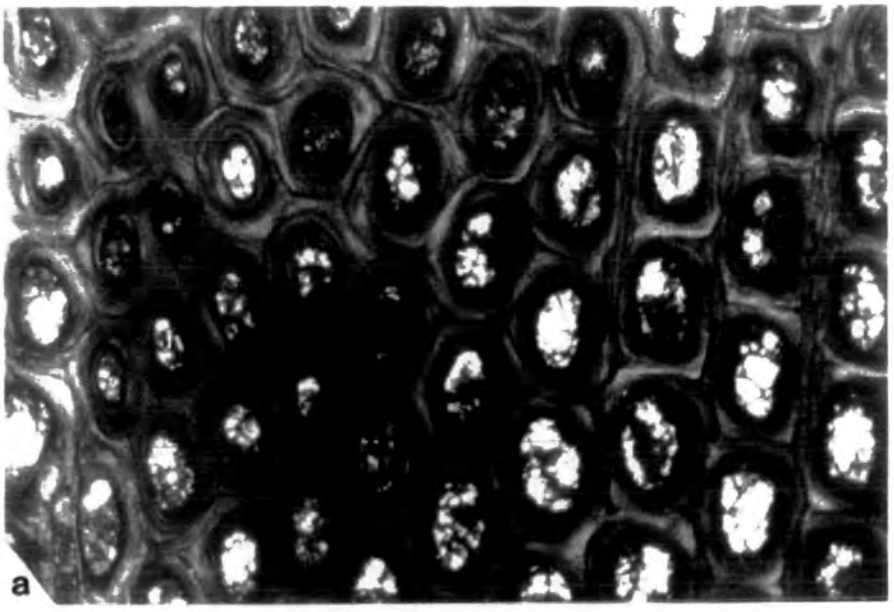
a

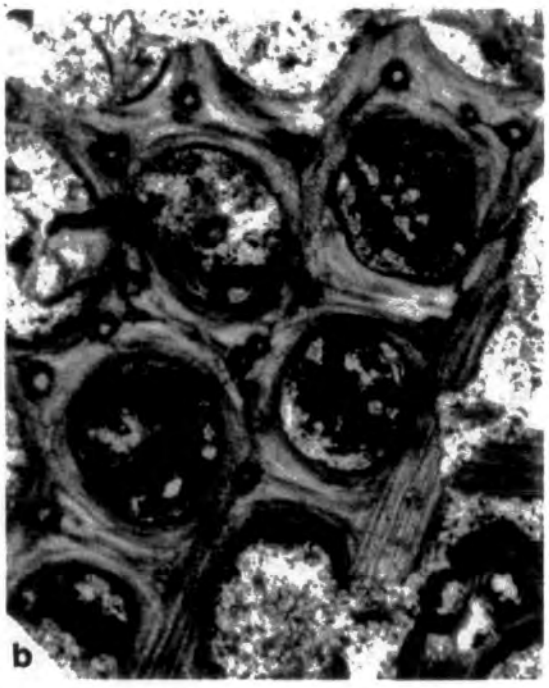
b

Plate 48. Fenestella plebeia McCoy

fig.a. Lectotype. NMI F.6035. Asbian, Carboniferous slate, Killybrone, Killala. X1.5.

fig.b. Type of Fenestella ejuncida McCoy. NMI F.6042. Asbian, Upper Limestone, Blacklion, Enniskillen. X1.8.

figs c and d. Two views of a large slightly foliaceous conical colony. NMI F.5286. Kildare. XO.62.

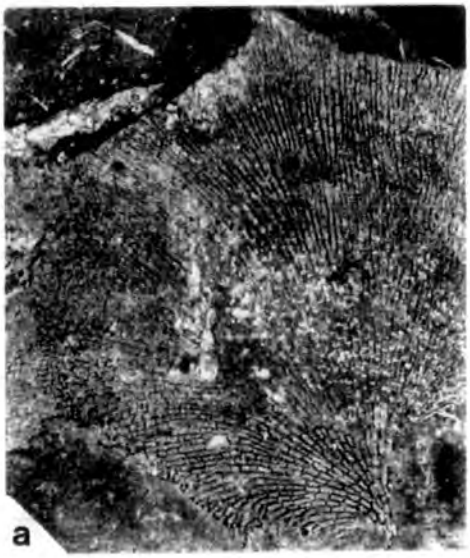

a

b

c

d

Plate 49. Fenestella plebeia McCoy

fig.a. High angle conical colony. BOM 25-09-220. Brigantian, Black Limestone, Halkyn Mountain, Clwyd. X1.7.

fig.b. Low angle horn-shaped conical colony. NMI F.6079. Asbian, Lower Limestone, Kilcommock, Londford. XO.6.

fig.c. Proximal area of a large high angle conical colony. BOM GWS+ 0.12. Brigantian, Black Limestone, Halkyn Mountain. X1.7.

fig.d. Planar fan-shaped colony. BOM 25-09-226

Horizon and locality as for fig.c.

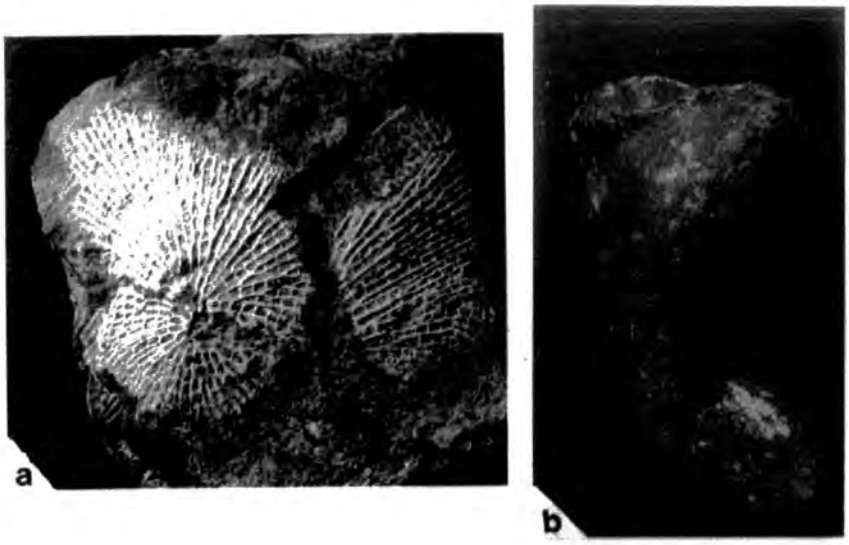
a
b

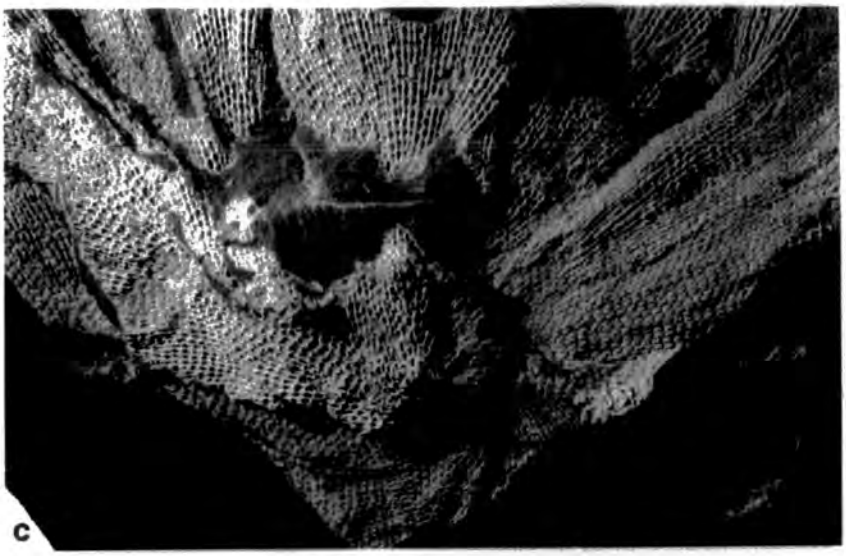
c

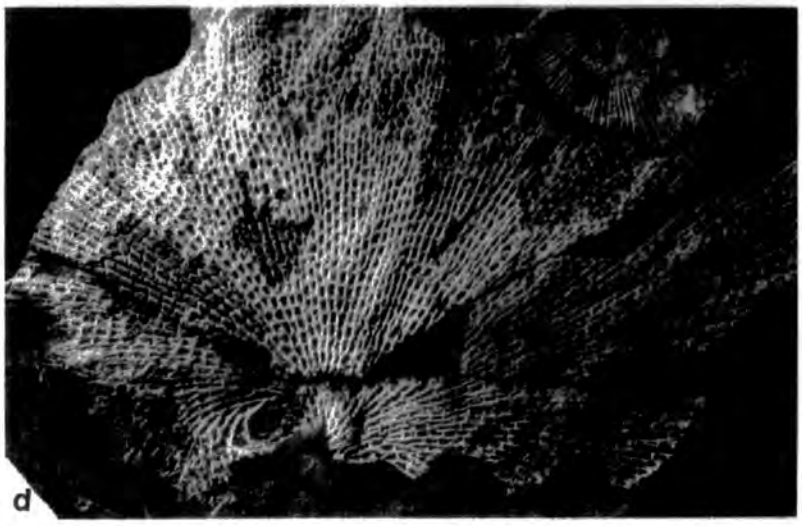
d

Plate 50. Fenestella plebeia McCoy

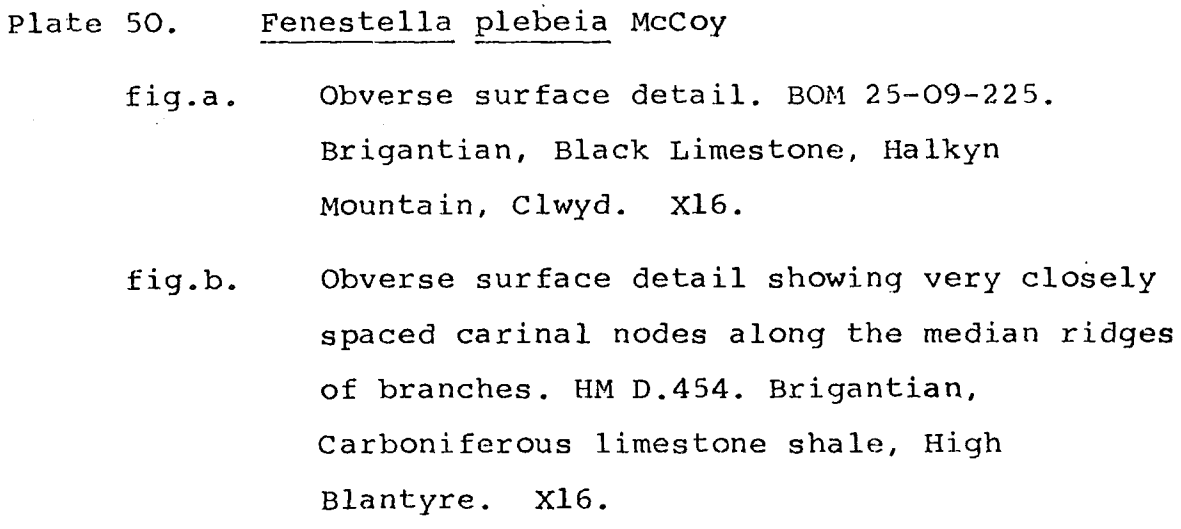

fig.a. Obverse surface detail. BOM 25-09-225. Brigantian, Black Limestone, Halkyn Mountain, Clwyd. X16.

fig.b. Obverse surface detail showing very closely spaced carinal nodes along the median ridges of branches. HM D.454. Brigantian, Carboniferous limestone shale, High Blantyre. X16.

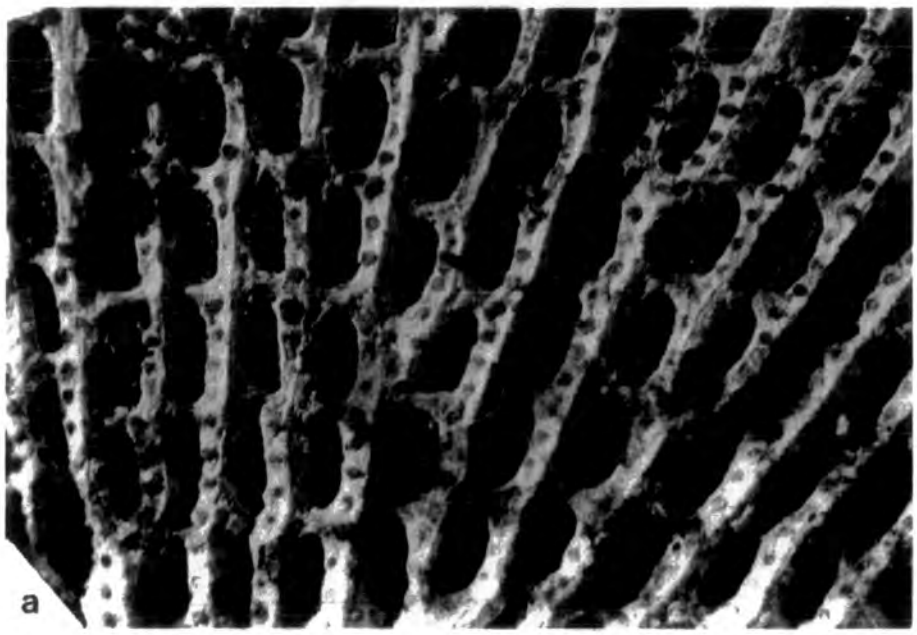
a


b

Plate 51. Fenestella plebeia McCoy

fig.a. Obverse surface detail. ABP 4. Asbian, Alston Group, Fifth Limestone, Penruddock. X16.

fig.b. As for fig.a. X16.

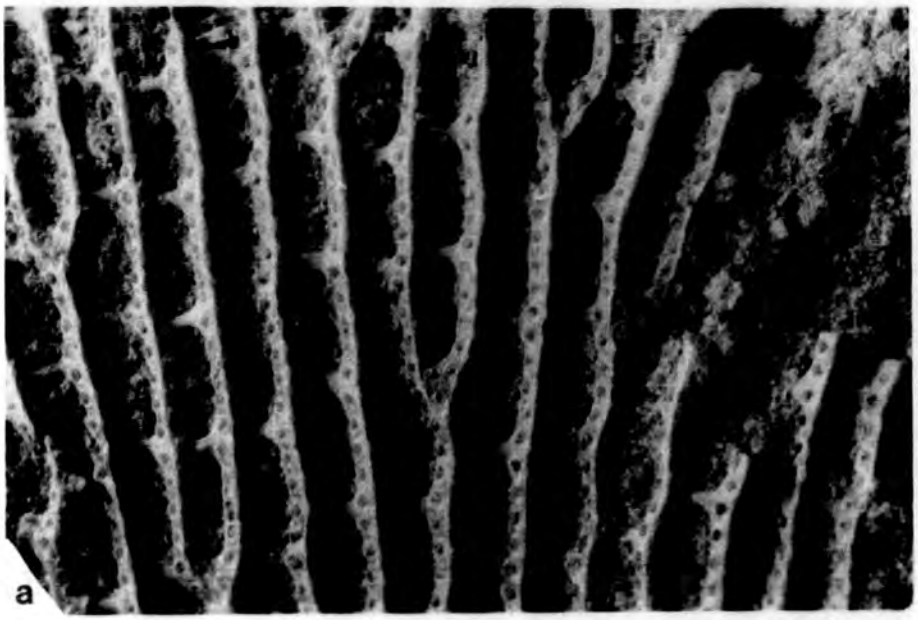
a


b

Plate 52. *Fenestella plebeia* McCoy

fig.a. Reverse surface detail, HM D.12:1.

Brigantian, Lower Limestone Group, High Blantyre. X16.

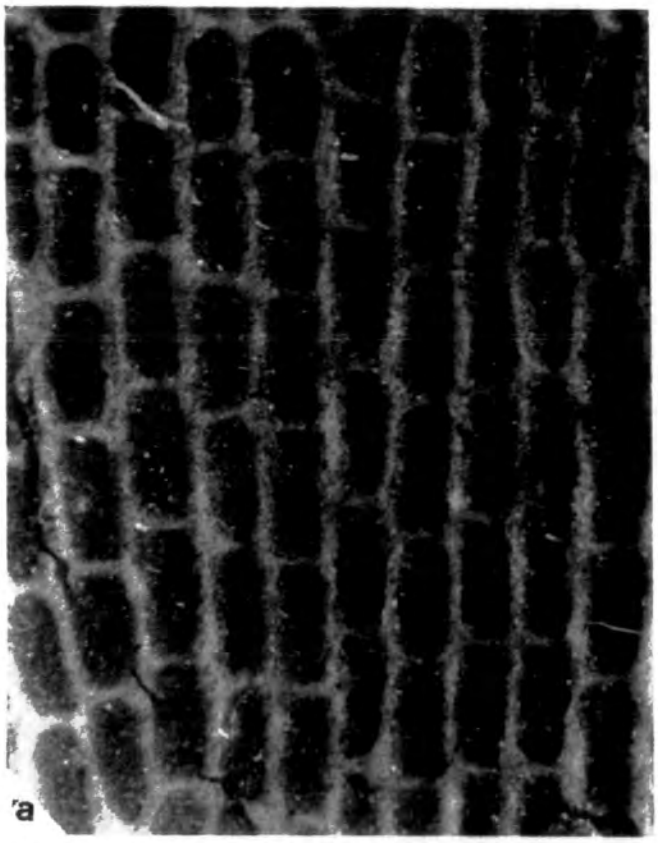
a

Plate 53. Fenestella papillata (McCoy)

fig.a. Lectotype; colony form. NMI F.6070. Asbian, Upper Limestone, Blacklion, Enniskillen. X2.

fig.a. As for fig.a. but showing obverse surface detail revealed in a polished ground down section. X12.

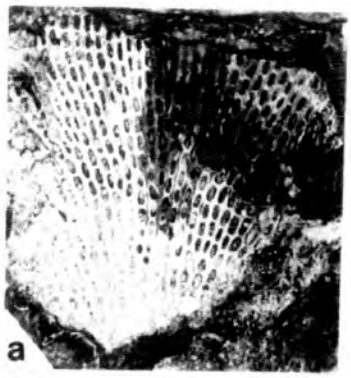
a


b

Plate 54. Fenestella papillata (McCoy)

fig.a. Lectotype; reverse surface detail. NMI F.6070. Asbian, Upper Limestone, Blacklion, Enniskillen. X12.

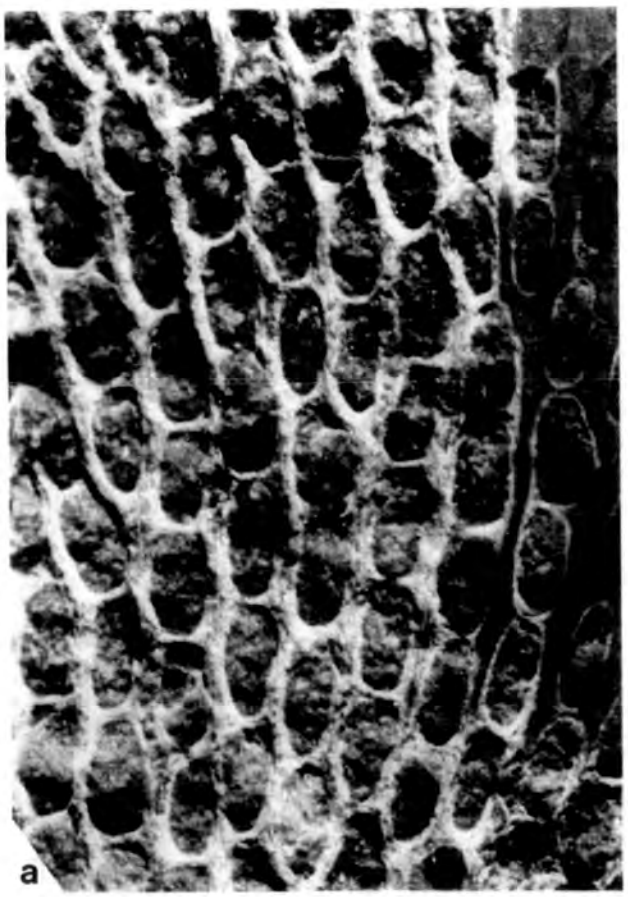
a

Plate 55. *Fenestella morrisii* McCoy

fig.a. Lectotype; colony form. NMI F.6034. Holkerian or Asbian, Lower Limestone, Little Island, Cork. Xl.2.

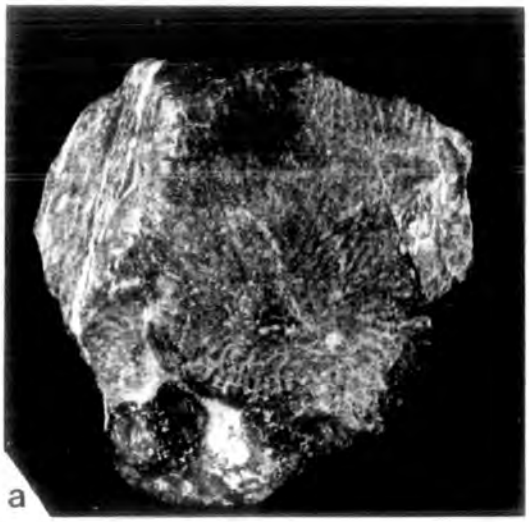

a

Plate 56. Fenestella polyporata (Phillips)

fig.a. Syntype of Fenestella multiporata McCoy showing colony form. NMI F.6041. Asbian, Upper Limestone?, Killymeal, Dungannon. X1.2.

fig.b. As for fig.a. but showing obverse surface detail. X16.

a

b

Plate 57. Fenestella polyporata (Phillips)

fig.a. Obverse surface detail. ABMG 26. Brigantian, Hardraw Shales, Mill Gill, Askrigg. X13.

fig.b. Obverse surface detail. ABMG 27. Horizon and locality as for fig.a. X13.


a


b

Plate 58. Fenestella polyporata (Phillips)

fig.a. Obverse surface detail; showing very closely spaced carinal nodes. ABMG 28. Brigantian, Hardraw Shales, Mill Gill, Askrigg. X13.

fig.b. Obverse surface detail. ABMG 26. Horizon and locality as for fig.a. X18.5.

a

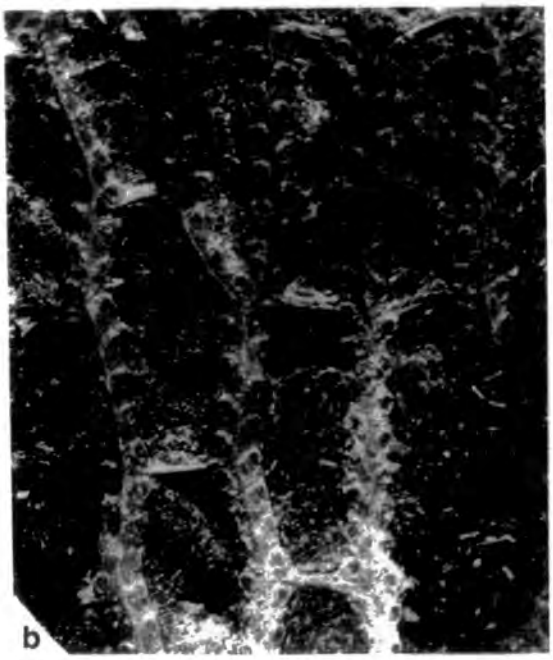

b

Plate 59. Fenestella polyporata (Phillips)

fig.a. Colony form. BOM 25-09-195. Asbian?, Castleton, Derbyshire. Xl.7.

fig.b. Weathered reverse surface showing detail of autozooecial chamber bases. BOM 25-09-192. Asbian?, Castleton, Derbyshire. Xll.


a

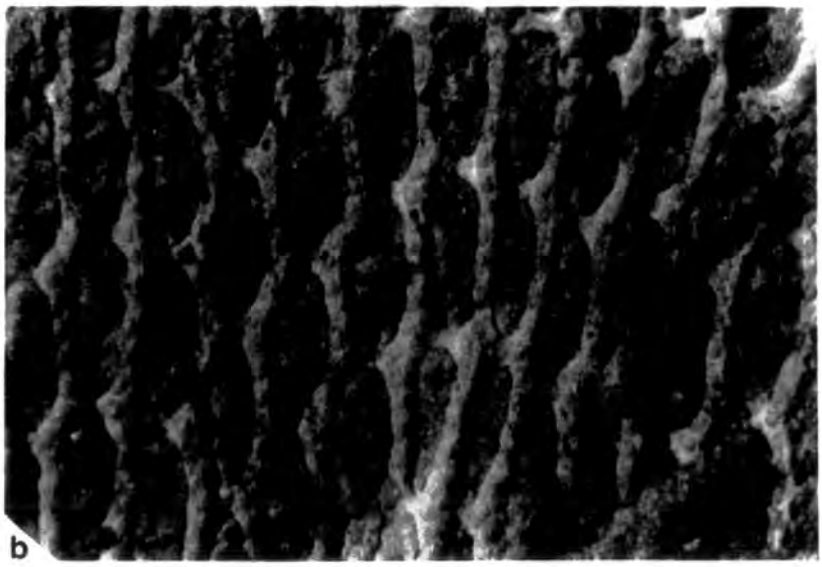
b

Plate 60. Fenestella quadridecimalis McCoy

fig.a. Lectotype; colony form. NMI F.6036. Asbian, Upper Limestone, Blacklion, Enniskillen. X1.76.

fig.b. Lectotype; polished ground down section revealing obverse surface detail. X16.

fig.c. Obverse surface detail. HM D.4/1. Arnsbergian, Upper Limestone Group, shale above the Gillfoot Limestone, Carluke. X17.

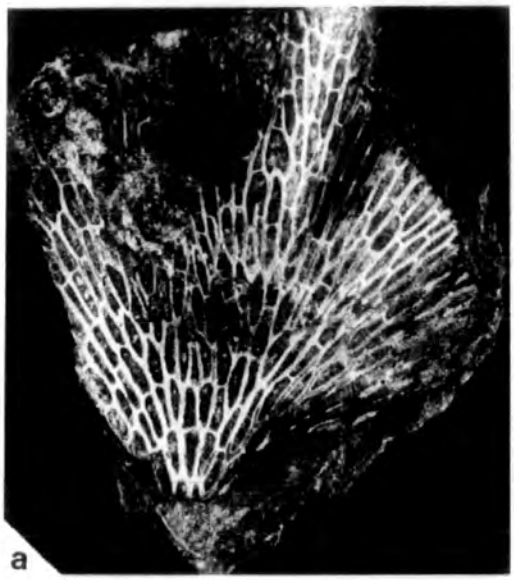

a

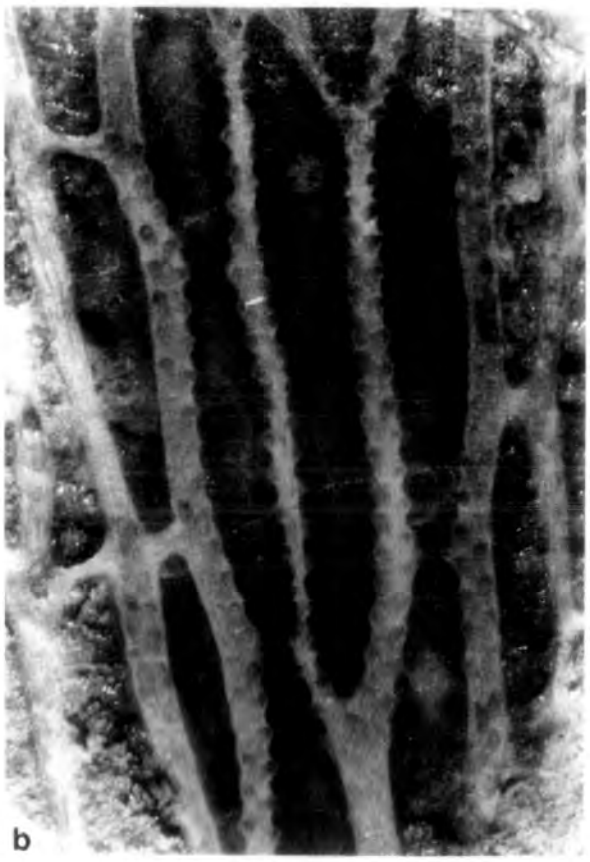

b

c

Plate 61. Minilya plummerae(Moore)

fig.a. Obverse surface detail. ABP 153. Asbian, Alston Group, Fifth Limestone Penruddock. X13.5.

fig.b. As for fig.a. but with some of the positions of carinal nodes indicated. X18.


a


b

Plate 62. Minilya nodulosa (Phillips)

fig.a. Obverse surface detail. ABP 135. Asbian, Alston Group, Fifth Limestone, Penruddock. X14.

fig.b. Obverse surface detail. ABAF 3. Asbian, Alston Group, Knipe Scar Limestone, Ashfell Edge, Cumbria. X18.5.

a

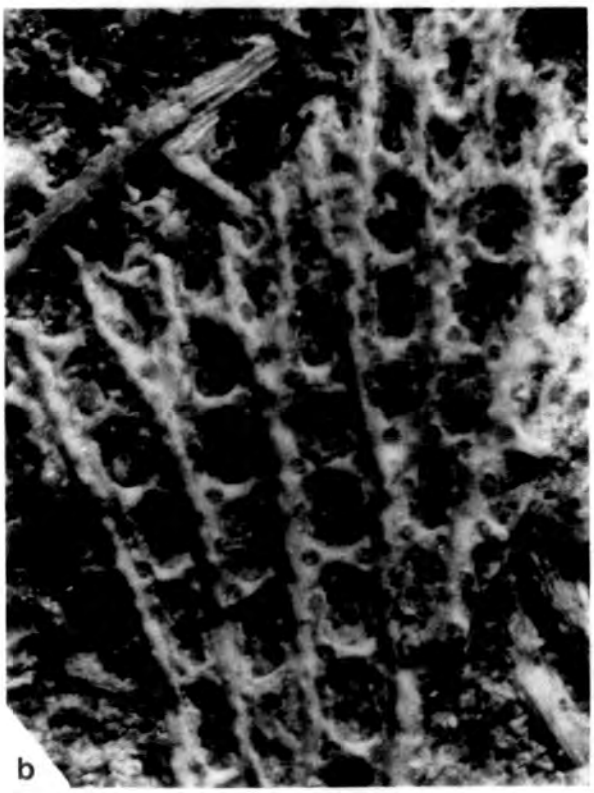

b

Plate 63. *Minilya nodulosa* (Phillips)

fig.a. Obverse surface detail; the positions of some of the carinal nodes are indicated. ABP 131. Asbian, Alston Group, Fifth Limestone, Penruddock. X18.

fig.b. Obverse surface detail. ABCL 18. Asbian, Calp Shale-Upper Limestone, Carrick Lough. X11.

fig.c. Reverse surface detail of specimen shown in fig.b. X18.

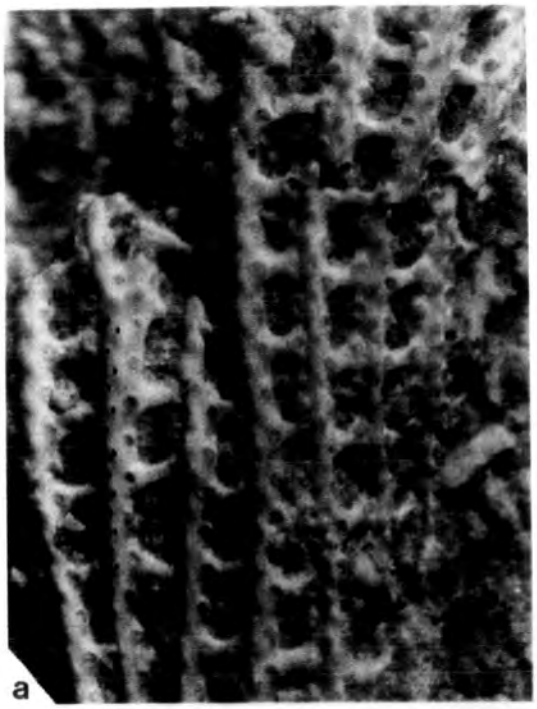
a

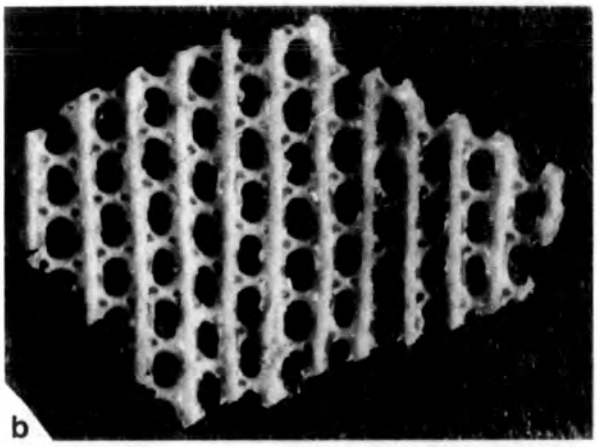
b

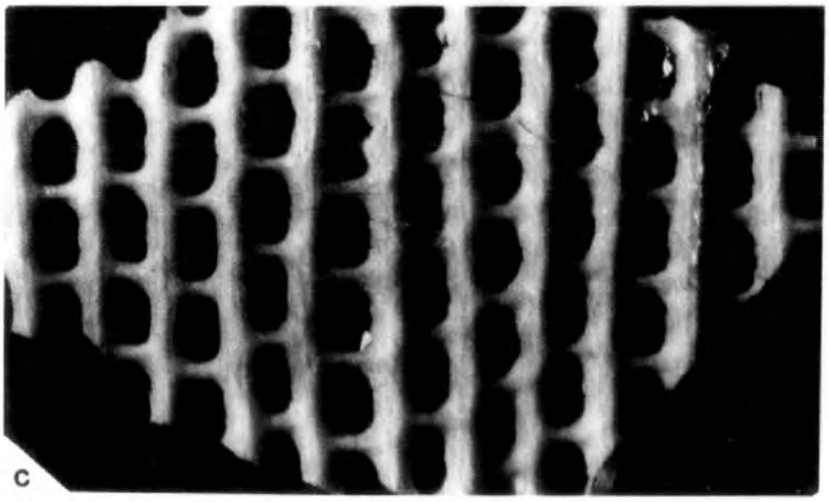
c

Plate 64. Ptiloporella varicosa (McCoy).

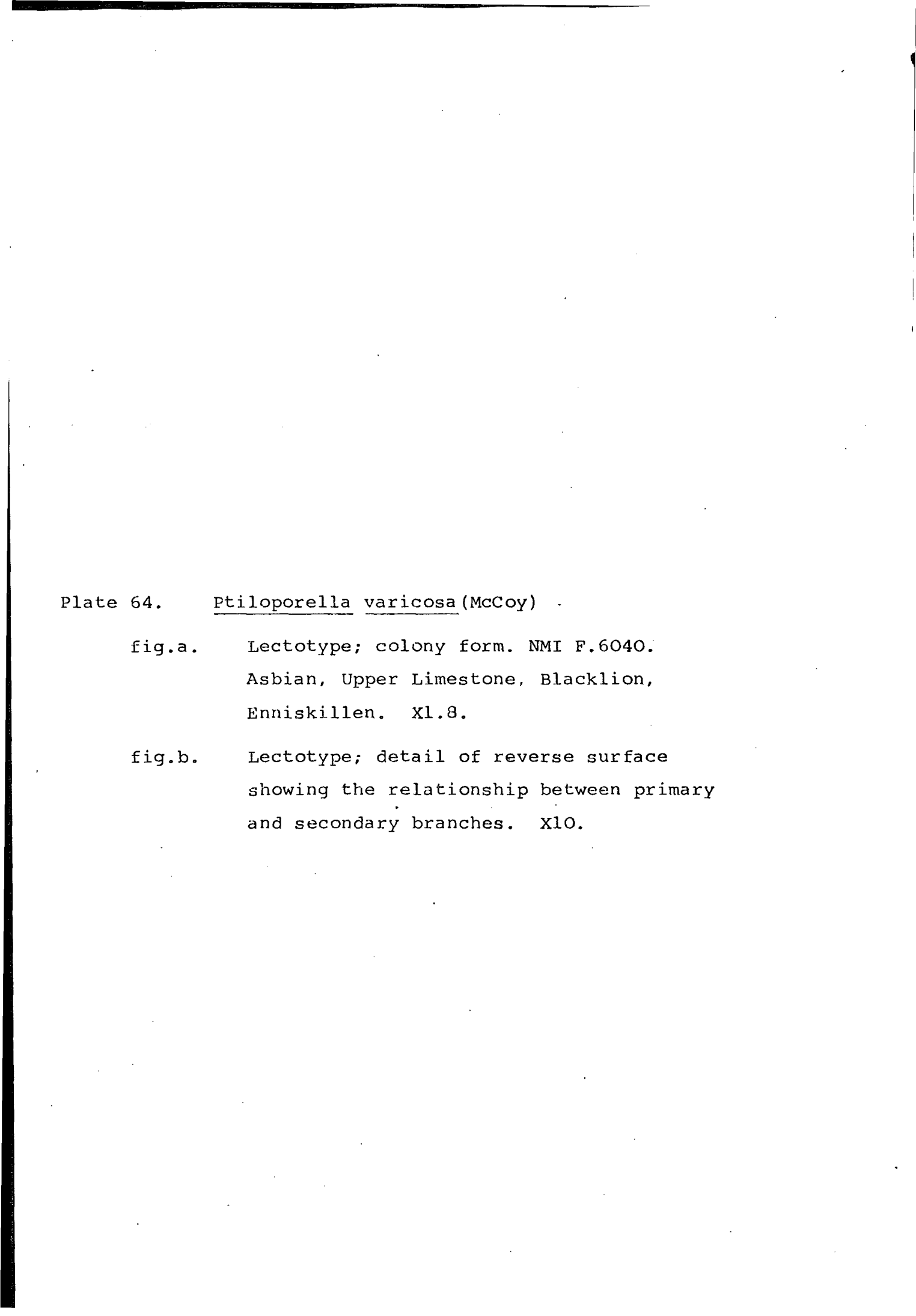

fig.a. Lectotype; colony form. NMI F.6040. Asbian, Upper Limestone, Blacklion, Enniskillen. X1.8.

fig.b. Lectotype; detail of reverse surface showing the relationship between primary and secondary branches. X10.

a

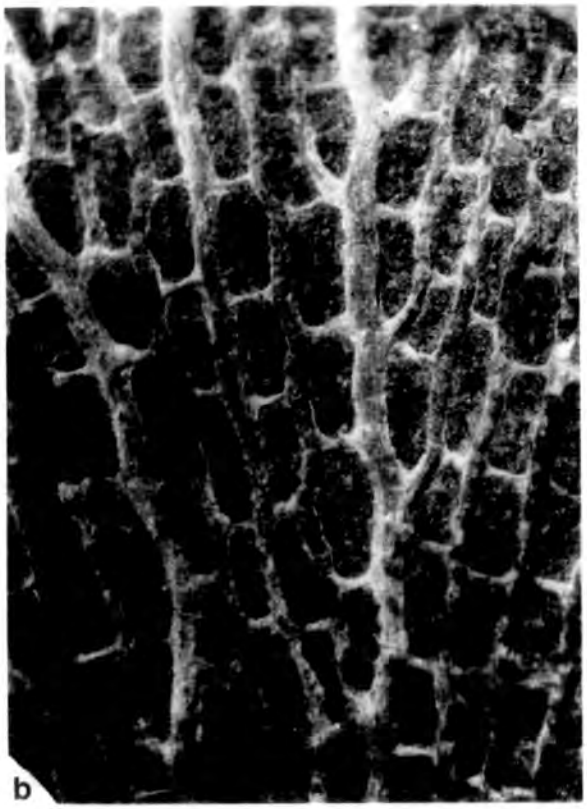

b

Plate 65. Hemitrypa hibernica McCoy

figs a and b. Lectotype; two views showing the low angle conical colony form. NMI F.6022. Holkerian or Asbian. Lower Limestone, Little Island, Cork. X1.7.

fig.c. Lectotype; detail of the superstructure. X10.


a
b

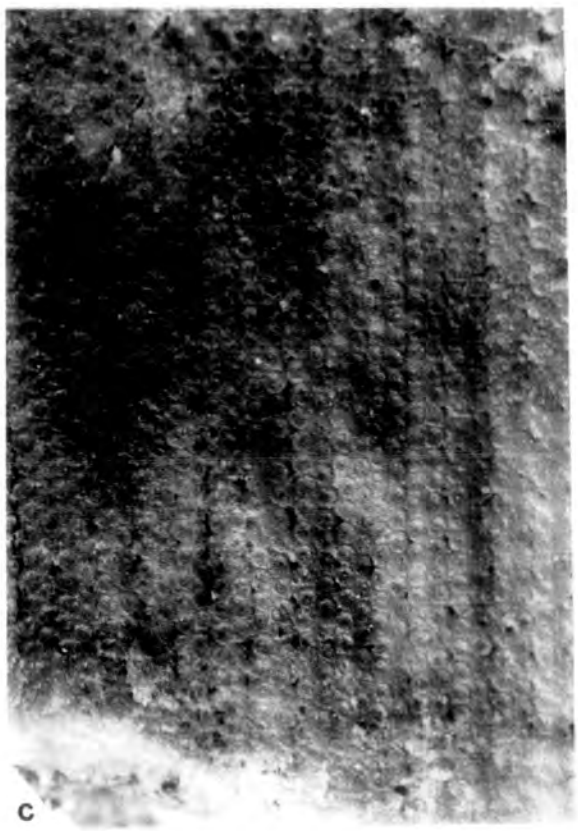
c

Plate 66. Hemitrypa hibernica McCoy

fig.a. Syntype; showing a deformity in the growth of a low angle conical zoarium. NMI F.6080. Holkerian or Asbian, Lower Limestone, Little Island, Cork. Xl.3.

fig.b. Syntype; colony form showing a low angle conical zoarium with crenulations developed. NMI F.6081. Horizon and locality as for fig.a. X76.

fig.c. Syntype. NMI F.6065. Asbian, Calp, Ballintrillick, Bundoran, Donegal. Xl.3.

fig.d. Syntype. NMI F. 6066. Horizon and locality as for fig.c. Xl.3.

a

b

c

d

Plate 67. Hemitrypa hibernica McCoy

fig.a. Syntype, showing detail of the superstructure that has partly broken away to reveal the obverse surface of the main fenestellid meshwork below. NMI F.6065. Asbian, Calp, Ballintrillick, Bundoran, Donegal. X11.

fig.b. Syntype, showing detail of the superstructure that has partly broken away to reveal moulds of the fenestellid meshwork below. NMI F.6066. Horizon and locality as for fig.a. X11.

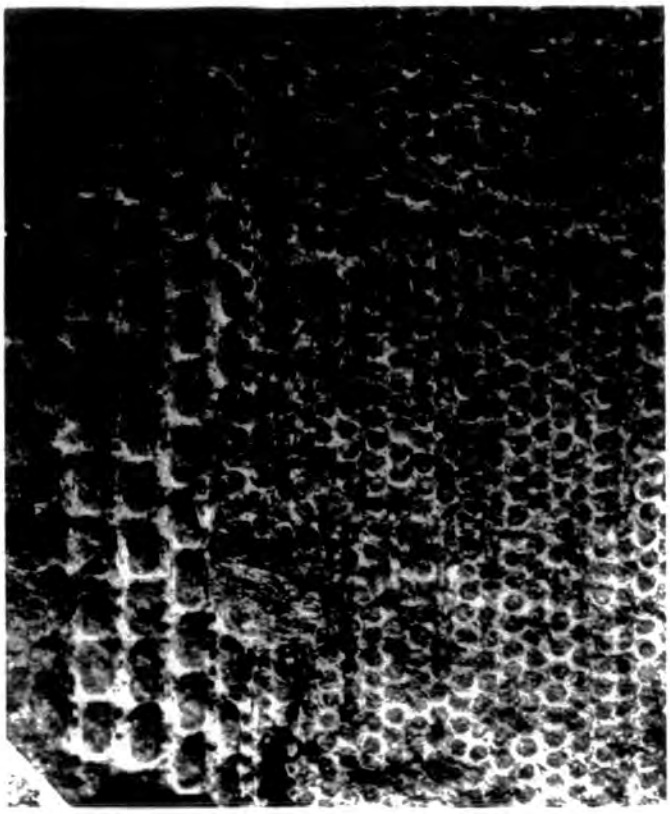


b

Plate 68. Hemitrypa hibernica McCoy

fig.a. Type of Fenestella carinata McCoy. NMI F.6033. Asbian, Carboniferous Shale, Enagh, Tynan. X1.3.

fig.b. Detail of the perforate superstructure, also showing stout supporting spines. ABCL 20. Asbian, Calp Shale-Upper Limestone, Carrick Lough. X13.

a

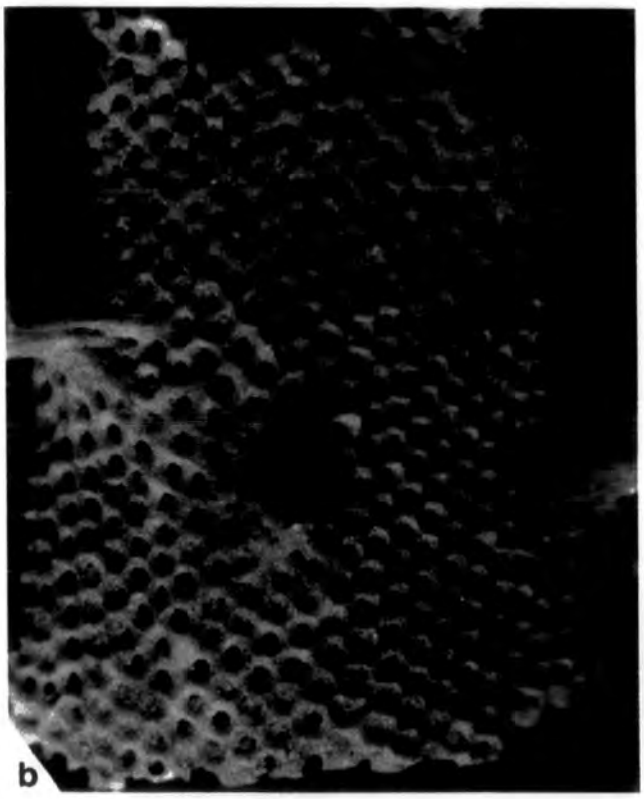

b

Plate 69. Hemitrypa hibernica McCoy

figs a and b show detail of the superstructure. It has a stouter construction above branches to which it is connected by the pillar like carinal nodes. The roughly hexagonal shape of the individual meshwork units is evident, but the perforations, that are situated directly above apertures on the branches below, are quite well rounded.

fig.a. ABP 107. Asbian, Alston Group, Fifth Limestone, Penruddock. X13.

fig.b. As for fig.a. X19.

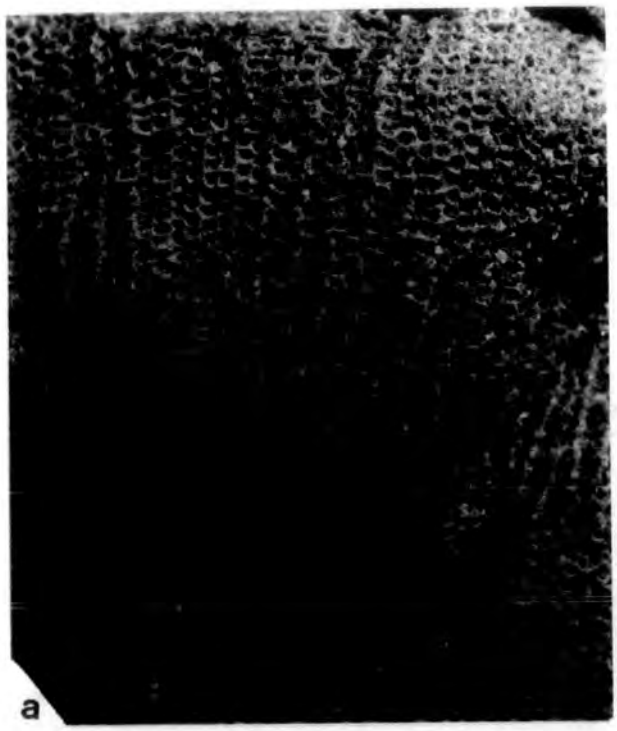
a


b

Plate 70. Hemitrypa hibernica McCoy

figs a and b show silicified colony fragments with the superstructure preserved in position by the pillar-like carinal nodes above branches.

fig.a. ABCL 20. Asbian, Calp Shale-Upper Limestone, Carrick Lough. X13.

fig.b. As for fig.a. X13.

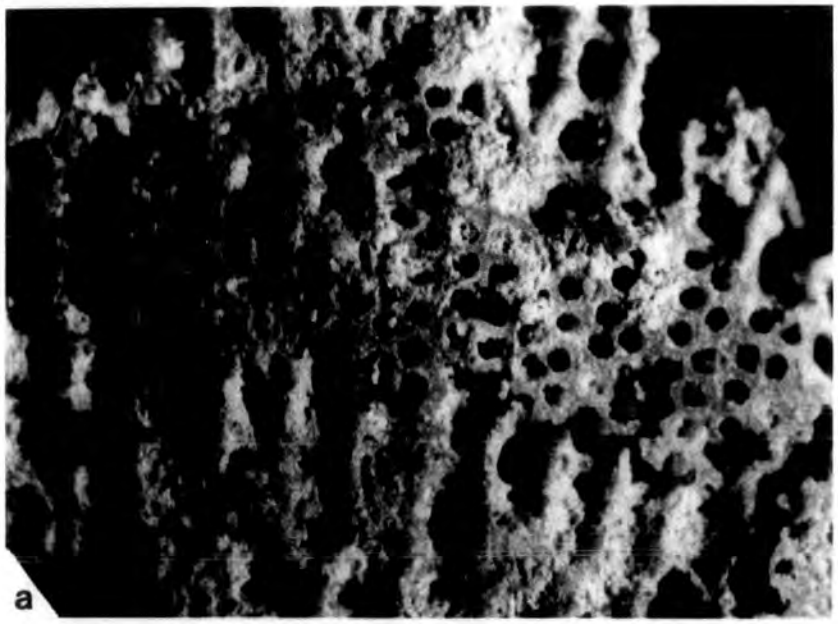
a

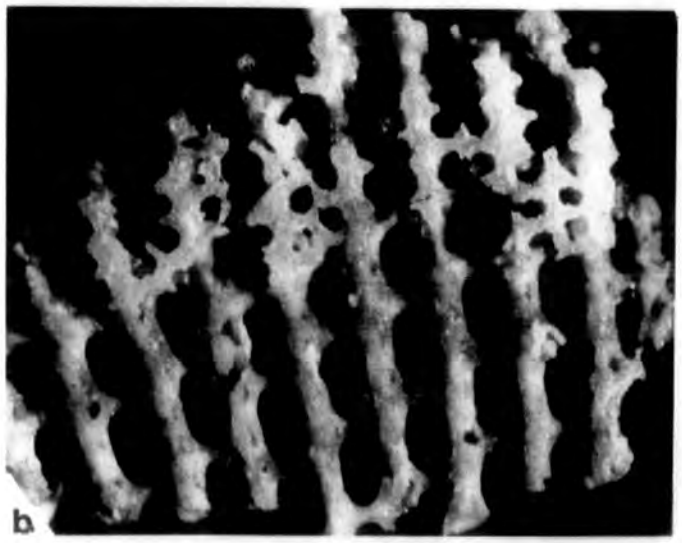
b

Plate 71. Hemitrypa hibernica McCoy

fig.a. The superstructure has partially broken away revealing the obverse surface of the main fenestellid meshwork below. ABP 100. Asbian, Alston Group, Fifth Limestone, Penruddock. X13.

fig.b. As for fig.a., but showing detail of the obverse surface of branches. X19.


a


b

Plate 72. Hemitrypa hibernica McCoy

fig.a. Obverse surface detail of the fenestellid meshwork, also showing large ovicellular cavities. ABCL 20. Asbian, Calp Shale-Upper Limestone, Carrick Lough. X17.

fig.b. Lateral view showing the superstructure supported at a uniform distance above branches by the pillar-like carinal nodes. ABCL 20. Horizon and locality as for fig.a. X17.

fig.c. Reverse surface detail. ABP 114. Asbian, Alston Group, Fifth Limestone, Penruddock. X18.5.

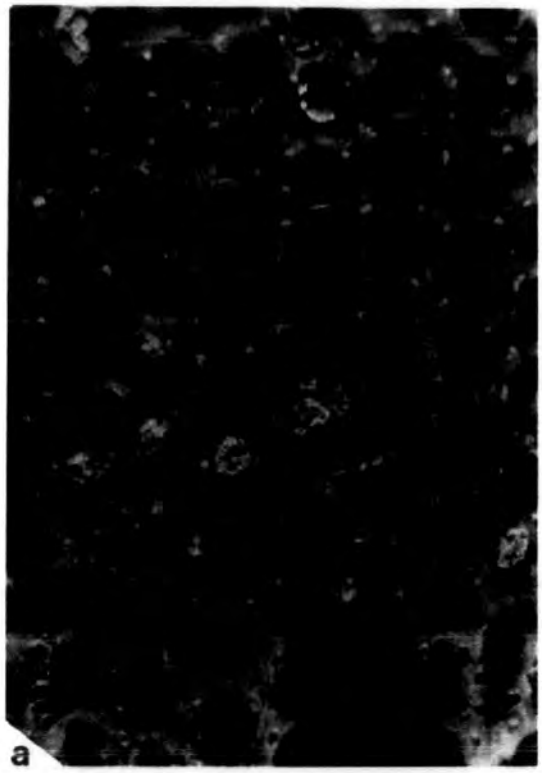
a


b

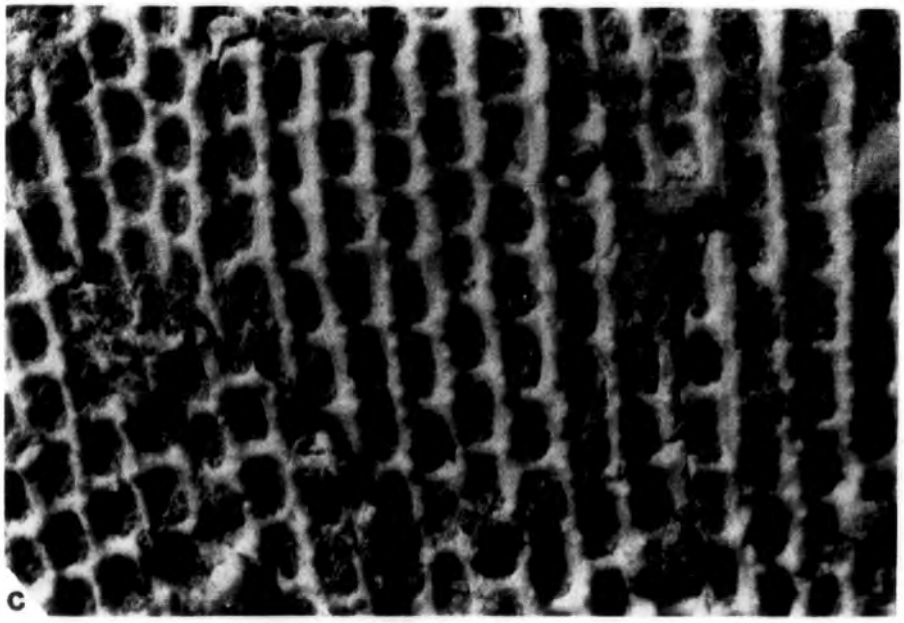
c

Plate 73. Hemitrypa hibernica McCoy

fig.a. Oblique tangential section showing the variation in the shape of autozooecial chambers with depth. ABRE 243. Holkerian, Orton Group, Seventh Limestone, Redmain. X51.

fig.b. Tangential section showing detail of autozooecial chamber bases and surrounding skeletal tissues. ABRE 243. Horizon and locality as for fig.a. X145.


q


e

Plate 74. Hemitrypa hibernica McCoy

fig.a. Longitudinal section. ABRE 254. Holkerian, Orton Group, Seventh Limestone, Redmain. X34.

fig.b. As for fig.a. X130.

fig.c. Longitudinal section showing detail of the outer secondary laminated skeleton. ABRE 254. Horizon and locality as for fig.a. X240.

a

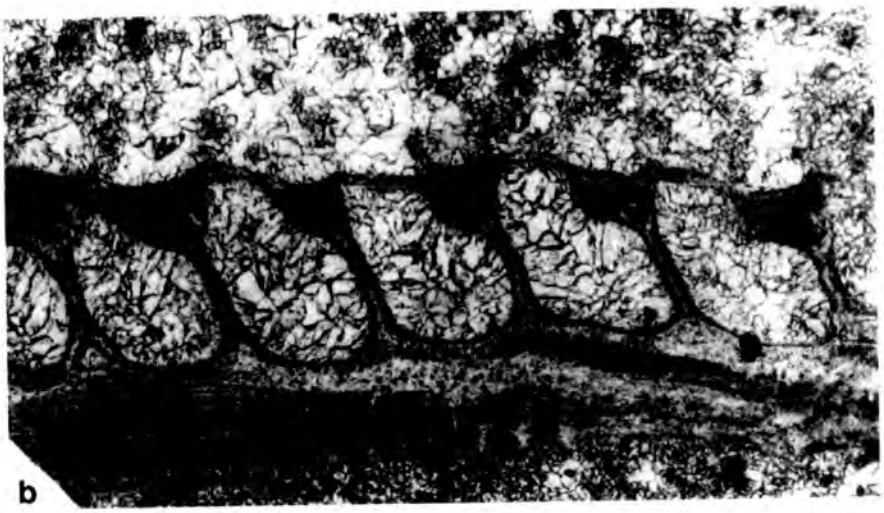

b

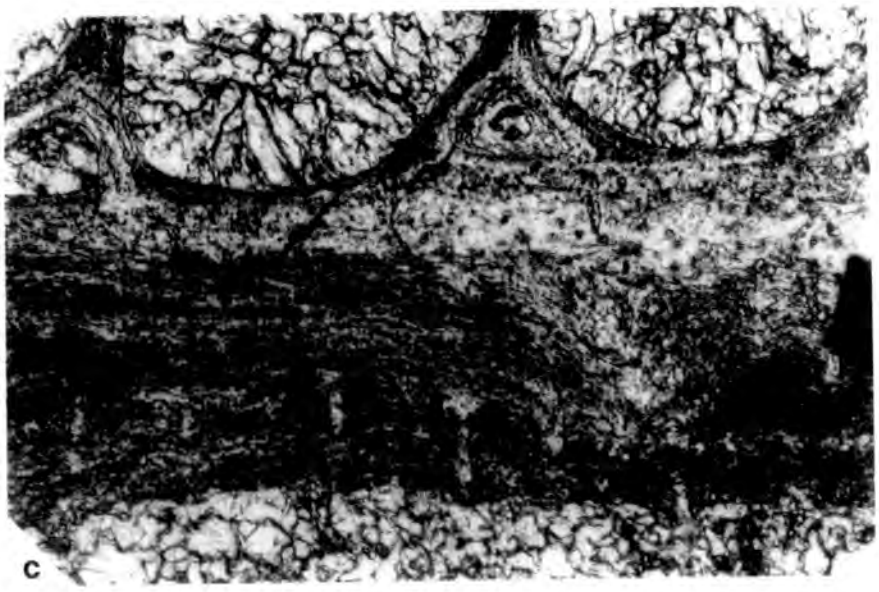

c

Plate 75. Hemitrypa hibernica McCoy

fig.a. Longitudinal section showing the connection of the superstructure and branch by the supporting pillar-like carinal nodes at a uniform distance above the branch surface. ABRE 250. Holkerian, Orton Group, Seventh Limestone, Redmain. X37.

fig.b. As for fig.a. X93.

fig.c. Transverse section showing the connection of the superstructure and branches by supporting pillar-like carinal nodes at a uniform distance above the obverse surface of branches. ABRE 236. Horizon and locality as for fig.a. X39.

fig.d. Transverse section showing a colony of Fistulipora incrustans (Phillips) encrusting the surface of the superstructure. ABRE 236. Horizon and locality as for fig.a. X39.


a

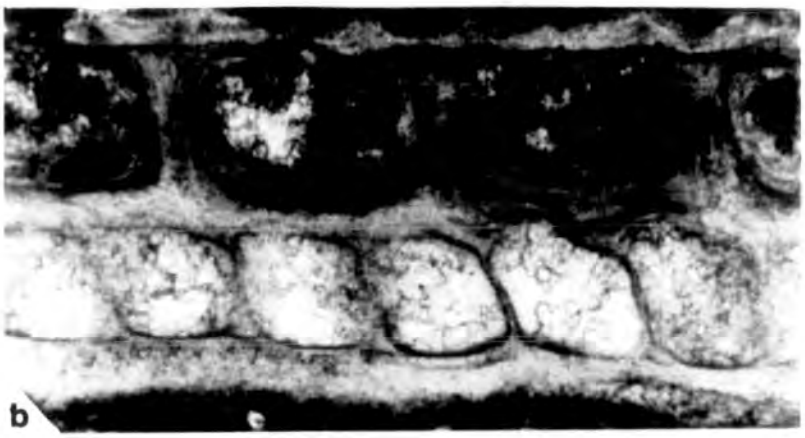
b


c

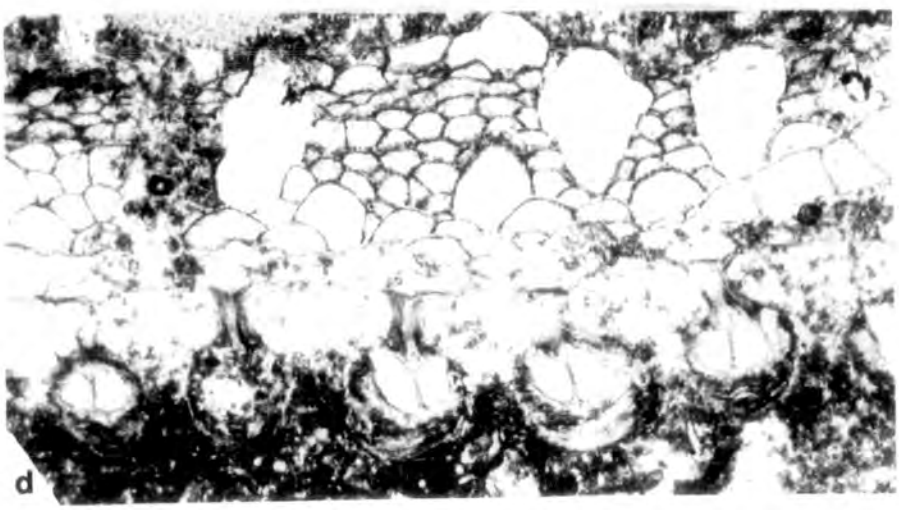
d

Plate 76. Hemitrypa hibernica McCoy

fig.a. Transverse section showing colony of Fistulipora incrustans (Phillips) encrusting the surface of the superstructure. ABRE 236. Holkerian, Orton Group, Seventh Limestone, Redmain. X55.

fig.b. Transverse section showing detail of the skeletal tissues of a branch, pillar-like carinal node, and the supported superstructure. ABRE 236. Horizon and locality as for fig.a. X227.

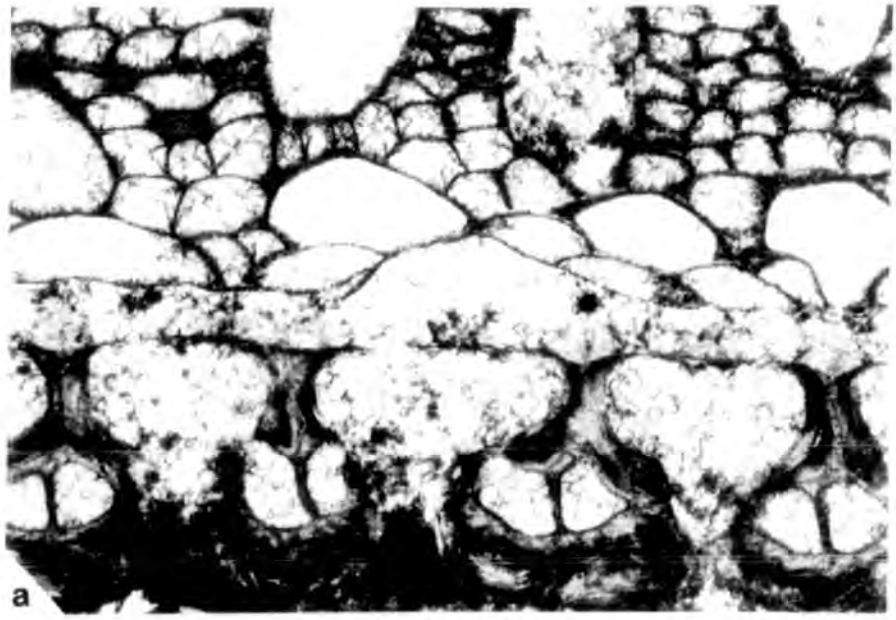

a

b

Plate 77. Hemitrypa hibernica McCoy

fig.a. Transverse section showing detail of the skeletal tissues of a branch, pillar-like carinal node and the supported superstructure. A very thin primary granular layer surrounds autozooecial chambers and forms the central narrow core of the pillar-like carinal nodes, and is seen to be continuous into the superstructure forming its central core. The thicker outer secondary laminated tissues of the branch are seen to be continuous along the length of the pillar-like carinal node and the superstructure where it also encloses the primary granular layer. ABRE 236. Holkerian, Orton Group, Seventh Limestone, Redmain. X400.

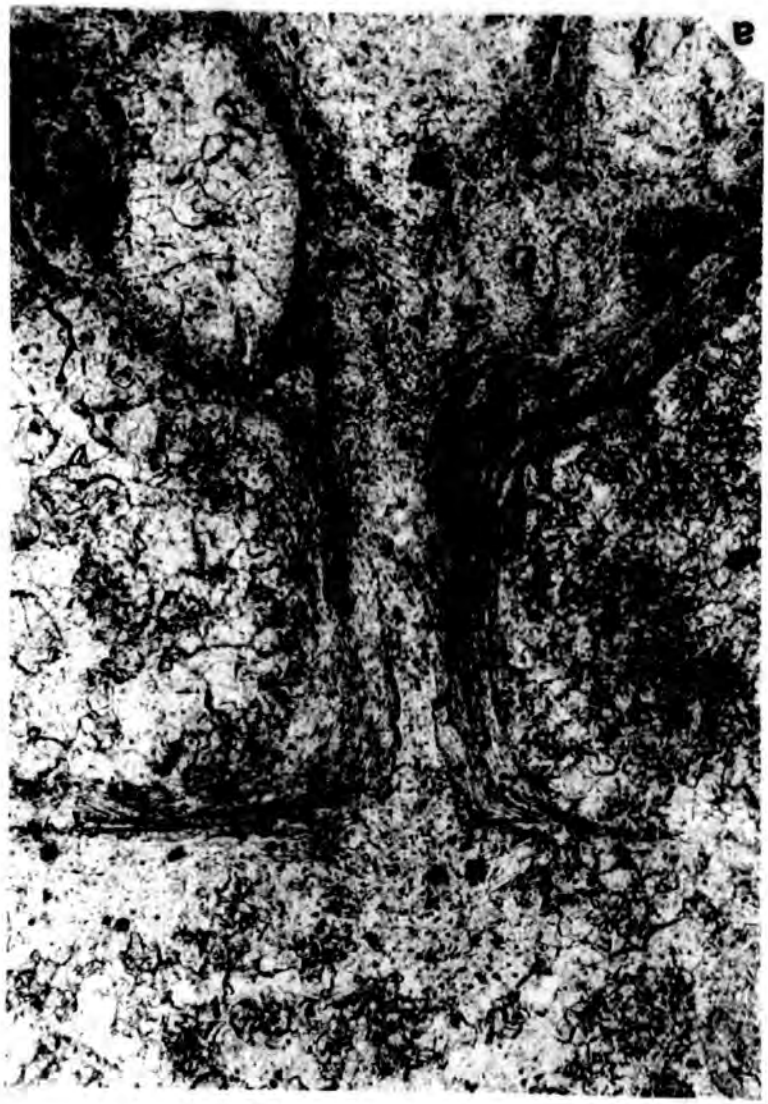
e

Plate 78. Polypora dendroides McCoy

fig.a. Lectotype; colony form. NMI F.6073. Courceyan, Hookhead Formation, Hookhead, Fethard. Xl.5.

fig.b. Colony form. ABHH 20. Horizon and locality as for fig.a. Xl.5.

fig.c. Lectotype; obverse surface detail. Xll.

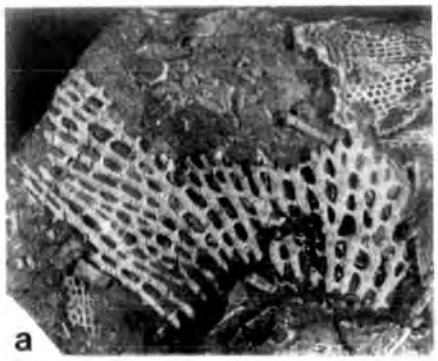
a


b

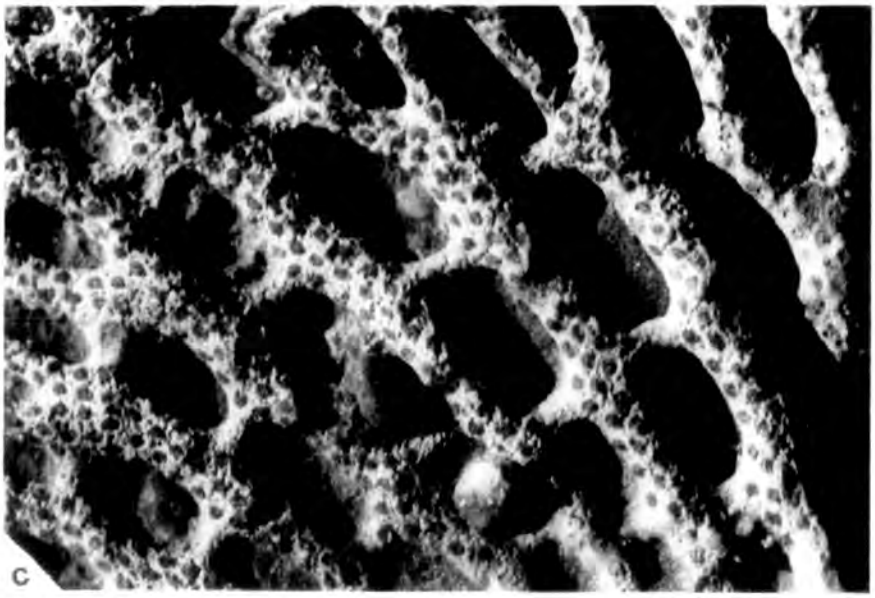
c

Plate 79. Polypora dendroides McCoy

fig.a. Lectotype; obverse surface detail.
NMI F.6073. Courceyan, Hookhead Formation
Hookhead, Fethard. X11.

fig.b. Syntype; obverse surface detail.
NMI F.6085. Horizon and locality as for
fig.a. X11.


a

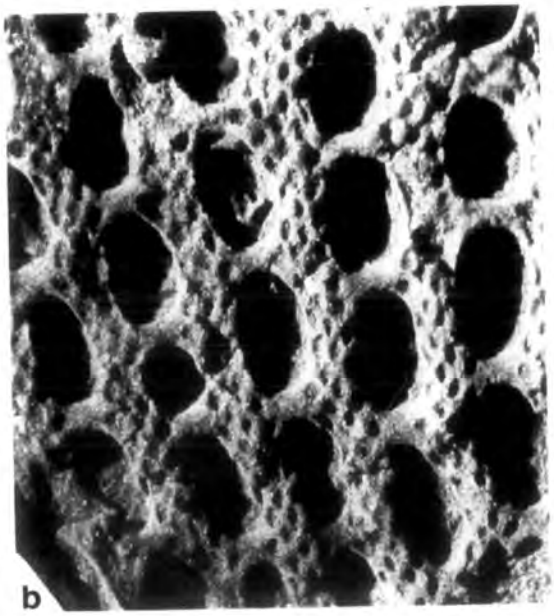
b

Plate 80. Polypora dendroides McCoy

fig.a. Lectotype; shallow tangential section showing the occurrence of closely spaced narrow rods of the inner primary granular layer around autozooecial apertures, and their irregular distribution over the zoarial surface. NMI F.61039. Courceyan, Hookhead Formation, Hookhead, Fethard. X90.

fig.b. Shallow tangential section showing the same detail as for fig.a. NMI F.6100. Horizon and locality unknown. X90.

fig.c. Oblique tangential section showing detail of autozooecial chamber bases. NMI F.6100. Horizon and locality unknown. X35.

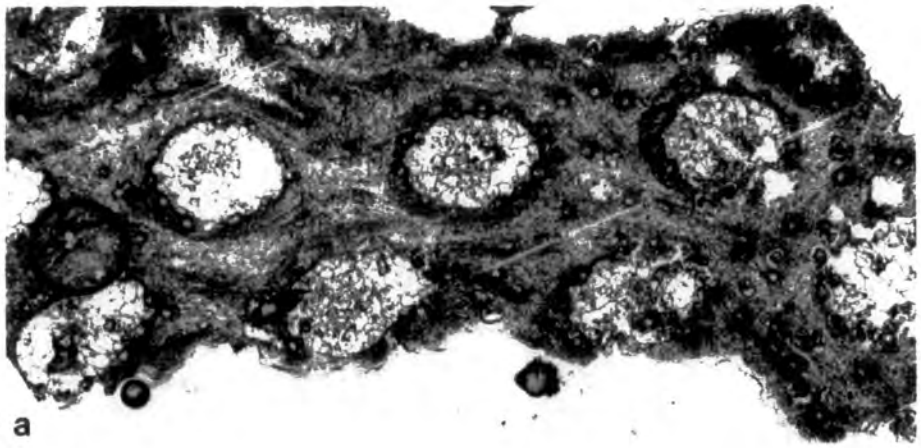

a

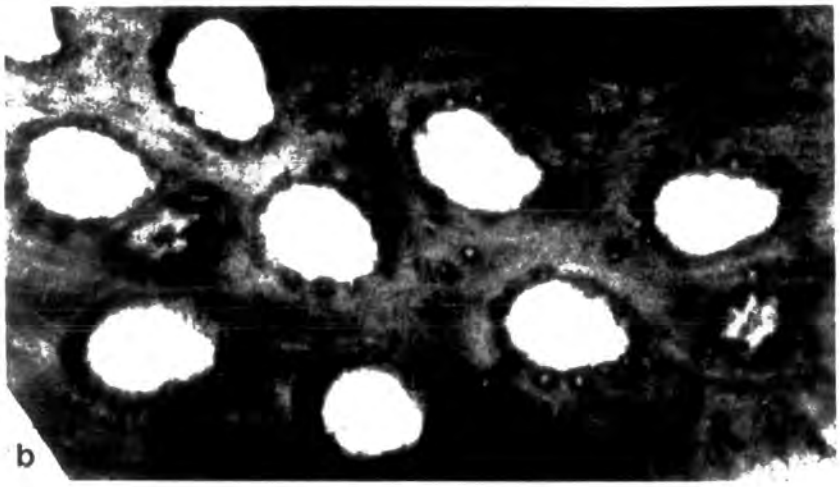

b

c

Plate 81. Polypora dendroides McCoy

fig.a. Tangential section showing detail of autozooecial chamber bases; lateral chamber bases are hemihexagonal while those of the median row are rhombic. NMI F.6100. Horizon and locality unknown. X86.

fig.b. Oblique tangential section showing detail of the outer secondary laminated skeleton through which closely and regularly spaced narrow cylindrical rods of the inner primary granular skeleton extend. NMI F.6100. Horizon and locality unknown. X86.

fig.c. As for fig.b. X35.

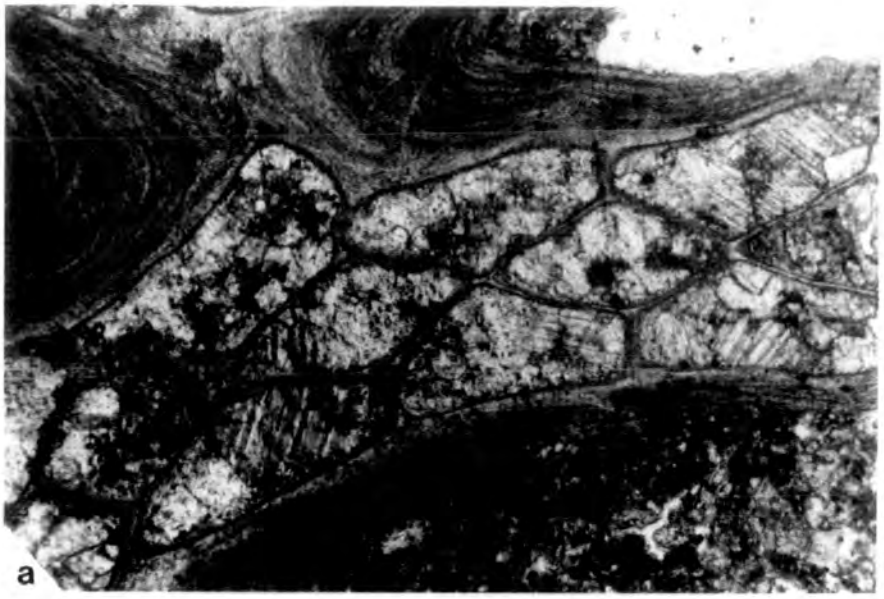

a

b

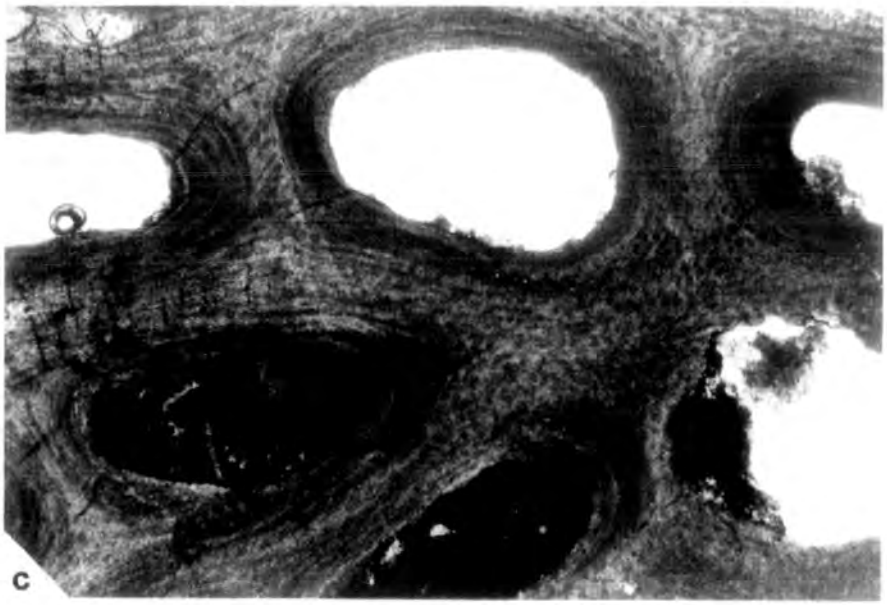

c

Plate 82. Polypora dendroides McCoy

fig.a. Lectotype; longitudinal section. NMI F.6103d. Courceyan, Hookhead Formation, Hookhead, Fethard. X34.

fig.b. As for fig.a. but showing detail of skeletal tissues, with the narrow cylindrical rods of the inner primary granular skeleton extending out into the outer secondary laminated tissues. X91.

fig.c. As for fig.b. but showing the narrow cylindrical rods of the inner primary granular skeleton curving distally outwards into the outer secondary laminated skeleton. X91.

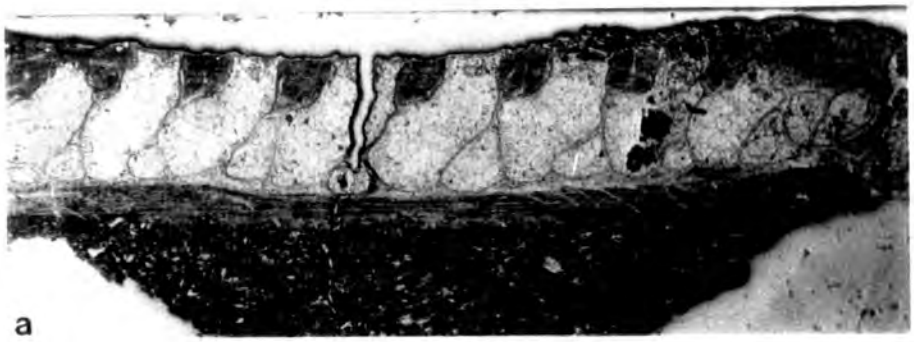

a

b

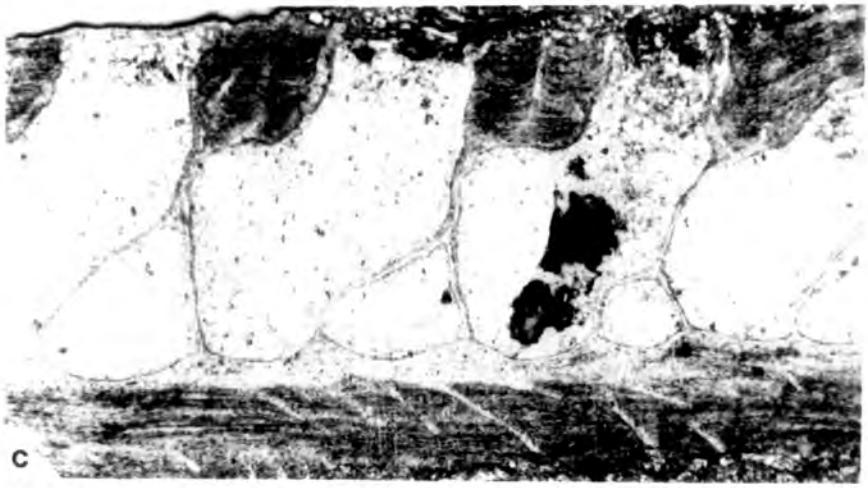

c

Plate 83. *Polypora dendroides* McCoy

fig.a. Lectotype; longitudinal section showing detail of the inner zooecial laminated skeleton lining autozooecial chambers, the surrounding thin primary granular skeleton and the thick outer secondary laminated skeleton. Narrow cylindrical rods of the primary granular skeleton curve distally outwards into the outer secondary laminated skeleton. NMI F.6103d. Courceyan, Hookhead Formation, Hookhead, Fethard. X210.

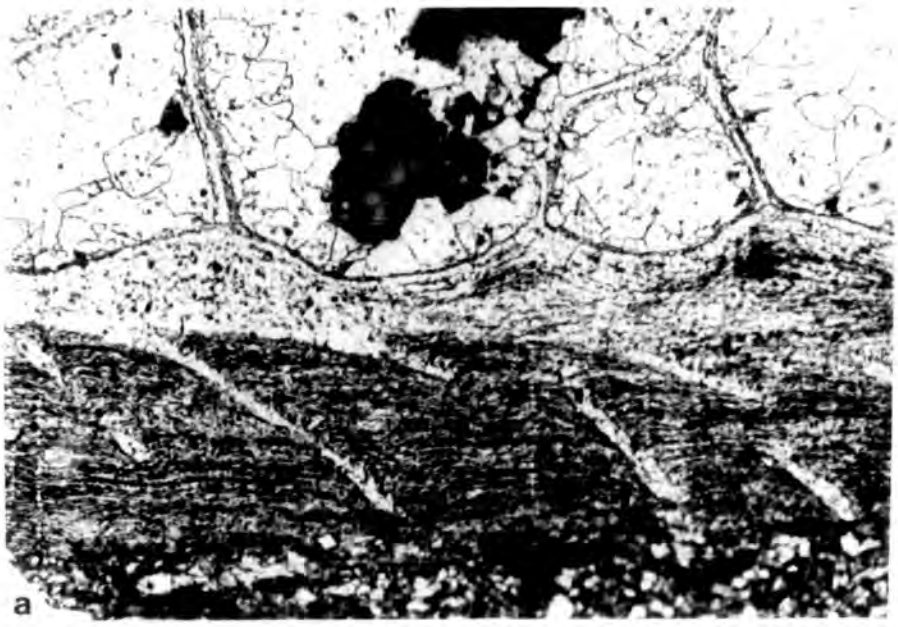
a

Plate 84. *Polypora verrucosa* McCoy

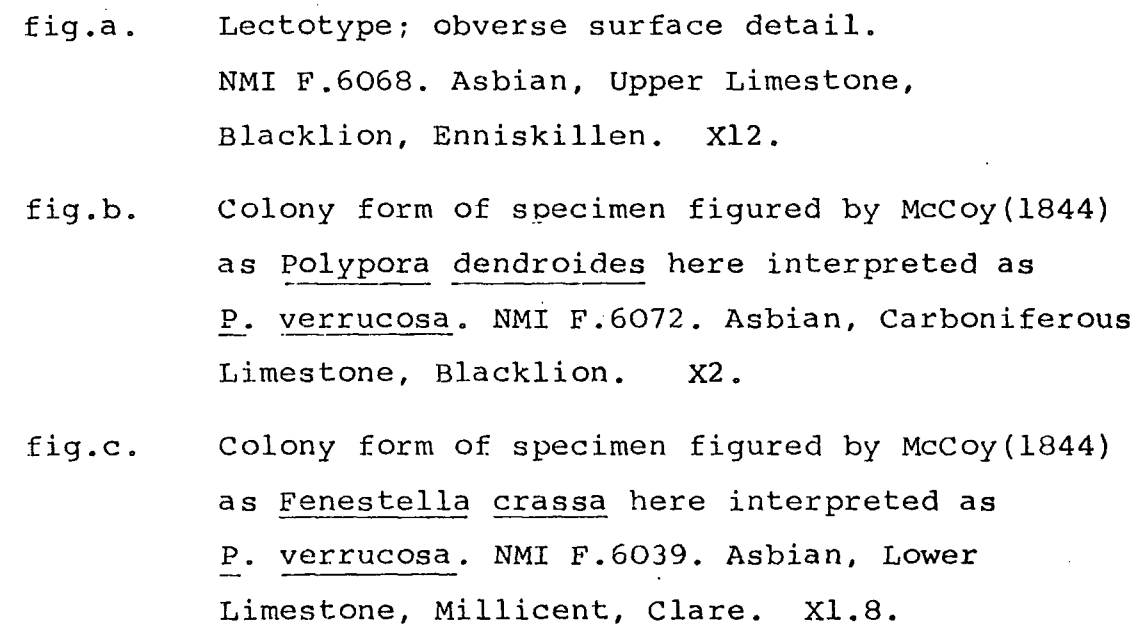

fig.a. Lectotype; obverse surface detail. NMI F.6068. Asbian, Upper Limestone, Blacklion, Enniskillen. X12.

fig.b. Colony form of specimen figured by McCoy(1844) as *Polypora dendroides* here interpreted as *P. verrucosa*. NMI F.6072. Asbian, Carboniferous Limestone, Blacklion. X2.

fig.c. Colony form of specimen figured by McCoy(1844) as *Fenestella crassa* here interpreted as *P. verrucosa*. NMI F.6039. Asbian, Lower Limestone, Millicent, Clare. X1.8.


a

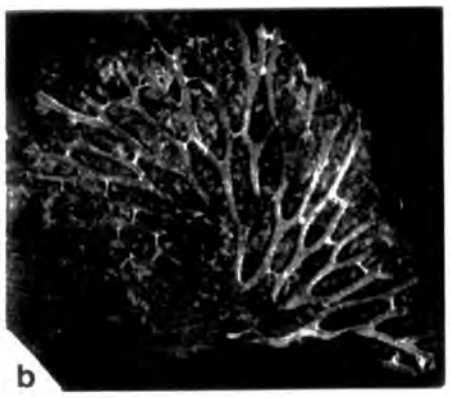
b

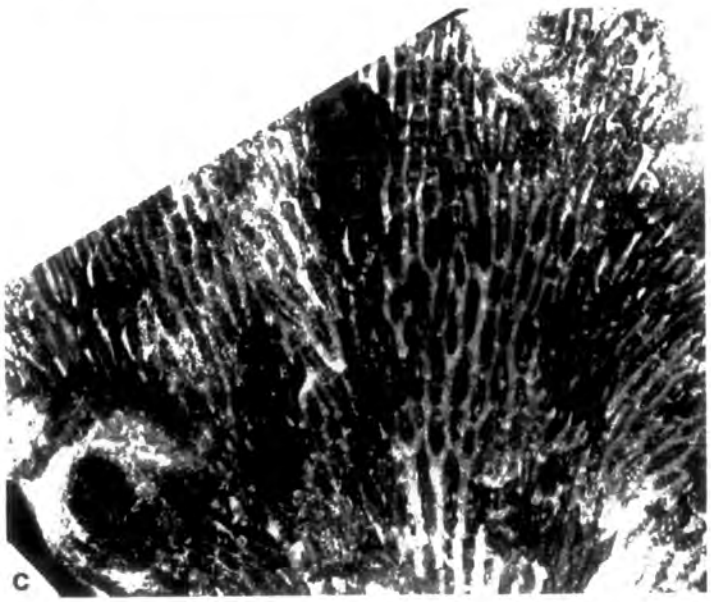
c

Plate 85. Polypora verrucosa McCoy

fig.a. Colony form. NMI F.6082. Asbian?, Kildare. X1.6.

fig.b. Reverse surface detail. NMI F.6072. Asbian, Blacklion. X11.

a

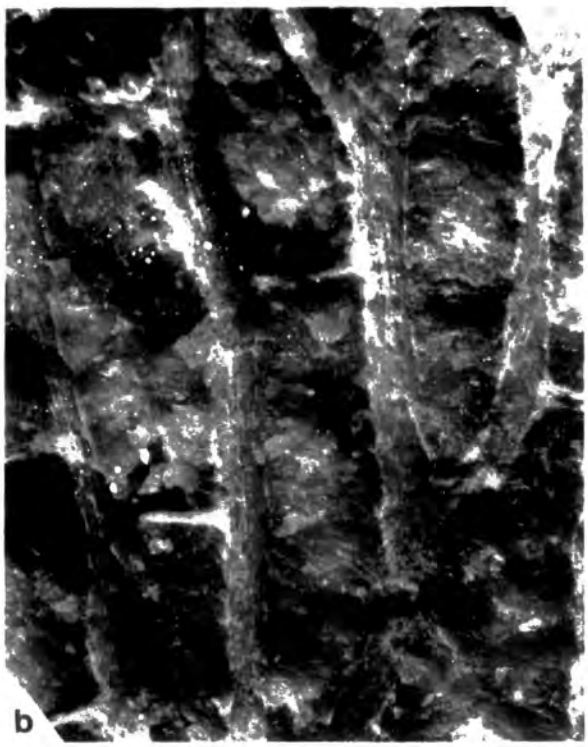

b

Plate 86. Polypora verrucosa McCoy

fig.a. Reverse surface detail; the removal of some of the branches has revealed moulds of autozooecial apertures on the obverse surface. NMI F.6072. Asbian, Carboniferous Limestone, Blacklion. X11.

fig.b. S.E.M. photomicrograph showing obverse surface detail. ABWB 1. Brigantian, Middle Limestone Group, Morpeth Scar Limestone, West Burton. X8.

fig.c. As for fig.b. X26.

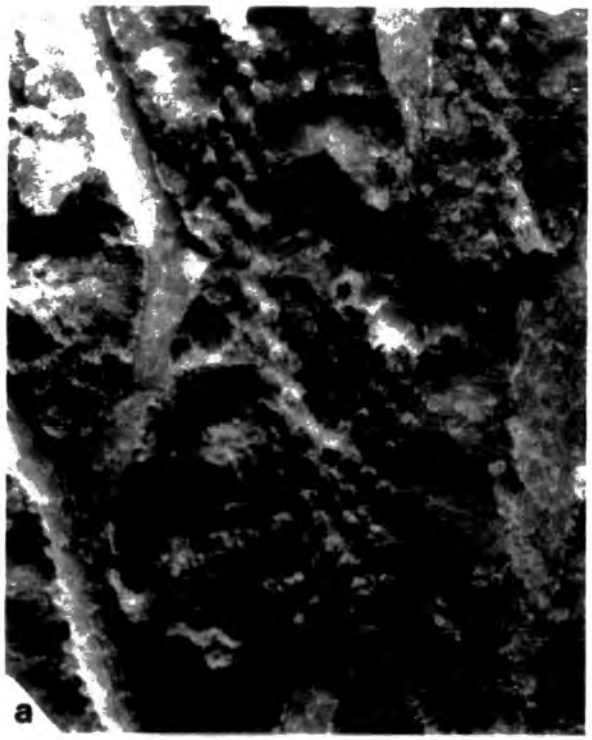
a

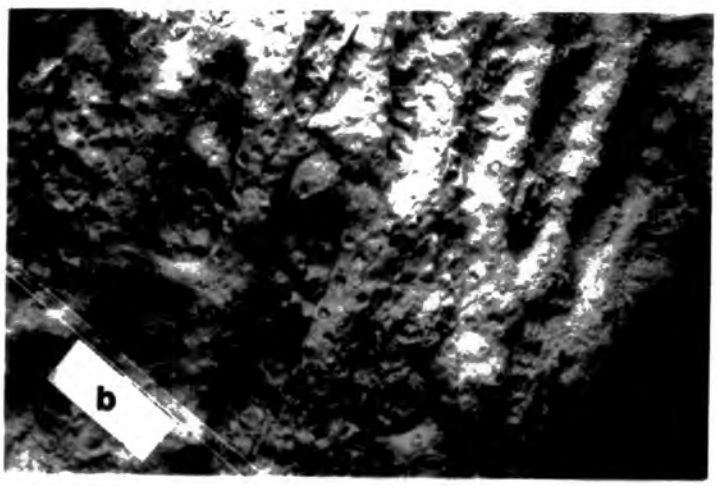
b

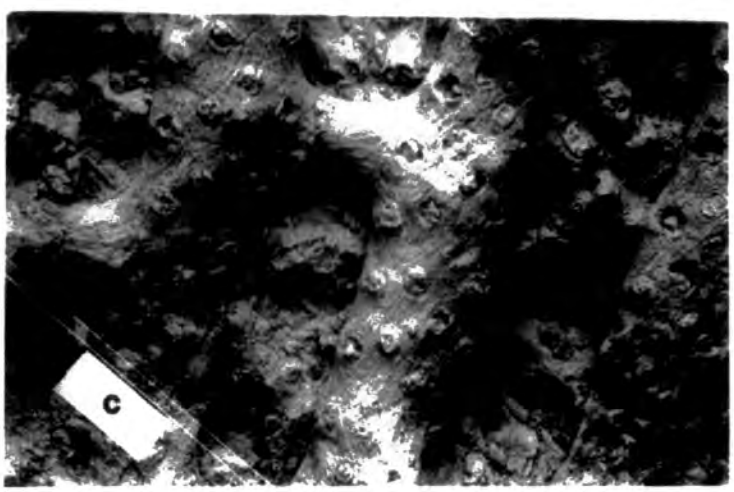
c

Plate 87. Polypora verrucosa McCoy

fig.a. S.E.M. photomicrograph showing obverse surface detail. ABWB 1. Brigantian, Middle Limestone Group, Morpeth Scar Limestone, West Burton. X66.

fig.b. Tangential section of the type specimen of Fenestella crassa McCoy, showing autozooecial chamber bases. There are four rows of autozooecia developed on branches, lateral rows have hemi-hexagonal shaped chamber bases while median rows are rhombic. NMI F.6105b. Asbian, Lower Limestone Group, Millicent, Clare. X17.


q


e

Plate 88. Polypora verrucosa McCoy

fig.a. Tangential section showing detail of autozooecial chamber bases. NMI F.6105b. Asbian, Lower Limestone, Millicent, Clare. X49.

fig.b. Longitudinal section. NMI F.6105e. Horizon and locality as for fig.a. X49.


a


b

Plate 89. Polypora verrucosa McCoy

fig.a. Transverse section. NMI F.6105d. Asbian, Lower Limestone, Millicent, Clare. X46.

fig.b. As for fig.a. X46.

fig.c. Transverse section showing microstructural details of the skeletal tissues of a branch. The zooecial laminated skeleton is very thin; the surrounding primary granular layer is thin, and skeletal ridges of the primary granular skeleton are only very poorly developed. The outer secondary laminated skeleton is thick. NMI F.6105d. Horizon and locality as for fig.a. X115.

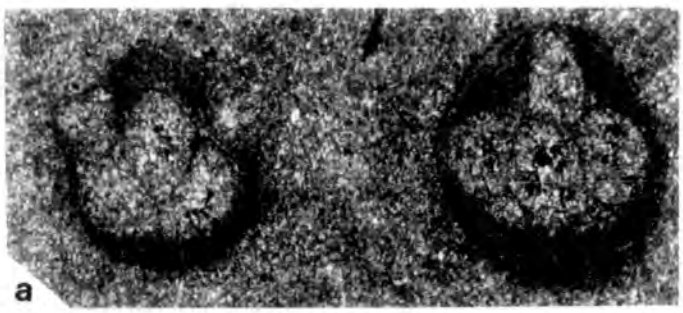

a

b

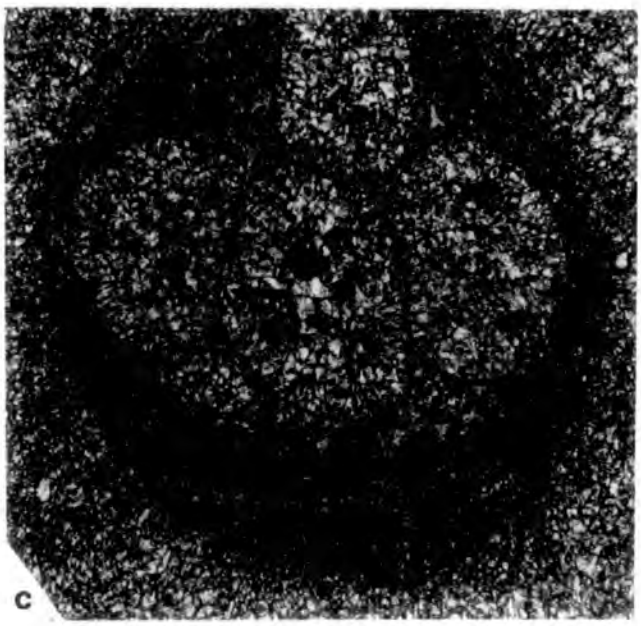

c

Plate 90. Polypora marginata McCoy

fig.a. Lectotype; colony form. NMI F.6071. Asbian, Upper Limestone, Killymeal, Dungannon. X1.5.

fig.b. Lectotype; polished ground down section showing obverse surface detail. X11.

fig.c. Lectotype; reverse surface detail. X11.

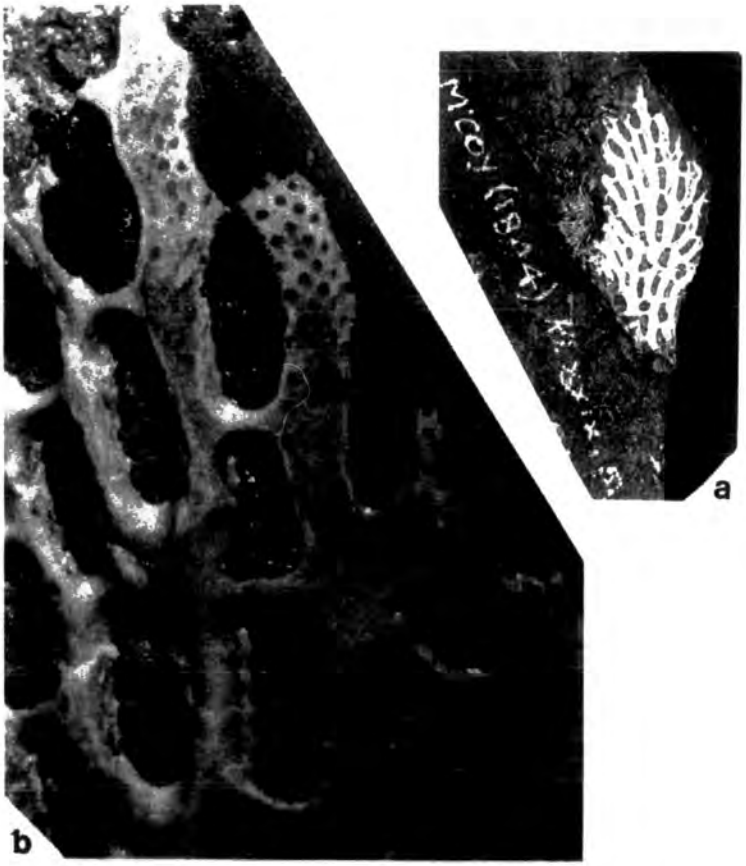
M'Coy (1844)
a
b


c

Plate 91. Polypora sp.nov. A

fig.a. Holotype; showing the very high angle conical zoarial form. HM D.356. Brigantian, Corrie Burn. X1.35.

fig.b. Holotype; showing obverse surface detail. X13.5.

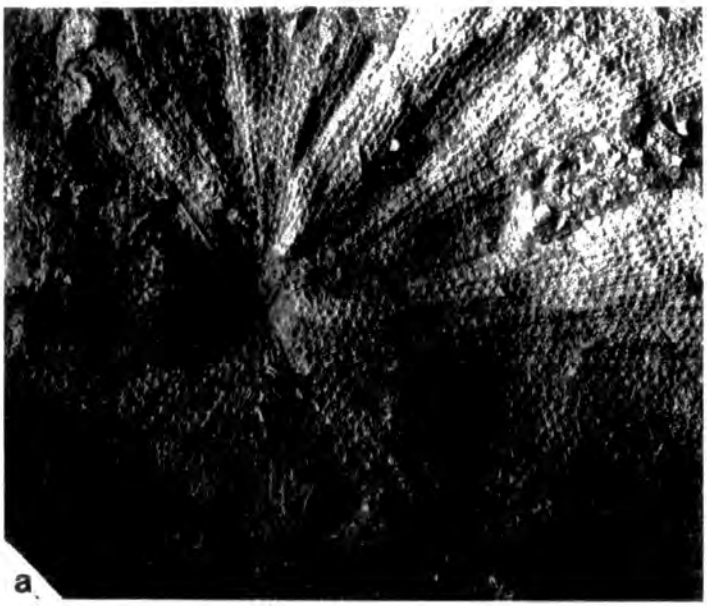

a

b

Plate 92. Polypora sp. nov. A

fig.a. Holotype; showing obverse surface detail.
HM D.356. Brigantian, Corrie Burn. X13.5.

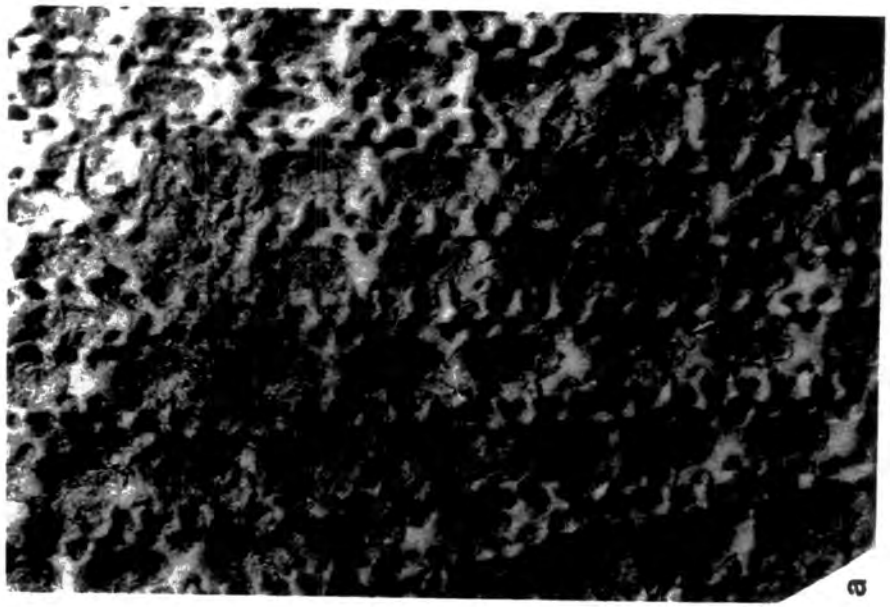

Plate 93. Diploporaria marginalis (Young and Young)

fig.a. Colony form. BOM 25-09-202. Brigantian, Lower Limestone Group, Hosie Limestone, Hairmyres, E. Kilbride. X11.

fig.b. Obverse surface detail. The specimen on the right hand side is the lectotype. HM D.122. (Lectotype is number HM D.122:14) Horizon and locality as for fig.a. X18.

fig.c. Obverse surface detail. HM D.122. Horizon and locality as for fig.a. X17.

fig.d. Obverse and reverse surface detail. HM D.122. Horizon and locality as for fig.a. X17.

fig.e. S.E.M. photomicrograph showing obverse surface detail. ABH 1. Horizon and locality as for fig.a. X33.

fig.f. As for fig.a. X120.

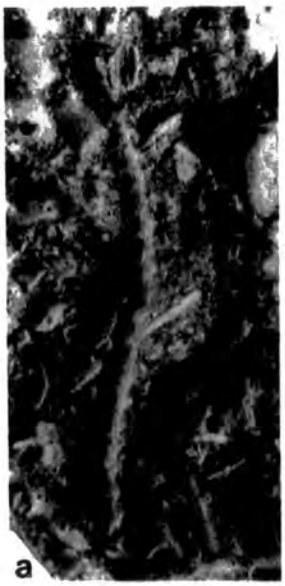
a

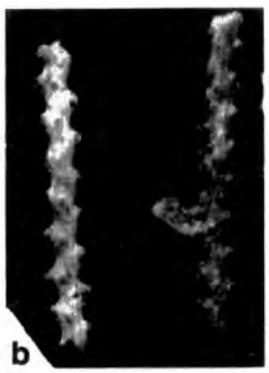
b


c


d


e


f

Plate 94. Diploporaria marginalis (Young and Young)

fig.a. S.E.M. photomicrograph showing reverse surface detail. ABH 2. Brigantian, Lower Limestone Group, Hosie Limestone, Hairmyres, E. Kilbride. X72.

fig.b. As for fig.a. X236.

fig.c. Oblique tangential section. GAGM 01-53vt. Horizon and locality as for fig.a. X35.

fig.d. Shallow tangential section showing a superior hemiseptum situated at the base of vestibular regions in each autozooecium. GAGM 01-53vt. X64.

fig.e. Tangential section showing the trapezoidal shape of autozooecial chamber bases. GAGM 01-53vt. Horizon and locality as for fig.a. X64


a

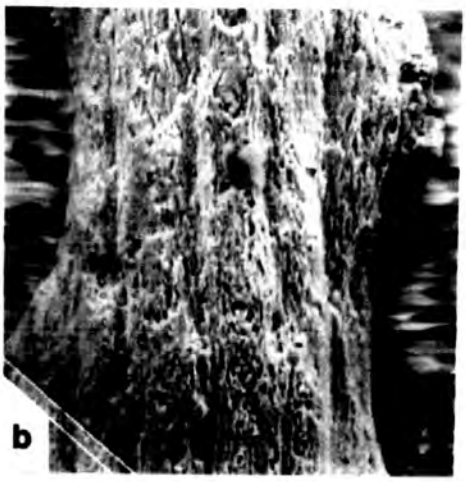
b

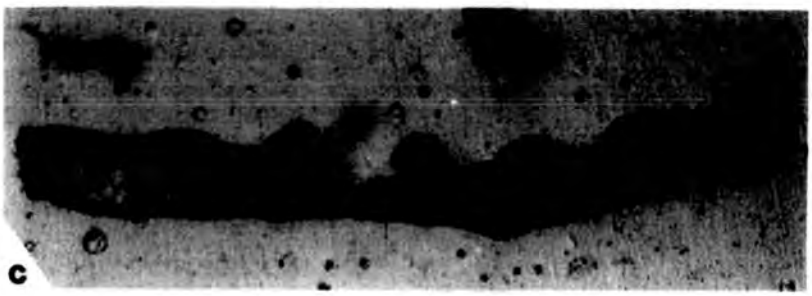
c


d


e

Plate 95. Diploporaria marginalis (Young and Young)

fig.a. Shallow tangential section showing the position of the superior hemiseptum situated at the base of the vestibular region in each autozooecium. GAGM 01-53vu(-2). Brigantian, Upper Limestone, Boghead, Hamilton. X152.

fig.b. Longitudinal section showing the position of the superior hemiseptum. GAGM 01-53vu(-1). Horizon and locality as for fig.a. X162.


b


a

Plate 96. Diploporaria marginalis (Young and Young)

fig.a. Transverse section showing an autozooecium opening low down on a branch side, and detail of the thin primary granular skeleton with its fairly short narrow ridges projecting out into the thick outer secondary laminated skeleton. GAGM 01-53vu(-1). Brigantian, Upper Limestone, Boghead, X180.

fig.b. Transverse section. GAGM 01-53vt. Brigantian, Lower Limestone Group, Hosie Limestone, Hairmyres. X383.

a

b

Plate 97. Pennireteporá stellipora (Young and Young)

fig.a. Obverse surface detail. ABHR 1. Arnsbergian, Shales above the Main Limestone, Hurst. X15.

fig.b. Obverse surface detail. GAGM 01-53vs. Arnsbergian, Upper Limestone Group, Gare, Carluke. X15.

fig.c. Reverse and obverse surface detail. HM D.128. The specimen second from the right is the Lectotype (HM D.128-4). Brigantian, Lower Limestone Group, Hosie Limestone, Hairmyres. X15.

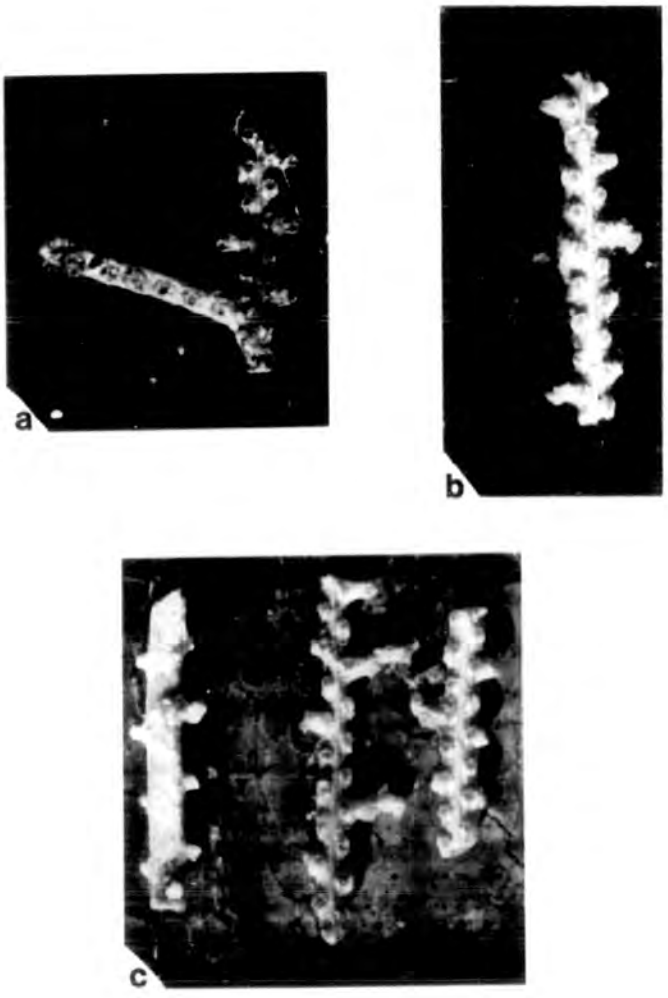
a
b
c

Plate 98. Penniretepora spinosa (Young and Young)

fig.a. Obverse surface detail. GAGM 01-53vr. Brigantian, Lower Limestone Group, Hosie Limestone, Hairmyres, E. Kilbride. X17.

fig.b. Obverse surface detail. GAGM 01-53vr. Horizon and locality as for fig.a. X17.

fig.c. Lectotype; obverse surface detail. HM D.128:17. Horizon and locality as for fig.a. X17.

fig.d. Reverse surface detail. HM D.128. Horizon and locality as for fig.a. X17.

fig.e. S.E.M. photomicrograph showing obverse surface detail, also an ovicell on the top left hand side lateral branch. ABH 29. Horizon and locality as for fig.a. X43.

fig.f. S.E.M. photomicrograph showing detail of an ovicell. ABH 29. Horizon and locality as for fig.a. X120.

fig.g. S.E.M. photomicrograph showing detail of a denticulated autozooecial aperture. HM D.128:21. Horizon and locality as for fig.a. X400.

fig.h. S.E.M. photomicrograph showing detail of denticulated autozooecial apertures. ABH 28. Horizon and locality as for fig.a. X180.

a
b
c
d
e
f
g
h

Plate 99. Pennireteporaspinosa (Young and Young)

fig.a. S.E.M. photomicrograph showing detail of a denticulated autozooecial aperture. ABH 28. Brigantian, Lower Limestone Group, Hosie Limestone, Hairmyres, E. Kilbride. X280.

fig.b. Shallow tangential section. GAGM 01-53vr. Horizon and locality as for fig.a. X96.

fig.c. Tangential section showing the trapezoidal shape of autozooecial chamber bases. GAGM 01-53vr(-2). Horizon and locality as for fig.a. X96.

fig.d. Transverse section. GAGM 01-53vr. Horizon and locality as for fig.a. X230.

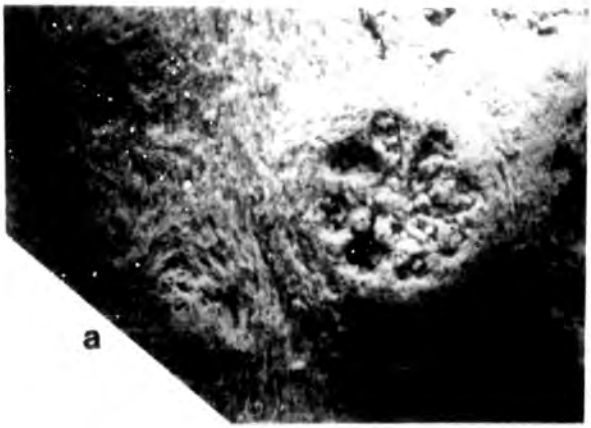
a


b


c


d

PLate 100. Pennireteporа sp. nov. A

fig.a. Holotype; obverse surface detail. HM D.62(-1). Brigantian, Shale above the Second Kingshaw Limestone, Carluke. X16.

fig.b. Paratype; reverse surface detail. HM D.62(-2). Horizon and locality as for fig.a. X11.

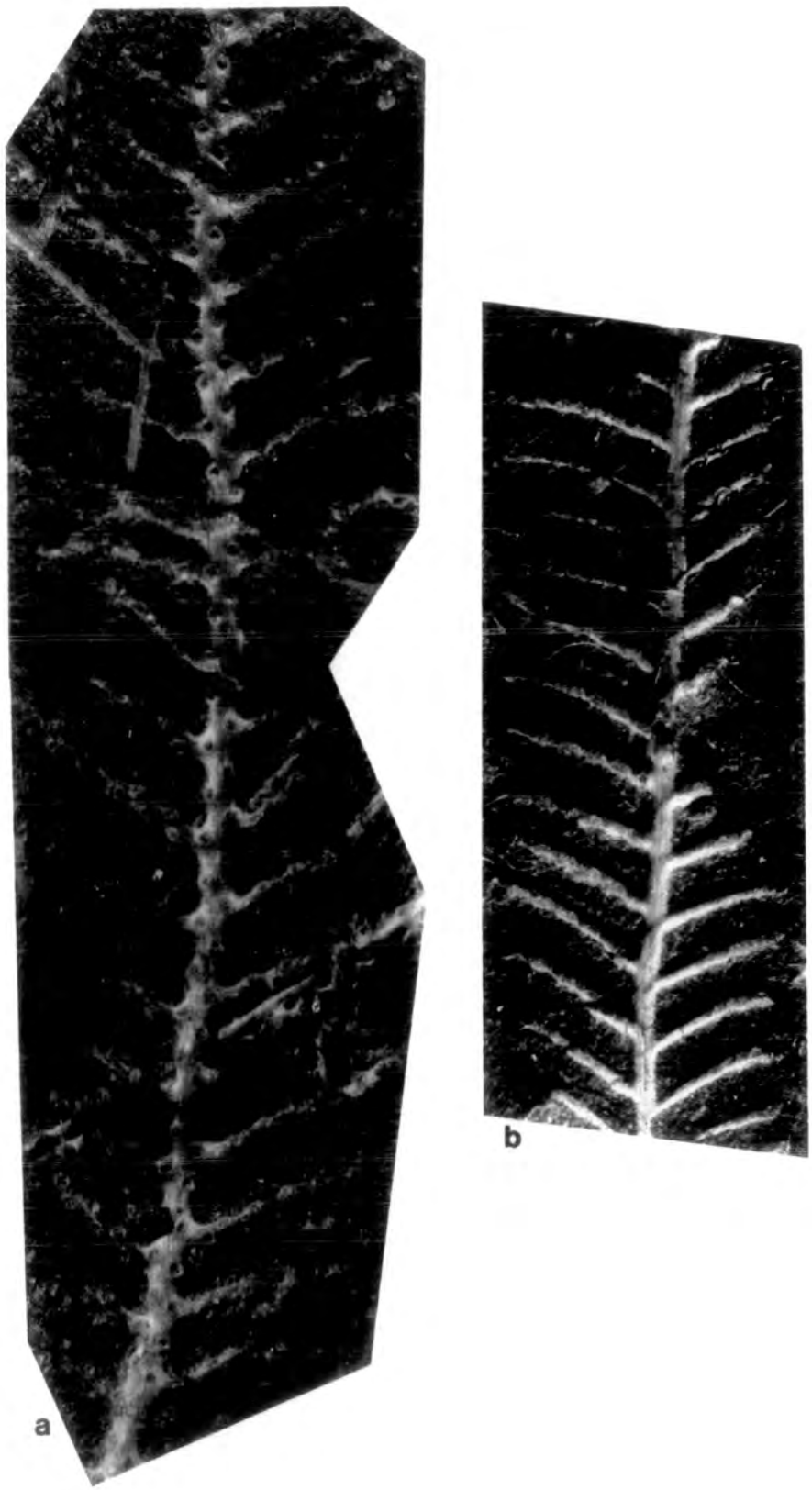
a
b

Plate 101. Penniretepora sp.nov. B.

fig.a. S.E.M. photomicrograph of holotype showing obverse surface detail. ABHR A6(-1). Arnsbergian, Shales above the Main Limestone, Hurst, N. Yorkshire. X18.5.

fig.b. S.E.M. photomicrograph of paratype showing obverse surface detail and the occurrence of ovicells. ABHR A6(-4). Horizon and locality as for fig.a. X19.

fig.c. S.E.M. photomicroraph showing detail of an ovicell. ABHR A6(-4). Horizon and locality as for fig.a. X130.

fig.d. S.E.M. photomicrograph showing detail of an ovicell. ABHR A6(-4). Horizon and locality as for fig.a. X153.

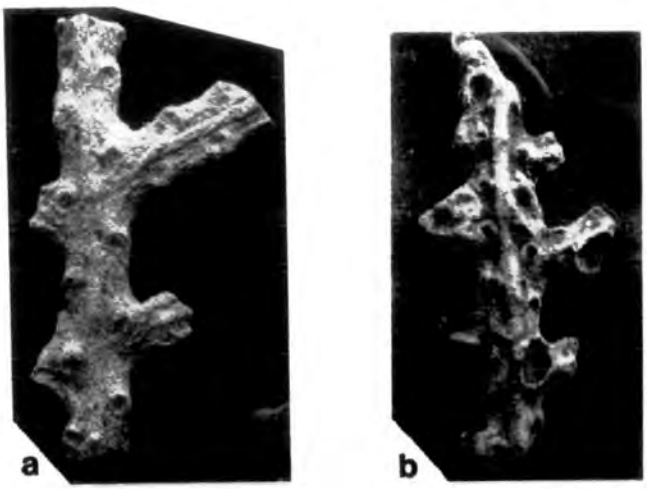
a
b

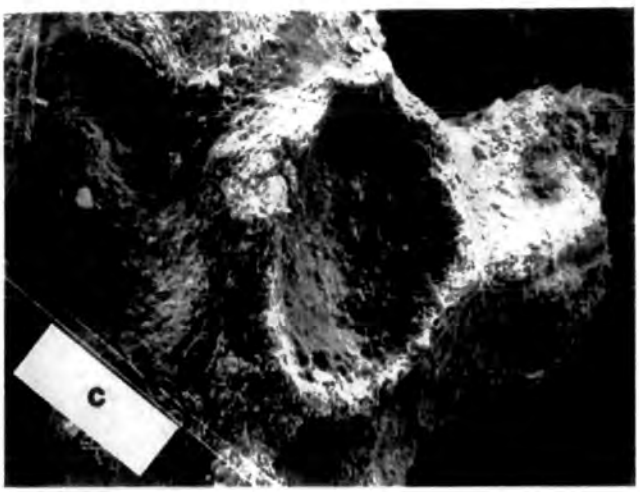
c

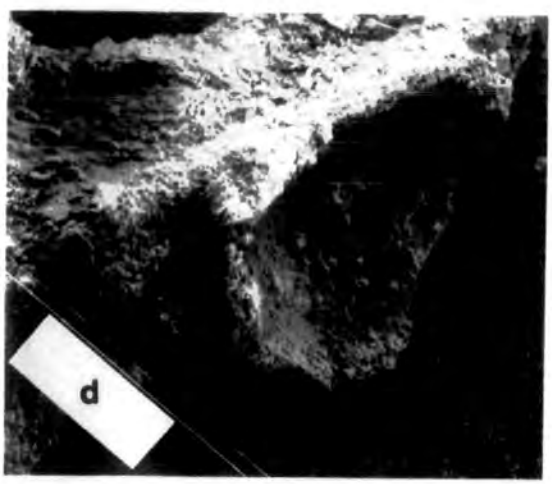
d

Plate 102. Penniretepora flexicarinata (Young and Young)

fig.a. Obverse surface detail. HM D .121. The lectotype is second from the left (HM D.121 -8). Brigantian, Lower Limestone Group, Hosie Limestone, Hairmyres, E. Kilbride. X16.

fig.b. Obverse surface detail. HM D.121. Horizon and locality as for fig.a. X16.

fig.c. Reverse surface detail. HM D.121. Horizon and locality as for fig.a. X16.

fig.d. Obverse surface detail. GAGM 01-53vz. Horizon and locality as for fig.a. X13.

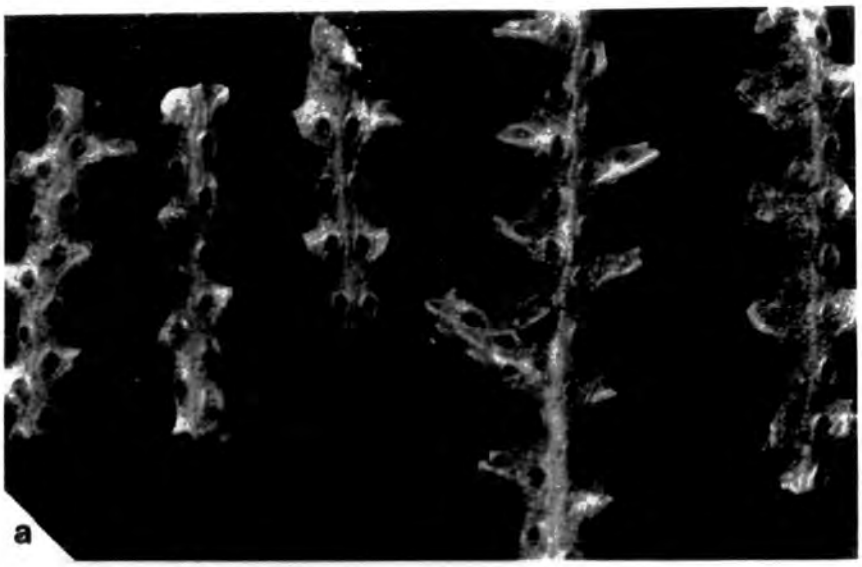
a

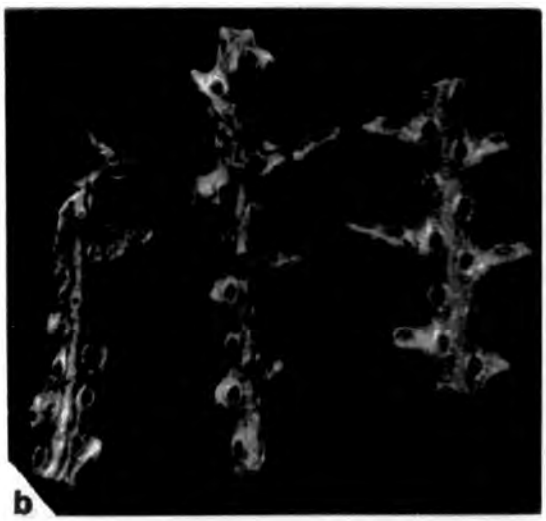
b


c


d

Plate 103. Penniretepora flexicarinata (Young and Young)

fig.a. S.E.M. photomicrograph showing obverse surface detail. ABH 23. Brigantian; Lower Limestone Group, Hosie Limestone, Hairmyres. X20.

fig.b. S.E.M. photomicrograph showing obverse surface detail. Detail as for fig.a. X88.

fig.c. Colony form of Grahams (1975) lectotype of Penniretepora recticarinata (Young and Young), here placed in synonomy with P. flexicarinata. HM D.455. Brigantian; Lower Limestone Series, Dykehead Pit, High Blantyre. X2.

fig.d. As for fig.c. but showing obverse surface detail. X21.

a

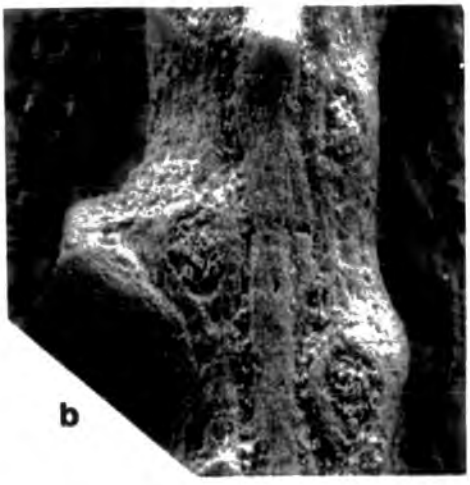

b

c

d

Plate 104. Penniretepora pulcherrima McCoy

fig.a. Lectotype; colony form. NMI F.6023. Asbian, Upper Limestone, Blacklion, Enniskillen. X2.5.

fig.b. Lectotype; reverse surface detail. X15.5.


a


b

Plate 105. Penniretepora pulcherrima McCoy

fig.a. Colony form; abundant pinnate colonies showing a prefered orientation. GAGM 01-53us. Brigantian, Lower Limestone Group, Hosie Limestone, Hairmyres. X.84.

fig.b. Obverse and reverse surface detail. HM D.125. Horizon and locality as for fig.a. X16.

fig.c. As for fig.b. X16.


a

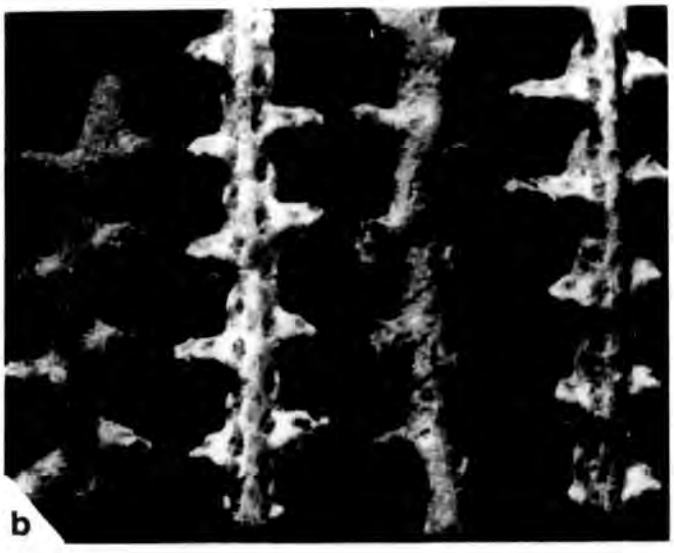
b

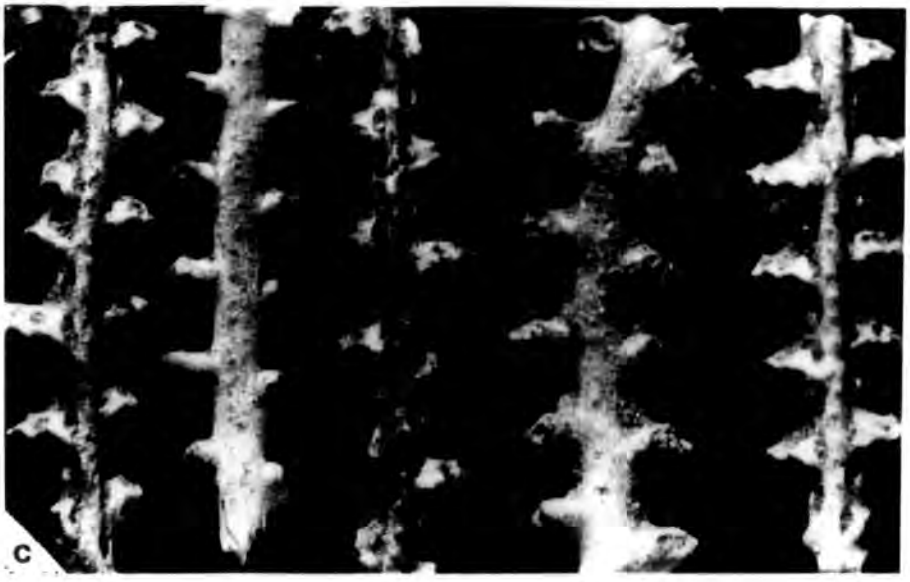
c

Plate 106. Penniretepora pulcherrima McCoy.

fig.a. S.E.M. photomicrograph showing obverse surface detail. Each autozooecial aperture is sealed by a secondary nanozooid. ABH 17. Brigantian, Lower Limestone Group, Hosie Limestone, Hairmyres. X22.

fig.b. As for fig.a. X51.

fig.c. S.E.M. photomicrograph showing detail of an autozooecial aperture sealed by a secondary nanozooid. ABH 17. Horizon and locality as for fig.a. X160.

fig.d. S.E.M. photomicrograph showing reverse surface detail. ABH 18. Horizon and locality as for fig.a. X56.

fig.e. Tangential section showing the trapezoidal shape of autozooecial chamber bases. HM D.127. Horizon and locality as for fig.a. X11.

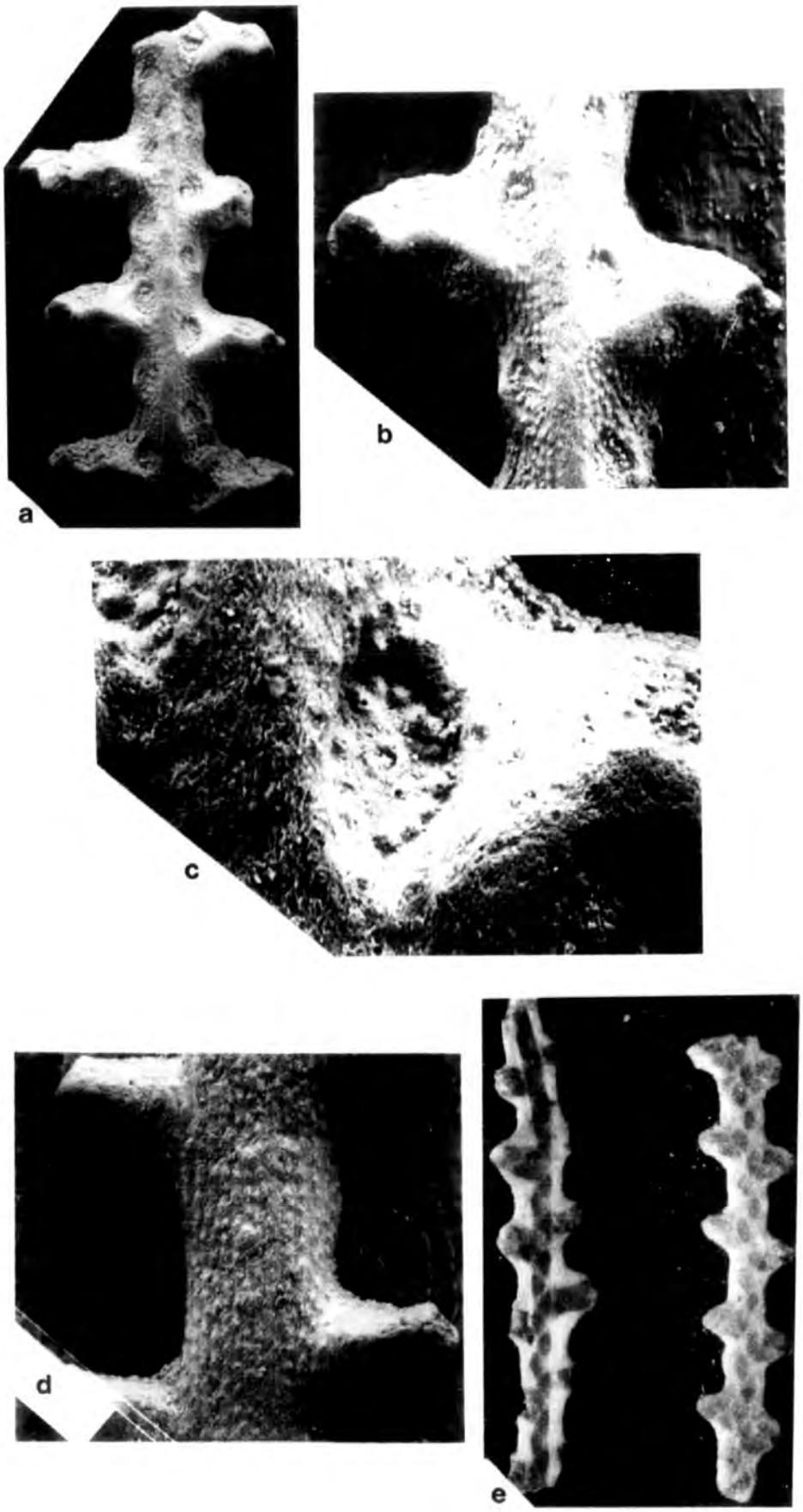
a
b
c
d
e

Plate 107. Penniretepora robusta (Young and Young)

fig.a. Lectotype: obverse surface detail. HM D.54-1. Brigantian; Shale above the Gillfoot Limestone, Carluke. X10.

fig.b. Reverse surface detail. HM D.54-2. Horizon and locality as for fig.a. X13.5.

fig.c. Reverse surface detail. HM D.54-3. Horizon and locality as for fig.a. X10.

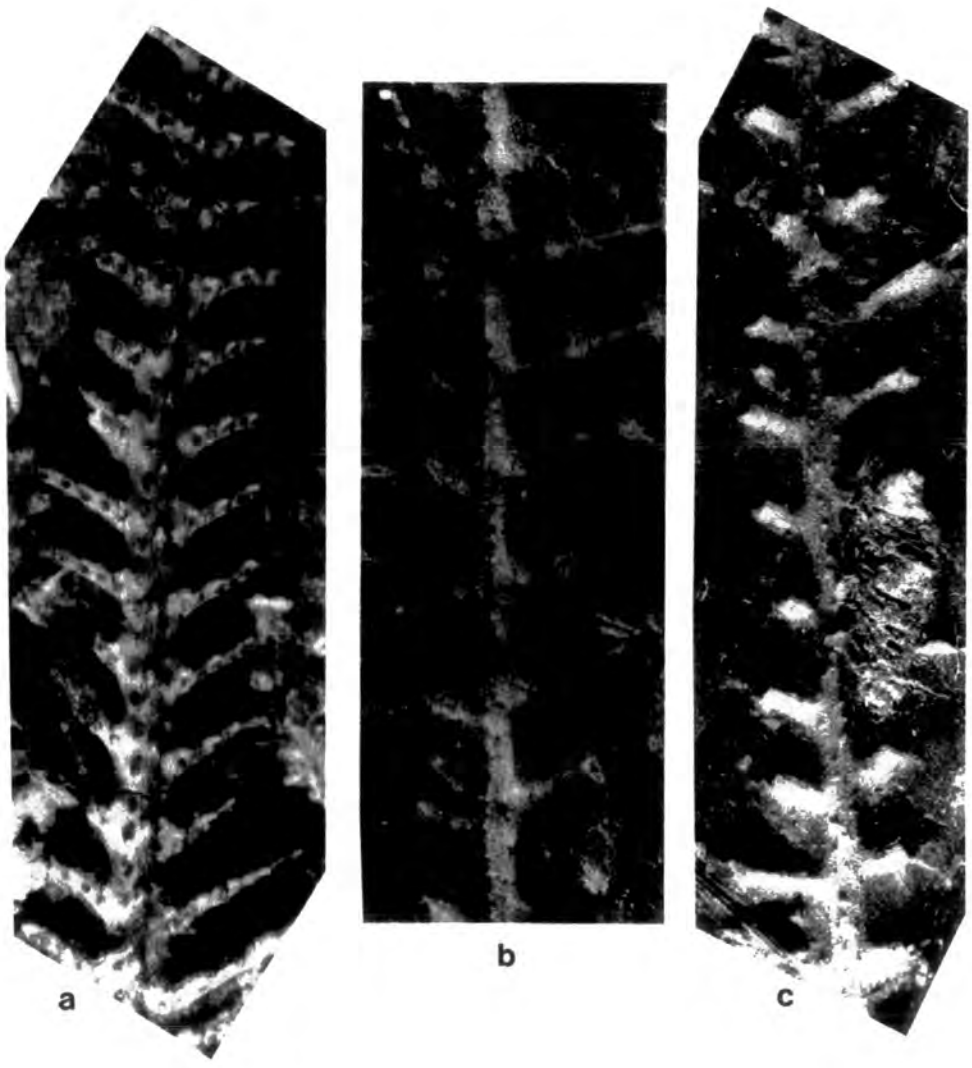
a
b
c

Plate 108. Penniretepora elegans (Young and Young)

fig.a. Colony form. GAGM 01-53wf. Brigantian, Dykehead Pit, High Blantyre. X1.3.

fig.b. Colony form. GAGM 01-53wg. Horizon and locality as for fig.a. X1.3.

fig.c. Colony form.HM D.13. Horizon and locality unknown. X1.9.

fig.d. Obverse surface detail. GAGM 01-53wj. Horizon and locality as for fig.a. X14.


a


b


c


d

Plate 109. Penniretepora elegans (Young and Young).

fig.a. Lectotype, obverse surface detail. GAGM 01-53wd(-6). Brigantian, Lower Limestone Group, Hosie Limestone, Hairmyres. X13.

fig.b. Lectotype, reverse surface detail. X13. (figs. a and b are reproduced from Graham 1975 Pl. 1, figs. 3.3a)

fig.c. Obverse surface detail. HM D.124. Horizon and locality as for fig.a. X18.

fig.d. S.E.M. photomicrograph showing obverse surface detail. Each autozooecial aperture is sealed by a secondary nanozooid. ABH 19. Horizon and locality as for fig.a. X17.

fig.e. Obverse surface detail. HM D.124. Horizon and locality as for fig.a. X17.

fig.f. S.E.M. photomicrograph showing detail of autozooecial apertures sealed by secondary nanozooids. Horizon and locality as for fig.a. X78.

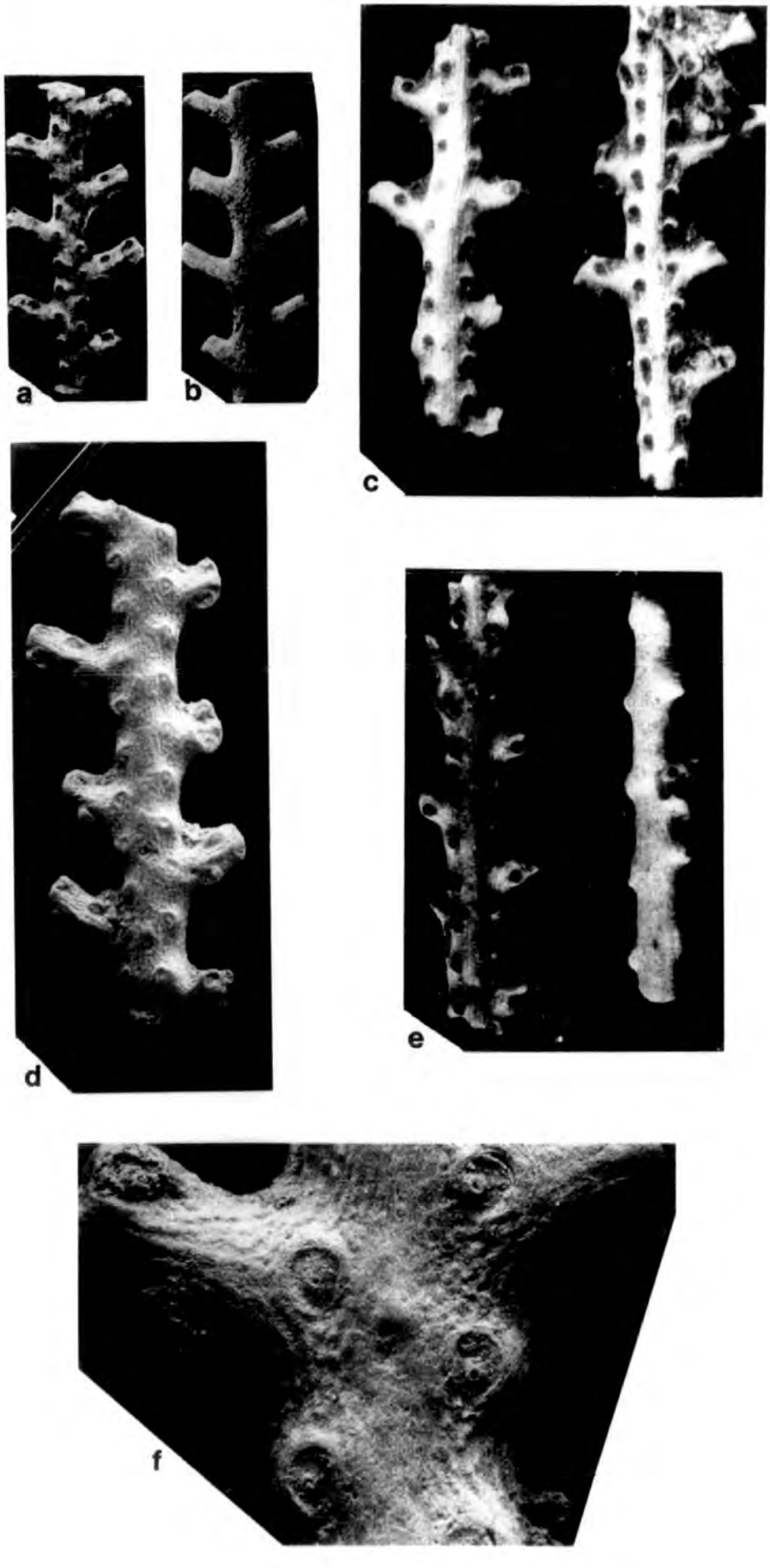
a
b
c
d
e
f

Plate 110. Penniretepora elegans (Young and Young).

fig.a. S.E.M. photomicrograph showing detail of secondary nanozooids. ABH 19. Brigantian, Lower Limestone Group, Hosie Limestone, Hairmyres. X144.

fig.b. Shallow tangential section. HM D.123(-2). Horizon and locality as for fig.a. X99.


a


b

Plate 111. Penniretepora elegans (Young and Young).

fig.a. Longitudinal section. HM D.123(-1). Brigantian, Lower Limestone Group, Hosie Limestone, Hairmyres. X37.

fig.b. As for fig.a. X99.


b


a

Plate 112. Penniretepora laxa (Young and Young).

fig.a. Lectotype, obverse surface detail. GAGM 01-53vk(-9). Brigantian, Lower Limestone Group, Hosie Limestone, Hairmyres. X9.

fig.b. Lectotype, reverse surface detail. X9.

fig.c. Obverse surface detail. GAGM 01-53vk. Horizon and locality as for fig.a. X9.

fig.d. Reverse surface detail. Horizon and locality as for fig.a. X9.
(figs.a-d are reproduced from Graham 1975, Pl.2, figs.9.9a,10.10a).

fig.e. Obverse surface detail. GAGM 01-53vk. Horizon and locality as for fig.a. X16.

fig.f. Obverse surface detail. HM D.131. Horizon and locality as for fig.a. X16.

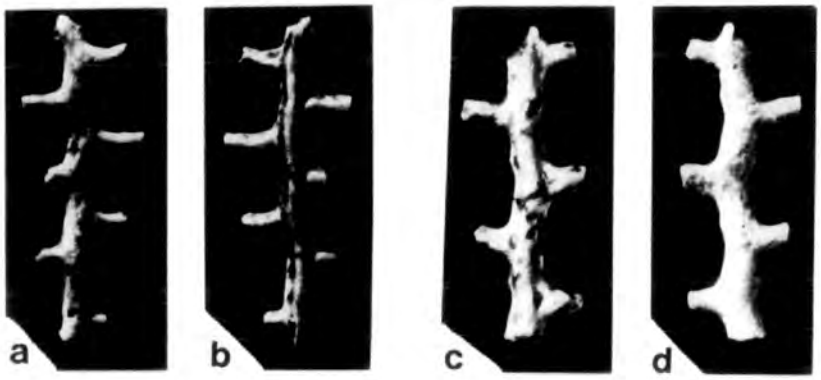
a
b
c
d

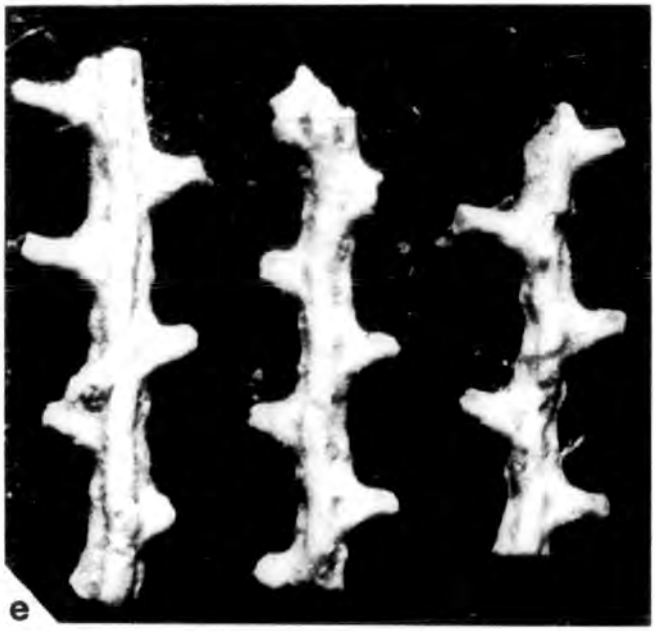
e


f

Plate 113. Penniretepora laxa (Young and Young).

fig.a. Reverse and obverse surface detail. GAGM 01-53clj. Brigantian, Lower Limestone Group, Hosie Limestone, Hairmyres. X17.

fig.b. Type of Glauconome elegantula Etheridge. G.S.E.2109. Brigantian, Lower Limestone Group, Harelaw Quarry, Longniddry, East Lothian. X13.

fig.c. Type of Glauconome elegantula Etheridge. G.S.E.2096. Horizon and locality as fig.b. X13.

(figs.b and c are reproduced from Graham 1975, Pl.6. figs.1.2).


a


b


c

Plate 114. Penniretepora grandis McCoy.

fig.a. Lectotype; colony form. NMI F.6024. Asbian; Meelick Chapel, Clare. X1.6.

fig.b. Lectotype; obverse surface detail. X13.

fig.c. Lectotype; obverse surface detail. X13.


a

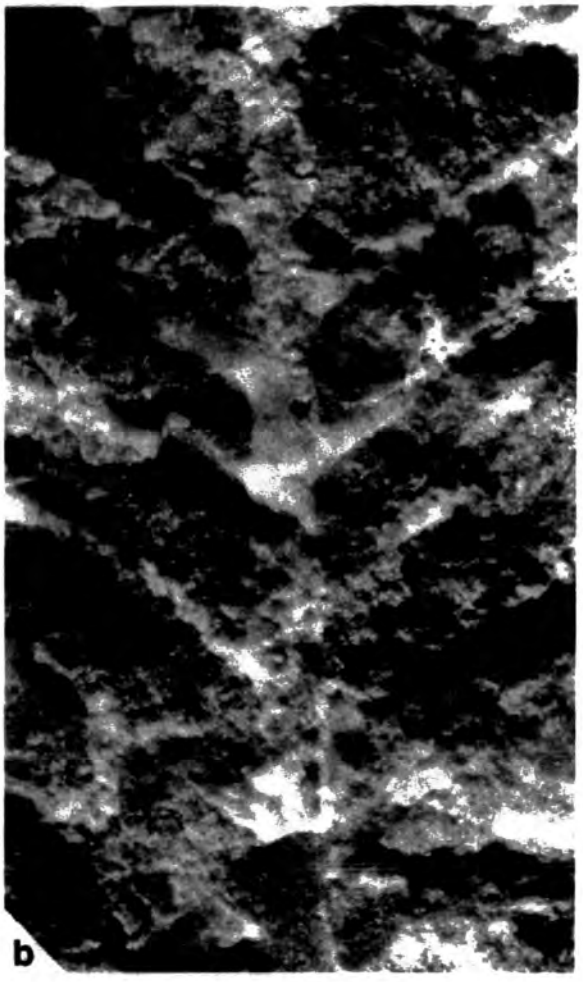
b

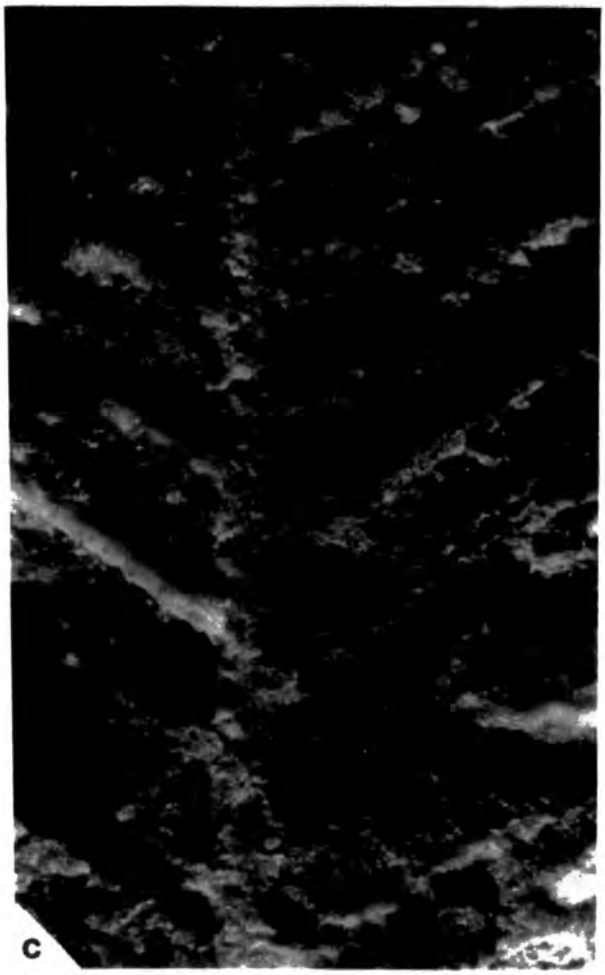
c

Plate 115. *Ptylopora pluma* McCoy.

fig.a. Lectotype; colony form. NMI F6046.
Courceyan, Hookhead formation, Hookhead. X1.5.

fig.b. Lectotype; obverse surface detail. X10.

fig.c. Lectotype; obverse surface detail. X10.

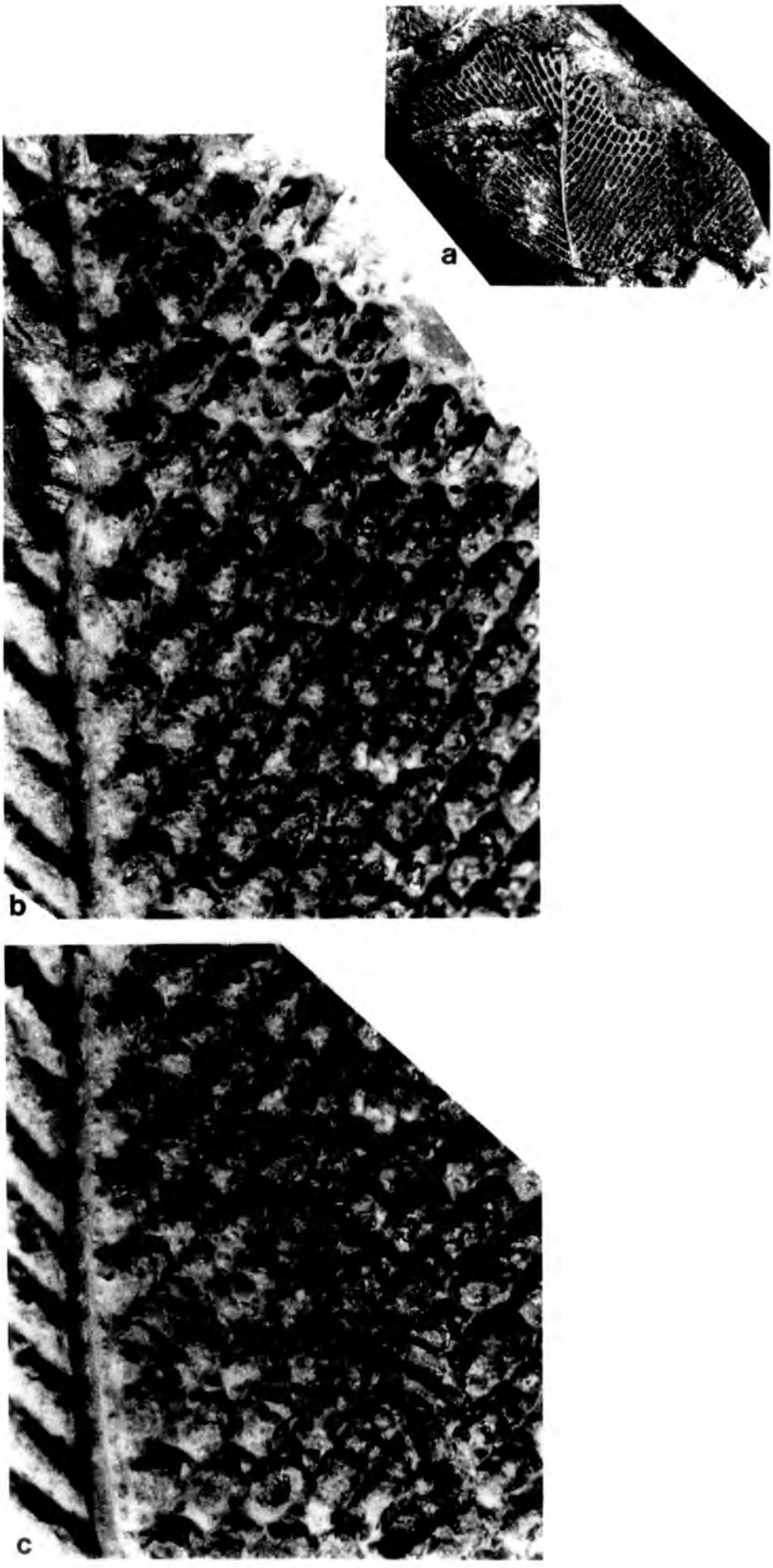
a
b
c

Plate 116. Ptylopora pluma McCoy

fig.a. Topotype; colony form. NMI F.6096(-1). Courceyan, Hookhead Formation, Hookhead, Fethard. X1.5.

fig.b. Topotype; colony form. NMI F.6096(-2). Horizon and locality as for fig.a. X2.2.

fig.c.. Colony form. HM 891. Brigantian, Corrieburn. X1.7.

fig.d. Obverse surface detail. ABCL 21. Asbian, Calp Shale-Upper Limestone, Carrick Lough, X11.

fig.e. Ptylopora flustriformis McCoy, colony form. (P. flustriformis is here placed in synonomy with P. pluma.). NMI F.6089(-1). Asbian, Kildare. X1.5.


a

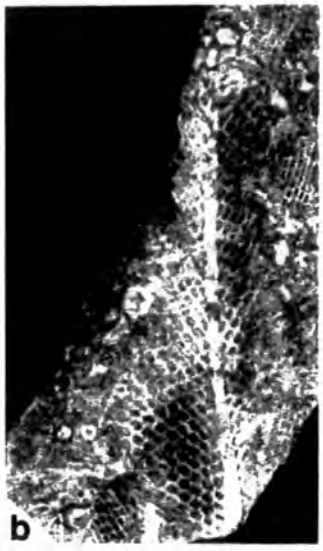
b


c

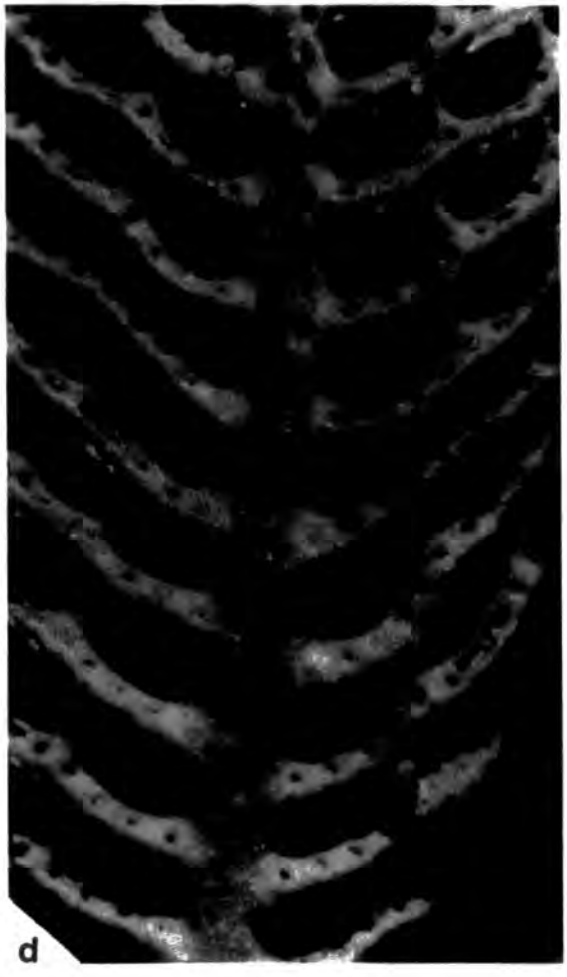
d


e

Plate 117. Ptylopora pluma McCoy

fig.a. Ptylopora flustriformis McCoy. NMI F.6089(-2). Asbian, Kildare. X2.0.

fig.b. Ptylopora macropora McCoy. NMI F.6088. (P. macropora is here placed in synonomy with P. pluma) Asbian. Carboniferous slate. Poulscadden Howth. X1.4.

fig.c. Ptylopora phillipsi Vine. (P. phillipsi is here placed in synonomy with P. pluma) Colony form. BOM 29-05-175(-1). Asbian(?), Castleton Derbyshire. X1.7.

fig.d. As for fig.c. X1.7.

fig.e. Ptylopora phillipsi Vine. Plan of a conical colony. BOM 29-05-175(-2). Horizon and locality as for fig.c. X2.0.

fig.f. Ptylopora phillipsi Vine. Colony form. BOM 29-05-175(-3). Horizon and locality as for fig.c. X2.3.


a


b


c


d


e


f

Plate 118. Ptylopora pluma McCoy

fig.a. Ptylopora phillipsi Vine, obverse surface detail showing lateral branches diverging from the midrib at low acute angles. BOM 29-05-175(-2). Asbian(?), Castleton, Derbyshire. X10.

fig.b. Ptylopora phillipsi Vine, obverse surface detail showing the convergence of lateral branches at low acute angles on the opposite side of the cone to the midrib. BOM 29-05-175(-1). Horizon and locality as for fig.a. X10.

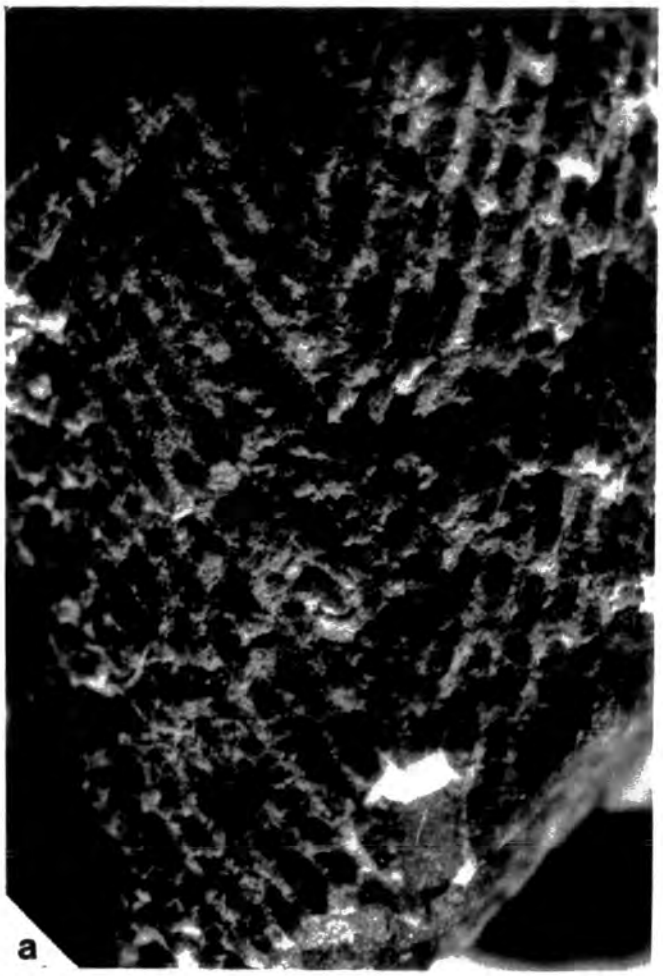
a


b

Plate 119. Ptylopora pluma McCoy

fig.a. Ptylopora phillipsi Vine; poorly preserved specimen with moulds of the branches showing the convergence and fusion of lateral branches in a plane parallel to the midrib on the opposite surface of the cone. BOM 29-05-175(-1). Asbian(?), Castleton, Derbyshire. X10.

fig.b. As for fig.a. X10.

a

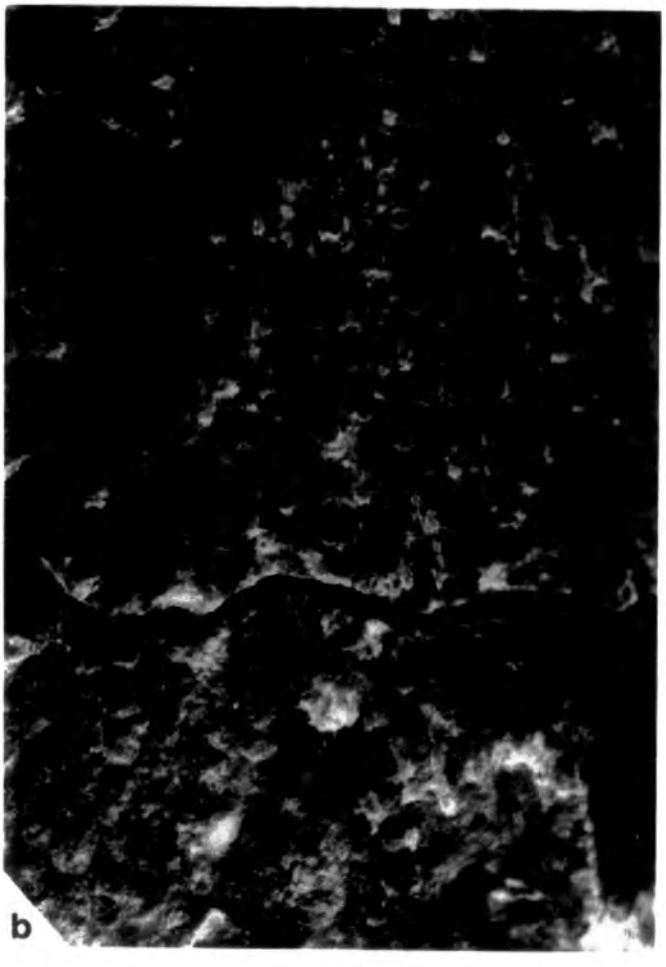

b

Plate 120. Ptylopora pluma McCoy

fig.a. Tangential section through the midrib and proximal areas of lateral branches showing autozooecial chamber bases. NMI F.6102a. Courceyan, Hookhead formation, Hookhead, Fethard. X40.

fig.b. As for fig.a. X104.


a


b

Plate 121. Ptylopora pluma McCoy

fig.a. Longitudinal section through the midrib showing the extremely thick secondary outer laminated skeleton. NMI F.6102f. Courceyan, Hookhead Formation, Hookhead, Fethard. X34.

fig.b. Transverse section through the midrib (far right) and two lateral branches. NMI F.6102d. Horizon and locality as for fig.a. X34.

fig.c. Transverse section through the midrib showing details of the skeletal microstructure. The primary granular layer that surrounds autozooecial chambers is thin, and short, narrow ridges of this granular layer radiate outwards into the very thick outer secondary laminated skeleton which has a chevron-like structure. NMI F.6102d. Horizon and locality as for fig.a. X92.

a

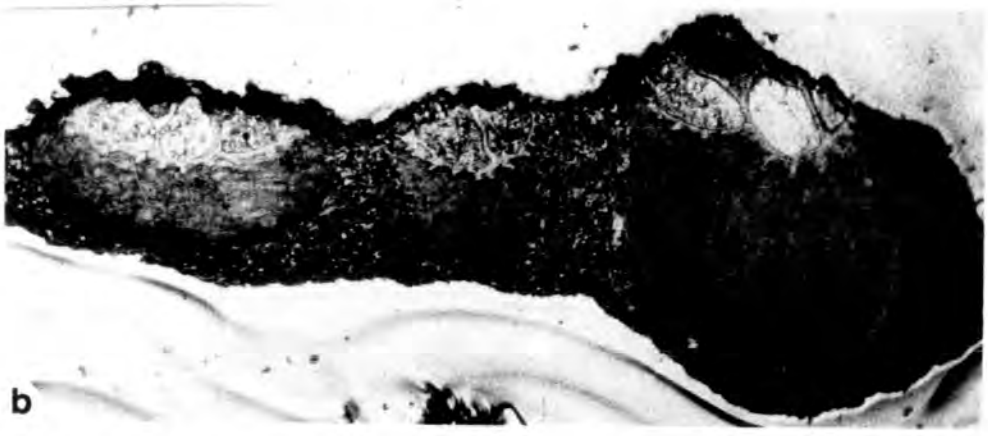

b

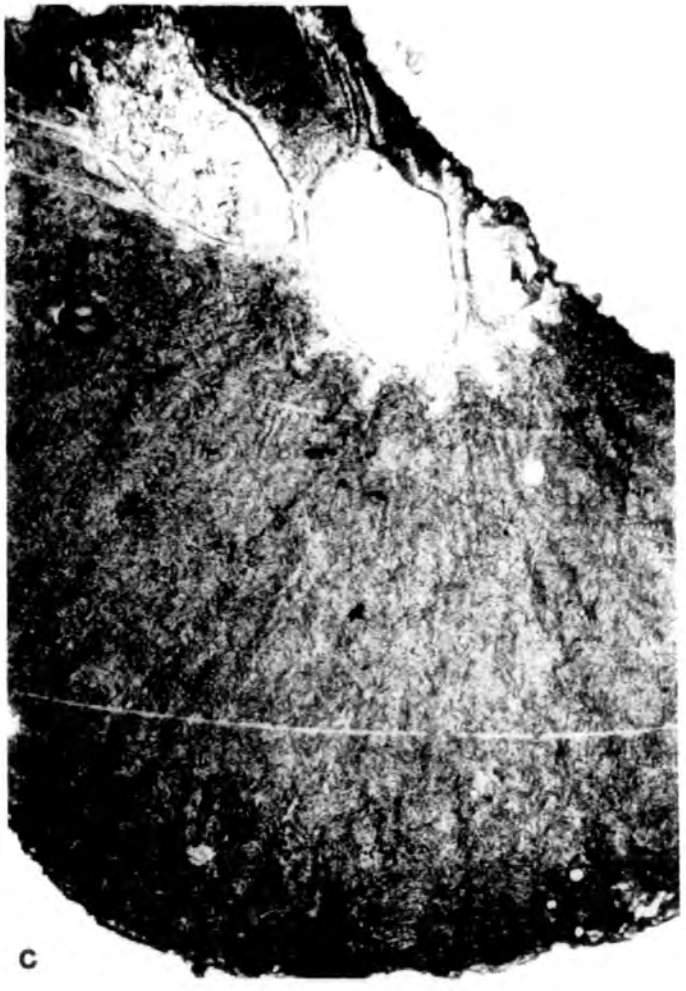

c

Plate 122. Ptylopora pluma McCoy

fig.a. Transverse section showing detail of the skeletal microstructure of the midrib. A thin finely laminated secondary skeleton lines autozooecial chambers. A thin primary granular layer surrounds chambers and narrow short ridges radiate outwards into the surrounding thick outer secondary laminated skeleton. The outer secondary laminated skeleton is orally flexed around the ridges of the primary granular skeleton. NMI F.6102d. Courceyan, Hookhead Formation, Hookhead, Fethard. X220.

fig.b. As for fig.a. X400.

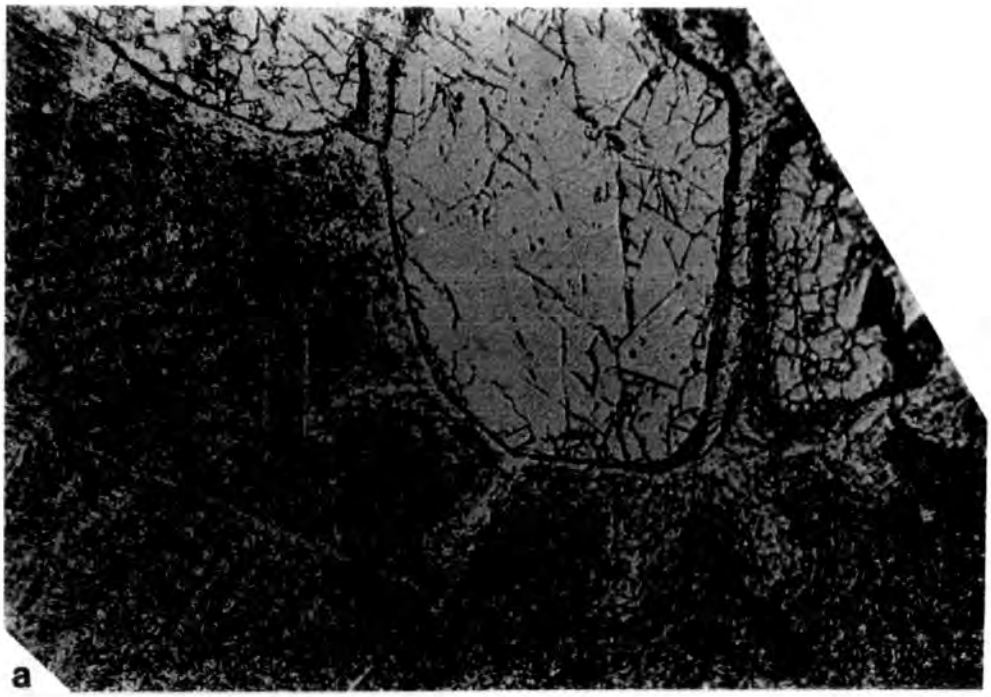

a

b

Plate 123. *Ptylopora pluma* McCoy

fig.a. Transverse section through the midrib showing detail of the outer secondary laminated skeleton with its chevron-like structure. NMI F.6102d. Courceyan, Hookhead Formation, Hookhead, Fethard. X400.

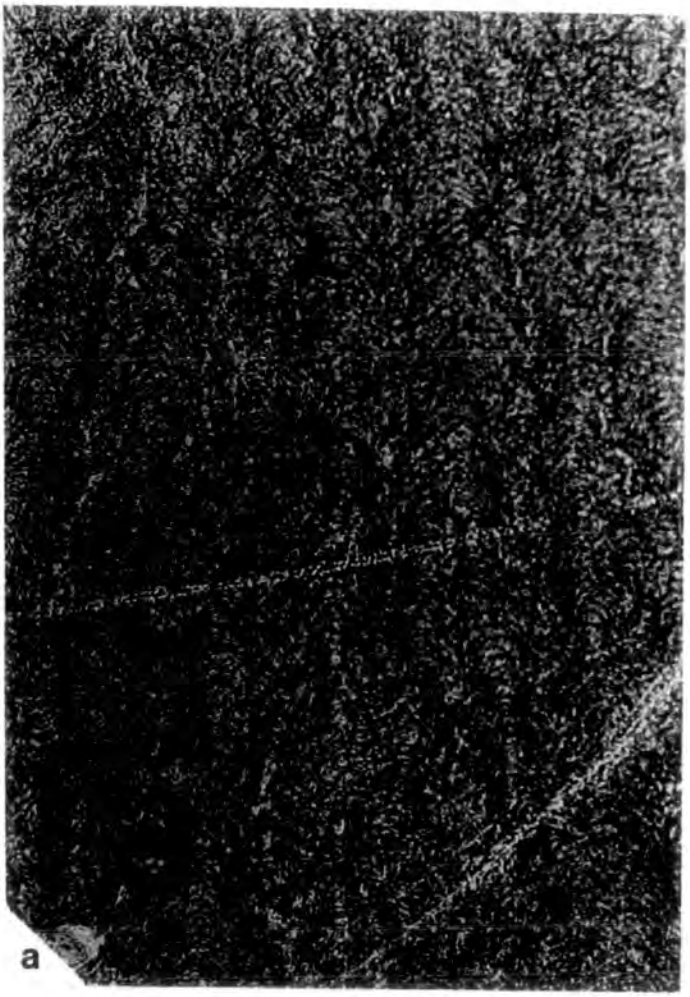
a

Plate 124. Secondary Overgrowths

fig.a. Longitudinal section showing detail of an overgrowth in a colony of Dyscritella miliaria (Nicholson). The point of origin of the overgrowth is seen and autozooecia of the overgrowth grew in a proximal direction down the sides of the parent branch. HM D.21. Asbian, Lower Limestone Group, Redesdale Ironstone Shale, Ridsdale, Northumberland. X37.

fig.b. Longitudinal section showing detail of the the overgrowth in the same colony as illustrated in fig.a. X37.


a
b

Plate 125. Secondary Overgrowths

fig.a. Longitudinal section showing detail of an overgrowth in a colony of Stenodiscus tumida (Phillips). The basal lamina of the overgrowth is shown and the endozones of the overgrowth autozooecia are very short and poorly developed. HM D.10. Asbian, Lower Limestone Group, Redesdale Ironstone Shale Ridsdale, Northumberland. X47.


a

Plate 126. Zooecial Boundaries

fig.a. Tangential section showing the laminated nature of skeletal laminae throughout the entire width of the interzooecial wall in the thin walled portion of the exozone wall in Tabulipora urii (Fleming). Laminae only turn over in a very narrow dark coloured zone along the median line of interzooecial wall where they are orientated parallel to the plane of section. HM D.787b. Brigantian, Lower Limestone Group, Hosie Limestone, Hairmyres. X400.

fig.b. Longitudinal section showing the occurrence of an irregularly sinuous narrow dark zone along the median line of interzooecial walls in the thin walled portion of an exozone wall. Laminae turn over abruptly in this zone. Tabulipora urii (Fleming). Horizon and locality as for fig.a. X90.

a

b

Plate 127. Zooecial Boundaries

fig.a. Longitudinal section showing the gradual dissapearance of the dark coloured narrow median line in interzooecial walls accompanying the development of a thick walled monila as the pitch of the laminae decreases and they turn gently over across a wider area. Tabulipora urii (Fleming). HM D.902. Brigantian, Lower Limestone Group, Hosie Limestone, Hairmyres. X91.

fig.b. Longitudinal section showing the occurrence of a narrow dark line along the median line of interzooecial walls in the exozone region. The line appears at the anterior ends of monilae with the development of a thin walled portion (higher pitch of laminae) and dissapears in the proximal portion of the succeeding monilae as the pitch of the laminae decreases. Tabulipora urii (Fleming). HM D.902. X360.


a


b

Plate 128. Ring Septa

fig.a. Longitudinal section showing detail of the laminar microstructure of ring septa. Skeletal laminae comprising ring septa are only continuous with interzooecial wall laminae in the proximal portions of septa. Along most of the septums length laminae extend from its anterior surface at low angles and gradually gently curve inwards and turn over quite abruptly fairly close to the posterior septum wall. The posterior curvature of the septal rims is developed by the accretion of laminae at increasing angles away from the anterior surface. Tabulipora urii (Fleming). HM D.787a. Brigantian, Lower Limestone Group, Hosie Limestone, Hairmyres. X360.

fig.b. Longitudinal section showing the occurrence of a dark narrow line developed where laminae of the ring septum turn over abruptly in the posterior portion of the septum. Tabulipora urii (Fleming). HM D.787a. Horizon and locality as for fig.a. X360.

b

a

Plate 129. Ring Septa

fig.a. Longitudinal section showing morphological variation of septal rims on opposite margins in Tabulipora urii (Fleming). HM D.787a. Brigantian, Lower Limestone Group, Hosie Limestone, Hairmyres. X230.

fig.b. Longitudinal section showing thickened anterior surfaces of septal rims. Tabulipora urii (Fleming). HM D.787a. Horizon and locality as for fig.a. X360.

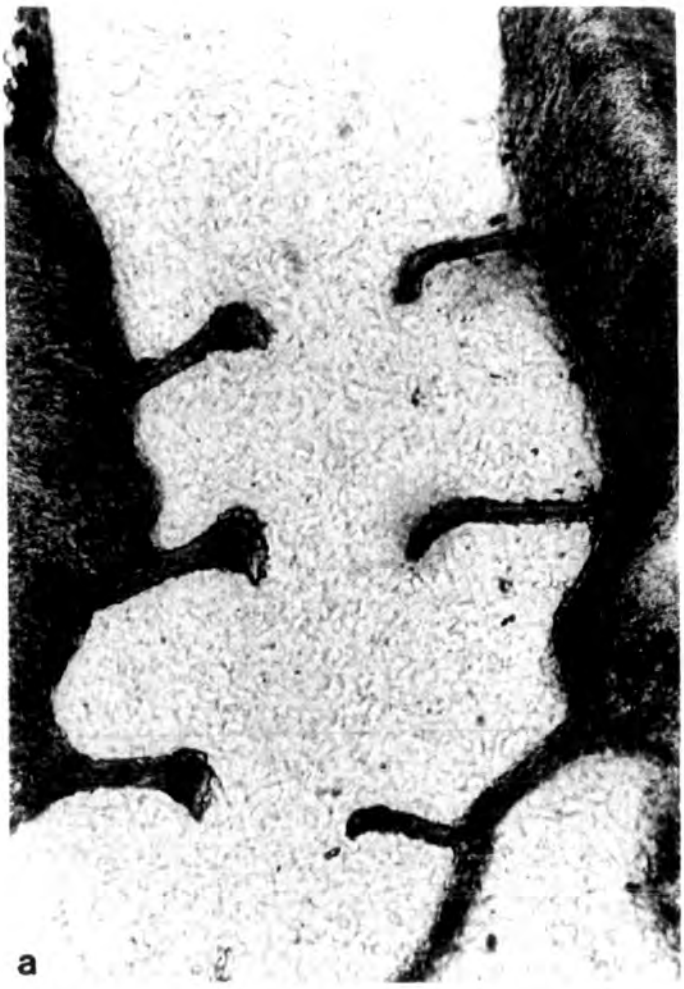

a

b

Plate 130. *Tabulipora urii* (Fleming)

fig.a. Paralectotype; colony encrusting a crinoid stem. HM D.300. Brigantian, Lower Limestone Series, Trearne, Beith. X1.9.

fig.b. Paralectotype; colony encrusting the brachiopod *Composita ambigua*. HM D.786c. Brigantian, Lower Limestone Series, Hosie Limestone, Hairmyres. X13.

fig.c. Paralectotype; adnate colony. HM D.785. Horizon and locality as for fig.b. X13.

a

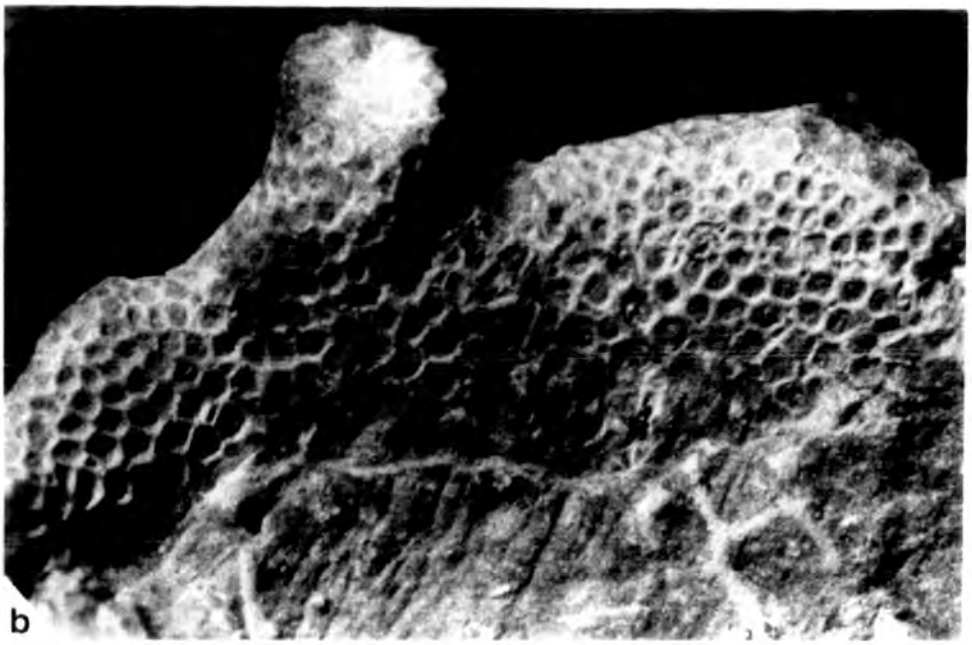

b

c

Plate 131. Tabulipora urii (Fleming)

fig.a. Paralectotype; detail of the zoarial surface showing the irregular shape, size and distribution of autozooecial apertures, and the irregular distribution of exilazooecia. HM D.907. Brigantian, Lower Limestone Group, Hosie Limestone, Hairmyres. X11.

fig.b. As for fig.a. X11.

fig.c. As for fig.a. X18.

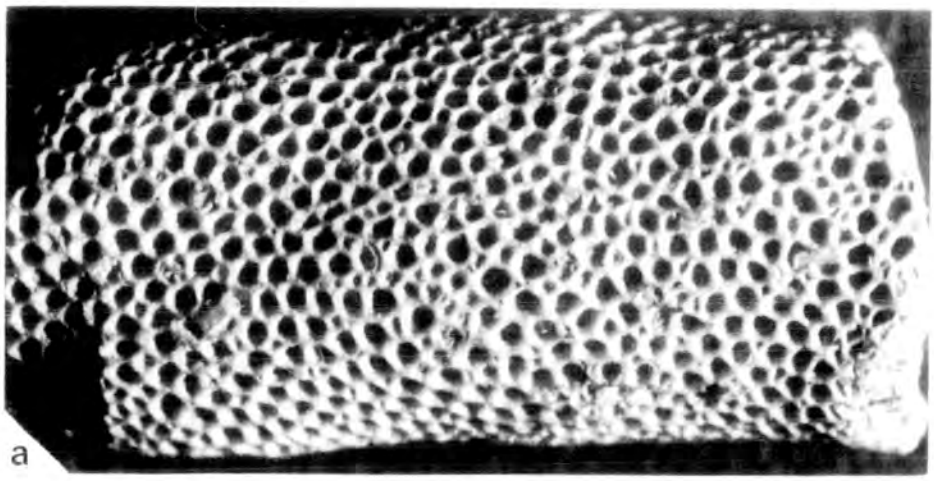

a

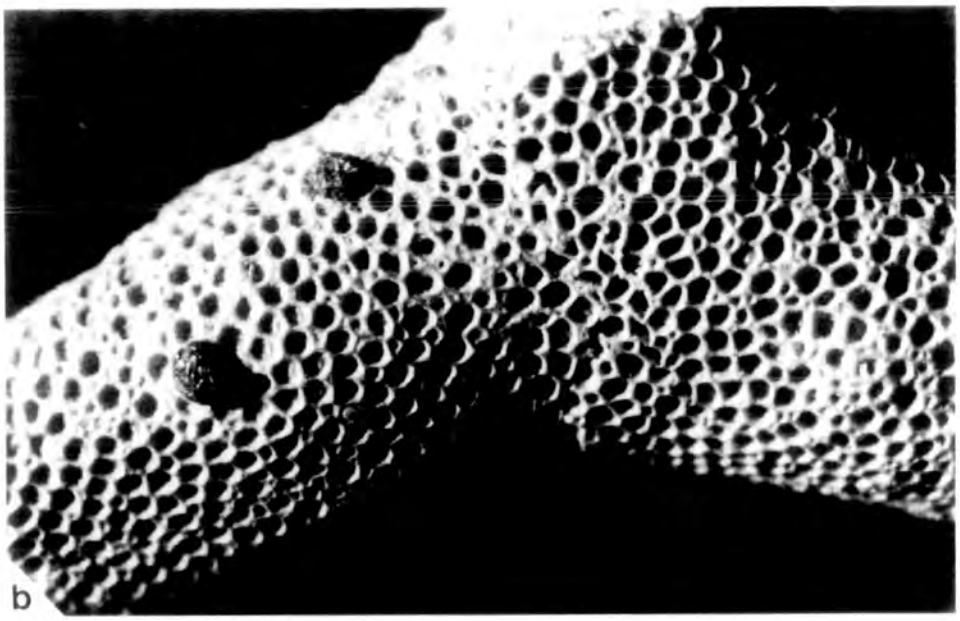

b

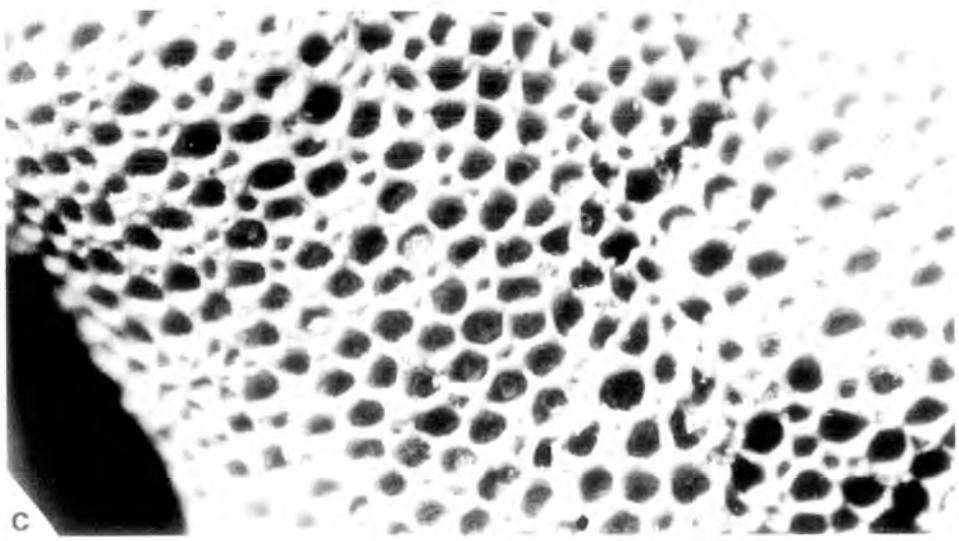

c

Plate 132. Tabulipora urii (Fleming)

fig.a. Paralectotype; zoarial surface detail showing the distribution of stylets with large type A stylets situated at interapertural angles and small type C stylets closely spaced between. HM D.907. Brigantian, Lower Limestone Group, Hosie Limestone, Hairmyres. X18.

fig.b. Lectotype; shallow tangential section showing the distribution of stylets. HM D.787d. Horizon and locality as for fig.a. X37.

fig.c. Shallow tangential section. GAGM 01-53bxx. Brigantian, Capelrig, E. Kilbride. X16.

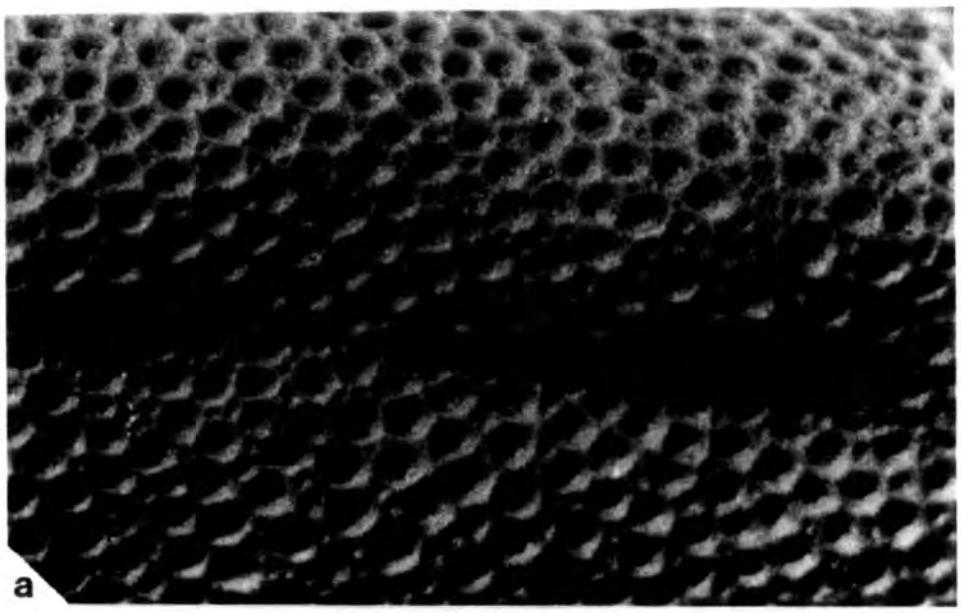
a

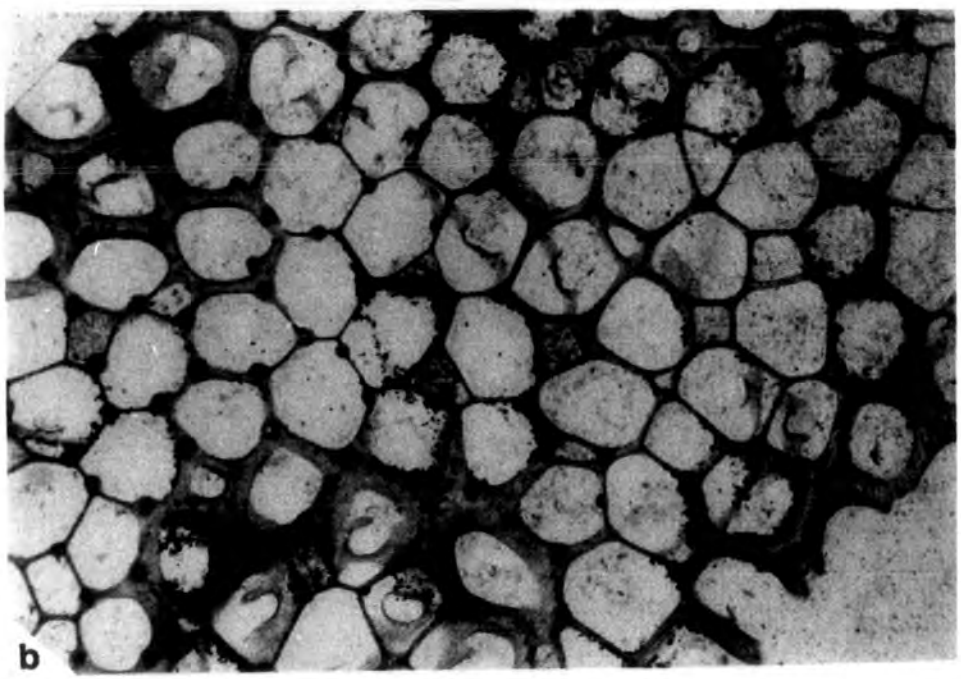
b

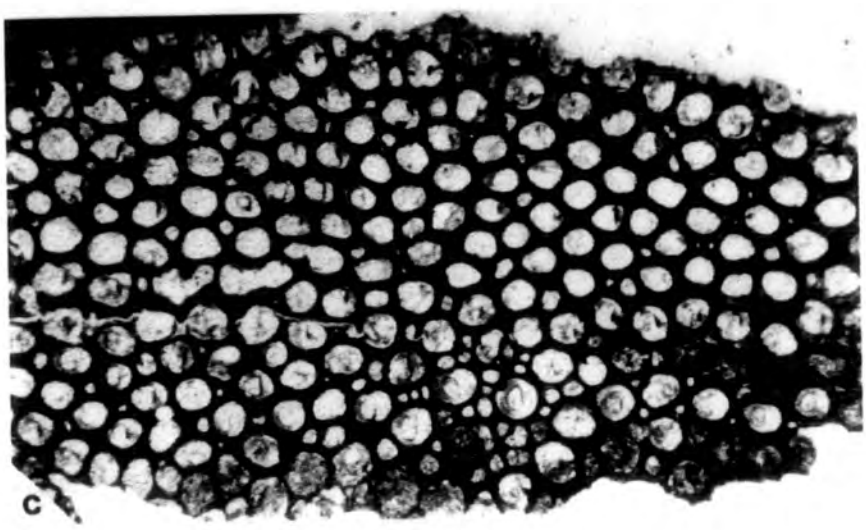
c

Plate 133. Tabulipora urii (Fleming)

fig.a. Lectotype; tangential section showing the distribution of stylets on interzooecial walls, large type A stylets are situated at interzooecial angles and small type C stylets are closely spaced between. Type C stylets are absent in thin walled portions. The reniform shape of the perforations in ring septa are shown. HM D.787b. Brigantian, Lower Limestone Group, Hosie Limestone, Hairmyres. X88.

fig.b. Lectotype; tangential section showing detail of the distribution of stylets. Horizon and locality as for fig.a. X230.

fig.c. Lectotype; tangential section showing type A stylets situated at, and close to interzooecial angles, and their projection beyond the margins of interzooecial walls in a narrow thin walled portion of the exozone wall. Horizon and locality as for fig.a. X200.

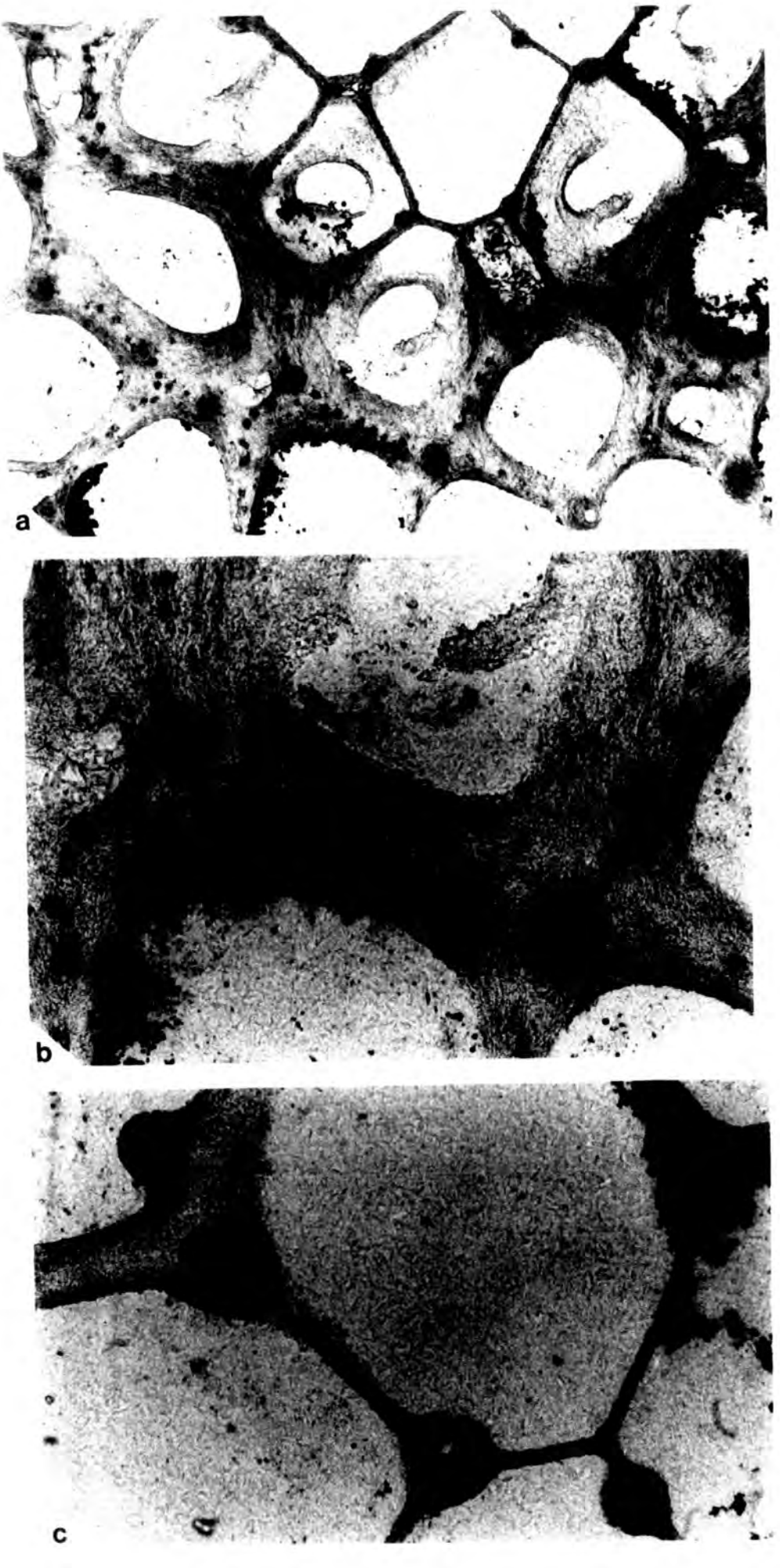
a
b
c

Plate 134. Tabulipora urii (Fleming)

fig.a. Transverse section showing the exozone region with a long thick walled portion, also the origin of a lateral branch. Lateral branch development is initiated with the development of a long thin walled endozone portion on the exozone wall of the parent branch.
GAGM 01-53bxs. Brigantian, Hillhead Quarry, Beith. X16.

fig.b. Lectotype; transverse section showing the irregularly budded autozooecia in the endozone region, also a long thick walled portion and a very short thin walled portion in the exozone region. HM D.787c. Brigantian, Lower Limestone Group, Hosie Limestone, Hairmyres. X37.

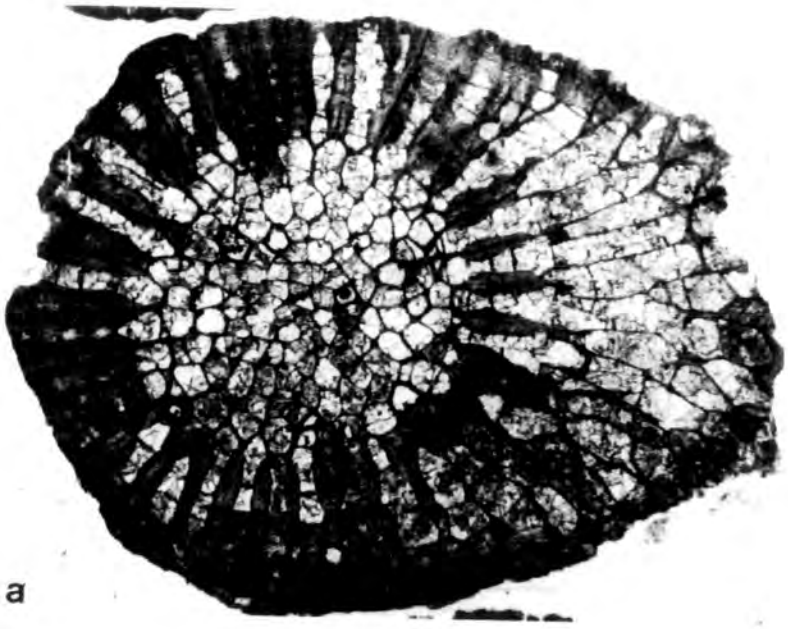

a

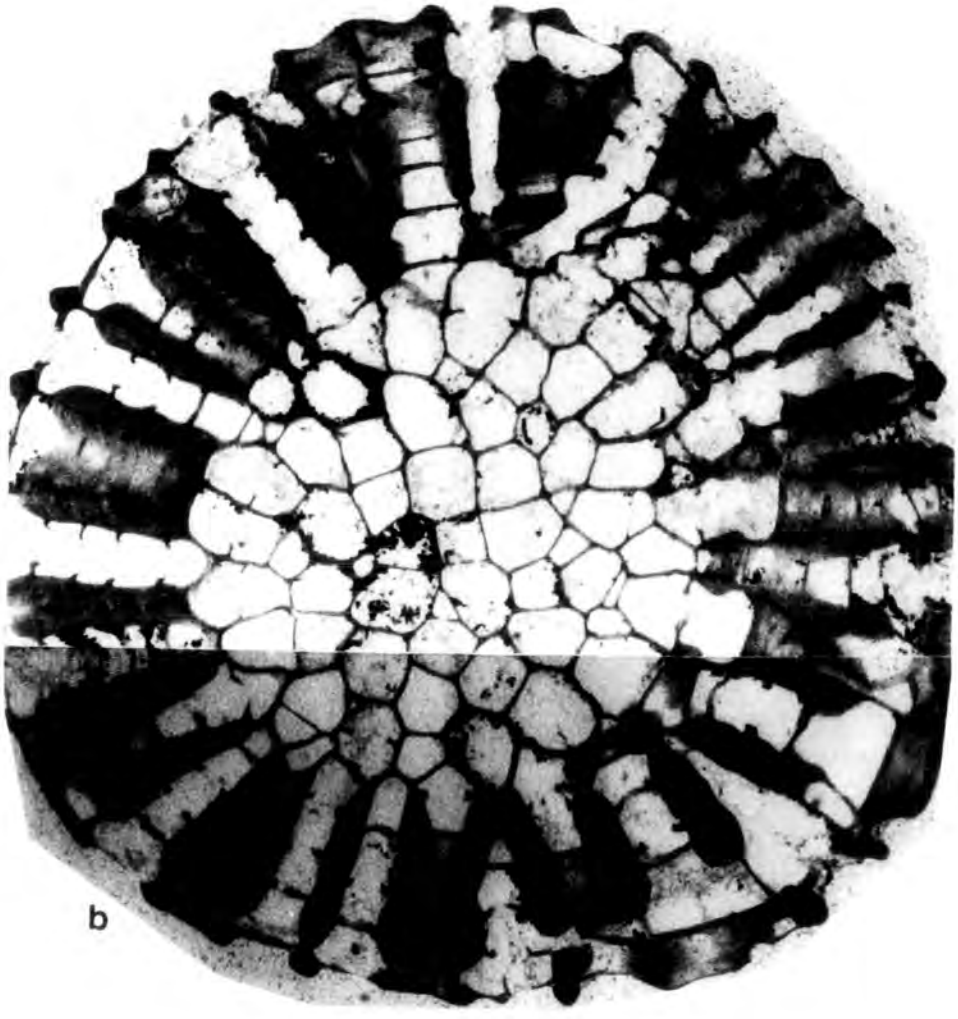

b

Plate 135. *Tabulipora urii* (Fleming)

fig.a. Lectotype; transverse section showing exozone detail. The irregularly developed narrow dark sinuous median line of interzooecial walls is shown, and type A stylets are seen in the upper part of interzooecial walls. HM D.787c. Brigantian, Lower Limestone Group, Hosie Limestone, Hairmyres. X90.

fig.b. Lectotype; longitudinal section showing the interzooecial allignment of ring septa and monilae in the exozone region. X16.

fig.c. Lectotype; longitudinal section showing the interzooecial allignment of monilae and ring septa in the exozone region. X35.

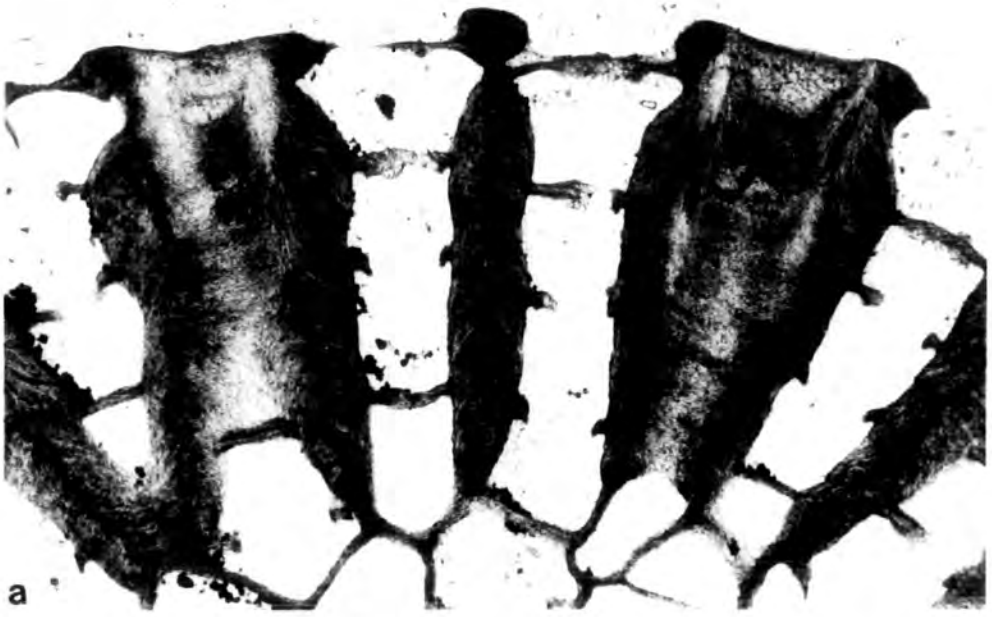
a

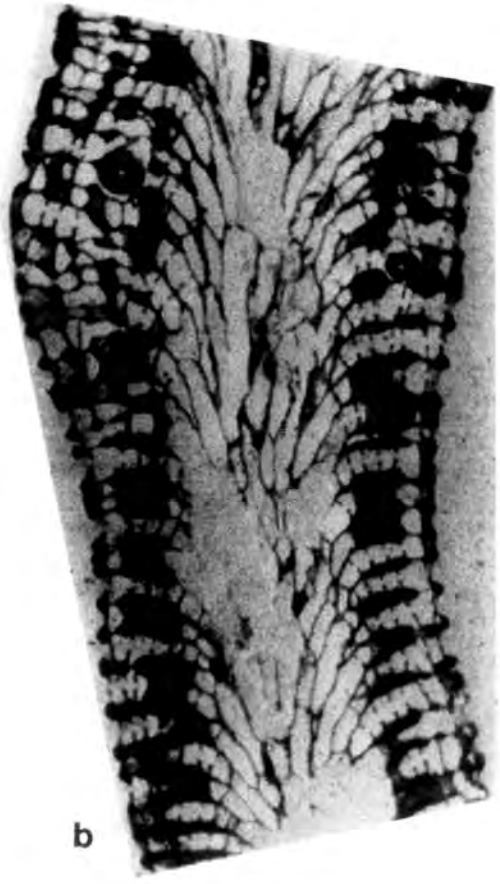
b

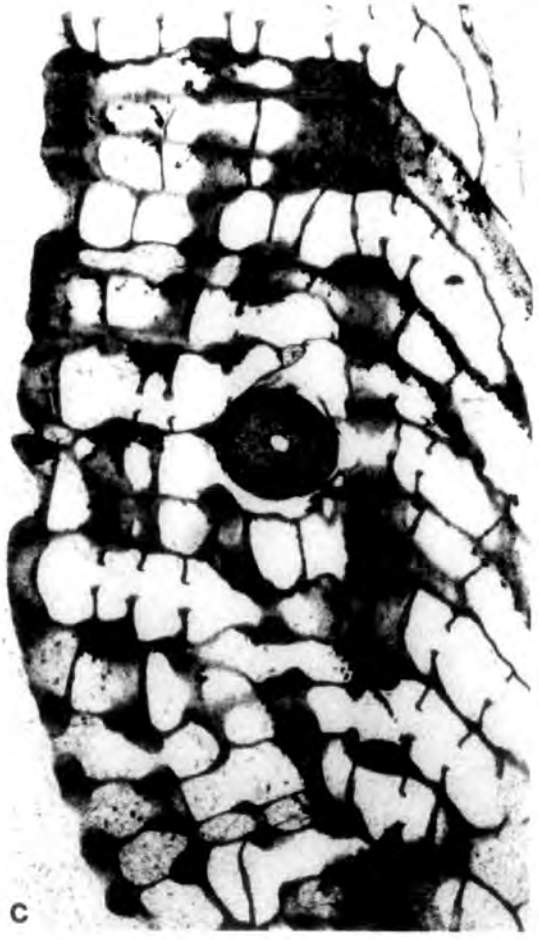
c

Plate 136. Tabulipora urii (Fleming)

fig.a. Lectotype; longitudinal section showing the interzooecial allignment of monilae and ring septa and the irregular development of the dark narrow sinuous median line in the thick walled portions of exozone interzooecial walls. HM D.787a. Brigantian, Lower Limestone Group, Hosie Limestone, Hairmyres. X34.

fig.b. Paralectotype; longitudinal section showing thin exozone interzooecial walls with monilae only poorly developed, and the interzooecial allignment of ring septa. HM D.900. Horizon and locality as for fig.a. X16.

fig.c. Paralectotype; longitudinal section showing the occurrence of a thicker and better developed proximal (lower) side to ring septa compared to distal (upper) sides. HM D.900. Horizon and locality as for fig.a. X38.


a


b


c

Plate 137. Tabulipora urii (Fleming)

fig.a. Paralectotype; longitudinal section showing the interzooecial allignment of monilae and ring septa in the exozone region. HM D.902. Brigantian, Lower Limestone Group, Hosie Limestone, Hairmyres. X16.

fig.b. As for fig.a. X37.

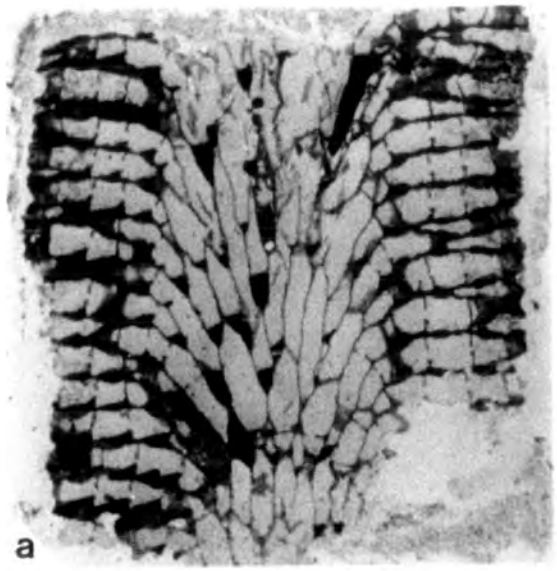

a

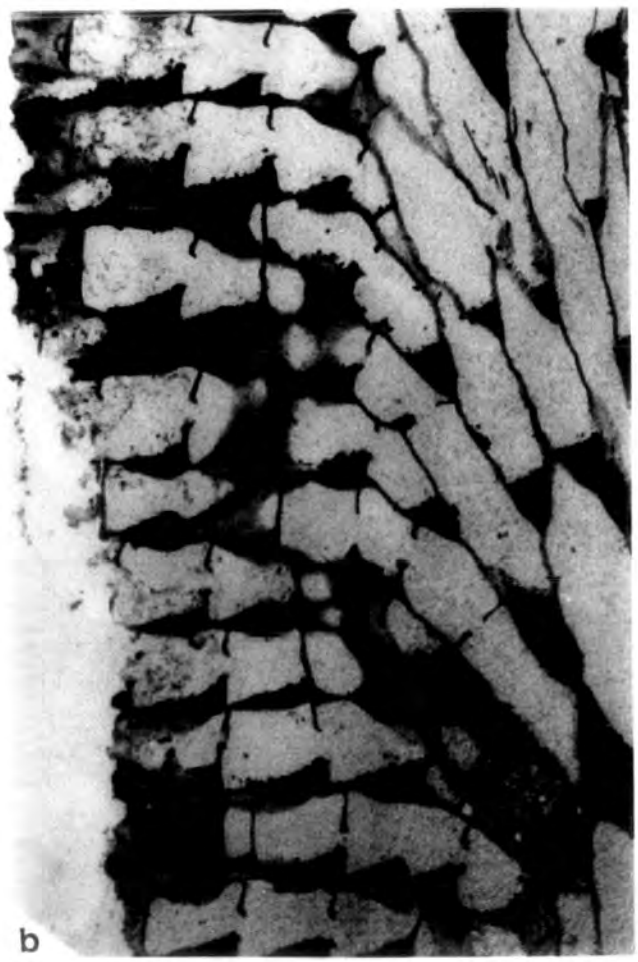

b

Plate 138. Tabulipora urii (Fleming)

fig.a. Paralectotype; longitudinal section showing interzooecial allignment of monilae and ring septa in the exozone region. HM D.902. Brigantian, Lower Limestone Group, Hosie Limestone, Hairmyres. X38.

fig.b. Paralectotype; longitudinal section showing the better developed thicker and longer proximal (lower) margins of ring septa compared to distal (upper) margins. HM D.902. Horizon and locality as for fig.a. X93.

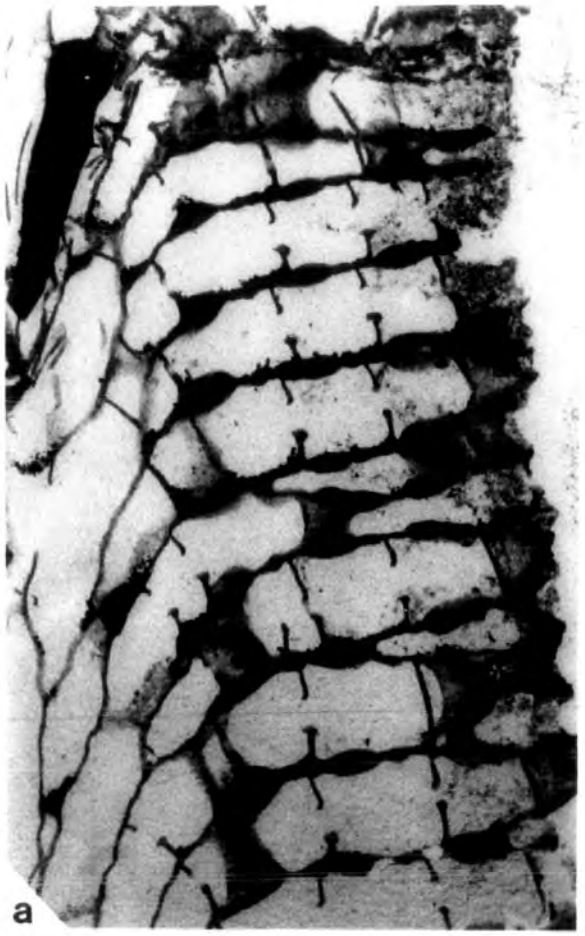
a


b

Plate 139. Tabulipora howsii (Nicholson)

fig.a. Specimens attached to a card showing the regular arrangment of monticules. The specimen on the bottom left is a cut and polished section showing the interzooecial allignment of monilae in the exozone region. NH G.155.83(1-6). Asbian, Lower Limestone Group, Redesdale Ironstone Shale, Ridsdale, Northumberland. XO.6.

fig.b. Colony fragment showing the regular arrangment of monticules. NH G.155.86(-5). Horizon and locality as for fig.a. X2.3.

a

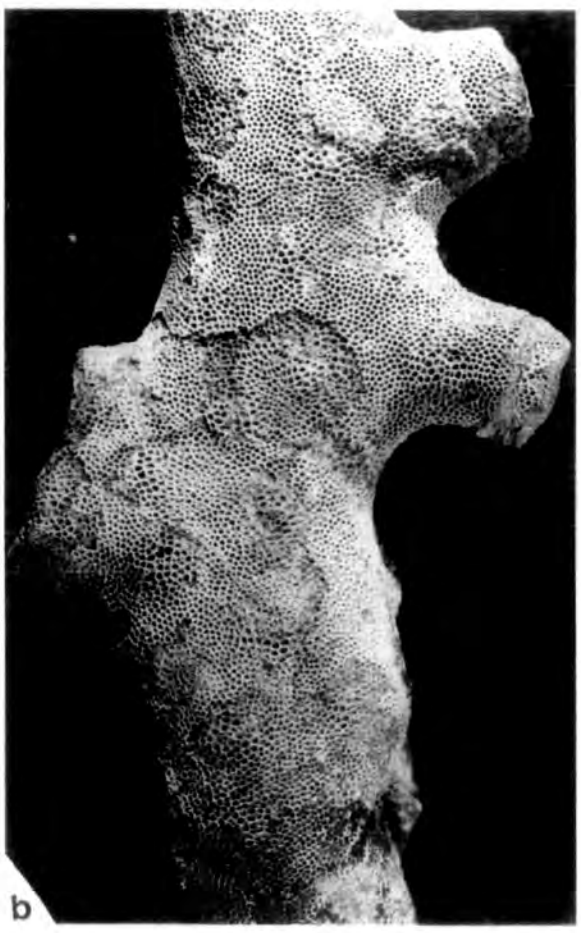

b

Plate 140. Tabulipora howsii (Nicholson)

fig.a. Zoarial surface detail showing the regular arrangement of monticules. NH G.155.86(-4). Asbian, Lower Limestone Group, Redesdale Ironstone Shale, Ridsdale, Northumberland, X2.4.

fig.b. Zoarial surface detail showing the regular arrangement of monticules and the occurrence of acrothoracian type borings. NH G.155.87(-6). Horizon and locality as for fig.a. X2.4.

fig.c. Zoarial surface detail showing the variation in the shape, size and the irregular distribution of autozooecial apertures; also the distribution of stylets with large type A stylets situated at interapertural angles and small closely spaced type C stylets between. NH G.155.87(-6). Horizon and locality as for fig.a. X20.

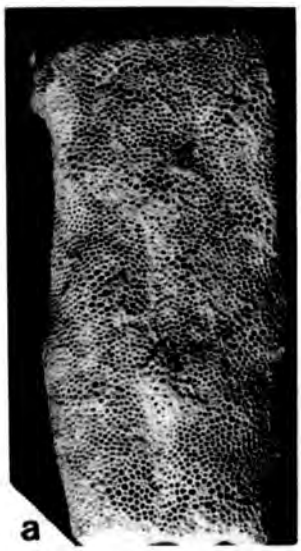
a

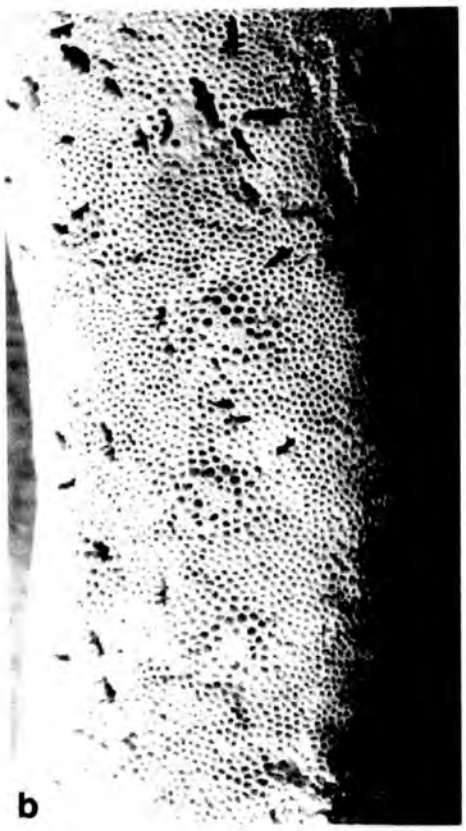
b

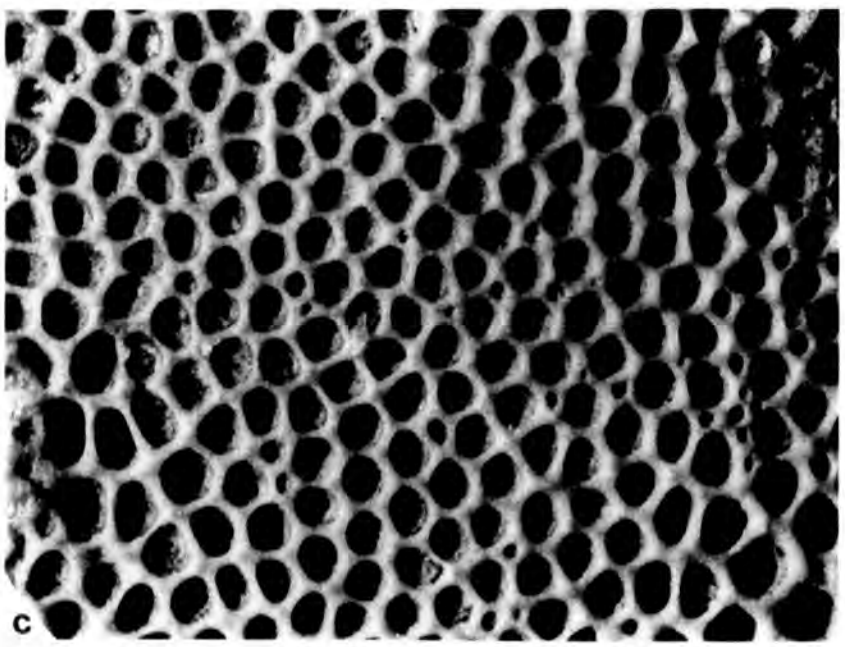
c

Plate 141. Tabulipora howsii (Nicholson)

figs.a. to c. show zoarial surface detail of a monticule. The summit area is comprised of very small exilazooecia and is surrounded by autozooecial apertures of a larger than average size. Autozooecial apertural dimensions decrease in size away from this region to intermonticular areas. The distribution of stylets is also shown with large type A stylets situated at interapertural angles and small type C stylets closely spaced between.

fig.a. ABR 116. Asbian, Lower Limestone Group, Redesdale Ironstone Shale, Ridsdale, Northumberland. X 20.

fig.b. NH G.155.87(-6). Horizon and locality as for fig.a. X20.

fig.c. NH G.155.87(-1). Horizon and locality as for fig.a. X20.

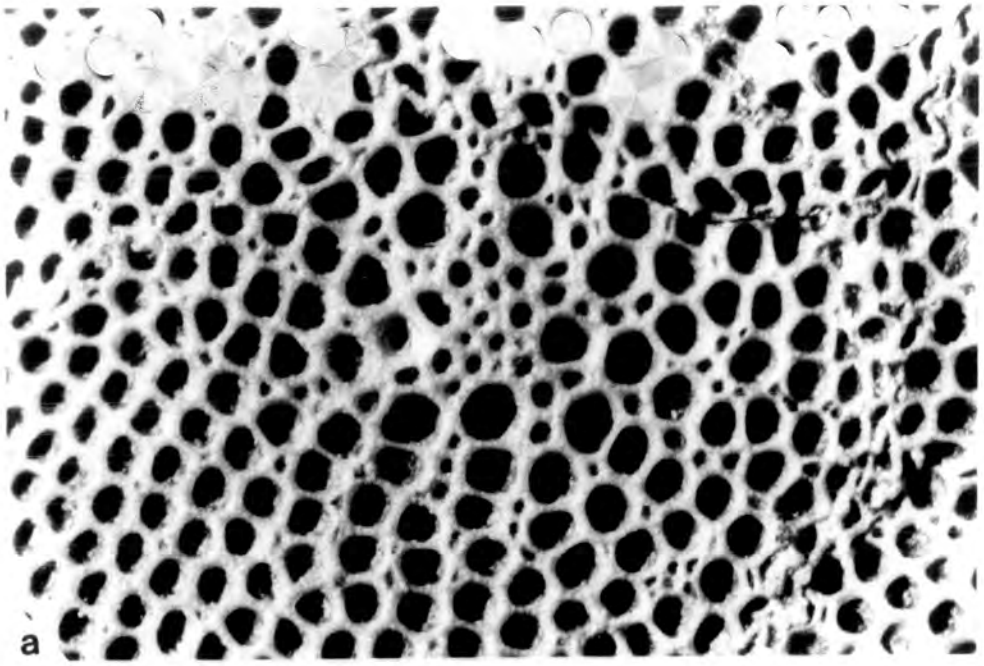
a

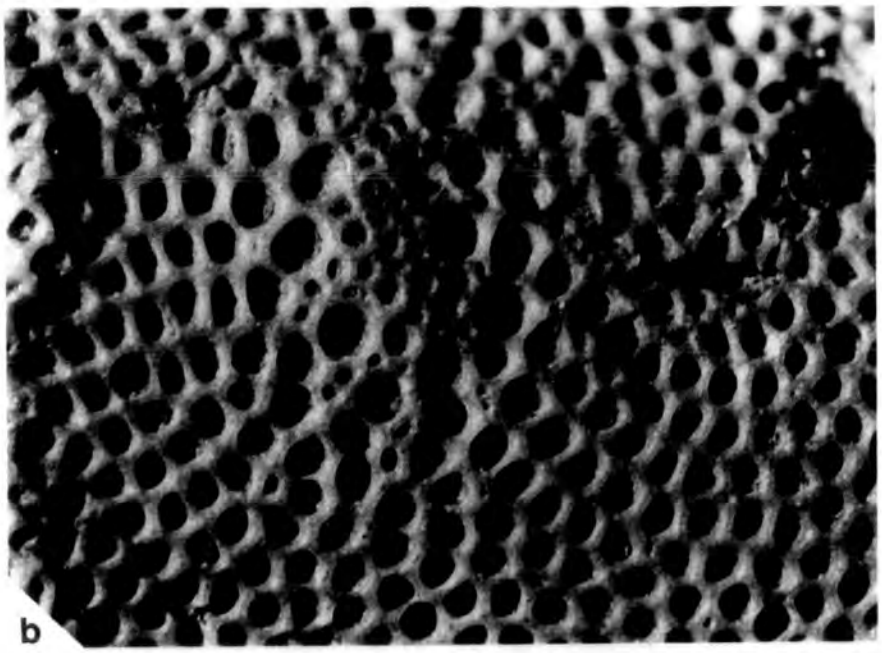
b

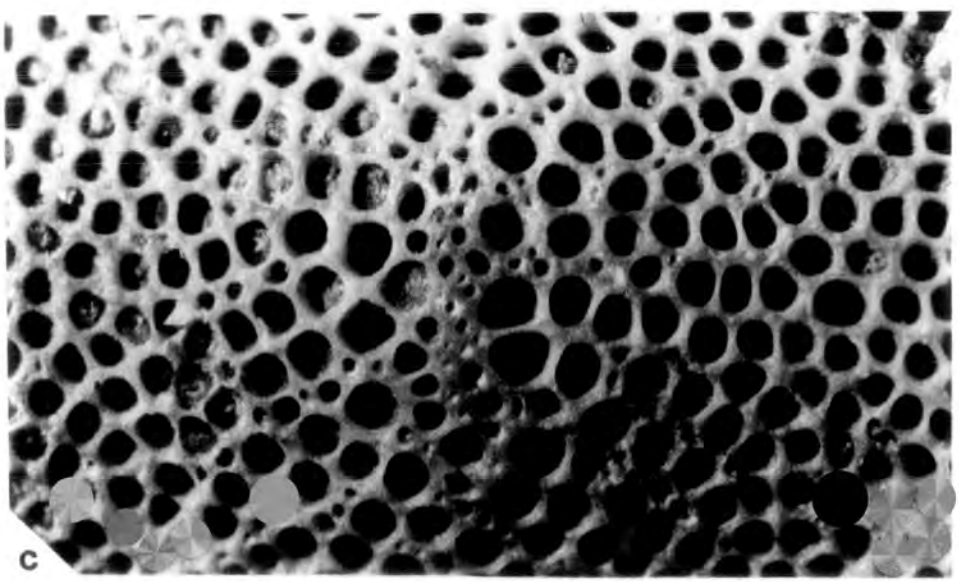
c

Plate 142. Tabulipora howsii (Nicholson)

fig.a. S.E.M. photomicrograph showing zoarial surface detail. ABR 116. Asbian, Lower Limestone Group, Redesdale Ironstone Shale, Ridsdale, Northumberland. X73.

fig.b. S.E.M. photomicrograph showing zoarial surface detail of a monticule. ABR 116. Horizon and locality as for fig.a. X36.

fig.c. S.E.M. photomicrograph showing zoarial surface detail, also showing the occurrence of ring septa situated close to the zoarial surface and their oval foramina. ABR 116. Horizon and locality as for fig.a. X55.

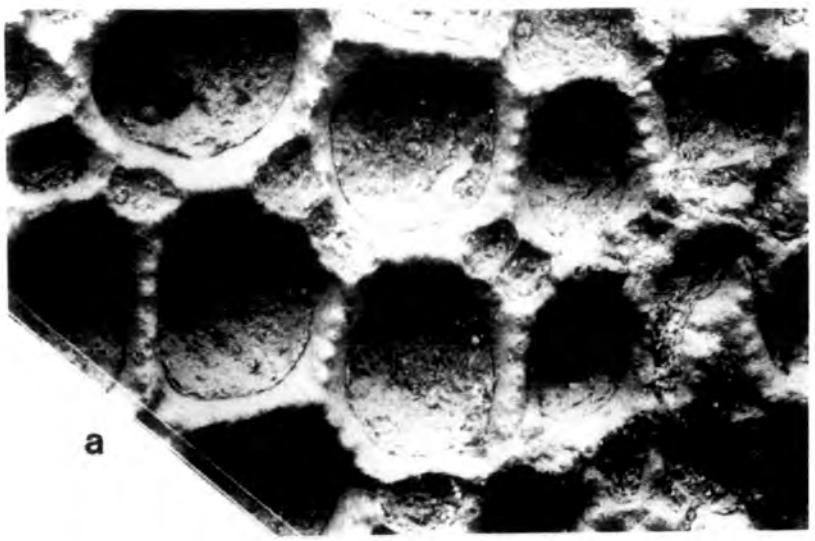

a

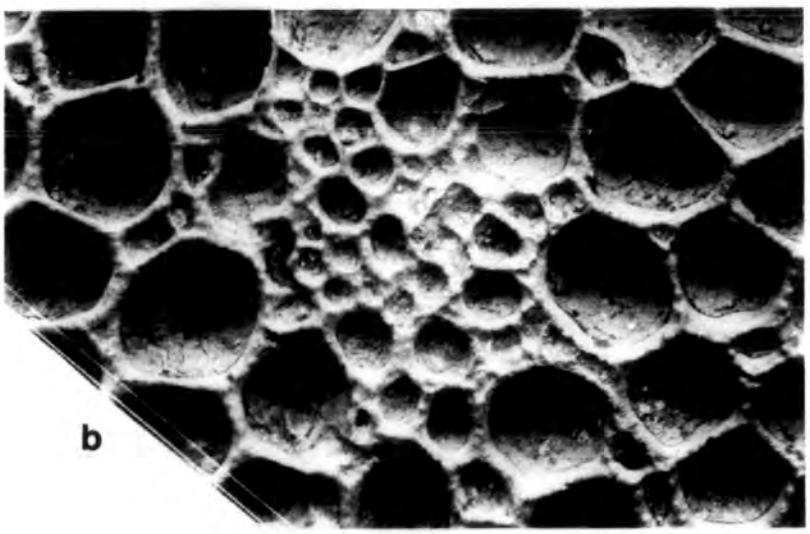

b

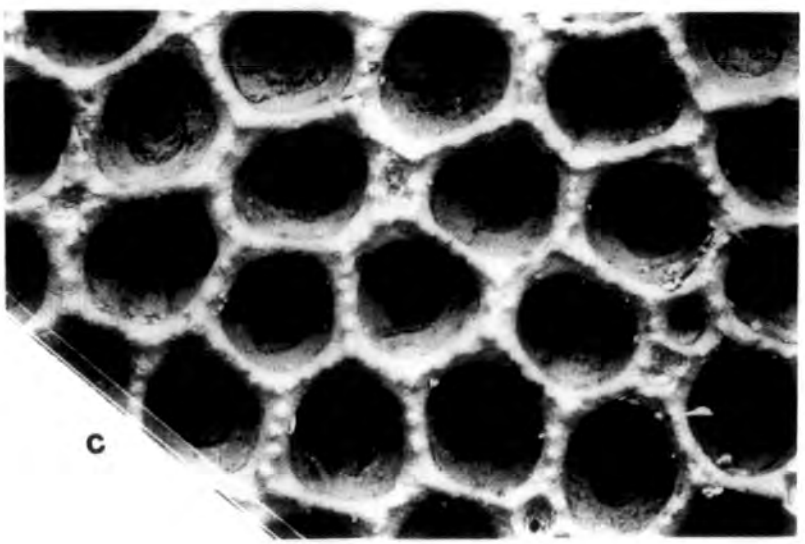

c

Plate 143. Tabulipora howsii (Nicholson)

fig.a. S.E.M. photomicrograph showing detail of ring septa situated close to the zoarial surface. The foramena are oval and are symmetrically positioned. ABR 116. Asbian, Lower Limestone Group, Redesdale Ironstone Shale, Ridsdale, Northumberland. X129.

fig.b. Broken portion of a branch showing the wide exozone region with autozooecia crossed by many closely spaced ring septa. NH G.155.86(-1). Horizon and locality as for fig.a. X3.2.

fig.c. Lectotype; transverse section showing the wide exozone region with thin moniliform interzooecial walls and autozooecia crossed by many closely spaced ring septa. GAGM 01-53bxw. Brigantian, Trearne, Beith. X16.

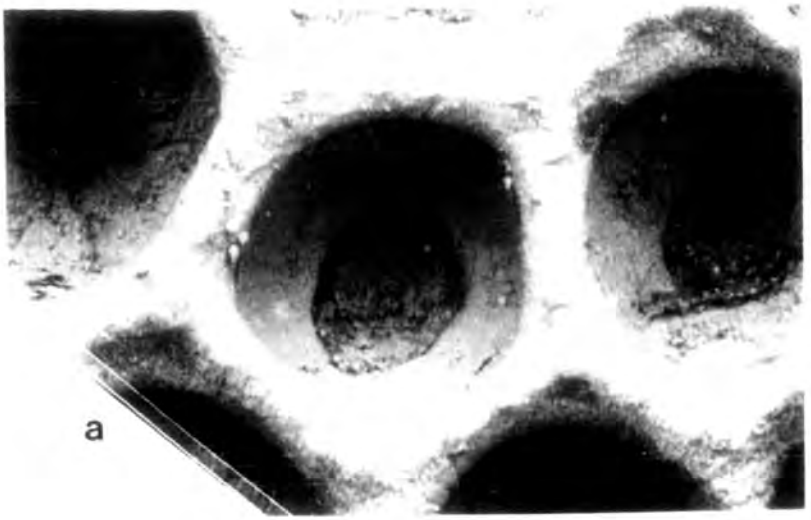
a


b

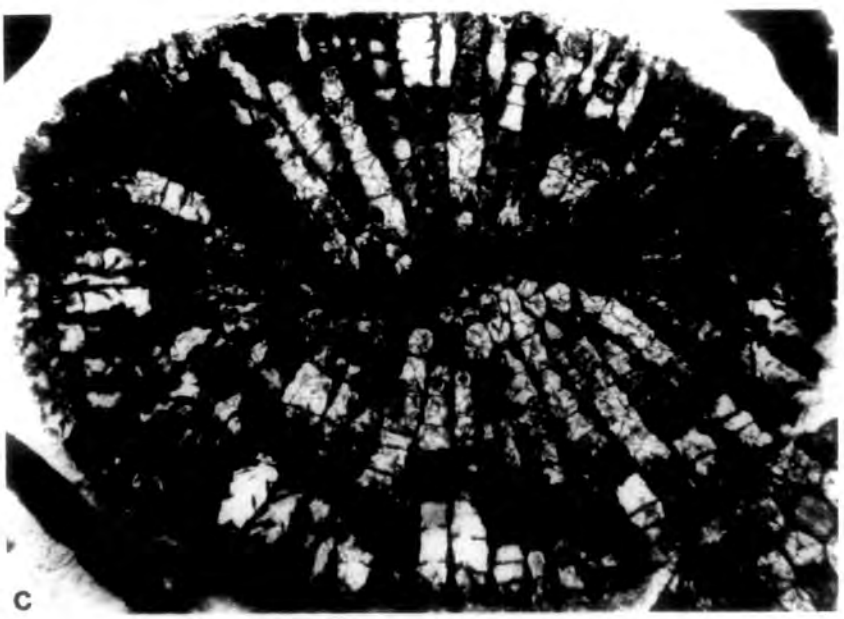
c

Plate 144. Tabulipora howsii (Nicholson)

fig.a. Lectotype; transverse section showing detail of the exozone region. The small oval monilae are more abundant than ring septa. GAGM 01-53bxw. Brigantian, Trearne, Beith. X37.

fig.b. Topotype; transverse section showing the wide exozone region. GAGM 01-53bxw. Brigantian, Trearne, Beith. X16.

fig.c. Topotype; transverse section showing detail of exozone interzooecial walls and ring septa. GAGM 01-53bxw. X37.

a

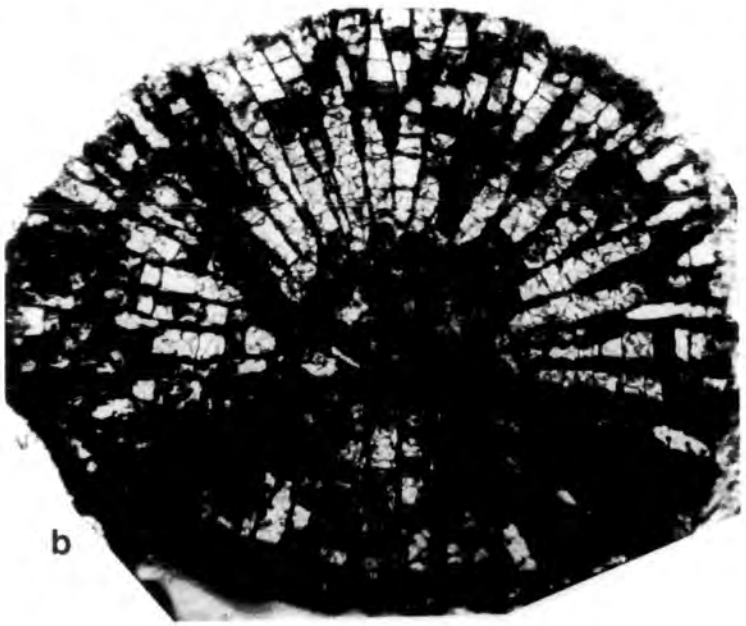

b

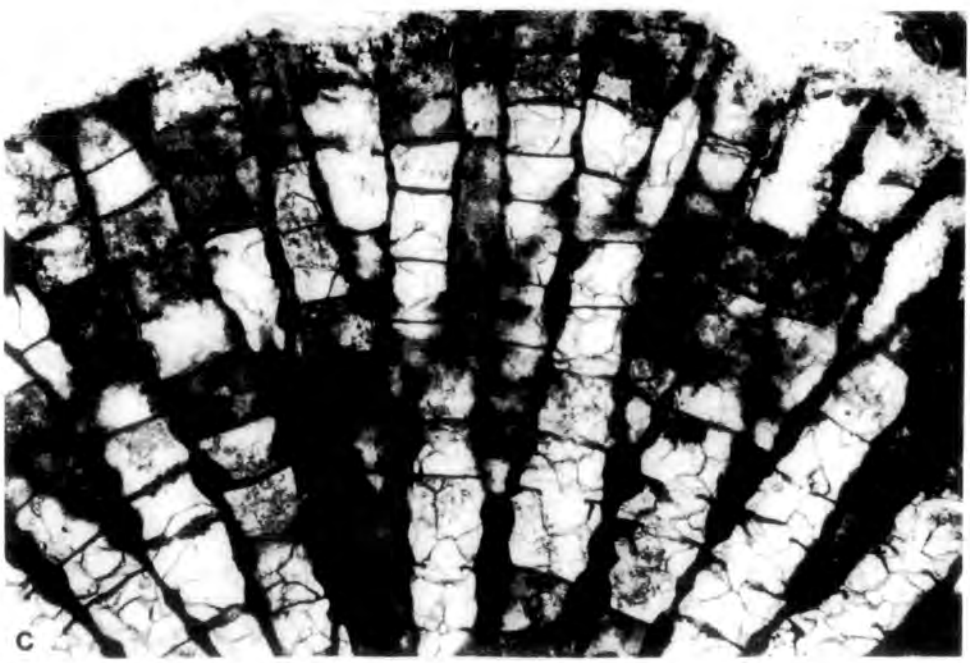

c

Plate 145. Tabulipora howsii (Nicholson)

fig.a. Topotype; transverse section showing detail of exozone interzooecial walls and ring septa. GAGM 01-53bxw. Brigantian, Trearne, Beith. X37.

fig.b. Topotype; longitudinal section showing detail of the exozone region. Interzooecial walls show a continuous curvature from the endozone into the exozone and through to the zoarial surface. GAGM 01-53bxw. Horizon and locality as for fig.a. X16.

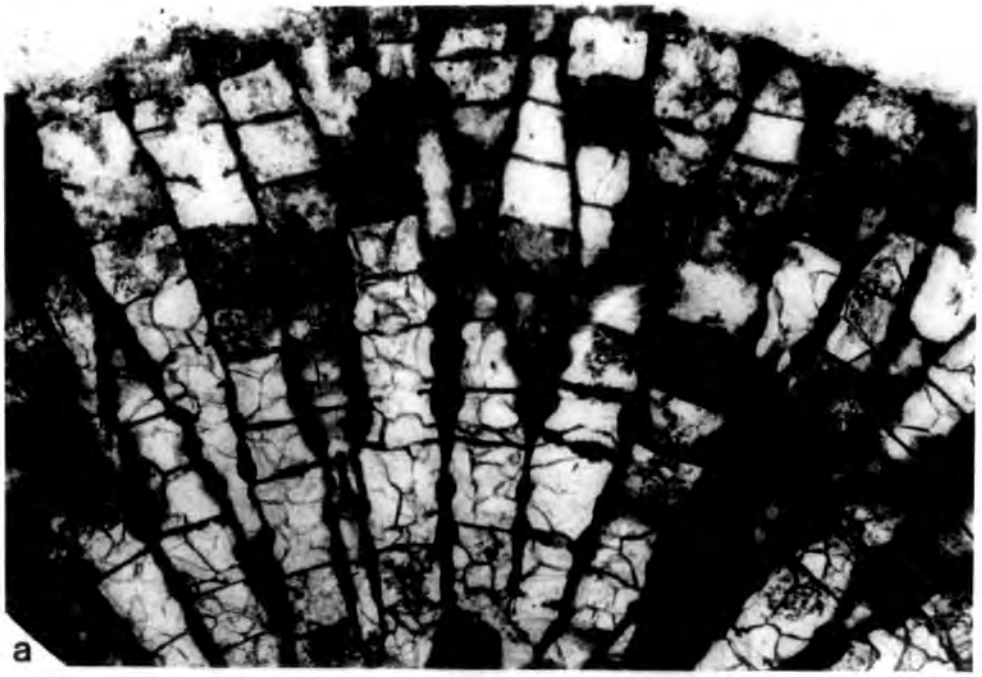

a

b

Plate 146. Tabulipora howsii (Nicholson)

fig.a. Topotype; longitudinal section showing detail of exozone interzooecial walls and ring septa. The small oval monilae are more abundant than ring septa. GAGM 01-53bxw. Brigantian, Trearne, Beith. X37.

fig.b. Topotype; longitudinal section showing the gradual curvature of interzooecial walls from the endozone through the exozone to the zoarial surface. GAGM 01-53bxw. Horizon and locality as for fig.a. X37.

a

b

Plate 147. Tabulipora minima Lee

figs .a. to e. show zoarial surface detail; the irregular arrangement and shape of autozooecial apertures; the distribution of stylets with large type A stylets situated at interapertural angles and small type C stylets closely spaced between; and the irregular distribution of exilazooecia.

fig.a. ABHR 1S(-2). Arnsbergian, Shales above the Main Limestone, Hurst. X16.

fig.b. ABHR 1S(-13). Showing an unusually high number of exilazooecia. Horizon and locality as for fig.a. X16.

fig.c. ABHR 1S(-15). Horizon and locality as for fig.a. X16.

fig.d. ABHR 1S(-4). Horizon and locality as for fig.a. X16.

fig.e. ABHR 1S(-3). Horizon and locality as for fig.a. X16.


a


b

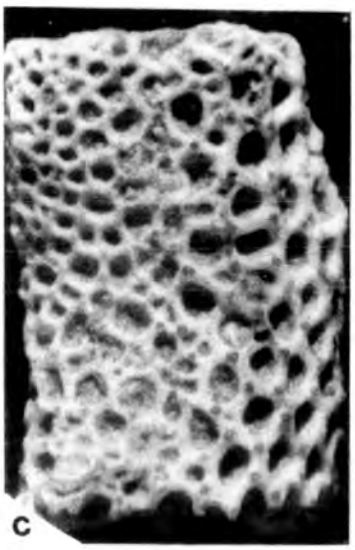
c


d

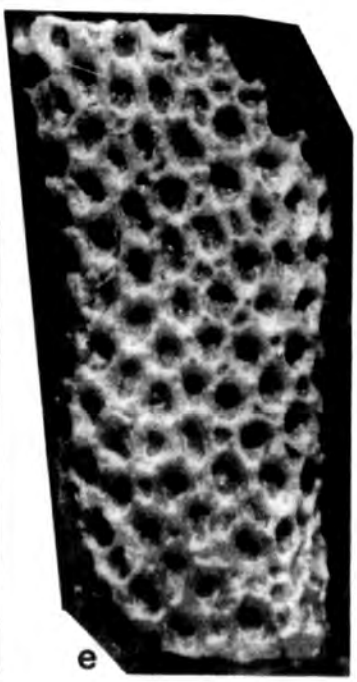
e

Plate 148. Tabulipora minima Lee

fig.a. Topotype; shallow tangential section showing the irregular shape and arrangement of autozooecial apertures, and the irregular distribution of exilazooecia and the distribution of stylets. GAGM 01-53byb. Brigantian, Lower Limestone Series, Howood Quarry, Renfreiwshire. X34.

fig.b. Topotype; shallow tangential section showing the distribution of stylets with large type A stylets situated at interapertural angles and small type C stlets irregularly arranged between. GAGM 01-53byb. Horizon and locality as for fig.a. X144.

a

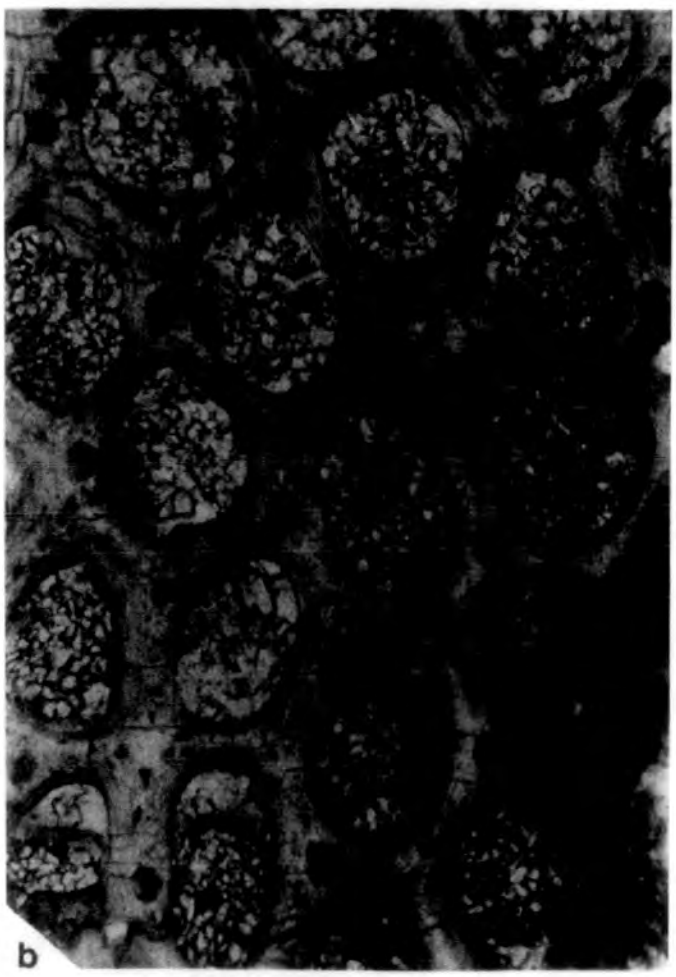

b

Plate 149. Tabulipora minima Lee

fig.a. Lectotype; longitudinal section showing the relatively narrow exozone region, club-like exozone interzooecial walls and the occurrence of about three ring septa per autozooecium. GAGM 01-53byb. Brigantian, Lower Limestone Series, Howood Quarry, Renfriewshire. X37.

fig.b. Topotype; longitudinal section, details as for fig.a. X37.

a

b

Plate 150. Tabulipora minima Lee

fig.a. Lectotype; longitudinal section showing exozone region detail. Exozone interzooecial walls are club-like, and the proximal(lower) margins of ring septa are better developed than distal (upper) margins. GAGM 01-53byb. Brigantian, Lower Limestone Series, Howood Quarry, Renfriewshire. X88.

fig.b. Lectotype; details as for fig.a. X88.

fig.c. Topotype; details as for fig.a. X88.

a

b

c

Plate 151. Tabulipora youngi Lee

fig.a. Lectotype; longitudinal section showing the uniform width of exozone interzooecial walls. GAGM 01-53bxr. Brigantian, Lower Limestone Series, Hillhead Quarry, Beith. X16.

fig.b. Lectotype; longitudinal section showing detail of exozone interzooecial walls - the intermittent development of a dark narrow irregularly sinuous zone along the median line of walls. Ring septa are interzooecially alligned. X36.


a


b

Plate 152. *Tabulipora youngi* Lee

fig.a. Lectotype; longitudinal section showing detail of exozone interzooecial walls- the intermittent development of a dark narrow irregularly sinuous zone along the median line of walls, GAGM 01-53bxr. Brigantian, Lower Limestone Series, Hillhead Quarry, Beith. X36.

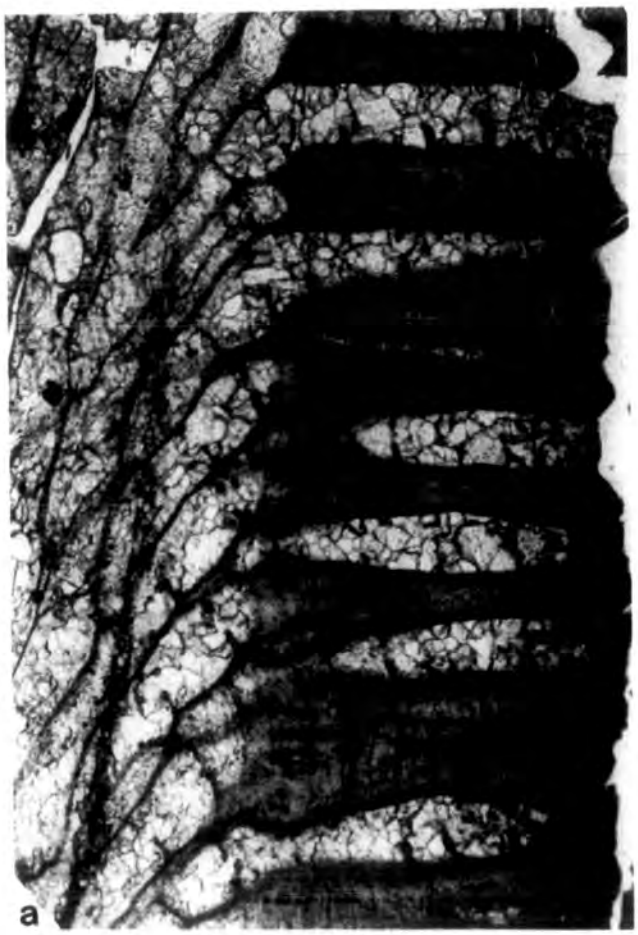
a

Plate 153. Stenodiscus tumida (Phillips)

fig.a. Colony form; the colony fragment with the growth tip shows quite regularly arranged maculae. NH G.155.81. Asbian, Lower Limestone Group, Redesdale Ironstone Shale, Ridsdale, Northumberland. X2.4.

fig.b. Zoarial surface detail showing well rounded autozooecial apertures, occasional exilazooecia, and large type A stylets situated at interapertural angles with closely spaced small type C stylets in uniserial rows between. NH G.155.82-7. Horizon and locality as for fig.a. X20.


a

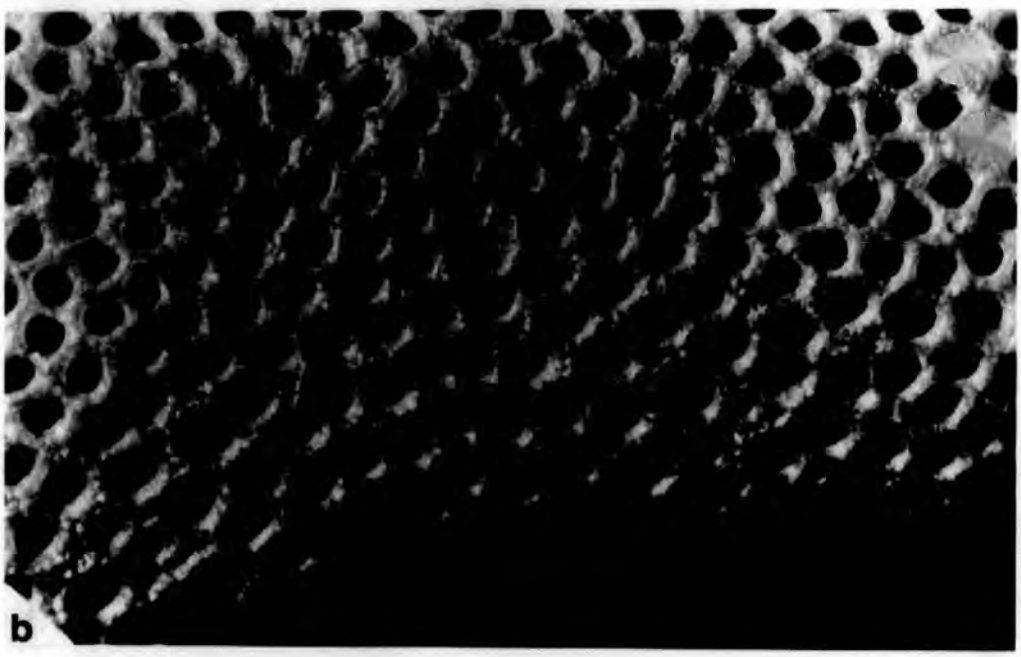
b

Plate 154. Stenodiscus tumida (Phillips)

fig.a. Zoarial surface detail showing the typically well rounded oval shape of autozooecial apertures. The macula is surrounded by enlarged autozooecial apertures. Type A stylets are situated at interapertural angles and closely spaced smaller type C stylets occur in uniserial rows between. NH G.155.82-7. Asbian, Lower Limestone Group, Redesdale Ironstone Shale, Ridsdale, Northumberland. X19.

fig.b. Zoarial surface detail showing a cluster of exilazooecia in the centre of the macula. NH G.155.81-11. Horizon and locality as for fig.a. X19.

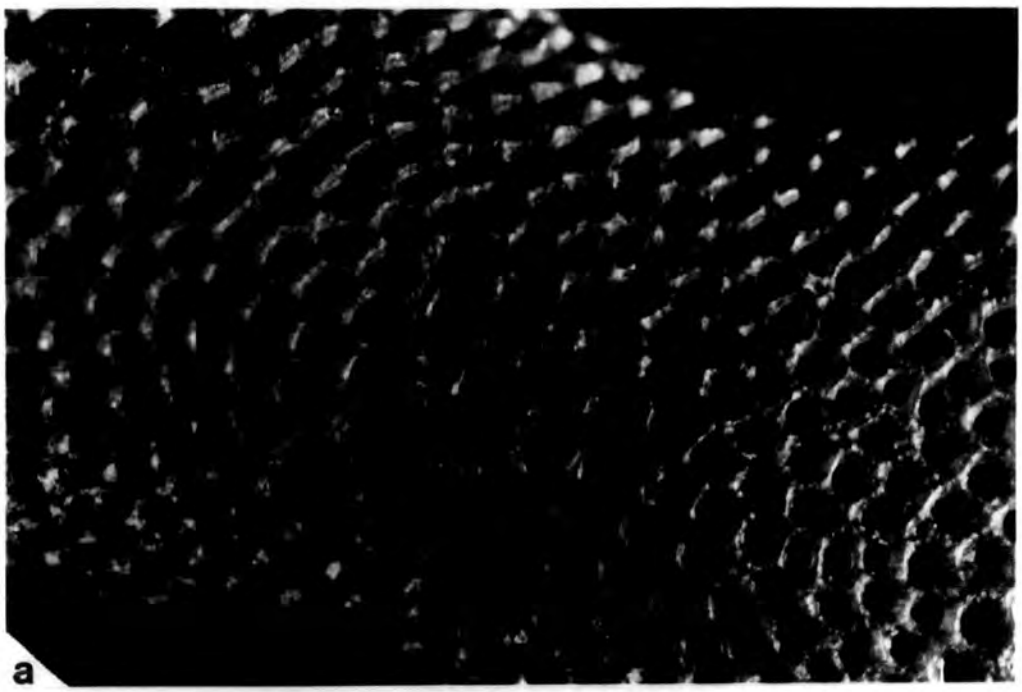

a

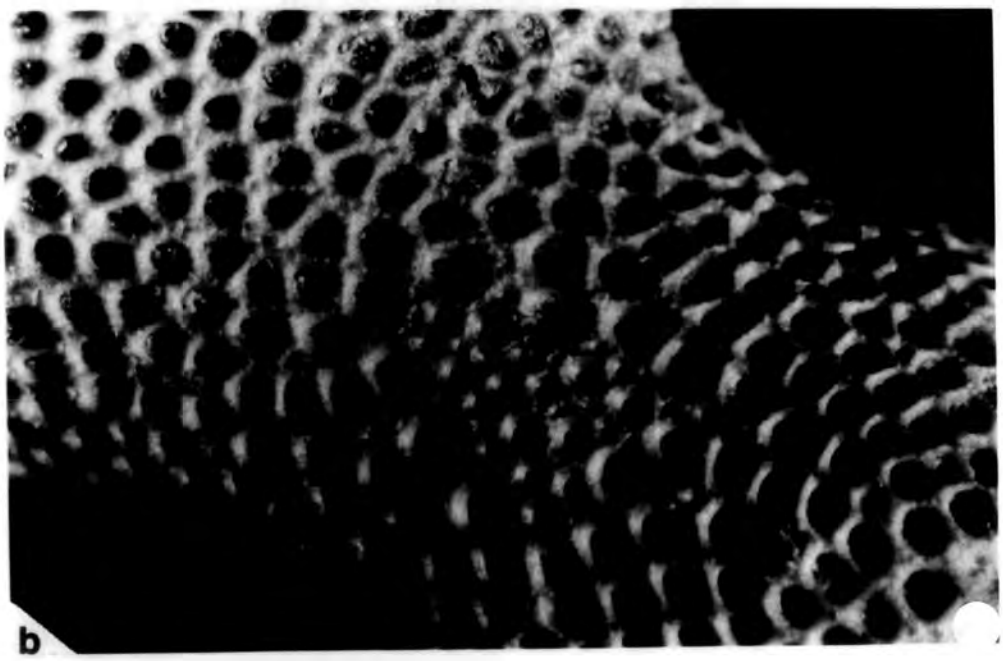

b

Plate 155. Stenodiscus tumida (Phillips)

fig.a. An erect ramose colony has developed from an adnate basal region which is encrusting a crinoid stem. NH G.155.80-13. Asbian, Lower Limestone Group, Redesdale Ironstone Shale, Ridsdale, Northumberland. X2.6.

fig.b. Detail of the growth front in the adnate basal portion of the colony shown in fig.a. X19.

a

b

Plate 156. Stenodiscus tumida (Phillips)

fig.a. Zoarial surface detail showing the regularity of budding in an adnate colony with autozooecia arranged in curved parallel lines. (The growth direction is left to right). NH G.155.83-2. Asbian, Lower Limestone Group, Redsedale Ironstone Shale, Ridsdale, Northumberland. X19.

fig.b. Shallow tangential section showing the well rounded autozooecial apertures and type A stylets situated at interzooecial angles. HM D.17. Horizon and locality as for fig.a. X51.

fig.c. Shallow tangential section through a macula showing the central area composed of a cluster of small exilazooecia. Autozooecia immediatly around the cluster are larger than average. HM D.17. Horizon and locality as for fig.a. X51.

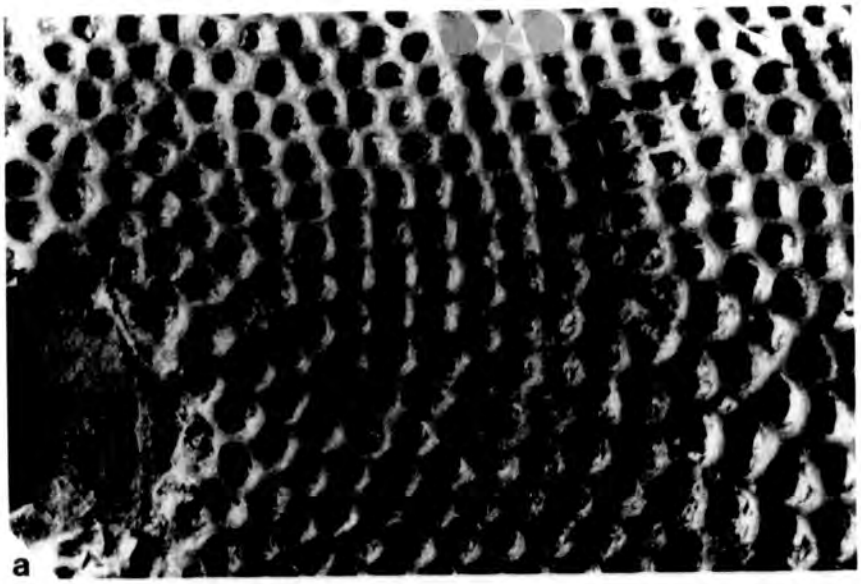

a

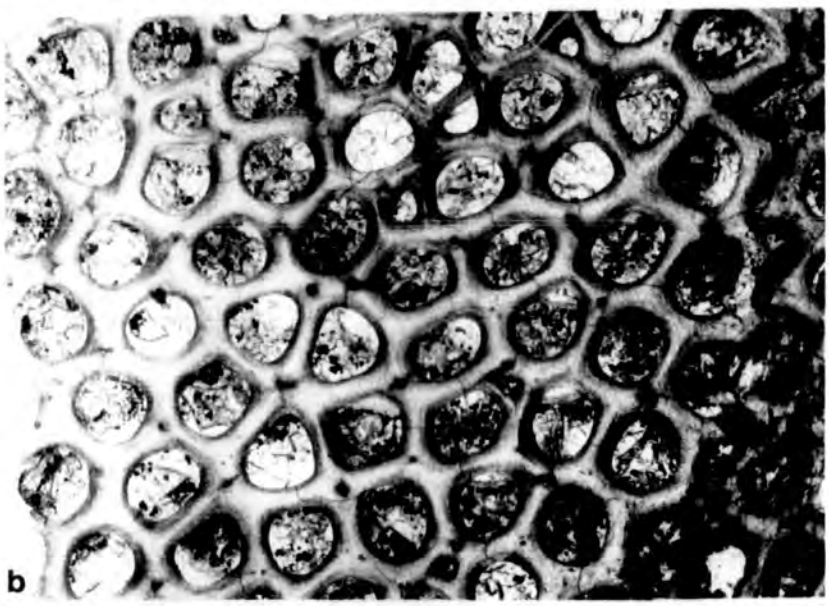

b

c

Plate 157. Stenodiscus tumida (Phillips)

fig.a. Shallow tangential section showing detail of type A stylets. The narrow central granular core is seen in the right hand stylet. HM D.17. Asbian, Lower Limestone Group, Redesdale Ironstone Shale, Ridsdale, Northumberland. X180.

fig.b. Longitudinal section showing the undulatory endozone interzooecial walls and the poorly moniliform exozone walls. Between three and four basal diaphragms cross autozooecial tubes. ABR 207. Horizon and locality as for fig.a. X15.

a

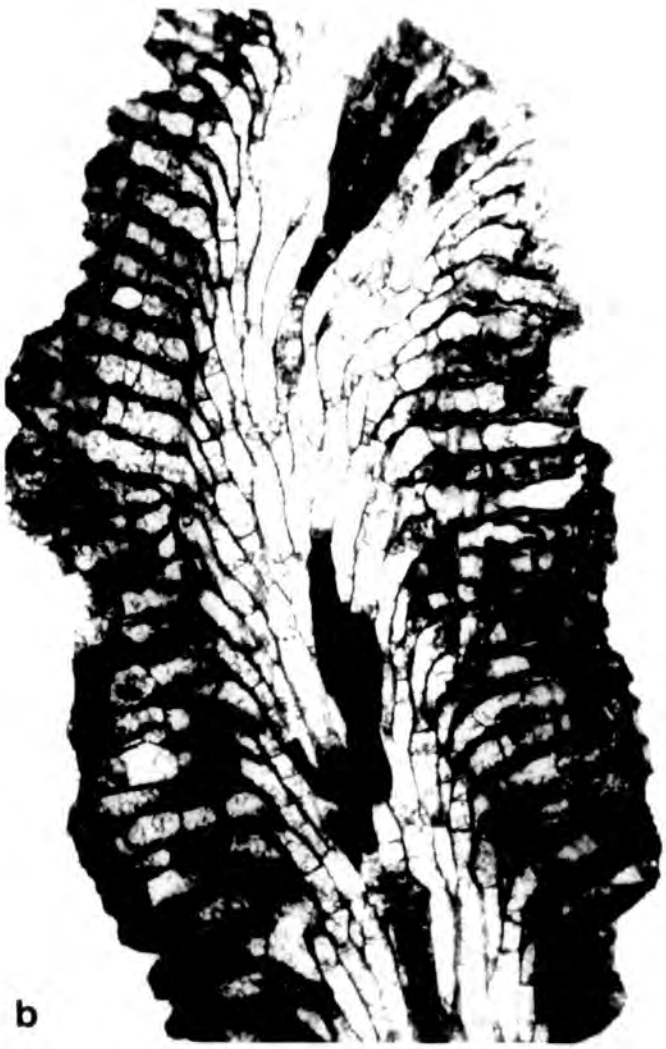

b

Plate 158. Stenodiscus tumida (Phillips)

fig.a. Longitudinal section showing the undulatory endozone interzooecial walls and the poorly moniliform exozone walls. ABR 202. Asbian, Lower Limestone Group, Redesdale Ironstone Shale, Ridsdale, Northumberland. X15.

fig.b. Longitudinal section showing the bulb-like nature of exozone interzooecial walls and the relatively narrow exozone region. ABR 205. Horizon and locality as for fig.a. X15.

a

b

Plate 159. Stenodiscus tumida (Phillips)

fig.a. Longitudinal section. AUGD 10642d. Asbian, Lower Limestone Group, Redesdale Ironstone Shale, Ridsdale, Northumberland.

fig.b. Longitudinal section showing detail of the exozone region. AUGD 10642d. Horizon and locality as for fig.a. X38.

a

b

Plate 160. Dyscritella miliaria (Nicholson)

fig.a. Neotype ; colony form- showing the bifurcation of a branch, and the fairly regular distribution of maculae. NH G.155.79-6. Asbian, Lower Limestone Group, Redesdale Ironstone Shale, Ridsdale, Northumberland. X4.0.

fig.b. Topotype; adnate zoarium encrusting a crinoid stem. NH G.155.79-3. Horizon and locality as for fig.a. X3.2.

fig.c. Topotype; zoarial surface detail showing the oval shape of autozooecial apertures and the abundant exilazooecia on interapertural walls. NH G.155.78-3. Horizon and locality as for fig.a. X19.

fig.d. Topotype; zoarial surface detail showing the circular to oval shape of autozooecial apertures and abundant exilazooecia on interapertural walls. HM D.11. Horizon and locality as for fig.a. X17.


a


b

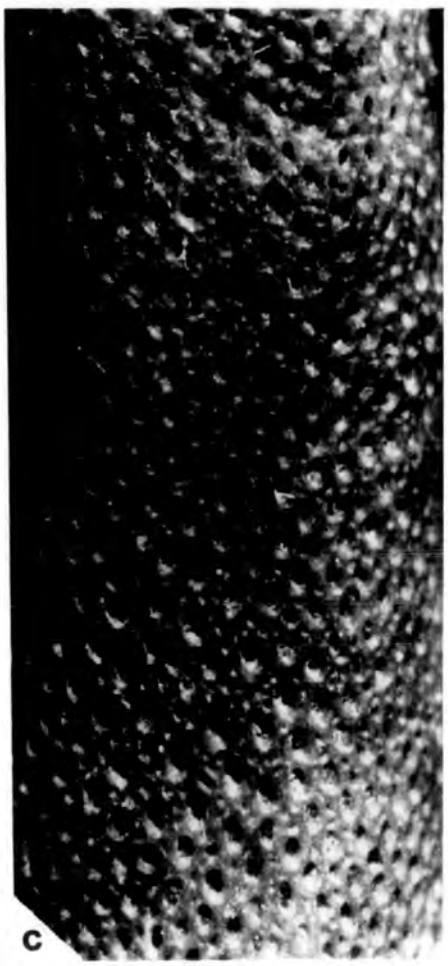
c


d

Plate 161. Dyscritella miliaria (Nicholson)

fig.a. Topotype; zoarial surface detail showing the fairly widely spaced autozooecial apertures, and abundant exilazooecia on interapertural walls. NH G.155.79-2. Asbian, Lower Limestone Group, Redesdale Ironstone Shale, Ridsdale, Northumberland. X20.

fig.b. Topotype; zoarial surface detail showing the circular shape of autozooecial apertures, which have low thin rounded peristome-like rims around them. HM D.11. Horizon and locality as for fig.a. X17.

fig.c. Topotype; zoarial surface detail showing the occurrence of a secondary overgrowth that has grown down in a proximal direction over the zoarial surface of an older portion of the parent branch. NH G.155.78-13. Horizon and locality as for fig.a. X20.

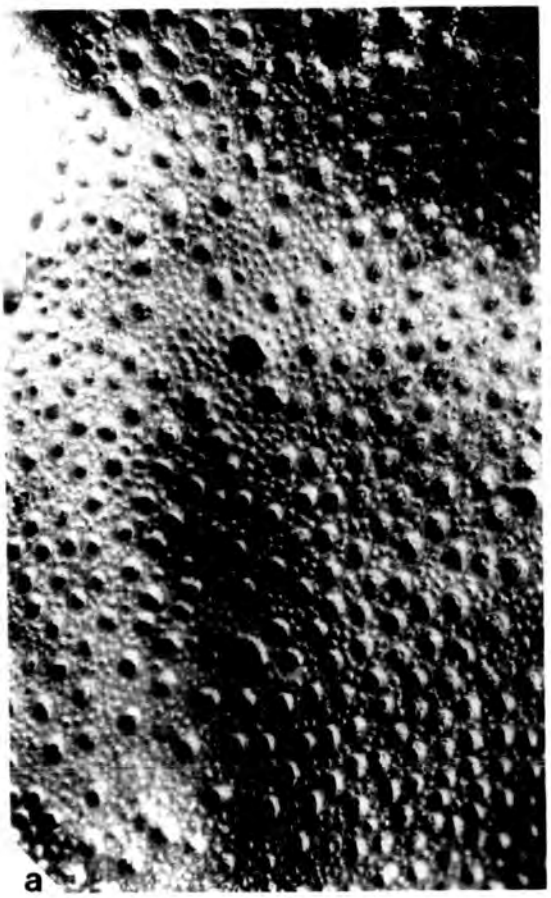
a

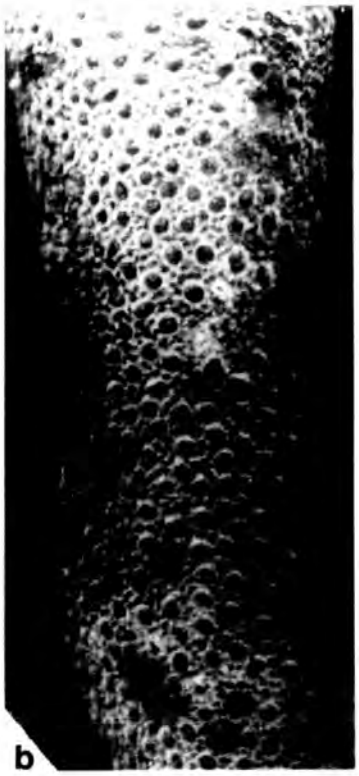
b


c

Plate 162. *Dyscritella miliaria* (Nicholson)

fig.a. Topotype; tangential section. HM D.10. Asbian, Lower Limestone Group, Redesdale Ironstone Shale, Ridsdale, Northumberland. X21.

fig.b. Topotype; transverse section. NH G.155.79-2. Horizon and locality as for fig.a. X10.


a

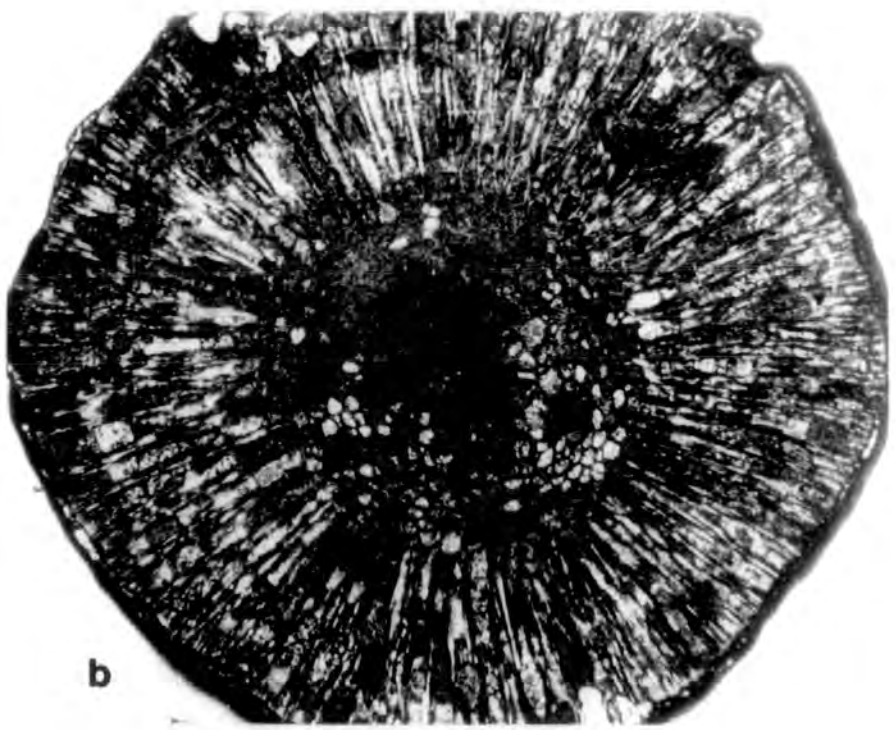
b

Plate 163. Dyscritella miliaria (Nicholson)

fig.a. Topotype; longitudinal section showing detail of autozooecial tubes, and exozone interzooecial walls. The development of exilazooecia is restricted to the exozone region. ABR 117. Asbian, Lower Limestone Group, Redesdale Ironstone Shale, Ridsdale, Northumberland. X23.

fig.b. Topotype; longitudinal section showing detail of the exozone region. Basal diaphragms occur in the exozone region of autozooecia and exilazooecia are restricted to the exozone region. Horizon and locality as for fig.a. X37.

a

b

Plate 164. *Dyscritella miliaria* (Nicholson)

fig.a. Topotype; longitudinal section showing detail of the exozone region. Exozone interzooecial walls are of fairly constant thickness to slightly undulatory (poorly moniliform). Autozooecial tubes are crossed by basal diaphragms in the exozone region. HM D.15. Asbian, Lower Limestone Group, Redesdale Ironstone Shale, Ridsdale, Northumberland. X37.

fig.b. As for fig.a. X37.


a


b

Plate 165. Vesicular Tissues

fig.a. Detail of vesicular tissues showing their simple bilamellar composition- with a lower primary thin dark grey granular layer on which lies a thicker pale grey secondary granular-prismatic layer. The individual curved plates are stacked on one another and rest on the upper layer of adjacent vesicles. ABWB 315. Brigantian, Middle Limestone Group, Morpeth Scar Limestone, West Burton. X135.

fig.b. As for fig.a. X230.

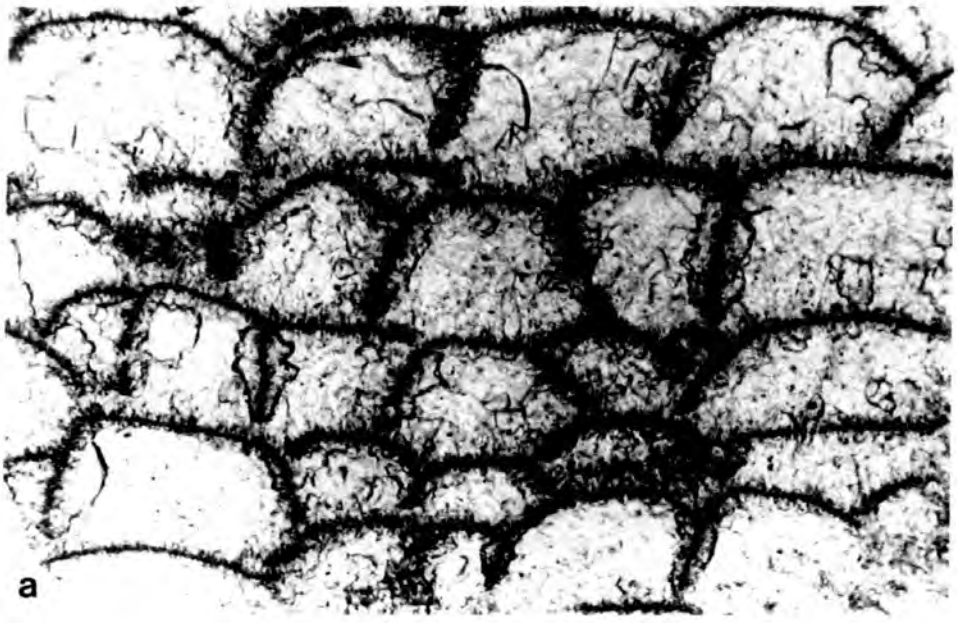

a

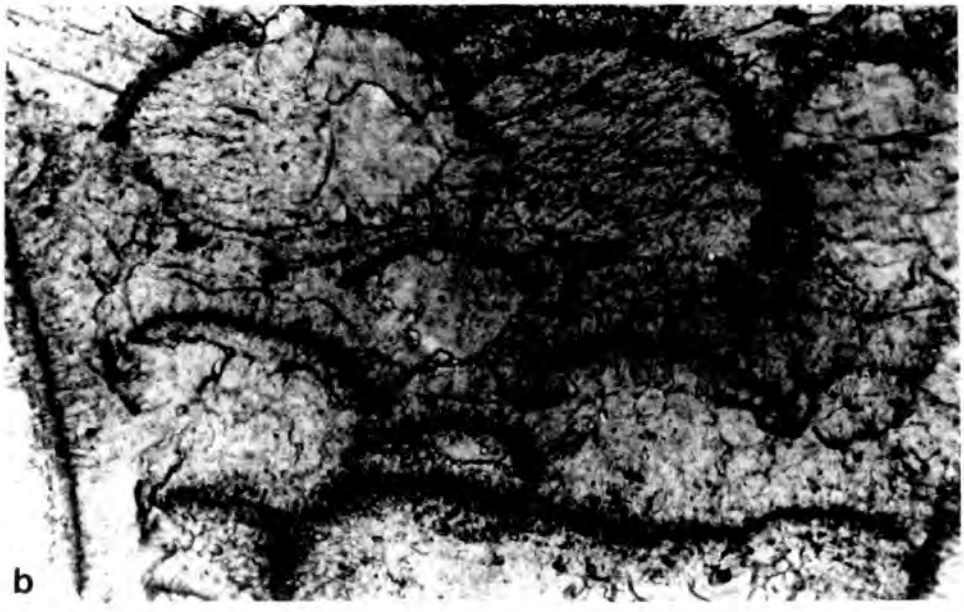

b

Plate 166. Fistulipora incrustans (Phillips)

fig.a. Large foliaceous colony. DUGD 8760-1. Chadian, Scandal Beck Limestone, Riggend Farm, Ravenstondale, Cumbria. XO.6.

fig.b. Thin unilamellar colony encrusting a crinoid stem. NH G.155.84-2. Asbian, Lower Limestone Group, Redesdale Ironstone Shale, Ridsdale, Northumberland. X2.4.

fig.c. Zoarial surface detail showing the regular arrangement of monticules. NH G.155.85-7. Horizon and locality as for fig.a. X3.4.

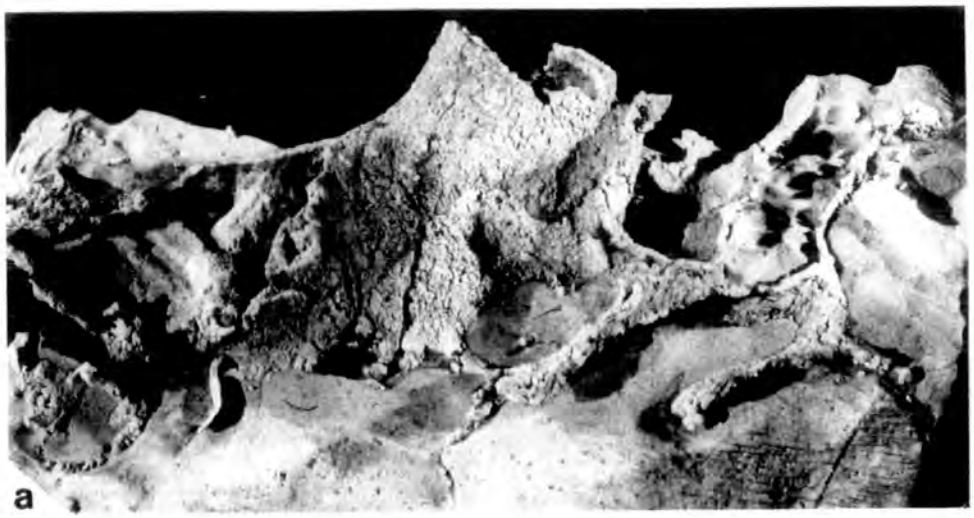

a

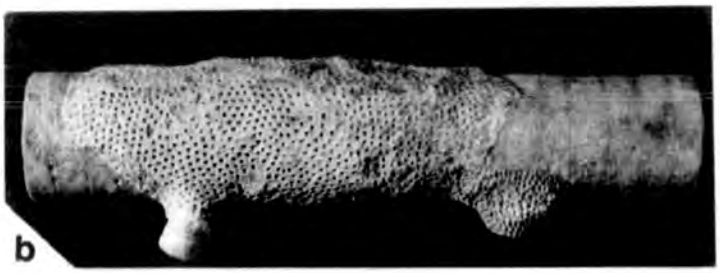

b

c

Plate 167. Fistulipora incrustans (Phillips)

fig.a. Immature colony showing the radial arrangement of autozooecia around the monticular-like growth origin. Autozooecia are immature and are orientated at oblique angles to the zoarial surface. ABP 88. Asbian, Alston Group, Fifth Limestone, Penruddock. X19.

fig.b. Zoarial surface detail showing the low very poorly developed lunaria of autozooecial apertures and the radial arrangement of apertures around a monticule. NH G.155.87-3. Asbian, Lower Limestone Group, Redesdale Ironstone Shale, Ridsdale, Northumberland. X20.

fig.c. Zoarial surface detail showing closely spaced autozooecial apertures which are separated by small well faceted vesicles. In the bottom right is a monticule, whose summit is devoid of apertures and around which autozooecial apertures are radially arranged. NH G.155.87-3. Horizon and locality as for fig.a. X19.

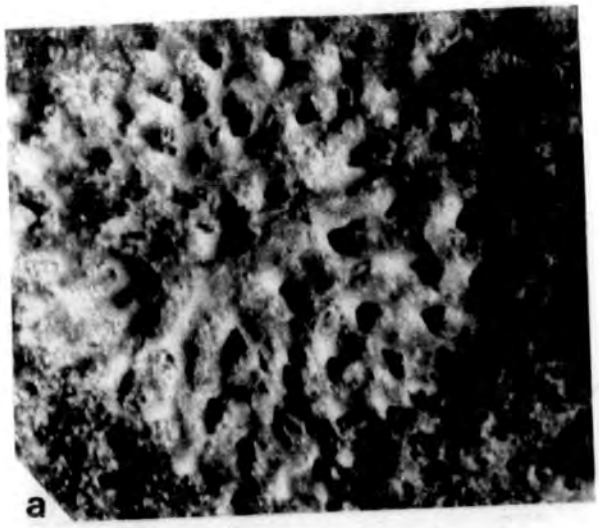

a

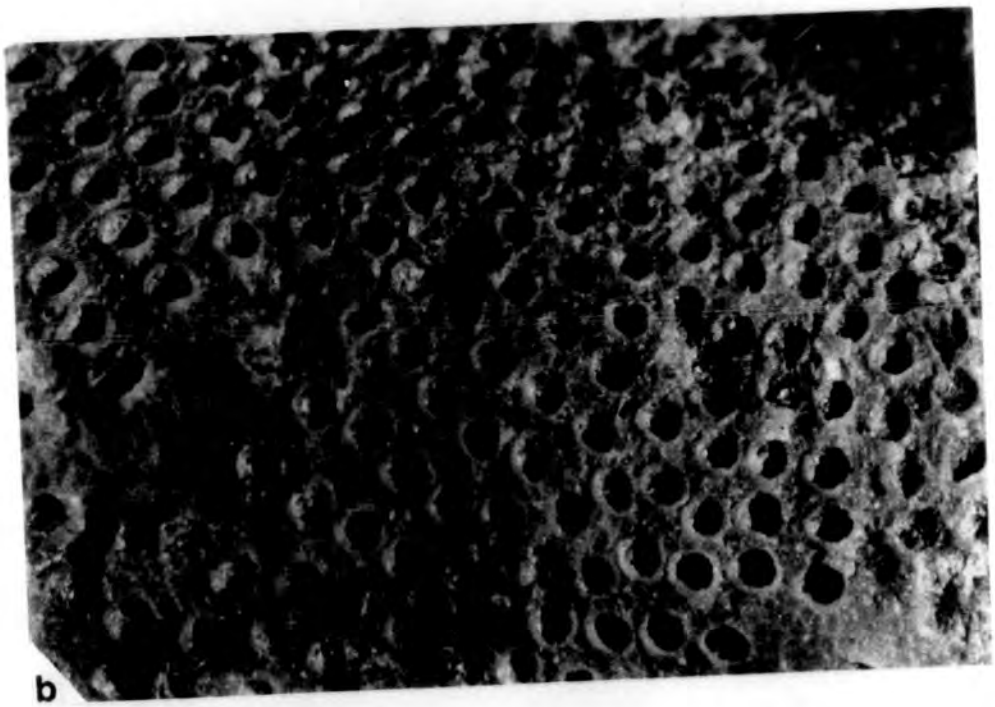

b

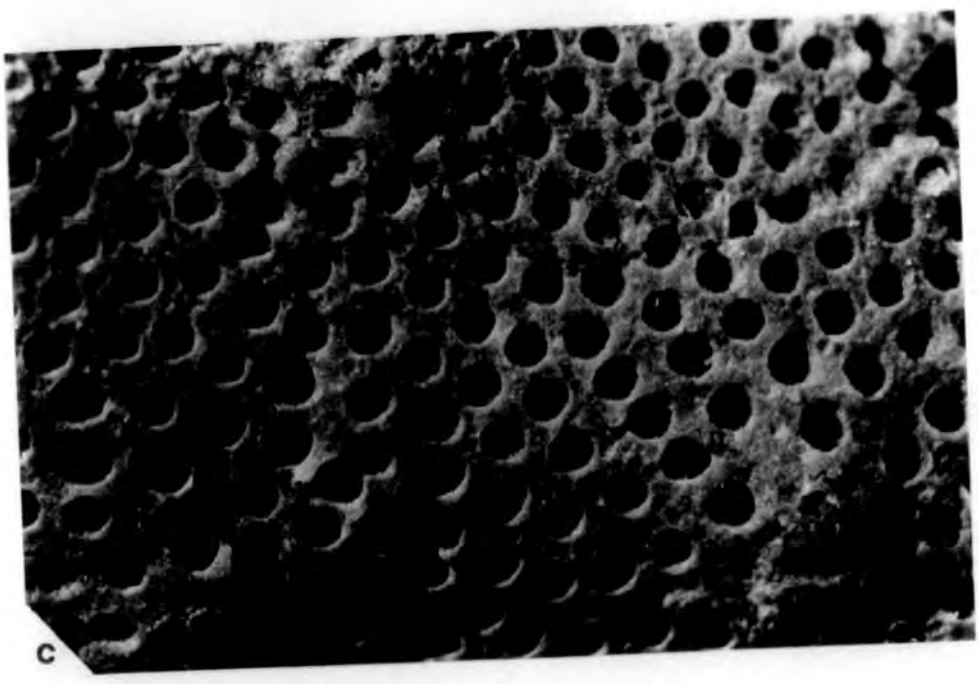

c

Plate 168. Fistulipora incrustans (Phillips)

fig.a. Zoarial surface detail showing the short crescent shaped low collar-like lunaria of autozooecial apertures. ABP 87. Asbian, Alston Group, Fifth Limestone, Penruddock. X13.

fig.b. S.E.M. photomicrograph showing zoarial surface detail with autozooecial apertures isolated by thin walled well faceted vesicles. ABP 86. Horizon and locality as for fig.a. X40.

fig.c. S.E.M. photomicrograph showing internal morphological detail in a broken colony fragment. ABCL 23. Asbian, Calp Shale-Upper Limestone, Carrick Lough. X9.0.

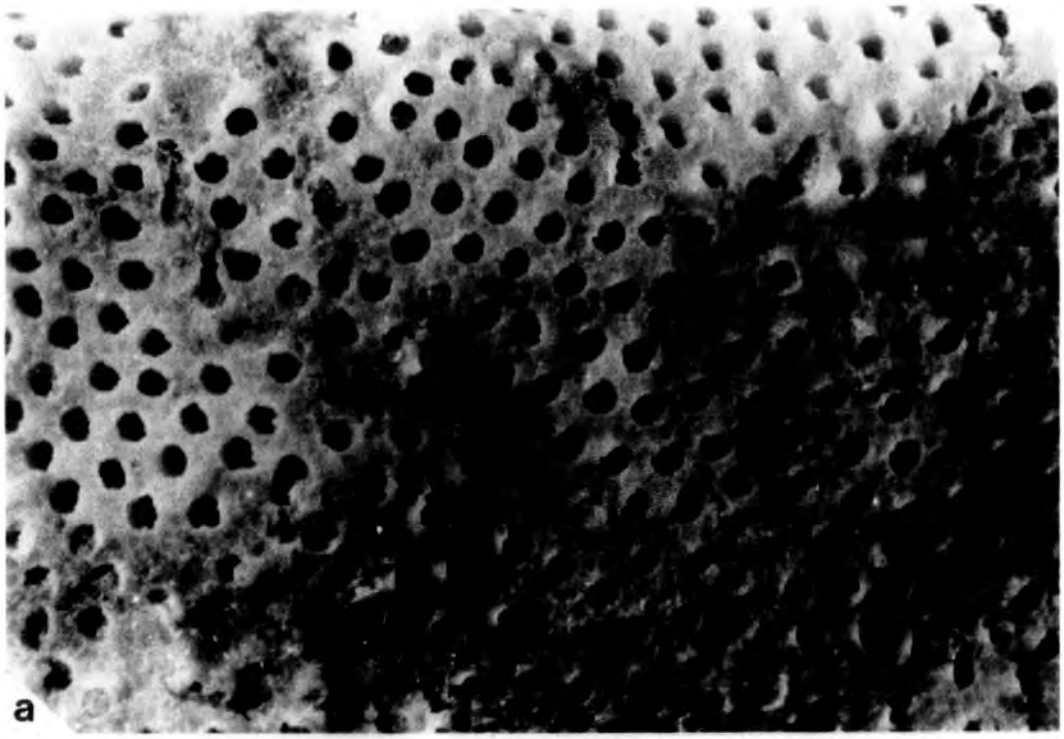
a

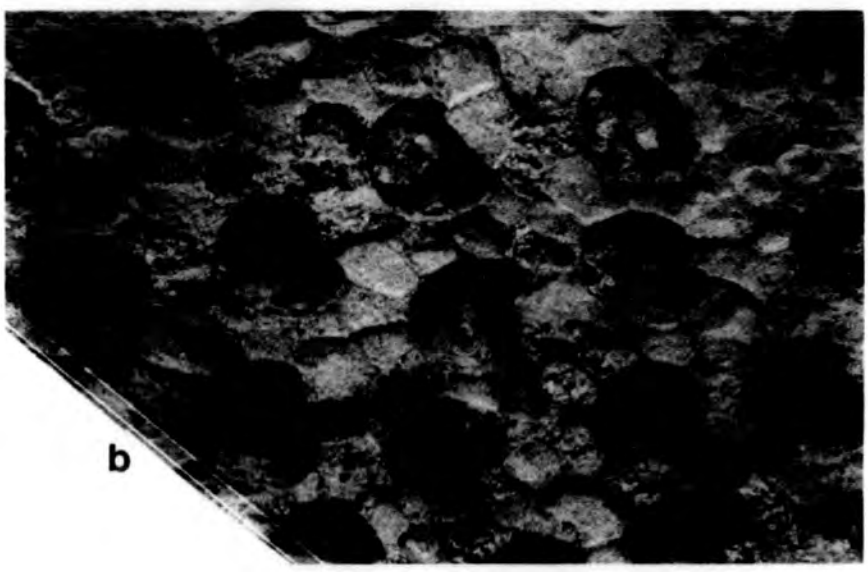
b

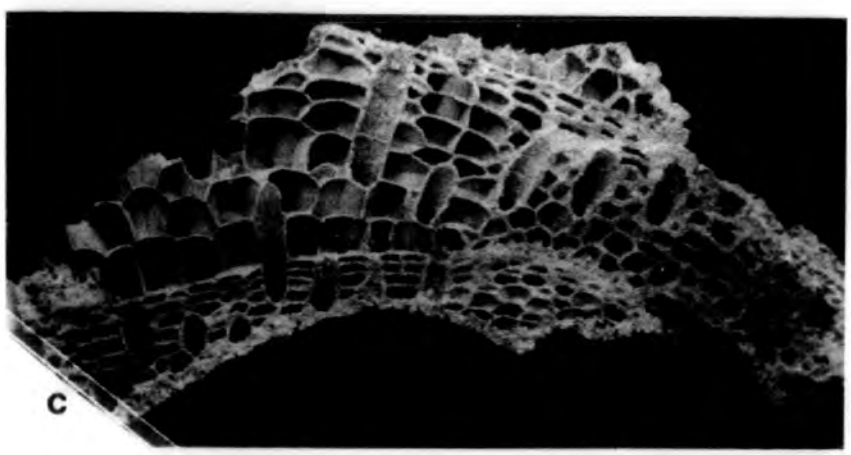
c

Plate 169. Fistulipora incrustans (Phillips)

fig.a. S.E.M. photomicrograph of a broken silicified colony fragment showing internal morphological detail. Basal diaphragms are seen in autozooecial tubes. ABCL 23. Asbian, Calp Shale-Upper Limestone, Carrick Lough. X28.

fig.b. Longitudinal section of a silicified colony fragment. ABCL 23. Horizon and locality as for fig.a. X10.

fig.c. Shallow tangential section showing the circular to oval shape of autozooecia, their short crescent shaped lunaria and the small well faceted vesicles that isolate autozooecia. HM D.15. Asbian, Lower Limestone Group, Redesdale Ironstone Shale, Ridsdale, Northumberland. X34.

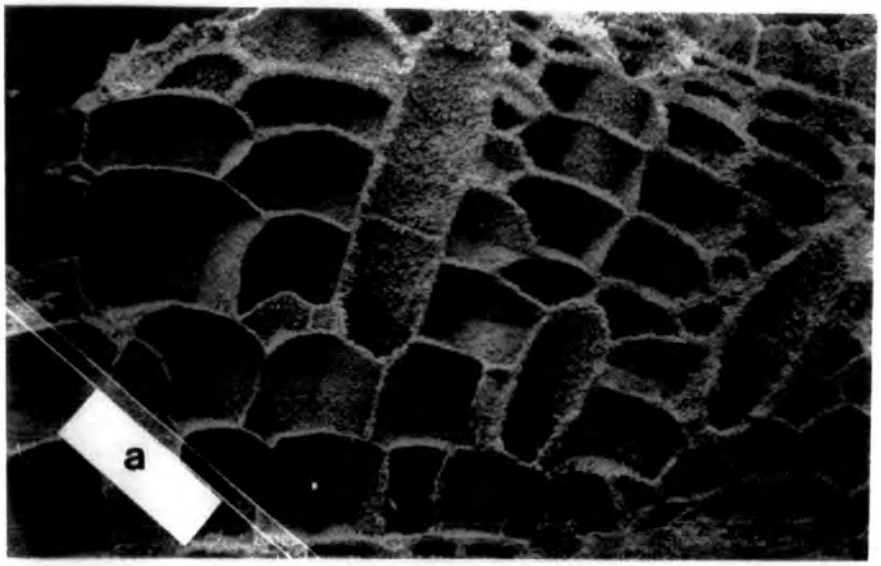
a

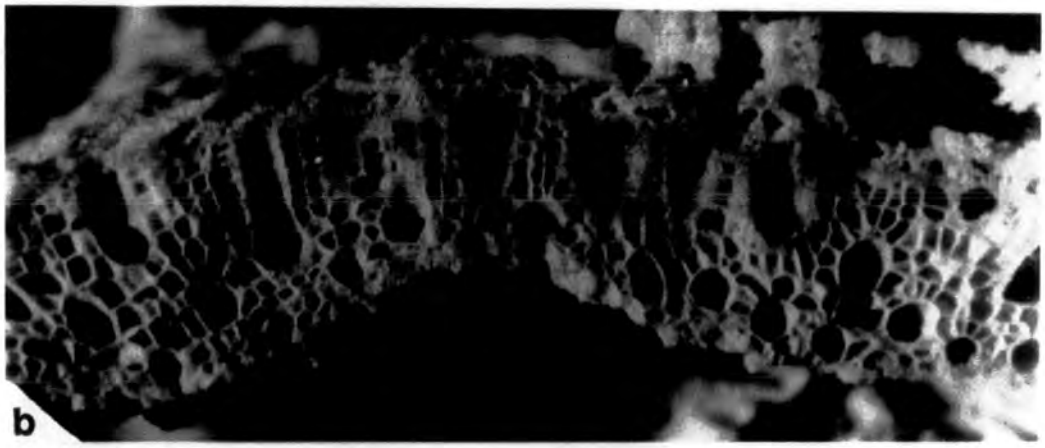
b

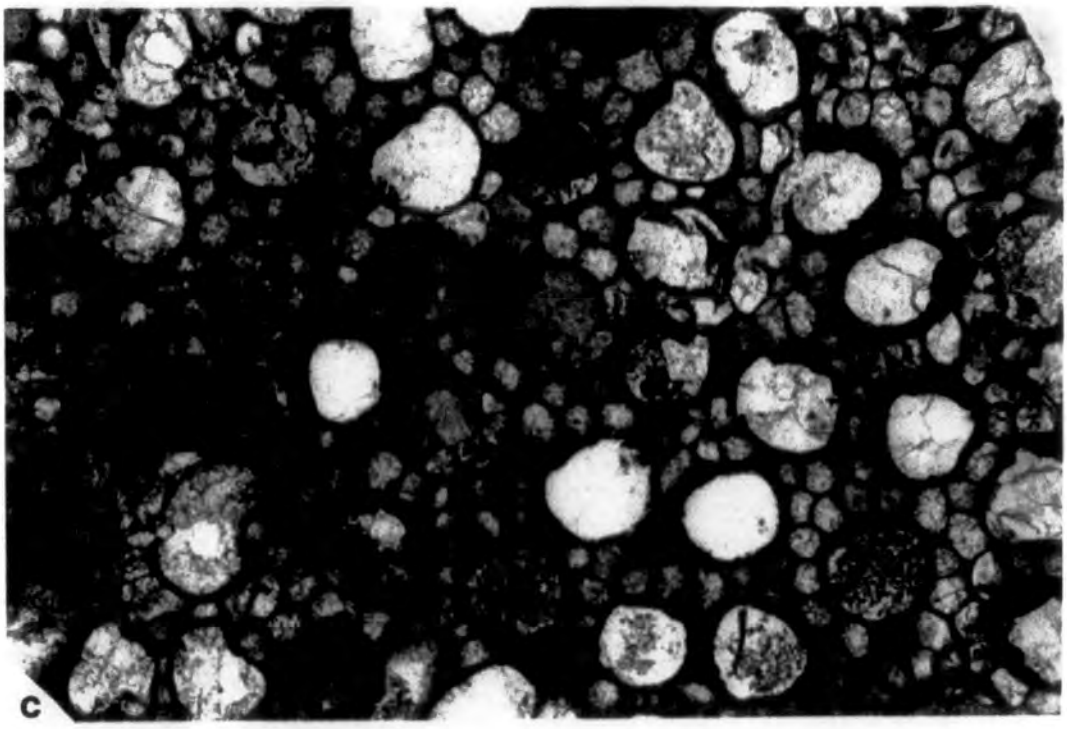
c

Plate 170. Fistulipora incrustans (Phillips)

Fig.a. Shallow tangential section. ABHR 123. Arnsbergian, Shales above the Main Limestone, Hurst, N. Yorkshire. X37.

fig.b. Shallow tangential section showing the short and poorly developed proximal lunarial portions of autozooecial walls, also the thin walled well faceted vesicles isolating autozooecia. HM D.15. Asbian, Lower Limestone Group, Redsedale Ironstone Shale, Ridsdale, Northumberland. X93.

fig.c. Longitudinal section through a colony, one autozooecium is crossed by five closely spaced basal diaphragms. HM D.15. Horizon and locality as for fig.b. X37.

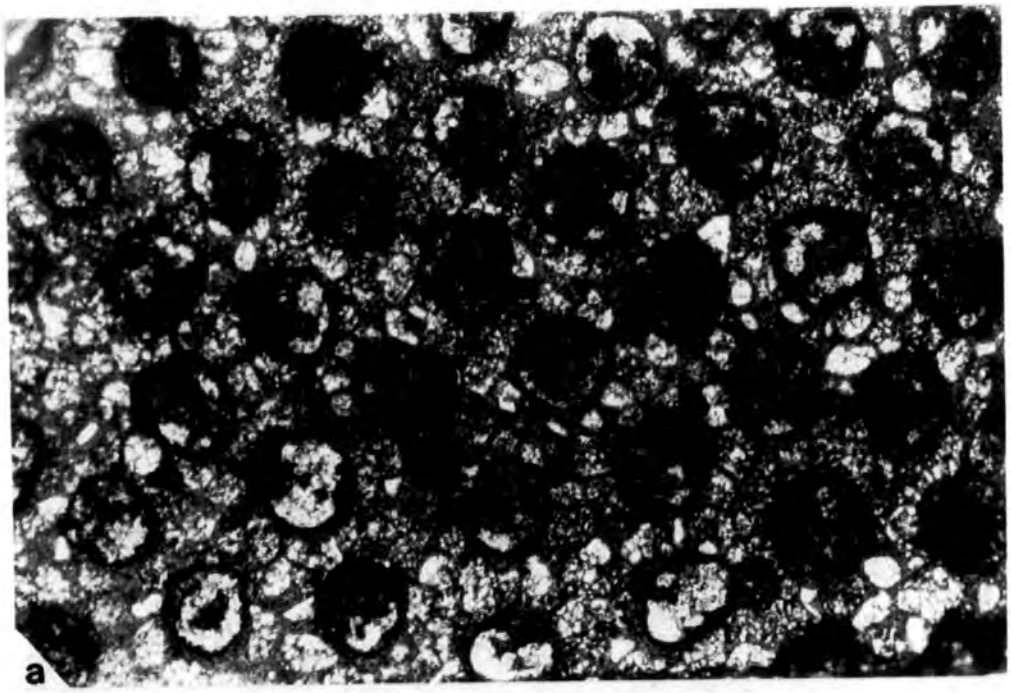
a

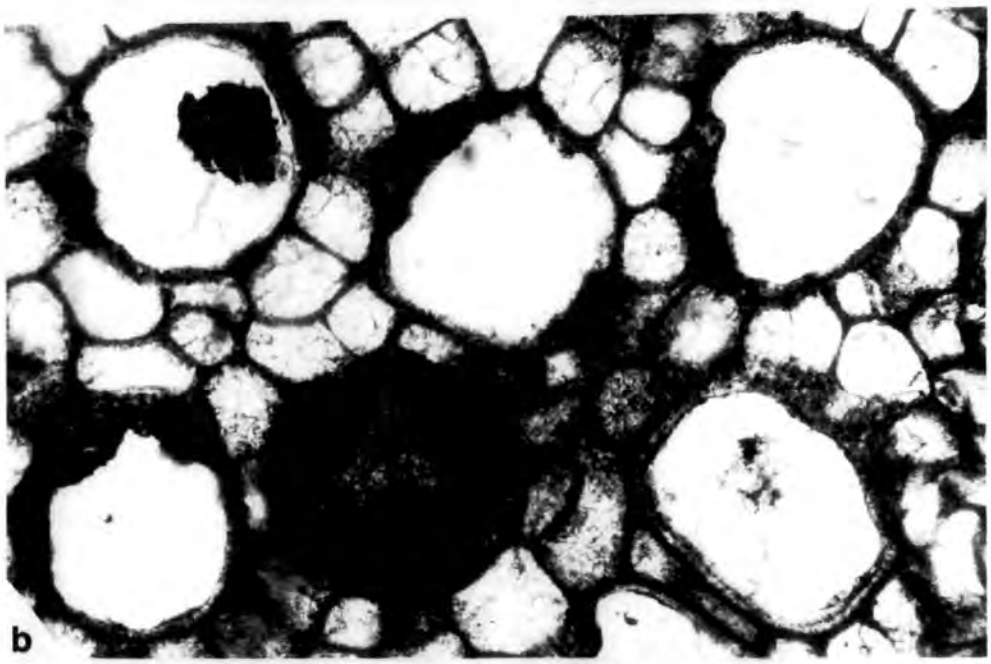
b


c

Plate 171. Fistulipora incrustans (Phillips)

fig.a. Longitudinal section through a colony encrusting the superstructure of the fenestrate Hemitrypa hibernica McCoy. ABRE 236. Holkerian, Orton Group, Seventh Limestone, Redmain, Cumbria. X37.

fig.b. As for fig.a. X37.

fig.c. Longitudinal section through a colony encrusting a branch of a stenoporid trepostome. ABWB 223. Brigantian, Middle Limestone Group, Morpeth Scar Limestone, West Burton. X37.

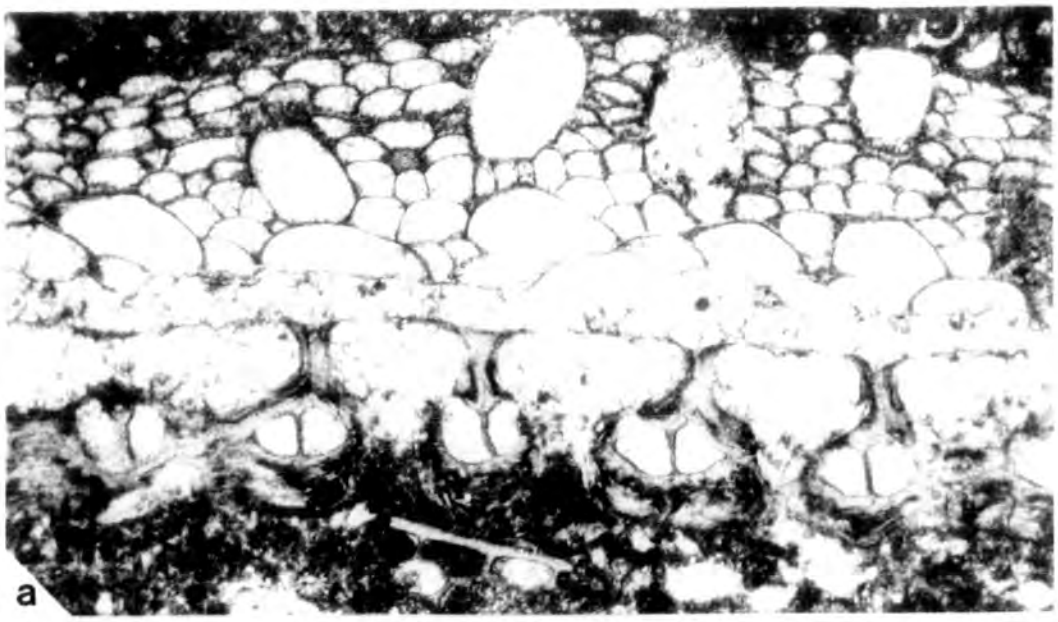
a


b

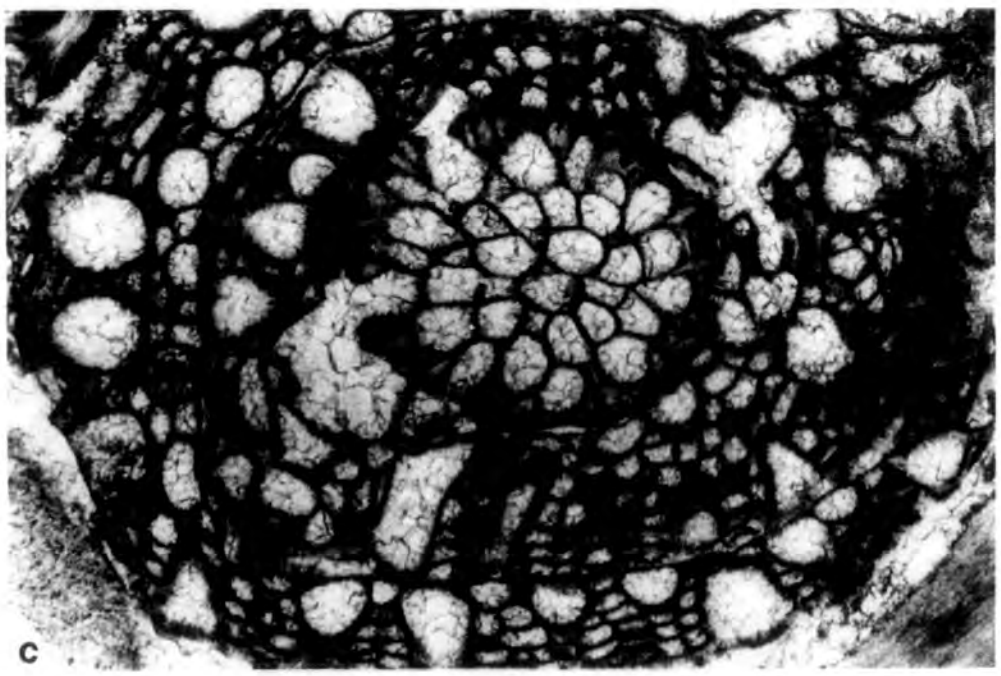
c

Plate 172. *Fistulipora incrustans* (Phillips)

fig.a. Longitudinal section through a colony encrusting the branch of a stenoporid trepostome. ABWB 200. Brigantian, Middle Limestone Group, Morpeth Scar Limestone, West Burton. X36.

fig.b. Longitudinal section through a colony encrusting the branch of a fenestellid. ABWB 315. Horizon and locality as for fig.a. X8.5.

fig.c. As for fig.b. X39.

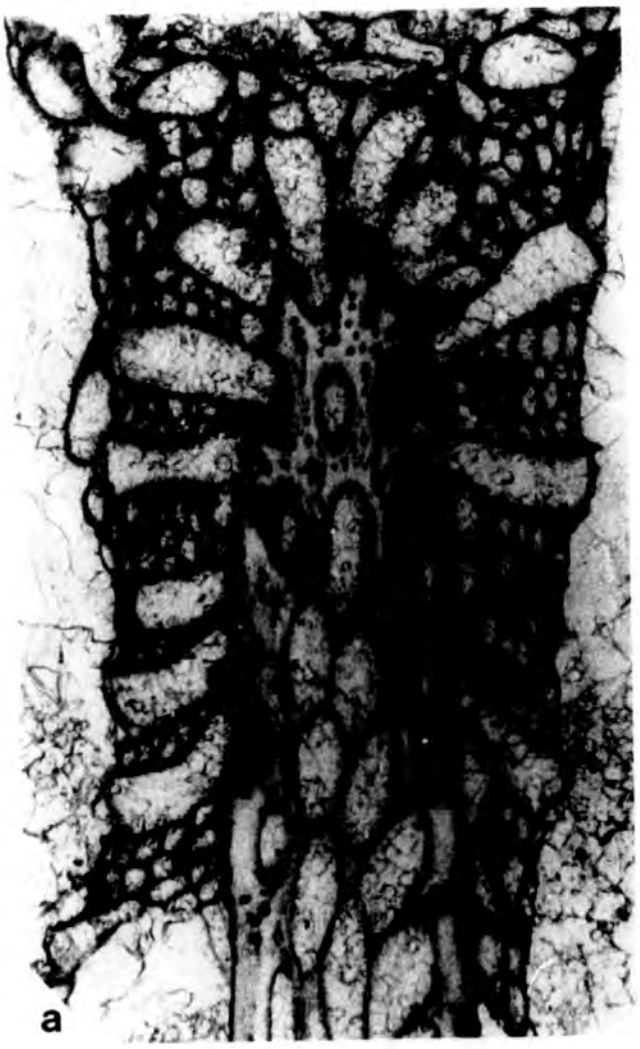
a

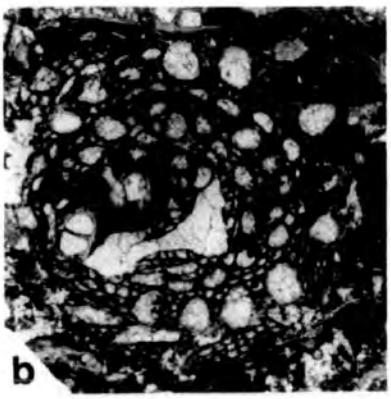
b

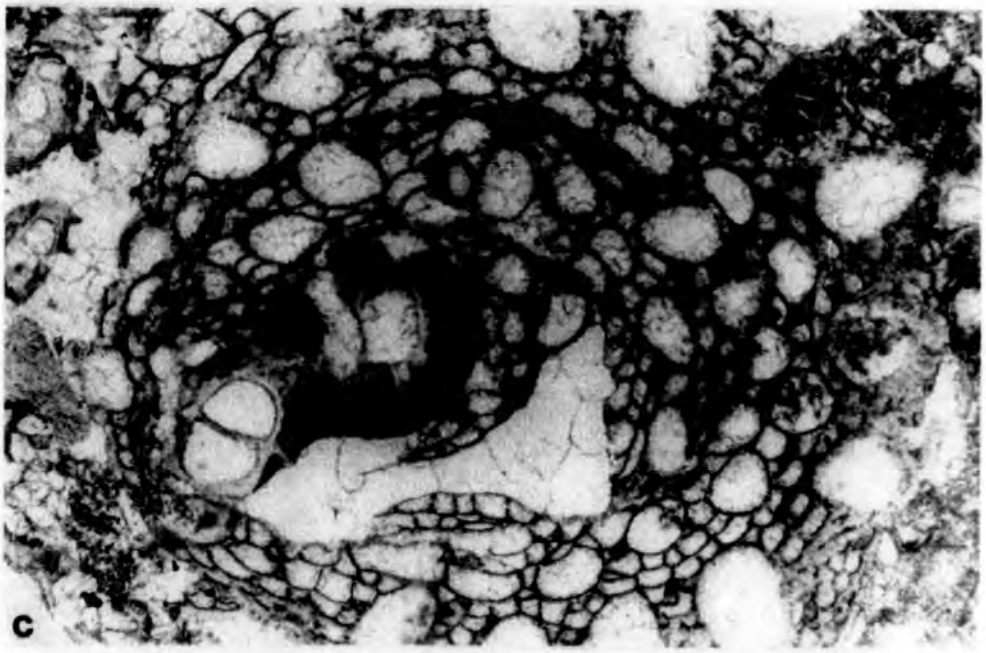
c

Plate 173. Eridopora beilensis Perkins and Perry

fig.a. Zoarial surface detail showing the growing edge of a colony, also the hood-like lunaria of more mature autozooecial apertures. ABHR.1E.1. Arnsbergian, Shales above the Main Limestone, Hurst. X16.

fig.b. Zoarial surface detail showing autozooecial apertures with their well developed hood-like lunaria. Apertures are radially arranged around a monticule whose centre is devoid of apertures. ABHR.1E.2. Horizon and locality as for fig.a. X16.

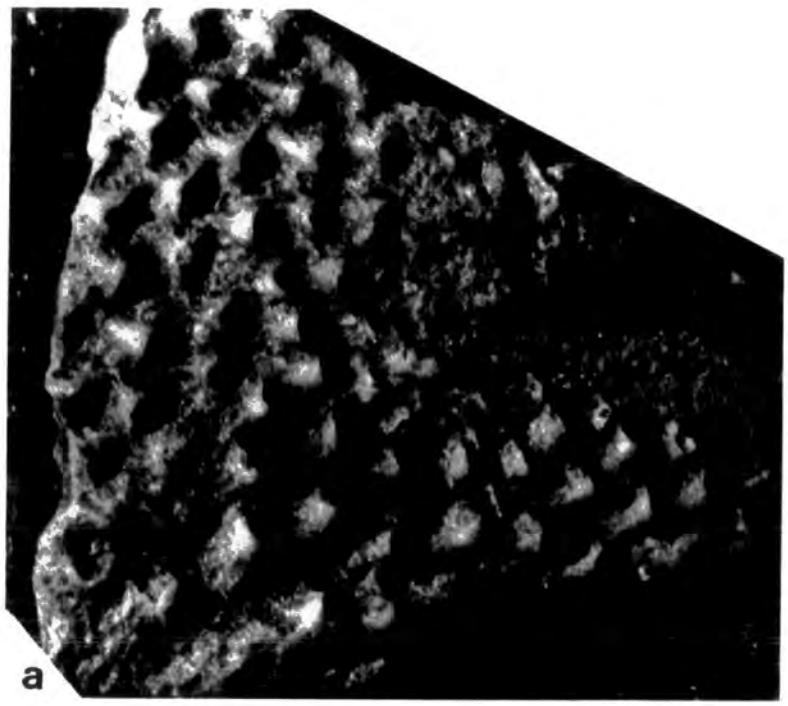
a

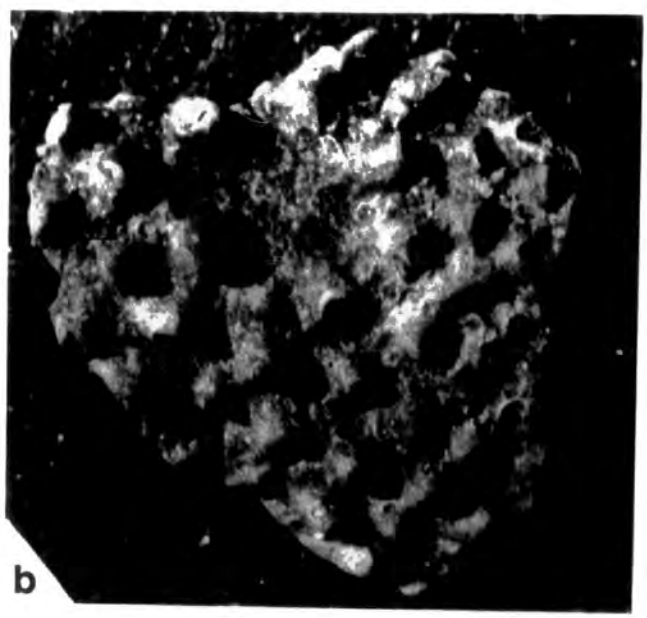
b

Plate 174. Eridopora beilensis Perkins and Perry.

fig.a. Shallow tangential section showing the pyriform shape of autozooecial apertures with their thick proximal lunarial walls, also the thin walled and well faceted angular shape of vesicles. ABHR 250. Arnsbergian, Shale above the Main Limestone, Hurst. X37.

fig.b. As for fig.a. X69.

fig.c. Shallow tangential section showing the pyriform shape of autozooecia. ABHR 101. Horizon and locality as for fig.a. X65.

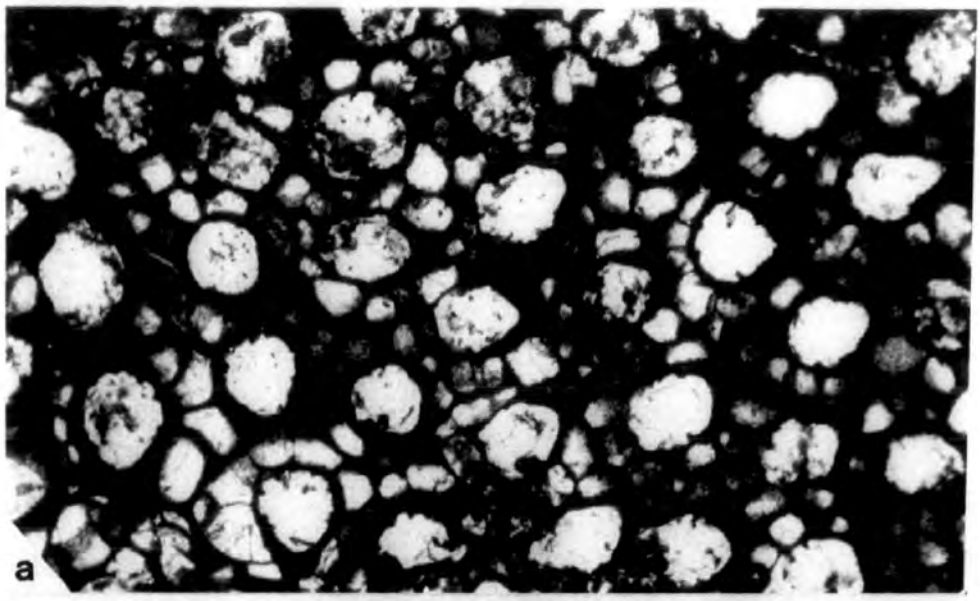
a

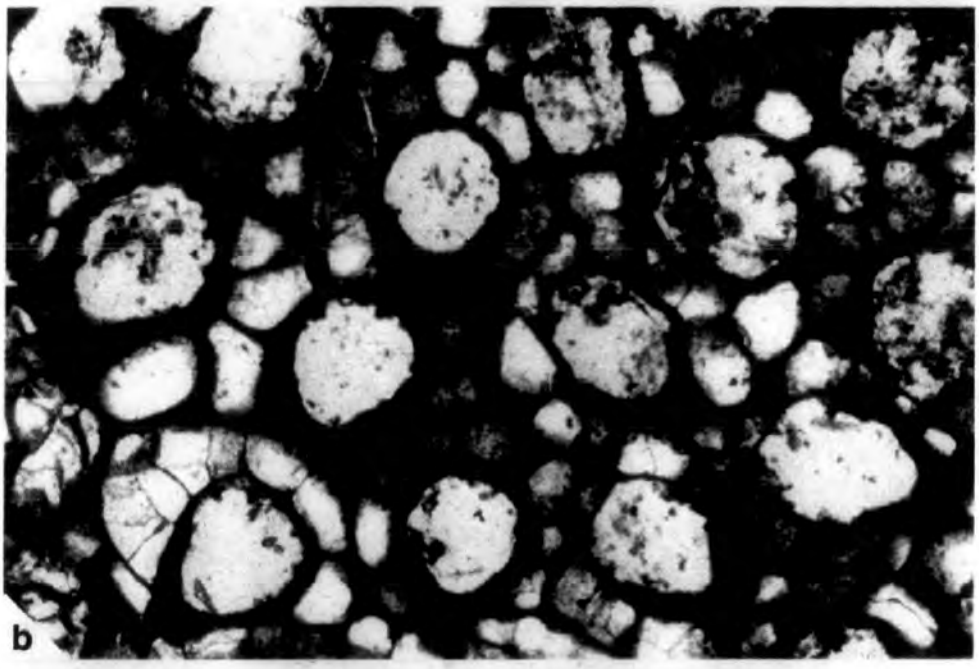
b

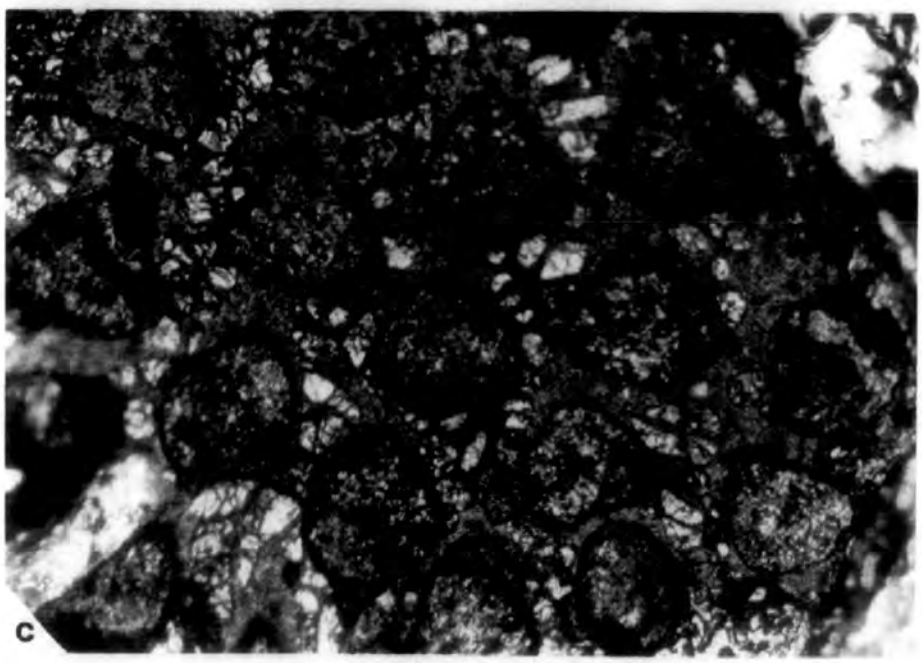
c

Plate 175. *Eridopora beilensis* Perkins and Perry

fig.a. Longitudinal section through a colony encrusting a brachiopod spine. ABHR 250. Arnsbergian, Shales above the Main Limestone, Hurst. X16.

a

Plate 176. Eridopora macrostoma Ulrich

fig.a. Zoarial surface detail showing the extremely closely spaced autozooecial apertures with their prominent helmet-like lunaria, also the poorly developed vesicles. ABHR 6. Arnsbergian, Shales above the Main Limestone, Hurst. X13.

fig.b. As for fig.a. X20.

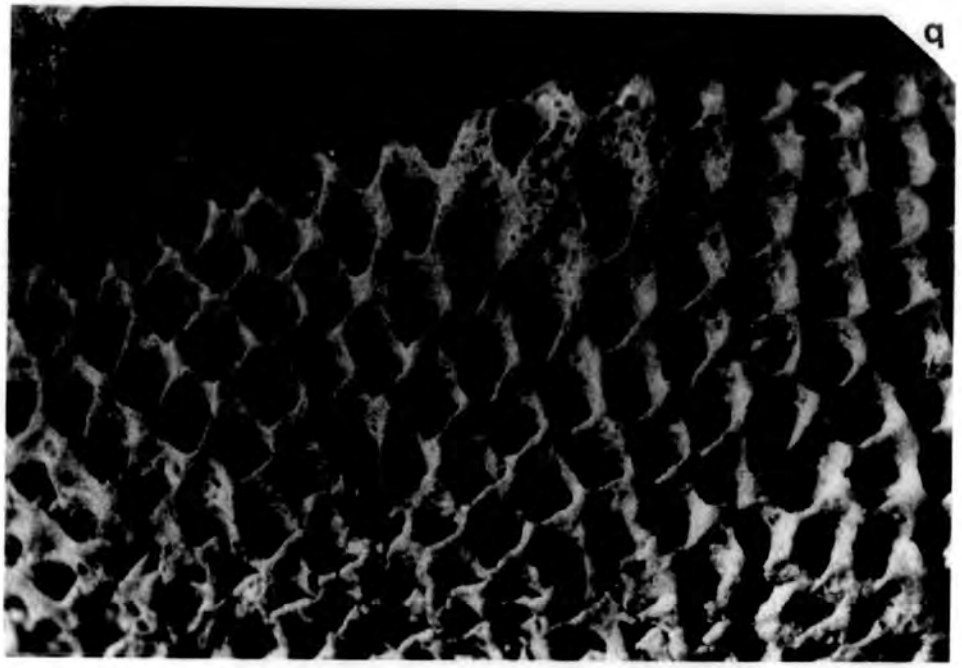
q

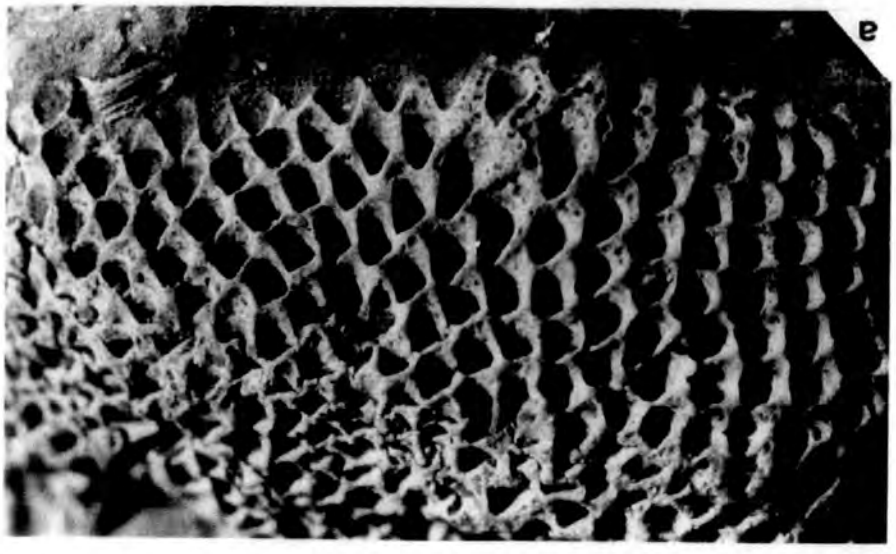
e

Plate 177. *Eridopora macrostoma* Ulrich

fig.a. Shallow tangential section showing the close spacing and pyriform shape of autozooecia. The proximal lunarial walls of autozooecia are very thick, and autozooecia are so closely spaced that very small vesicles are only occasionally developed between them. ABHR 116. Arnsbergian, Shales above the Main Limestone, Hurst. X68.

fig.b. As for fig.a. ABHR 115. X68.

fig.c. Shallow tangential section showing the thin walled and well faceted form of vesicles. ABHR 112. Horizon and locality as for fig.a. X82.

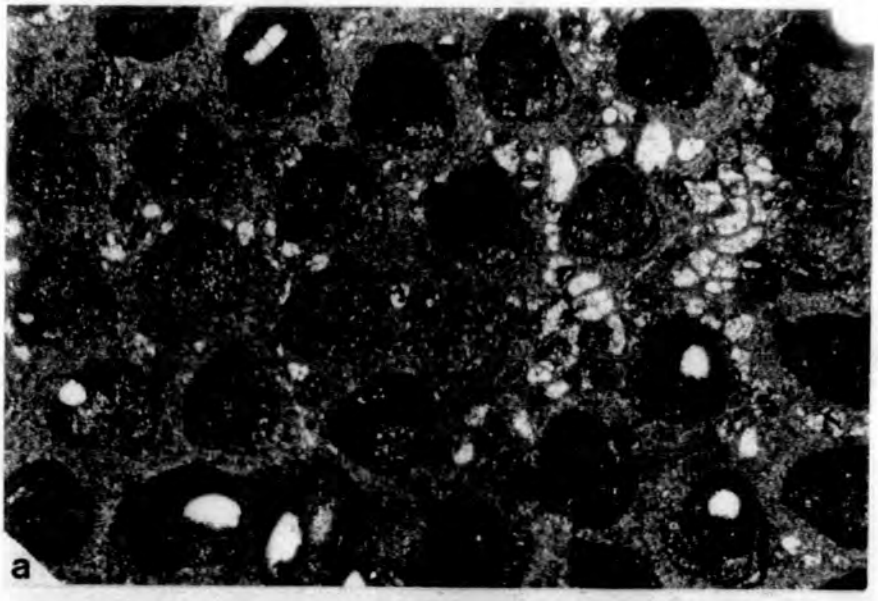
a

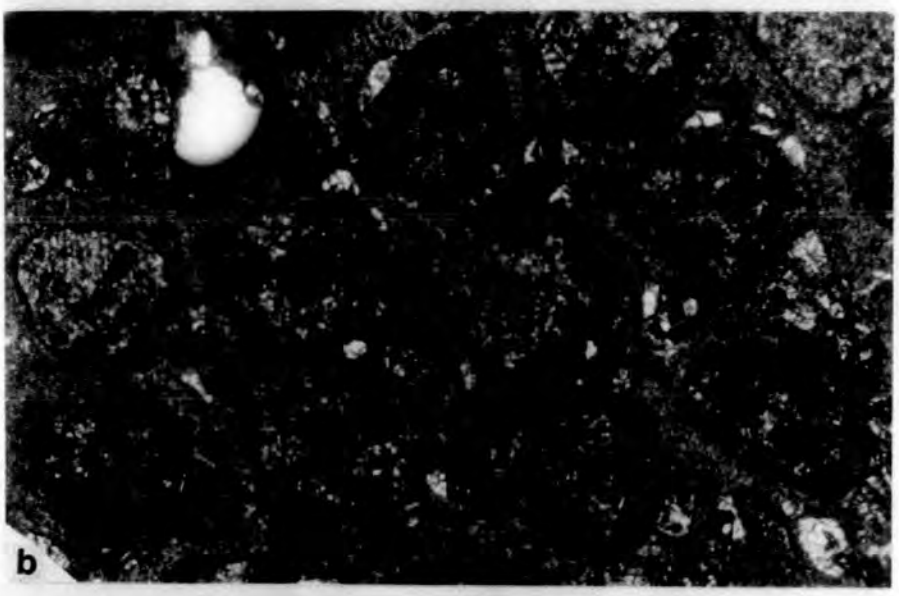
b

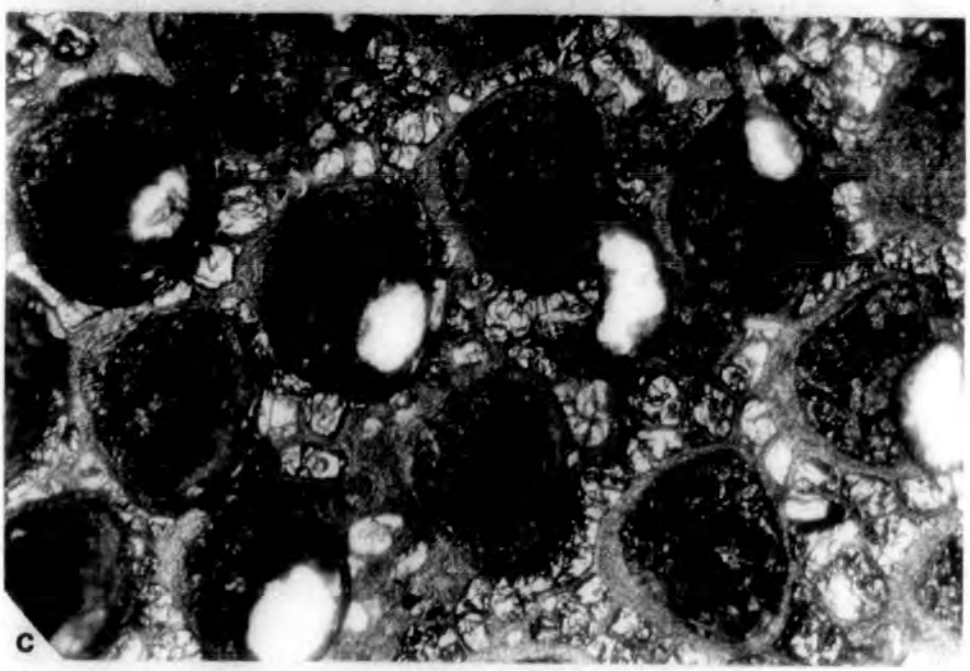
c

Plate 178. Eridopora macrostoma Ulrich

fig.a. Longitudinal section showing the bilamellar nature of vesicles, also their decrease in size and better vertical stacking towards the zoarial surface. ABHR 253. Arnsbergian, Shales above the Main Limestone, Hurst. X100.

fig.b. Longitudinal section. ABHR 257. Horizon and locality as for fig.a. X44.


a


b

Plate 179. Goniocladia cellulifera (Etheridge, Jun.)

fig.a. Colony form. YM 1983/657F. Carboniferous Limestone, Settle. X2.

fig.b. Zoarial surface detail. HM D.119. Brigantian, Lower Limestone Group, Hosie Limestone, Hairmyres, E. Kilbride. X21.

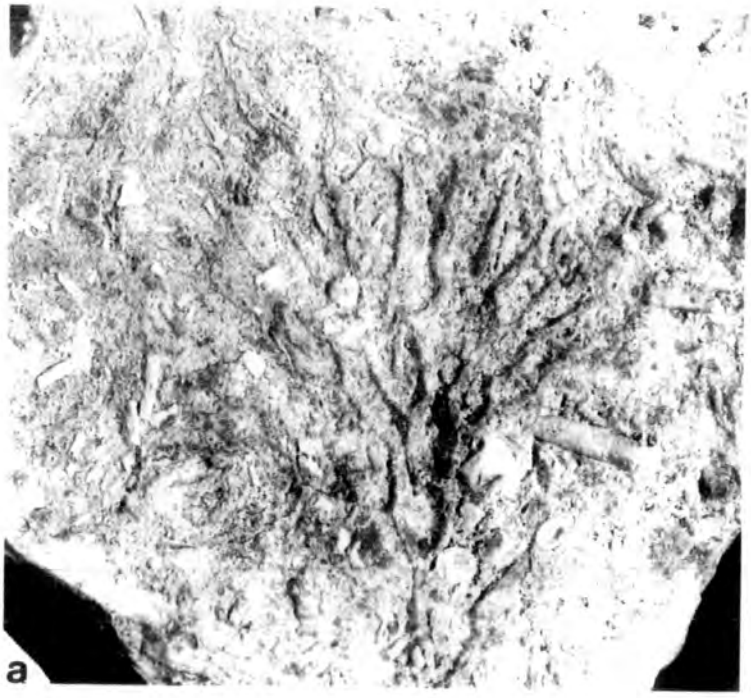

a

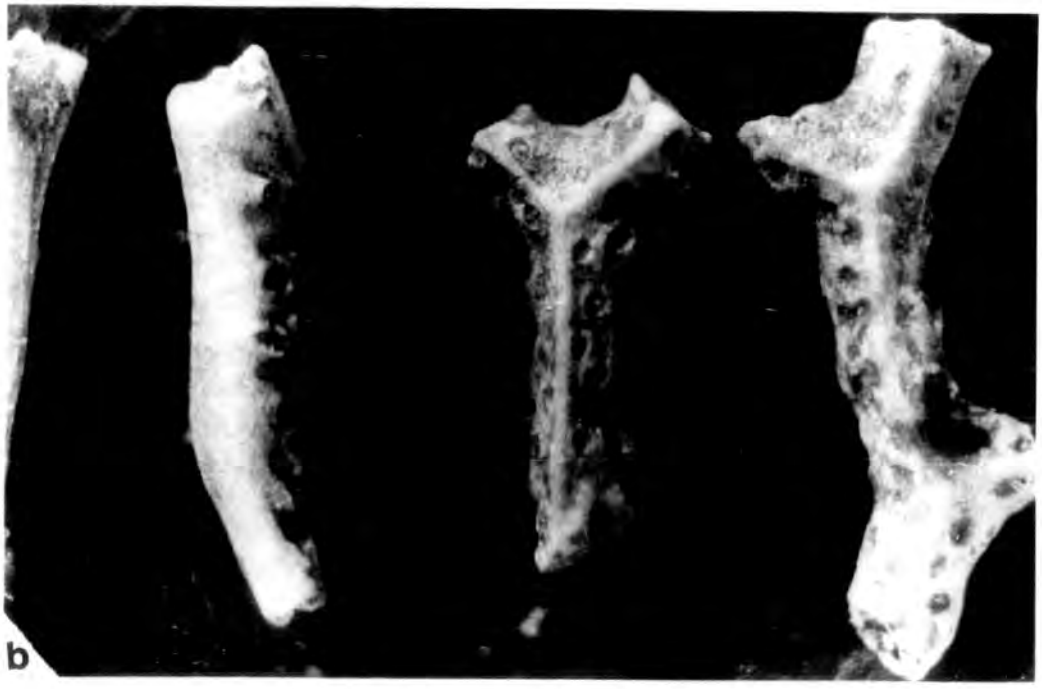

b

Plate 180. Gonoicladia cellulifera (Etheridge.Jun,)

fig.a. Shallow tangential section showing the compound structure of lateral and distal autozooecial walls, also the occurrence of thin walled well faceted vesicles. ABWB 287. Brigantian, Middle Limestone Group, Morpeth Scar Limestone, West Burton, Wensleydale. X46.

fig.b. Shallow tangential section. ABWB 319. Horizon and locality as for fig,a. X45.

fig.c. Topotype; shallow tangential section showing the compound structure of lateral and distal autozooecial walls. BMNH D.32637. Brigantian, Gair, near Carluke. X110.

b

c

Plate 181. Goniocladia cellulifera (Etheridge, Jun.)

fig.a. Topotype; shallow tangential section showing the compound structure of lateral and distal autozooecial walls. BMNH D.32637. Brigantian, Gair, near Carluke. X 276.

figs b to d are transverse sections through branches showing the pyriform shape of branches, also the compound median wall that completly bissects branches. Vesicles are only developed close to the median wall where autozooecia are recumbent, elsewhere the bilamellar structure of vesicles is only occasionally developed and most are infilled with stereom.

fig.b. ABWB 309. Brigantian, Middle Limestone Group, Morpeth Scar Limestone, West Burton, Wensleydale. X46

fig.c. ABWB 309. Horizon and locality as for fig.b. X46.

fig.d. ABWB 275. Horizon and locality as for fig.b. X46.


a


b


c


d

Plate 182. Goniocladia cellulifera (Etheridge, Jun.)

fig.a. Transverse section. ABWB 275. Brigantian, Middle Limestone Group, Morpeth Scar Limestone, West Burton, Wensleydale. X46.

fig.b. Longitudinal section showing internal morphological details. Autozooecia are developed from both sides of a straight compound median wall. Initially recumbent they diverge out towards the zoarial surface at constantly increasing angles. Vesicles are only developed close to the median wall elsewhere they are infilled with stereom. ABWB 267. Brigantian, Middle Limestone Group, Morpeth Scar Limestone, West Burton, Wensleydale. X46.

fig.c. Longitudinal section showing the compound structure of autozooecial walls. The median wall is compound. Vesicles have a simple bilamellar structure and are only developed close to the median wall elsewhere they are infilled with stereom. ABWB 267. Horizon and locality as for fig.b. X110.


a


b


c

Plate 183. Goniocladia cellulifera (Etheridge, Jun.)

fig.a. Longitudinal section showing the compound structure of distal autozooecial walls. ABWB 312. Brigantian, Middle Limestone Group, Morpeth Scar Limestone, West Burton, Wensleydale. X110.

fig.b. Topotype; longitudinal section. BMNH D.32637. Brigantian, Gair, near Carluke. X46.

a

b

Plate 184. *Goniocladia cellulifera* (Etheridge, Jun.)

fig.a. Longitudinal section through a large colony fragment showing branch bifurcation and fusion. ABWB 324. Brigantian, Middle Limestone Group, Morpeth Scar Limestone, West Burton, Wensleydale. X10.

a

Plate 185. Goniocladia cellulifera(Etheridge,Jun.)

fig.a. Topotype; longitudinal section showing the compound structure of autozooecial walls. BMNH D.32637. Brigantian, Gair, near Carluke. X276.

fig.b. Topotype; longitudinal section showing the compound structure of the median wall. BMNH D.32637. Horizon and locality as for fig.a. X276.

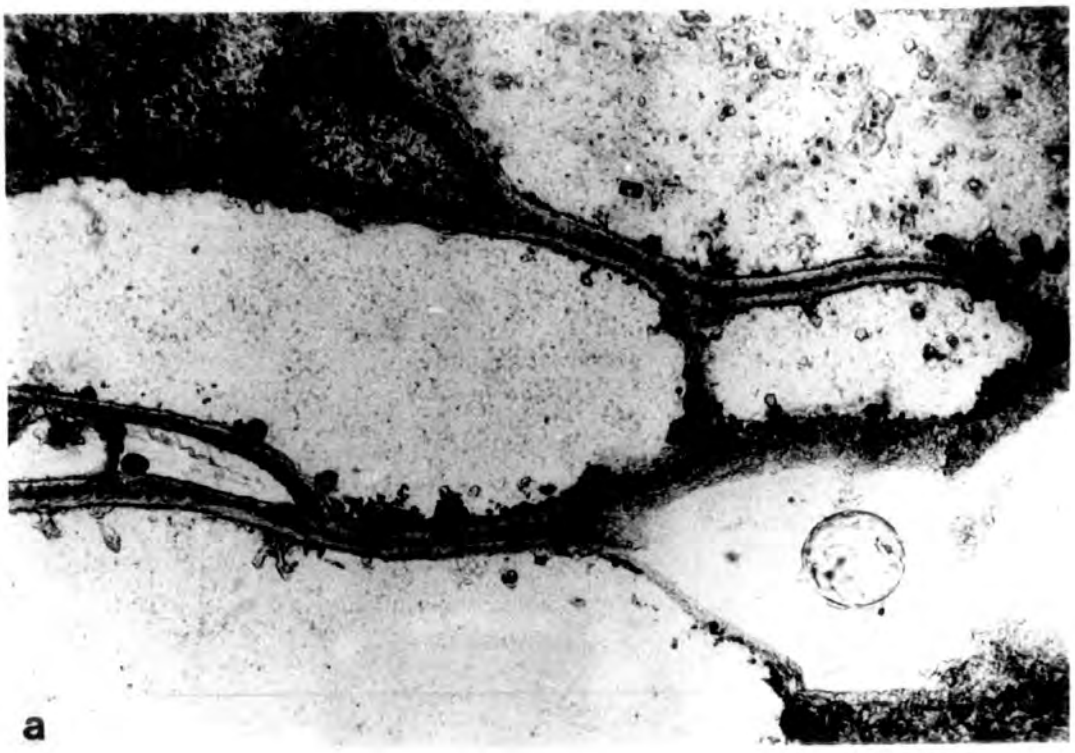
a


b

Plate 186. Sulcoretepora parallela(Phillips)

fig.a. Abundant large colony fragments. YM 1983,659F. Gilmerton, Edinburgh. X1.2.

fig.b. Abundant large colony fragments. HM D.288. Auchenskeoch Quarry, Dalry, Ayrshire. X1.2.

fig.c. Zoarial surface detail. ABHR 5. Arnsbergian, Shales above the Main Limestone, Hurst. X13.

a

b

c

Plate 187. Sulcoretepora parallela (Phillips)

figs a to e show zoarial surface detail. Autozooecial apertures are arranged in longitudinal rows, each separated by a narrow median ridge. All HM D.112. Brigantian, Lower Limestone Group, Hosie Limestone, Hairmyres, E. Kilbride. X21.

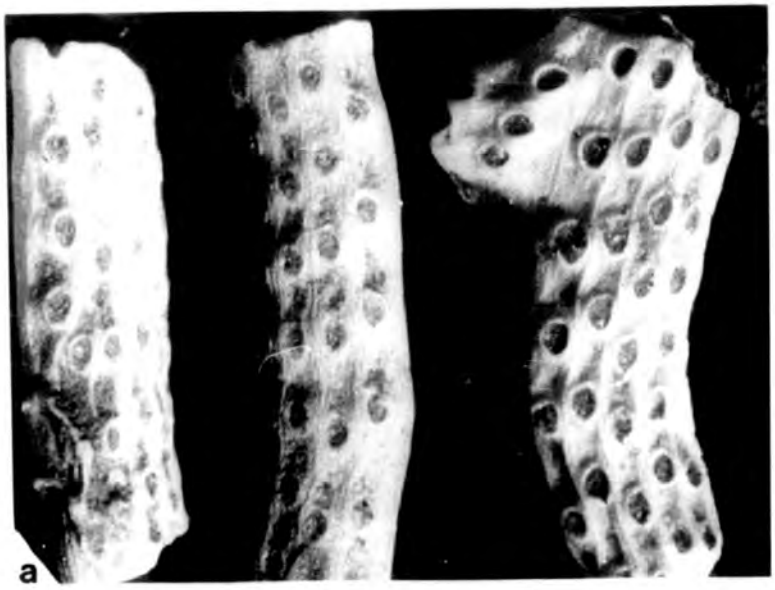

a

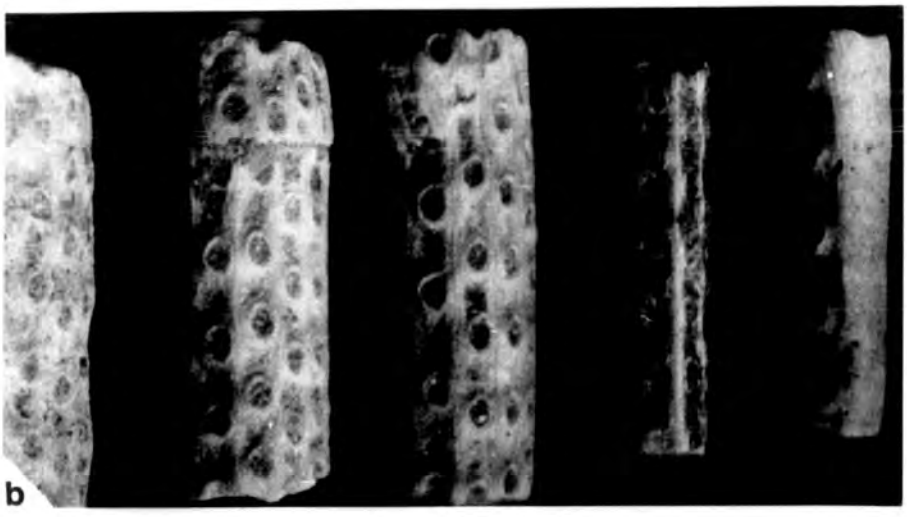

b

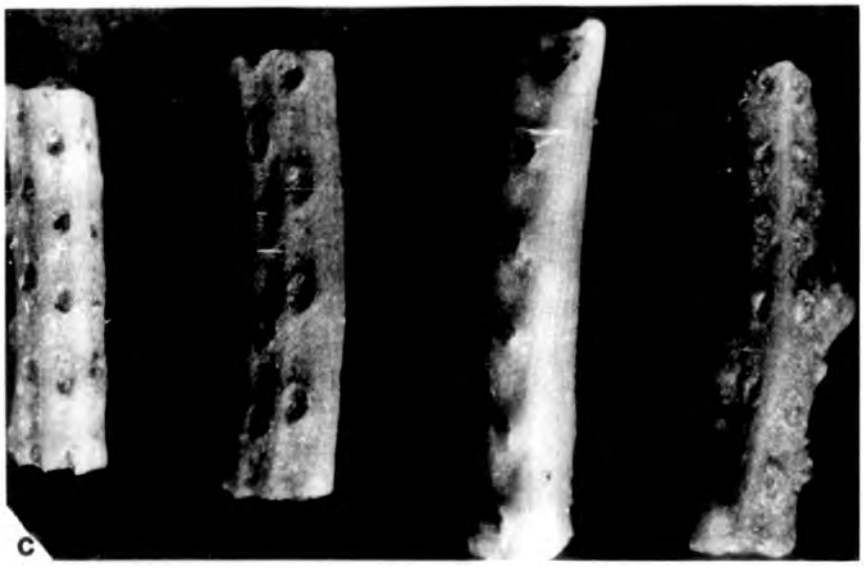

c

Plate 188. Sulcoretepora parallela (Phillips)

fig.a. Transverse section showing the acute elliptical shape of branches, the wedge shape of interzooecial walls and their compound structure. HM D.113-2. Brigantian, Lower Limestone Group, Hosie Limestone, Hairmyres, E. Kilbride. X109.

fig.b. Transverse section showing detail of the compound median and autozooecial walls. Vesicles are only occasionally developed and they are generally infilled with stereom. HM D.113-2. Horizon and locality as for fig.a. X290.

fig.c. Transverse section showing detail of the compound median and autozooecial walls. Horizon and locality as for fig.a. X290.


a
b
c

Plate 189. Sulcoretepora parallela (Phillips)

fig.a. Transverse section. HM D.113-3. Brigantian, Lower Limestone Group, Hosie Limestone, Hairmyres, E. Kilbride. X107.

fig.b. Transverse section showing detail of the compound median and autozooecial walls. Vesicles are only developed adjacent to the median wall and the recumbent portion of autozooecia, elsewhere they are infilled with stereom. HM D.113-3. Horizon and locality as for fig.a. X287.

fig.c. Transverse section through a parent branch and its lateral branch. HM D.113-5. Horizon and locality as for fig.a. X43.

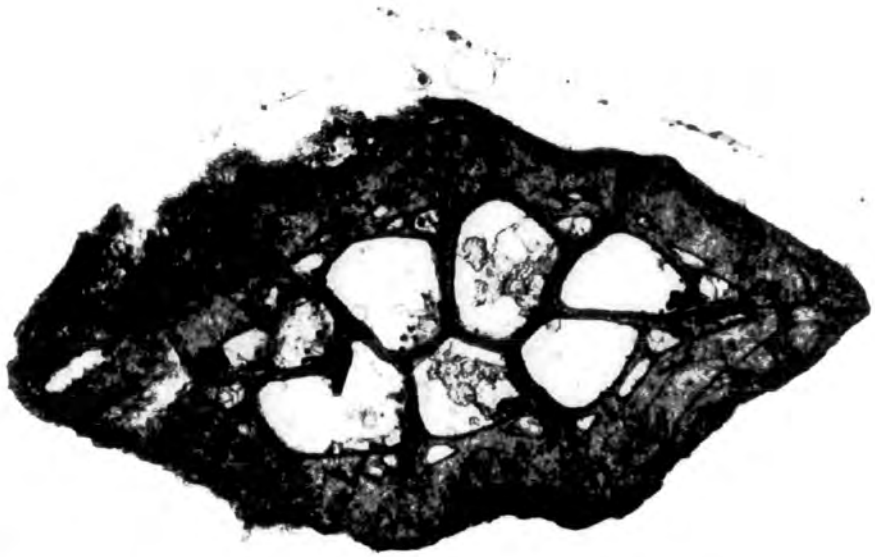

a

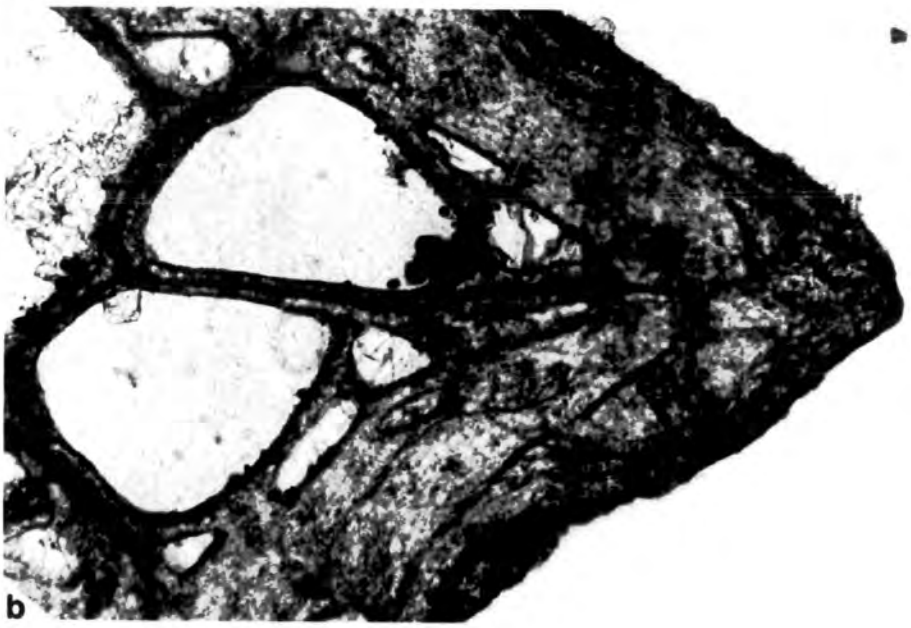

b

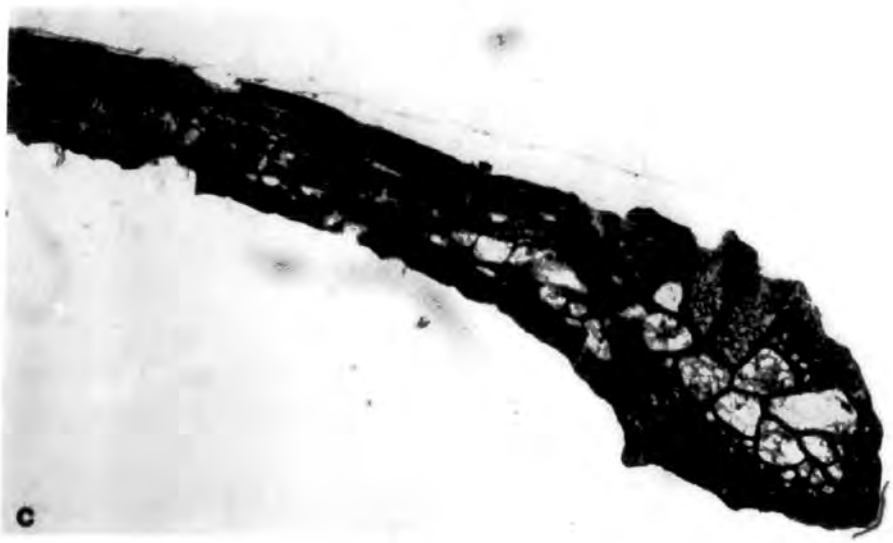

c

Plate 190. Sulcoretepora parallela (Phillips)

fig.a. Transverse section showing the occurrence of vesicles close to the autozooecial walls. Throughout most of the thickness of interzooecial walls they are infilled with stereom. HM D.113-5. Brigantian, Lower Limestone Group, Hosie Limestone, Hairmyres, E. Kilbride. X108.

fig.b. Shallow tangential section. HM D.113-4. Horizon and locality as for fig.a. X43.

fig.c. Oblique tangential section showing the recumbent portions of adjacent autozooecia, in the same longitudinal row, in contact. HM D.113-1. Horizon and locality as for fig.a. X43.

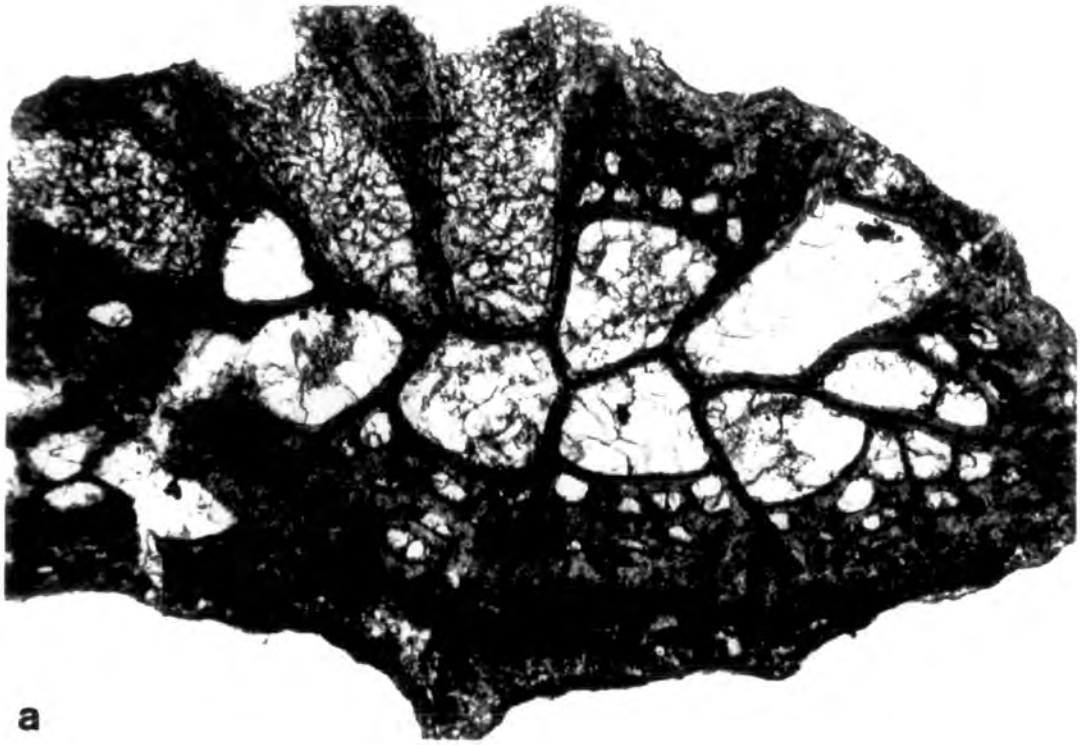

a

b

c

Plate 191. Sulcoretepora parallela (Phillips)

fig.a. Tangential section showing the compound structure of the longitudinal ridges between adjacent longitudinal rows of autozooecia. the ridges have a compound structure formed partially by the lateral walls of autozooecia. The vesicles between autozooecia are small thin walled, well faceted and structurally simple. HM D.113-1. Brigantian, Lower Limestone Group, Hosie Limestone, Hairmyres, E. Kilbride. X108.

fig.b. Longitudinal section showing the long recumbent portion of autozooecia and the small irregularly developed vesicles that form low hemispherical to box-like units. HM D.113-4. Horizon and locality as for fig.a. X108.

fig.c. As for fig.b. X107.


a

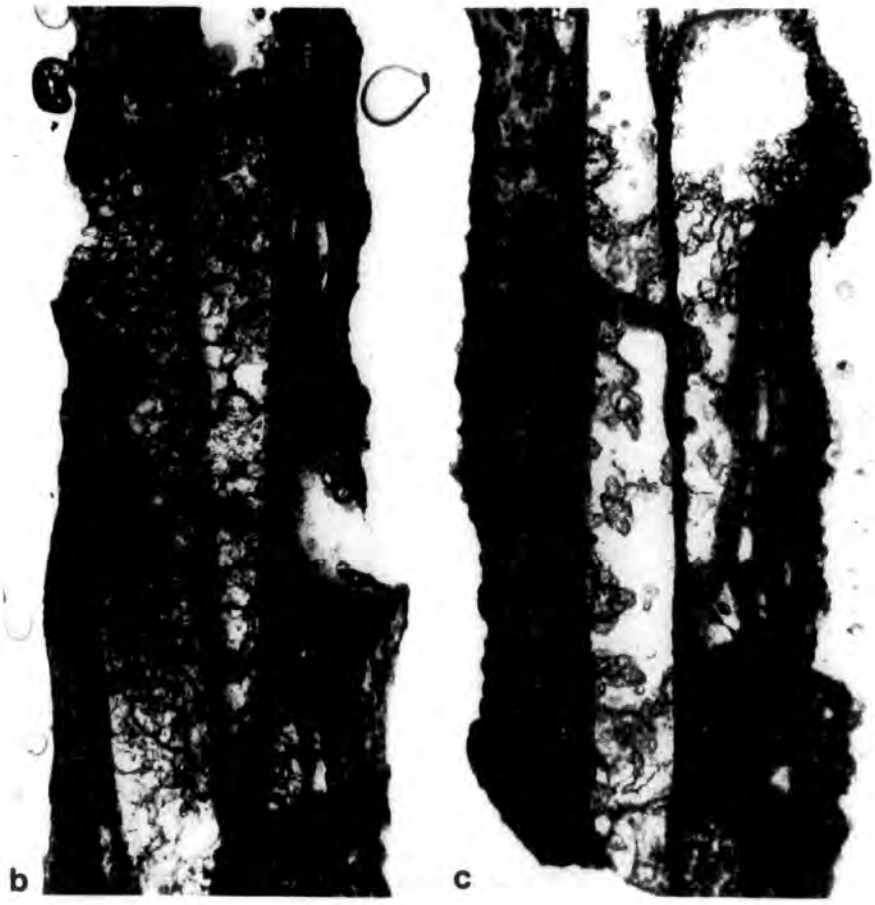
b
c